Electrospun antimicrobial and antibiofouling nanofibres

by

Nonjabulo Prudence Gule

Dissertation presented in fulfilment of the requirements for the degree
Doctor of Philosophy in Polymer Science at Stellenbosch University

Supervisor: Prof. Bert Klumperman
Co-supervisor: Prof. Thomas Eugene Cloete

Faculty of Science

Department of Chemistry and Polymer Science

December 2011

Declaration

By submitting this dissertation electronically, I declare that the entirety of the work contained therein is my own, original work, that I am the sole author thereof (save to the extent explicitly otherwise stated), that reproduction and publication thereof by Stellenbosch University will not infringe any third party rights and that I have not previously in its entirety or in part submitted it for obtaining any qualification.

December 2011

Abstract

The main objective of this study was to develop electrospun nanofibres with both antimicrobial and antibiofouling properties for possible application in water filtration. To do this, two routes were investigated: firstly, the use of biocides and bactericidal copper salts to introduce bactericidal properties on electrospun nanofibres. Secondly, the modification of polymers using furanone compounds to obtain nanofibres with the ability to repel microbial attachment.

Fabrication of biocide-containing PVA nanofibres was successful. This was achieved through direct doping of PVA solutions with AquaQure which is an aqueous biocide comprising of mainly Cu^{2+} and Zn^{2+}, prior to the electrospinning process coupled with chemical crosslinking using glyoxal. The conventional needle based electrospinning technique was used to fabricate these nanofibrous mats. The presence of the constituents of AquaQure on surfaces of PVA/AquaQure nanofibrous mats was confirmed using energy dispersive x-ray analysis (EDX). ATR/FTIR, XRD, TGA, DSC and SEM techniques were used to do chemical and thermal analysis of the nanofibres in comparison with pristine PVA nanofibres. These nanofibres demonstrated antimicrobial activity of up to 5 log against the Gram-positive strain *S. aureus* Xen 36 and Gram-negative strains *E. coli* Xen 14, S. *typhimurium* Xen 26, *P. aeruginosa* Xen 5 and *K. pneumoniae* Xen 39. Because of crosslinking, these fibres also demonstrated good water stability. Leaching of the ions constituting AquaQure was limited and compared with South African national standards for drinking water, the water filtered through these nanofibress was deemed safe for human consumption. Bioluminescence imaging and fluorescence microscopy were used to confirm antimicrobial activity results obtained from plate counting. These nanofibres demonstrated satisfactory antimicrobial efficiency but did not repel microbial attachment.

The second part of this study entailed the investigation of copper-doped PVA and SMA nanofibres for antimicrobial activity. Although bactericidal properties of copper are well documented, its selection was based on the fact that it is the main constituent of the AquaQure. Bubble electrospinning was used instead of needle electrospinning to upscale nanofibre production. Similar techniques as those used in PVA/AquaQure nanofibres were used to characterize the copper functionalized nanofibres. Even though these nanofibres demonstrated exceptional antimicrobial efficacy (up to 5 log) for all the strains, bioluminescence imaging indicated a trend for these cells to enter a dormant state on contact with the copper containing-nanofibres.

The last part of this project involved testing of free furanone compounds as well as surface-tethered furanone-modified nanofibres for their antibiofouling potentials. To do this, blends of 2,5-dimethyl-4-hydroxy-3(2H)furanone (DMHF) (5% wt/vol) with PVA (10% wt/vol) were prepared and electrospun to produce PVA/DMHF nanofibres. The free furanones and furanone-modified nanofibres

demonstrated not only antibiofouling properties but also antimicrobial activity. Other furanone compounds with 3(2H) and 2(5H) cores were synthesized. The synthesis of these furanone compounds (5-(2-(2-aminoethoxy)ethoxy)methyl)-2(5H)furanone and 4-(2-(2-aminoethoxy)-2,5-dimethyl-3(2H)-furanone) was successful. Their structures and molar masses were confirmed using ^{1}H NMR and ES mass spectroscopy. These furanones were then covalently immobilized on the SMA backbone. To test their antimicrobial and antibiofouling activity, the furanone-modified polymer was dissolved in an ethanol and methanol mixture (1:1) and electrospun to produce nanofibres. The free furanone and furanone-modified SMA nanofibres derived from 4-(2-(2-aminoethoxy)-2,5-dimethyl-3(2H)-furanone demonstrated high antibiofouling and antimicrobial efficiency against the Gram-positive strain *S. aureus* Xen 36 and Gram-negative strains *E. coli* Xen 14, S. *typhimurium* Xen 26, *P. aeruginosa* Xen 5 and *K. pneumoniae* Xen 39. The 2(5H) furanone on the other hand had limited activity against the strains. These nanofibres were also characterized and compared with their pristine polymer counterparts and leaching experiments were conducted using GC-MS.

Opsomming

Die hoofdoel van hierdie studie was om nanovesel filtrasie nanofibre met beide antimikrobiese en aanpakwerende eienskappe te ontwikkel. Twee verskillende metodes is ondersoek. Eerstens is biosiede en bakteriee-dodende koper soute gebruik om antimikrobiese nanovesels te lewer. Tweedens is nanovesels met furanoon samestellings gemodifiseer om nanovesels te lewer wat mikrobiese aanhegting voorkom.

Die fabrisering van biosied-bevattende PVA nanovesel nanofibre was suksesvol.
AquaQure, ’n biosied wat hoofsaaklik uit Cu^{2+} en Zn^{2+} bestaan, is direk by PVA oplossings gevoeg voor die elektrospin proses, en is gevolg deur chemiese kruisbinding deur middel van “glyoxal”. Die nanovesels is neergele in ’n ongeweefde mat deur middel van die konvensionele naald-gebasseerde elektrospin proses. Verspreidings X-staal analises (EDX) is gebruik om die teenwoordigheid van AquaQure komponente in en op die oppervlakte van die PVA/aquaqure nanovesel matte te bevestig. ATR/FTIR, UV-Vis, XRD, TGA, DSC en SEM tegnieke is gebruik vir chemiese en termiese analises om sodoende PVA/aquacure nanovesels met ongemodifiseerde PVA nanovesels te vergelyk. PVA/aquacure nanovesels het ’n antimikrobiese aktiwiteit van tot 5 log reduksie getoon teen Gram-positiewe *S. aureus* Xen 36 en Gram-negatiewe *E. coli* Xen 14, *S. typhimurium* Xen 26, *P. aeruginosa* Xen 5 en *K. pneumoniae* Xen 39. Die vesels was stabiel in water na kruisbinding. Slegs beperkte uitloging van Aquaqure Cu^{2+} en Zn^{2+} ione is waargeneem, en water wat deur die PVA/aquacure nanovesels gefiltreer is, is volgens Suid Afrikaanse Nasionale Standaarde vir drinkwater steeds veilig vir menslike gebruik. Behalwe vir die plaat-tellingsmetode het bio-lumiserende fotos en fluoroserende mikroskopie ook die antimikrobiese aktiwiteit van die vesels bevestig. Die vesels het bevredigende antimikrobiese efektiwiteit getoon, maar kon nie mikrobiese aanhegting voorkom nie.

In die tweede gedeelte van die werk is die antimikrobiese aktiwiteit van PVA en SMA vesels wat met koper verreik is, ondersoek. Alhoewel die bakteriee dodende eienskappe van koper reeds goed gedokumenteer is, is hierdie ondersoek gedoen op grond van die feit dat koper een van die hoof komponente van aquaqure is. Nanovesels is uit koper-verreikte oplossings van PVA en SMA deur middel van die borrel-gebasseerde elektrospin tegniek gefabriseer, ten einde die opbrengs van nanovesels te verhoog. Fisiese kruisbinding deur middel van hitte behandeling is toegepas ten einde die stabiliteit van die vesels in water te verbeter. Dieselfde karakteriseringstegnieke wat gebruik is vir die PVA/aquacure vesels is op hierdie vesels toegepas. Alhoewel die vesels uitstekende antimikrobiese aktiwiteit van tot 5 log reduksie gedemonstreer het, het bio-lumiserende beeldvorming getoon dat die selle ’n dormante stadium binnegaan na kontak met hierdie vesels.

In die laaste gedeelte van die projek is vrye furanoon samestellings en nanofibre met oppervlak-gehegde furanone getoets vir aanpakwerende potensiaal. Om dit te bewerkstellig was ‘n mengsel van 2,5 – dimethyl-4-hydroxy-3(2H) furanone (DMHF) (5% wt/vol) en PVA (10% wt/vol) voorberei en gebruik om PVA/DMHF nanovesel filtrasie nanofibre te produseer deur middel van die elektrospin proses. Die vrye furanone en furanoon-gemodifiseerde nanofibre het nie alleen aanpak weerstandbiedende einskappe gedemonstreer nie maar ook antimikrobiese eienskappe. DMHF was gebruik as die begin material om furanoon samestellings te produseer met 3(2H) en 2(5H) kerne. Die sintesis van hierdie furanone se samestellings (5-(2-(2-aminoethoxy)ethoxy)methyl)-2(5H)furanone en 4-(2-(2-aminoethoxy)-2,5-dimethyl-3(2H)-furanone) was suksesvol. Hulle strukture en molere massas was bevestig met ^{1}H NMR en ES massa spektrometrie. Hierdie furanone is daarna kovalent ge-immobiliseer op die SMA rugbeen. Om hulle antimikrobiese en aanpakwerende aktiwitiet te toets, is die furanoon-gemodifiseerde polimeer opgelos in ‘n etanol en metanol mengsel (1:1) en ge-elektrospin om nanovesel filtrasie nanofibre te produseer. Die furanone en furanoon-gemodifiseerde nanovesel filtrasie nanofibre afkomstig van 4-(2-(2-aminoethoxy)-2,5-dimethyl-3(2H)-furanone het hoe aanpakwerende en antimibrobiese effektiewitiet getoon teenoor die Gram-positiewe *S. aureus* Xen 36 en Gram-negatiewe *E. coli* Xen 14, S. *typhimurium* Xen 26, *P. aeruginosa* Xen 5 and *K. pneumoniae* Xen 39. Hierdie nanovesel filstrasie nanofibre is ook gekarakteriseer en vergelyk met die ongemodifiseerde polimeer. ‘n Uitlogings eksperiment is uitgevoer deur gebruik te maak van GC-MS.

List of Publications and Patents

Parts of this thesis have been patented, published, submitted to be published or presented at international conferences.

Patent

[1] *Patent number*: 2010/2091ZA00

Reference: Water filter assembly and filter element

Authors: Thomas Eugene Cloete, Marelize Botes, Michéle de Kwaadsteniet, Danielle Marguerite du Plessis, Nonjabulo Prudence Dlamini, Leon Milner Dicks

Publications (published; submitted or in preparation)

[1] An investigation into electrospun poly(vinyl alcohol) nanofibres with biocidal aditives for application in filter media. Part 1: Properties affecting electrospun fibre morphology and characterisation.

N.P. Dlamini, M. de Kwaadsteniet, T.E. Cloete, B. Klumperman (submitted)

[2] An investigation into electrospun poly(vinyl alcohol) nanofibres with biocidal additives for application in filter media. Part 2: Antimicrobial activity, reusability, leaching and water stability

N.P. Dlamini, M. de Kwaadsteniet, T.E. Cloete, B. Klumperman (submitted)

[3] Synthesis, characterization and antibiofouling efficacy of furanone compounds with the 3(2H) and 2(5H) furanone cores.

N.P. Dlamini, O. Bshena, M. de Kwaadsteniet, T.E. Cloete, B. Klumperman (in preparation)

[4] Antimicrobial and antibiofouling nanofibres derived from electrospun furanone modified poly(vinyl alcohol)

N.P. Dlamini, M. de Kwaadsteniet, T.E. Cloete, B. Klumperman (in preparation)

[5] Characterization and antimicrobial potential of electrospun nanofibres from copper doped polymer blends

N.P. Dlamini, M. de Kwaadsteniet, T.E. Cloete, B. Klumperman (in preparation)

Oral presentations

[1] Fabrication, characterization and antimicrobial efficacy of Cu^{+} functionalized polyacrylonitrile nanofibres. South African Microbiology Society Conference, November 2011

[2] Biofouling control using nanofibre containing furanone derivatives. IWA nano and water conference, Ascona, Zurich, Switzerland. 15-18 May 2011.

Poster presentations

[1] Fabrication and testing of the antimicrobial efficacy of PVA/Cu^{2+} nanofibres: 11th UNESCO/IUPAC Conference on Functional Polymeric Materials and Composites. April 2011.

Acknowledgements

I sincerely wish to thank the following people who contributed towards the success of this project:

- My supervisors Prof. Klumperman and Prof. Cloete for the opportunity to conduct this study under their leadership. Their experience, skill, determination and passion for research have made it an honour to study under their supervision. I would also like to thank them for their unswerving patience, encouragement and for always having time to give guidance when needed.
- My husband for being amazing through and through. For always being excited about my work even at times when I wasn't and for just seeing the best in me…I wouldn't have asked for a better person to share my life with.…Thank you for that reassuring smile my love!
- The Dlamini and Gule families for their prayers and support.
- My collegues from the Department of Microbiology Michele, Marelize, Danielle… You ladies are the best! Baie dankie. Michele, thank you for proof reading my work and for keeping me motivated.
- The Free Radical group and Ahson, you guys are just amazing.
- Welmarie, you are great my friend…you really helped me keep it together… Thank you for being who you are!
- Prof. L.M.T. Dicks and his group for welcoming me and for guidance during the time I spent in their laboratory.
- The central analytical facilities staff; for helping with sample analysis.
- The Andrew Mellon Foundation, Eskom and the National Research Foundation for funding this work.
- And to sum it all "TO GOD BE THE GLORY"…I wouldn't have done this without the Lord.

Clean, safe drinking water is scarce. It is the foundation of life, a basic human need. Yet today, all around the world, far too many people spend their entire day searching for it [United Nations, 2005].

Table of Contents

List of Figures

List of Tables

List of Schemes

List of Abbreviations

AA	Acrylic acid
AHL	*N*-Acyl homoserine lactone
ATP	Adenosine triphosphate
ATR-FTIR	Attenuated total reflectance-Fourier transform Infra red spectroscopy
BC	Before Christ
BLI	Bioluminescence imaging
CA	Cellulose acetate
CFU	colony forming units
DCM	Dichloromethane
DMF	Dimethylformamide
DMHF	2,5 dimethyl-4-hydroxy-3(2H)-furanone
DMSO	dimethylsulfooxide
DSC	Differential scanning calorimetry
EDCs	Endocrine disrupting compounds
EDTA	Ethylenediamine-N,N,N',N'-tetraacetic Acid
EPS	Extra polymeric substances
ES	Electrospinning
ES-MS	Electron spray-mass spectroscopy
EU	European Union
FRP	Free radical polymerization
GC-MS	Gas chromatograph coupled mass spectroscopy
HEMA	2-hydroxyethyl methacrylate
ICP-AES	Inductive coupled plasma-atomic emission spectroscopy
IR	Infrared spectroscopy
IVIS	*in vivo* imaging system
MeOH	Methanol
MF	Microfiltration
MIC	Minimum inhibitory concentration
$Na_2S_2O_3$	Sodium thiosulfate
NaOH	Sodium hydroxide
NF	Nanofiltration
NMR	Nuclear magnetic resonance spectroscopy
PA	Polyamide
PAAm	Polyacrylamide

PAN	Polyacrylonitrile
PCL	Polycaprolactone
PE	Polyethylene
PEG	Polyethylene glycol
PEI	Polyether imide
PP	Polypropylene
PPCPs	Pharmaceuticals and personal care products
PTFE	Polytetrafluoroethylene
PVA	Poly(vinyl alcohol)
PVC	Polyvinylchloride
PVDF	Poly(vinylidene fluoride)
PVP	Poly(vinyl pyrolidine)
QQ	Quorum quenching
QS	Quorum sensing
QSI	Quorum sensing inhibitors
RO	Reverse Osmosis
SANS	South African National Standards
SEM	Scanning electron microscopy
SMA	Poly(styrene-co-maleic anhydride)
SPIP	Scanning Probe Image Processor
SPME	Solid phase micro extraction
SRB	Sulphate reducing bacteria
TGA	Thermogravimetric analysis
THF	Tetrahydrofuran
UF	Ultrafiltration
UN	United Nations
UV	Ultra violet
UV-Vis	Ultra violet-visible
VNBC	viable but non-culturable
WHO	World health organization
XRD	X-ray diffraction

Chapter 1: Introduction

1.1 Background information

As the world population continues to grow, water resources are increasingly strained. Many areas around the world are turning to water reuse to augment their potable water supply. Modern biological wastewater treatment technologies are capable of removing suspended solids, organic constituents and nutrients. However, they do not completely remove many constituents of concern such as pathogenic bacteria and viruses, and traces of pharmaceuticals and personal care products (PPCPs) as well as endocrine disrupting compounds (EDCs). Membrane technology offers the water industry a simple and 'cost effective' treatment technique which can remove not only viruses, but also pharmaceuticals, personal care products and EDCs. Despite its wide use and promising applicability, membrane filtration technology remains limited due to fouling.[1, 2]

Fouling is a term used to describe the loss of throughput of a membrane device as it becomes chemically or physically changed by the process fluid. In membrane filtration applications, fouling emanates from the attachment or adherence of solutes onto the membrane surface or internal structure of the membrane. There are numerous reasons for a molecule, a colloid or a particle to settle on the membrane surface or inside the pores and to stay there. The main consequence is a change in flux, but also a change in the apparent porous structure of the membrane. The general trend reported is an increase of retention in fouled membranes compared to clean ones.[3] Based on the conditions causing membrane fouling, it can be divided into four types namely: inorganic, organic, silting and biofouling. Of all the types of fouling, biofouling which is caused by the growth of biofilms on membrane surfaces is the hardest to control.

In the last few years, significant milestones have been achieved in the area of membrane technology and realization of new organic and inorganic membranes and many academic and industrial research projects in this area are underway.[4] The production of nanofibres is one of the greatest breakthroughs in the water treatment industry because of the structural properties that these fibres have.[5] These properties include, a high surface to volume ratio which allows a higher adsorption rate of various trace organics and bacteria for improving water quality, a higher temperature and acid/base tolerance, longer membrane life span and flexibility which enables the membrane to be formed into various membrane modules for larger commercial application.[6]

Several techniques to fabricate nanofibres have been reported and electrostatic spinning or electrospinning is the most widely used. Electrospinning is a mechanical and electrical technique of producing ultrafine fibres in the submicron diameter range using high voltage.[6] This technique results

in continuous nanofibres which can be formed into various modules and can be produced on a large scale.[7] Various polymers can be electrospun into fibres using this process. Electrospinning is a well-established process for fabrication of nanofibre mats with high surface areas, large volume-to-mass ratios, and high porosities.[7-10] This process has been demonstrated to be suitable for scaling up nanofibre production at a relatively low cost.[11]

Even though membrane filtration is a promising technology, its large scale industrial applicability is limited partly due to poor intrinsic membrane properties but largely because of fouling of the membranes. The use of chemical biocides such as chlorine to control biofouling of membranes is widespread.[12-16] However, most of these chemical biocides are not very effective at higher pH values and they react with dissolved chemicals to produce harmful byproducts.[17] Physical means like pigging, brushing, swabbing and jetting have been reported, but only work best as secondary methods to other removal methods.[18] The use of bacteriophages,[19] electrical current[20] and nutrient control [21] have also been explored but these methods are either host specific or can take a long time to work and are not very cost effective.

The focus is now moving to modification of membrane surfaces to control fouling. Noble metal elements such as silver, copper, zinc, nickel, manganese, iron and lithium have been reported to be having antimicrobial properties.[22, 23] Some of these metals have been blended with polymers and made into fibres for use in filter media, wound dressing and other applications. Silver, has been extensively studied especially for wound dressing applications due to its antimicrobial nature.[24]

The use of furanone derivatives which inhibit quorum sensing in microorganisms is an area which has not been significantly explored in filtration systems. Furanones are analogs of homoserine lactones that appear to interfere with the development of typical biofilm structure, leaving these organisms more susceptible to treatment with biocides.[25] Targeting QS is also advantageous compared to the use of antibiotics since there is no risk of the bacteria developing resistance which causes serious control problems. Many natural products contain the core 3(*2H*)-furanone structure classified as a lactone.[26] Because of the high synthetic and biological importance of furanone compounds, their chemistry has received considerable attention over the past two decades.[27] Furanone moieties have been found to have various medicinal properties, such as anticancer, cardiotonic, analgesic, antimicrobial, antiviral, antifungal, and anti-inflammatory properties.[28-33] [34] Research on clinical applications is widespread but not much has been reported on filtration applications.

1.2 Motivation

Microbiologically safe drinking water is a scarce resource and many countries do not have sufficient water supplies to support their populations. With the changes in global climate and population growth, water will become an even scarcer resource especially in the developing world. Statistics released by

the World Health Organisation (WHO) on water shortage and the consequences associated with it indicate that almost a billion people in sub-Saharan Africa and the rest of the developing world lack access to safe water supplies. An estimate of 3.6 million people in the developing world die each year from water-related diseases and these are mostly children under the age of 15 years.[35] As Diallo said, "there is little doubt that satisfying humankind's demand for water in a sustainable manner requires visionary new approaches to management and conservation of water resources augmented by new technologies capable of dramatically reducing the cost of supplying clean fresh water-technologies that can best be derived from tightly coupled basic and applied research."[36] The application of conventional water treatment systems in the developing world is in most cases a daunting task due to lack of infrastructure and skills.[37, 38] Furthermore, dwellings of rural communities in the developing world are scattered over wide areas which makes it almost impossible to pipe water from centralized purification systems.[39-41] The application of membrane nanotechnology especially in point of use systems could be a viable alternative to providing safe drinking water for these areas. In this particular study, antimicrobial and antibiofouling nanofibres were fabricated and investigated for possible application in water filtration media with a possibility of further improvements to achieve industrial scalability.

1.3 Problem statement

Conventional water purification techniques involve the use of chemicals to clean water and these practices introduce harmful chemicals to the environment. These techniques also require skilled labour to operate the infrastructure and high energy is necessary to run the processes involved. This is in most cases not possible in remote rural areas where there is no electricity and skills. The trend in filtration plants is now moving towards membrane filtration technologies. Membrane water filtration is a cost effective and environmentally acceptable method of purifying large volumes of water. Due to these attributes, it is a viable method to meet the water demands of the growing population. The limitation to membrane filtration technology is the fouling of membranes which escalates maintenance costs and compromises water quality. Of all the types of membrane fouling, biological fouling which is fouling caused by biofilm attachment on membrane surfaces, is the most difficult to control. Researchers have come up with many solutions to the biofouling problem and most strategies are centred on either killing the bacteria before they form biofilms (inactivating them) or modifying membrane surfaces to produce membranes which will not allow biofilm attachment.

1.4 Objectives

The main goal of this study was to develop nanofibres with both antibacterial and anti-biofouling properties for possible application in filtration media. This means that the fabricated nanofibres should not only have surfaces which will repel microbial attachment, but also inactivate any bacteria which

may come into contact with it. The use of biocides containing transition metal elements which have widely demonstrated antimicrobial activity as well as furanone derivatives which inhibit (prevent) biofilm formation were explored in this study. The objectives of this study were therefore:

- To surface functionalize or modify polymers.
- To generate polymer nanofibres using the process of electrospinning.
- To determine antimicrobial potential of polymer nanofibres.
- To characterize nanofibres.
- To assess application in filter media

The dissertation is structured in such a way that, each of the major chapters has its own objective on how antimicrobial or antibiofouling activity was introduced to pristine polymers that otherwise do not possess any activity against microorganisms.

1.5 Methodology

This study focused on developing membranes using various durable, non-toxic and water-insoluble polymers (crosslinked) poly(vinyl alcohol) (PVA) and poly(styrene-co-maleic anhydride) (SMA). Electrospinnable solutions of the polymers with either a biocide (AquaQure) and/or copper salts to introduce antimicrobial functionality were prepared and electrospun using conventional needle electrospinning or bubble electrospinning. Post polymerization crosslinking of PVA using heat treatment and chemical crosslinking were explored. The nanofibres' antimicrobial efficiencies as well as water stability and leaching degree were tested. In the second part of this project free furanone compounds as well as nanofibres with immobilized furanone compounds were investigated for their antimicrobial and antibiofouling activities. Commercially available and synthesized furanone compounds were investigated.

1.6 Structure of thesis

The thesis comprises of six chapters as outlined in Figure 1.1. In Chapter 1 a brief introduction into membrane technology in water treatment is given. This chapter also highlights the motivation for this study. The problem statement puts forth the objective of developing antifouling nanofibres to solve the biofouling problem associated with current membrane filtration. Finally, the research methods adopted in this study are summarized.

An overall review on the fundamental theory of this study is given in Chapter 2. It describes membrane technology and then gives a detailed description on how membrane fouling limits its

application. The second part of this chapter focuses on electrospinning which is the technique used in this study for producing nanofibres.

In Chapter 3, functionalization of poly (vinyl alcohol) (PVA) with a known Cu containing biocide is reported. Factors affecting electrospinning of the polymeric solutions are investigated and characterization of the fibres is reported. The stability of the fibres in water and their antimicrobial efficiency are also reported.

Chapter 4 reports the fabrication and functionalization of nanofibre mats from PVA and SMA. Bactericidal copper salts were blended to spinning solutions and electrospun using bubble electrospinning to produce fibres in the nanometer range. PVA nanofibres were crosslinked through heat treatment to achieve stability in liquid filter media. Chemical and antimicrobial characterization of the nanofibres is also reported.

Furanones are known to inhibit quorum sensing and thus inhibit surface colonisation by biofilms. In chapter 5, a known furanone derivative was incorporated into PVA and electrospun to form fibres with the furanone functionality. Other furanone derivatives were also synthesized and covalently immobilised on poly(styrene-co-maleic anhydride) (SMA). The fibres resulting from both PVA/furanone blend and the synthesized furanone covalently immobilised to SMA were tested for their antibiofouling efficiencies.

Chapter 6 comprises of general conclusions from the study, a summary of the contribution as well as recommendations for future research in this field.

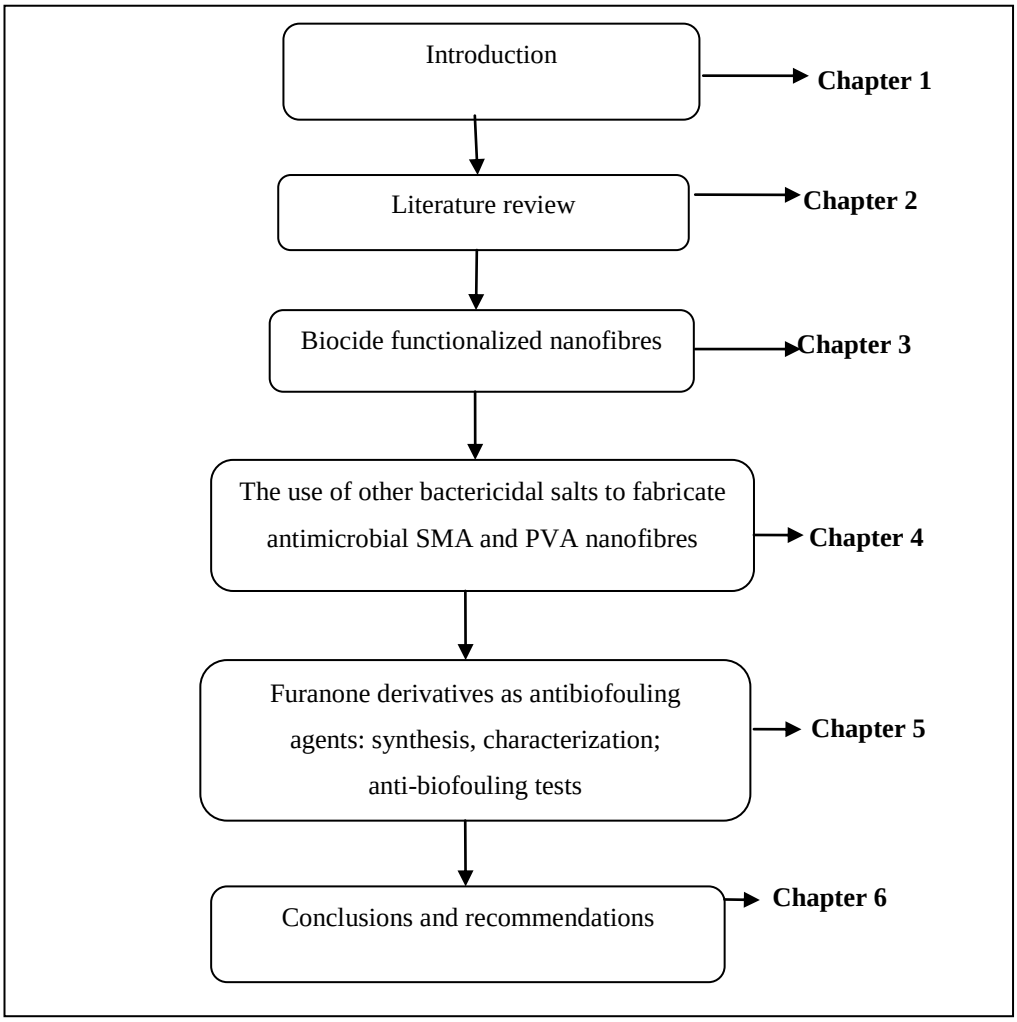

Figure 1.1: Thesis layout

1.7 References

1. Su T.J.; Lu J.R.; Cui Z.F. *Membrane Science* **2000,** 173, 167-178.
2. Cloete TE, V. S., Brozel S, Van Holy A. *International Biodeterioration and Biodegradation* **1992,** 29, 299-341.
3. Noble R.D.; Stern S.A., *Membrane Separations Technology: Principles and applications*. 1995.
4. Vrouwenvelder JS, W. L., Cornelissen ER, Heijman D, Van Der Kooij SG. Viallefont XD. *Journal of Membrane Science* **2007,** 287, 94-101.
5. Barker R.W., *Membrane Technology and Applicaions*. Wiley: 2004.
6. Huang Z-M.; Zhang Y-Z.; Kotaki M.; Ramakrishna S. *Composites Science and Technology* **2003,** 63, 2223-2253.
7. Ramakrishna S.; Fujihara K.; Teo W-E.; Lim T-C.; Ma Z., *An Introduction to Electrospinning and Nanofibres*. World Scientific Publishing Co. Pte. Ltd.: Toh Tuck Link, Singapore, 2005.
8. Baji A.; Mai Y-W.; Wong S-C.; Abtahi M.; Chen P. *Composites Science and Technology* **2010,** 70, 703-718.
9. Li D.; Xia Y. *Advanced Materials* **2004,** 16, 1151-1170.
10. Reneker D.H.; Yarin A.L.; Fong H.; Sureeporn K. *Journal of Applied Physics* **2000,** 87, 4531-4547.
11. Greiner A.; Wendorff J.H. *Angew Chem Int Edit* **2007,** 46, 5670-5703.
12. Chen X.; Stewart P.S. *Environmental Science and Technology* **1996,** 30, 2078-2083.
13. Kramer J.F., Biofilm control with bromo-chloro-dimethylhydantion. In *Corrosion NACE International. Paper number 1277*, Houston, Texas, 2001.
14. Vidella H.A. *International Biodeterioration and Biodegradation* **2002,** 49, 259-270.
15. Stewart P.; Roe F.; Rayner J.; Elkins F.G.; Lewandowski Z.; Ochsner U.A.; Hassett D.J. *Applied and Environmental Microbiology* **2000,** 66, 836-838.
16. Presterl E.; Suchomel M.; Eder M.; Reichmann S.; Lassnigg A.; Graninger W.; Rotter M. *Journal of Antimicrobial Chemotherapy* **2007,** 60, 417-420.
17. Richards M. Self immobilization of single and combinations of enzymes in spherical particles and evaluation of their anti-biofouling potential. University of Pretoria, Pretoria, South Africa, 2010.
18. Meyer B. *International Biodeterioration and Biodegradation* **2003,** 51, 249-253.
19. Curtin J.J.; Donlan R.M. *Antimicrobial Agents and Chemotherapy* **2006,** 50, 1268-1275.
20. Van der Borden A.J.; Van der Mei H.C.; Busscher H.J. *Journal of Biomedical Material Research* **2004,** 68B, 160-164.

21. Allison DG; Ruiz B; SanJose C; Jaspe A; Gilbert P. *FEMS Microbiology Letters* **1998,** 167, 179-184.
22. Al-Sha'alan N. *Molecules* **2007,** 12, 1080-1091.
23. Revanasiddappa H.D.; Vijaya B.; Kumar S.L.; Prasad K.S. *World Journal of Chemistry* **2010,** 5, 18-25.
24. Zhuang X.; Cheng B.; Kanga W.; Xua X. *Carbohydrate Polymers* **2010,** 82, 524-527.
25. Baveja J.K.; Willcox M.D.P.; Hume E.B.H.; Kumar N.; Odell R.; Poole-Warren L.A. *Biomaterials* **2004,** 25, 5003-5012.
26. Pe´rez A.G.; Olı´as R.; Olı´as J.M.; Sanz C. *Journal of Agricultural Food Chemistry* **1999,** 47, 655-658.
27. Mahajan V.A.; Borate H.B.; Wakharkar R.D. *Tetrahedron* **2006,** 62, 1258-1272.
28. Lattmann E.; Ayuko W.O.; Kinchinaton D.; Langley C.A.; Singh H.; Tisdale M.J. *Journal of Pharmacy and Pharmacology* **2010,** 55, 1259-1265.
29. Khan M.S.; Husain A. *Pharmazie* **2002,** 57, 448-452.
30. Leite L.; Jansone M.; Veveris M.; Cirule H.; Popelis Y.; Melikyan G.; Avetisyan A.; Lukevics E. *European Journal of Medical chemistry* **1999,** 34, 859-865.
31. Klunk W.E.; Covey D.F.; Ferrendelli J.A. *Molecular Pharmacology* **1982,** 22, 438-443.
32. Ali A.M.; Shahram H.; Jamshid C.; Ghadam Ali K.; Farshid H.; Fen-Tair L.; Tai W.L.; Kak-Shan S.; Chi-Feng Y.; Moti L.J.; Ramasamy K.; Cuihua X.; Manijeh P.; Gholam H. *Bioorganic & Medicinal Chemistry Letters* **2003,** 11, 4303-4313.
33. Wu H.; Song Z.; Hentzer M.; Andersen J.B.; Molin S.; Givskov M.; Høiby N. *Journal of Antimicrobial Chemotherapy* **2004,** 53, 1054-1061.
34. Gottesdiener K.; Mehlisch D.R.; Huntington M; Yuan W.; Brouwn P.; Gertz B.; Mills S. *Clinical therapeutics* **1999,** 21, 1301-1312.
35. Prüss-Üstün A.; Bos R.; Gore F. *Safer water, better health: Costs, benefits and sustainability of interventions to protect and promote health*; World Health Organization: Geneva, 2008.
36. Savage N.; Diallo M.; Duncan J.; Street A.; Rustich R., *Nanotechnology applications for clean water*. William Andrew Inc.: Norwich, NY, 2009.
37. Yu X.; Zhang S.; Zhang H. *The Status and Challenges of Water Infrastructure Development in China*; Institute of Urban Environment, Chinese Academy of Sciences: Xiamen, China, 2008.
38. Sengupta B.; Kumar P.; Ansari P.M.; Basu D.D.; Thirumurthy G.; Sharma A.; Gayithri H.V. *Status of water treatment plants in india*; Central Pollution Control Board (Ministry of Environment and Forests): India, 2009.
39. Swartz C.D. *A planning framework to position Rural water treatment in south Africa for the future* Water Research Commission: WRC Report No. TT 419/09: South Africa, 2009.
40. Momba MNB.; Tyafa Z.; Makala N.; Brouckaert B.M.; Obi C.L. *Water SA* **2006,** 32, 715-720.

41. Mandri-Perrott C. *OBA Aproaches* **2008,** 21.

Chapter 2: Literature review

2.1 Chapter summary

In this chapter, a review on the fundamental theory and historical milestones related to this study are given. Membrane technology and its application in water treatment are described as well as a detailed description on how membrane biofouling limits its application. Current strategies to control fouling are also discussed. New advancements in membrane technology have seen the rise in the use of nanotechnology to produce ultrafine fibres known as nanofibres through the electrospinning process for use in filter media. The second part of this chapter focuses on the production of nanofibres through electrospinning giving advantages of this process over other techniques which have been reported to fabricate nanofibres. It also gives an overview on how this process and resultant fibres can be manipulated to produce fibres with beneficial properties which the original polymers did not have.

2.2 Introduction

The word membrane is derived from the Latin word 'membrana' which means skin and was first used in popular English sometime before 1321.[1] A membrane can be described as a discrete, thin interface that moderates the permeation of species in contact with it.[2] This interface may be molecularly homogenous, that is, completely uniform in composition and structure or physically heterogeneous. Membrane technology has become one of the major separation technologies over the past decade. Advantages of membrane technology over other separation technologies are that it works without the addition of chemicals and uses relatively low energy.[2] According to the driving force behind membrane separation, membrane processes can be divided into four categories (Table 2.1). The membrane acts as a specific permeable barrier which allows some compounds to pass through it while restricting others (Figure 2.1). As the solution passes through the membrane, selective filtration takes place resulting in certain molecules making it to phase 2 (permeate).

Table 2.1: Membrane separation processes based on driving force.

Pressure	Concentration	Electric potential	Temperature
• Microfiltration • Ultrafiltration • Nanofiltration • Reverse osmosis • Pervaporation • Gas separation	• Dialysis • Osmosis • Forward osmosis	• Electrodialysis • Electrophoresis • Membrane electrolysis	• Membrane distillation

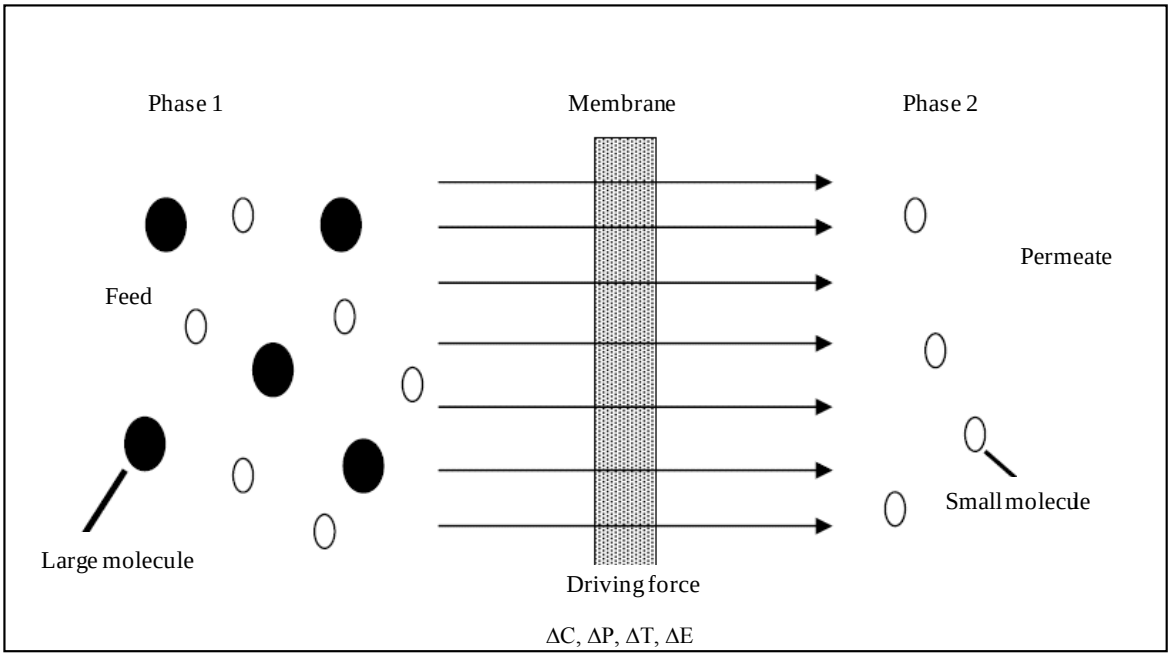

Figure 2.1: Principle of membrane operation.[2]

2.2.1 Historical development of membranes

Although membranes have existed and functioned in nature as long as life has existed on earth, there are no references to their applications until the middle of the eighteenth century. Thus, systematic studies on membranes can be dated back to the eighteenth century. In 1748 Jean-Antoine Nollet described the word 'osmosis' as the permeation of water through a diaphragm. Through research in the nineteenth and early twentieth centuries, membranes were used as laboratory tools to develop physical/chemical theories, but did not have any industrial or commercial uses. Since the first synthetic membranes became available approximately 50 years ago, the industry has grown enormously.[2, 3] The historical milestones in membrane technology are highlighted in Table 2.2. A breakthrough as far as industrial membrane applications are concerned was achieved by the development of cellulose acetate (CA) membranes by the Dreyfus brothers, which later made reverse osmosis (RO) a commercial reality. By the early 1980's, large plants based on a range of technologies were in operation around the world.[2]

Table 2.2: Developments in membrane technology.[1]

Year	Development	Scientists
1748	Osmosis: Permeation of water through pig bladders	A. Nollet
1833	The law of gas diffusion	T. Graham
1855	Phenomenological laws of diffusion	A. Fick
1860-1880s	Semi-permeable membranes: Osmotic pressure	M. Traube (1867), W. Pfeffer (1877), J.W. Gibbs (1878), J.H. Van't Hoff (1887)
1907-1920	Microporous membranes Prototype of Reverse Osmosis	R. Zsigmondy, L. Michaelis (1926); E. Manegod (1929), J.W. McBain (1931)
1930s	Electrodialysis membrane, modern membrane electrodes	T. Teorell (1935), K.H. Meyer and J.W. Sievers (1936)
1950s	Electrodialysis; Microfiltration; haemodialysis; ion exchange membrane	Many
1963	Defect free high flux anisotropic RO membrane	S. Loeb and S. Sourirajan
1968	Basics of pervaporation Spiral wound RO membrane	P. Aptel and J. Neel J. Westmorland
1977	Thin film composite membrane	J. Cadotte
1970-1980	Reverse osmosis (RO), Ultrafiltration (UF), microfiltration (MF), electrodialysis	Many
1988	Industrial gas separation processes	J.M.S. Henis and M.K. Tripodi
1989	Submerged membrane (bioreactor)	K. Yamamoto

2.2.2 Membrane technology in water treatment

Due to contamination of water sources by municipal and industrial effluents, there is a need for efficient and economic techniques to improve water quality, recover valuable materials from waste water and reuse waste water. Membrane water treatment technologies, compared to conventional technologies are simpler to improve for industrial operations and thus respond more efficiently to the requirements of process intensification. Membrane filtration techniques are very promising in the treatment of water due to their potential to remove particles, including organic pollutants, microorganisms, and inorganic compounds. Nanofiltration (NF) and reverse osmosis (RO) remove nutrients which can be transformed into biomass and this limits microbial regrowth in the distribution system. In addition, NF and RO can be used to remove viruses from water.[1]

2.3 Membrane filtration processes

Membranes can selectively separate components over a wide range of particle sizes and molecular weights, from macromolecular materials such as starch and protein to monovalent ions. Membrane separation processes currently used in the treatment of water can be classified into reverse osmosis

(RO), ultrafiltration (UF), nanofiltration (NF) and microfiltration (MF). Each of these technologies utilizes a membrane barrier that allows the passage of water but removes contaminants. Figure 2.2 and Figure 2.3 compare the four different processes based on the size of the contaminants they filter out. The following subsections describe each of the four membrane filtration processes, their shortcomings and applications.

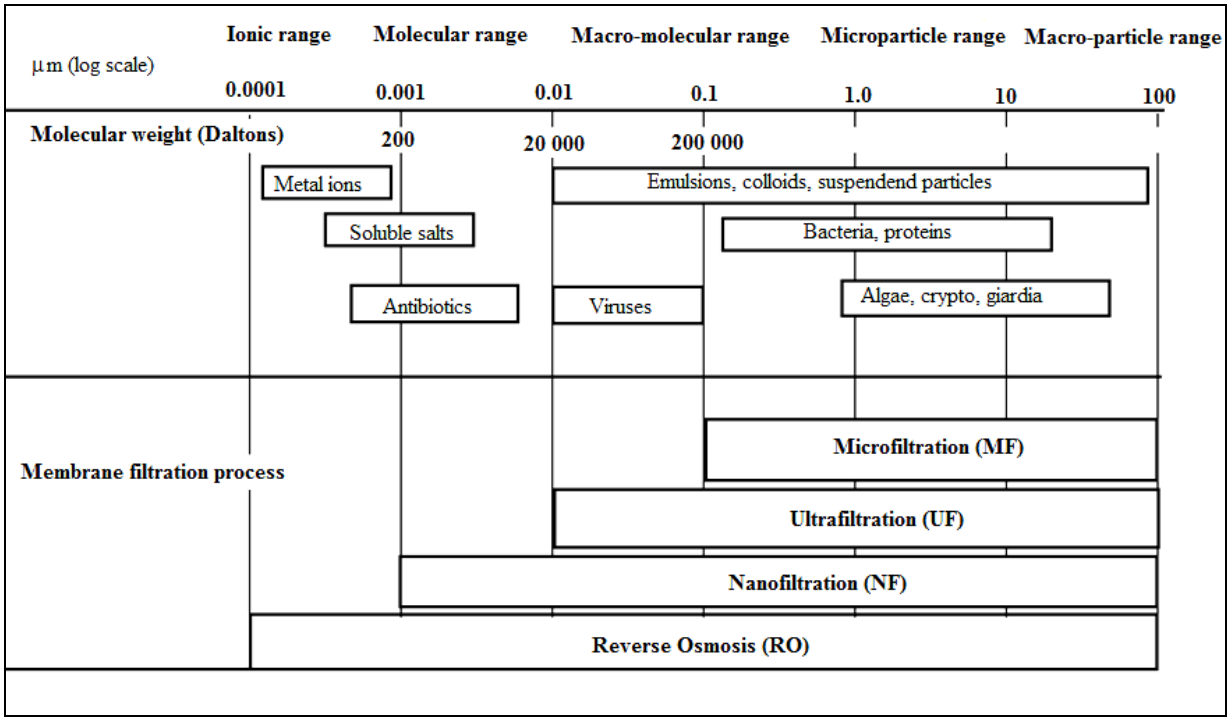

Figure 2.2: Membrane processes (modified from reference [4]).

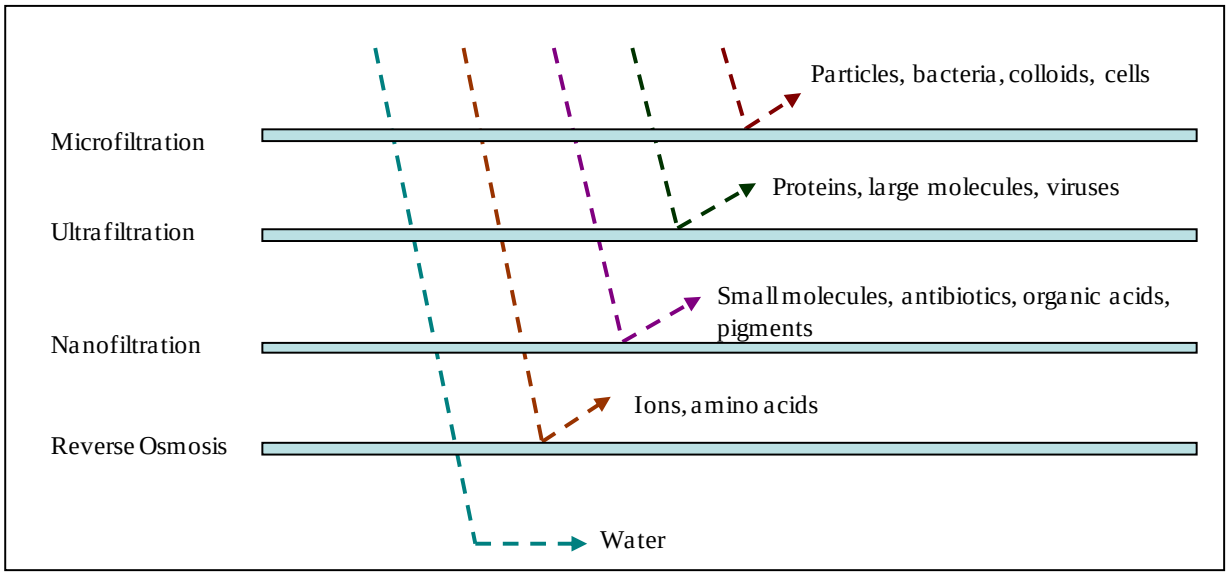

Figure 2.3*:* Separation capabilities of MF, UF, NF and RO for water and waste water treatment (modified from reference [5]).

2.3.1 Microfiltration (MF)

Microfiltration (MF) membranes have the largest pore sizes compared to the other pressure driven membrane filtration processes outlined in Table 2.1. A low pressure of between 1 and 2 bars is applied to the feed during the process.[6] MF is used for separating colloidal and suspended particles in the range of 0.1-5 microns. MF has also been considered as a pretreatment method for RO systems instead of existing physical and chemical treatment methods such as lime clarification and multimedia filtration.[7] MF can be implemented in many different water treatment and industrial processes where particles with a diameter greater than 0.1 mm need to be removed from a liquid.[8] Applications of MF in industry include: clarification of fermentation broth and biomass recovery. In the beverage industry MF membranes are used to sterilize beer and wines and also to clear fruit juices. MF is also used in separation of bacteria from water (biological wastewater treatment), separation of oil/ water emulsions, pre-treatment of water for NF or RO. MF removes micron-sized entities like cells, colloids, some bacteria and suspended solids. It however does not remove ions, viruses and low molecular weight organics (Figure 2.2).

2.3.2 Ultrafiltration (UF)

Ultrafiltration (UF) is a selective fractionation process utilizing pressures up to 1 bar. In UF, suspended solids and solutes of molecular weight greater than 1,000 are concentrated. The UF membrane pore diameters are in the range 10^{-3} -10 μm. The permeate contains low-molecular-weight organic solutes and salts. UF is widely used in the fractionation of milk and whey, and also finds application in protein fractionation. It is also used in the textile [9] and metal industry (oil/ water emulsions separation and paint treatment).10-13 These membranes are usually made from cellulose acetate (CA) and crosslinked polyamide. CA ultrafiltration membranes are resistant to chlorine and oxidation.1 They are also inexpensive when compared to those made from polyamide. CA ultrafiltration membranes are however limited due to their susceptibility to hydrolysis and biological attachment. The advantages of polyamide on the other hand include high fluxes and salt rejections. Polyamide UF membranes also have a wide temperature and pH tolerance compared to CA membranes. The major drawbacks of polyamide membranes include their reduced resistance to chlorine and increased susceptibility to oxidation.1

2.3.3 Nanofiltration (NF)

Nanofiltration (NF), which emerged in the mid-1980s, is a pressure driven process that represents the transition between ultrafiltration (UF) and reverse osmosis (RO).[14] Many separation problems can be solved economically by nanofiltration alone or in combination with other separation processes. For this reason, NF has been widely applied in many industrial fields, such as food and pharmaceutical industries,[15] textile wastewater reuse[16]and the regeneration of pulp and paper wastewater.[17] NF has also demonstrated efficient removal of dyes and colour [18-20] Nanofiltration can also be used to perform

separation applications that are not otherwise economically feasible for NF and RO, such as demineralization, colour removal, softening and desalination.[21] As illustrated in Figure 2.2, on top of the molecules which can be removed by MF and UF, NF membranes remove all multivalent ions and amino acids.[22, 23] However, the permeate in NF membranes contains monovalent ions and low-molecular-weight organic solutes like alcohols. One of the major drawbacks in NF membranes is the lack of reproducibility of the membrane pore size and pore size distribution.[1]

2.3.4 Reverse osmosis (RO)

The first membrane to be discovered was an osmosis membrane by Nollet in the 16th century. This then shows that the concepts of osmosis and reverse osmosis (RO) have been around for centuries. A lot of research was done on these membranes over the following centuries.[1]From these studies came what can be referred to as one of the largest milestones in membrane technology to date, which is the development of cellulose acetate (CA) membranes in the 1950's. CA membranes later made RO a commercial reality and also grew the membrane filtration industry enormously over the past 60 years. RO is a high-pressure technique and has been used in the concentration of low-molecular-weight substances in solution and in the purification of wastewater. Another major application of RO is in the desalination of seawater.[24-27] It has the capability to remove almost all water pollutants including monovalent ions (Figure 2.2).

RO systems can be used to remove both organic and inorganic pollutants simultaneously.[28] They also allow recovery of waste process streams without affecting the material being recovered.[28] As illustrated in Figure 2.2, RO removes not only particulate matter but also mineral ions from water.[5] This becomes a drawback in cases where people do not have access to adequate diets and depend on water to get necessary minerals like calcium.

2.4 Membrane materials

Membranes may be composed of natural, e.g. cellulose acetate (CA) or synthetic materials. Synthetic membrane materials include organic and inorganic materials such as organic and homogenous films, homogenous films (polymers), heterogeneous solids (polymeric mixes and mixed glasses) and liquids. Currently most commercial membranes are made from polymeric materials.[29] To be used as membrane materials, these polymers should demonstrate thermal stability over a wide range of temperatures and chemical stability over a wide pH range.[29, 30] They should also possess good mechanical strength, be good film formers, manage high permeate flows, have high selectivity, have good chemical and bacteriological resistance, be resistant to detergents and disinfectants and also be inexpensive. Early commercial membranes were based on cellulose acetate (CA) and polysulfone.[2, 29, 31] Nowadays, the number of polymers being used in membrane materials has increased considerably.

Polymers such as polyethersulfone, polyacrylonitrile, polyvinylidine fluoride, polycarbonate, polyamide and polyetherimide among others have been used in making membrane materials.[32]

2.5 Membrane systems

Membrane systems for water treatment are found in either dead end or cross flow configurations. In the dead end system, the feed suspension flows perpendicularly to the membrane surface. The feed is pressure driven through the membrane as shown in Figure 2.3 A. This can cause flux decline over time and the membrane needs to be frequently cleaned. On the other hand, in crossflow filtration, the feed suspension flows tangentially to the membrane surface.[33, 34] The feed water is reused and during recirculation, the feed water flows in a direction parallel to the membrane. Only little of the feed water is used for permeate while the other will leave the module.[33] Figure 2.3 B shows the cross-flow filtration system. Cross-flow filtration has a high energy cost. The feed water flows at a relatively high speed to minimise fouling and consequentially to the flow speed of the water. The high speed also enables the suspended solids to be carried away in the water flow. This system can achieve stable fluxes but cleaning process is still needed from time to time. This system is applied for RO, NF, UF and MF.[34]

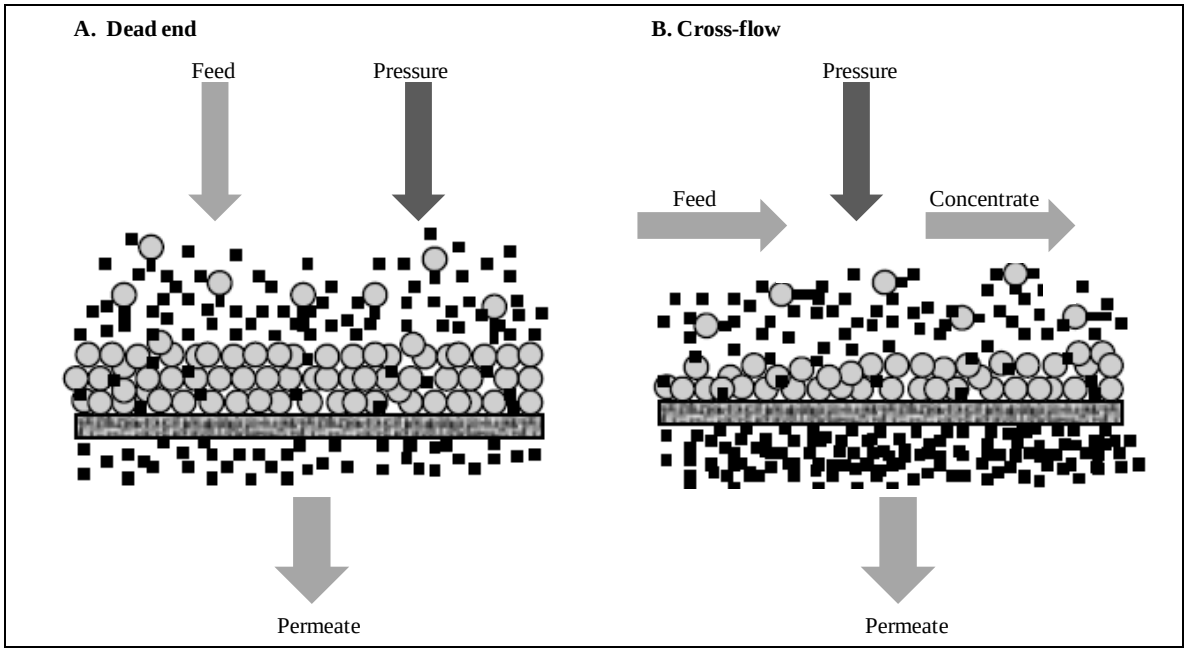

Figure 2.4: Dead end (A) and cross-flow (B) filtration systems.[34]

2.6 Membrane modules

The interest in membrane separation processes that began in the 1960s (Table 2.2) was prompted by two developments. Firstly the ability to produce high permeate fluxes and secondly the ability to form these membranes into compact, high surface area, economical membrane modules. Membrane media

are generally manufactured as flat sheets or as hollow fibres and then configured into membrane modules.[32]The common membrane modules used in filtration systems are spiral wound, plate and frame, tubular, hollow fibre and capillary modules. Packing density, membrane change (replacement), energy requirement, fouling control and cleaning are the important module characteristics for filtration membranes.[35] The following subsections discuss the various membrane modules, their applications as well as advantages and disadvantages of each one of them.

2.6.1 Plate and frame

Plate-and-frame modules were among the earliest types of membrane systems having been developed in the early 19th century.[36] Its design as illustrated in Figure 2.5, has its origin in the conventional filter press-concept. The feed solution is pressurized in the module and forced across the surface of the membrane. The permeate leaves the module through a permeate channel in a central tube. Plate and frame membranes flourished in the dairy industry for a long time. However, lack of improvements on the design coupled with inflexible prices more or less killed the design between 1989 and 1995.[32] These modules are now mostly used as laboratory test units and their industrial scale usage has drastically subsided. A limited number of RO and UF applications with highly fouling feeds also make use of plate and frame membrane modules. These units, however, are expensive and the exchange of the membranes is labor intensive and leaks through the gaskets required for each plate are a serious problem.[37]

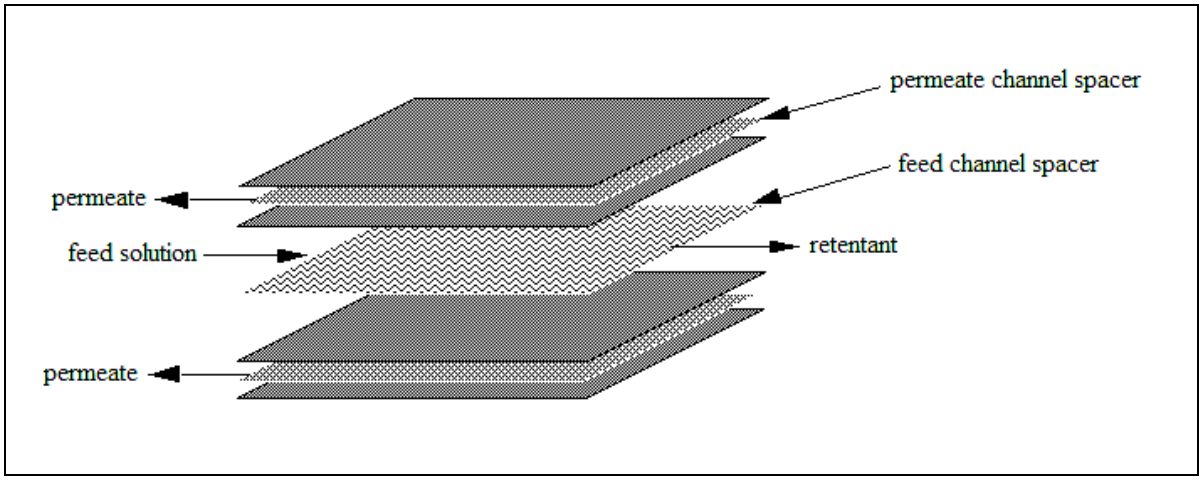

Figure 2.5: Schematic drawing illustrating the concept of a plate-and-frame membrane. [37]

2.6.2 Spiral wound

A variation of the basic plate-and-frame concept is the spiral-wound module (Figure 2.6). This design was initially made specifically for desalination of water, but it ended up attracting other industries because of its compact and low cost design.[32] To date spiral wound membrane modules are widely used today in reverse osmosis, and gas separation processes. Its basic design is illustrated in Figure 2.5. The design of a spiral wound membrane consists of membrane envelopes (leaves) and feed

spacers which wound around a perforated central collection tube. These modules were designed in an effort to pack as much membrane surface as possible into a given volume.[38, 39] Small scale spiral wound modules consist of a single membrane leaf wrapped around the collection tube. In the large membrane area module, using single membrane leaf might generate large pressure drop due to the longer path taken by the permeate to reach the central collection tube. Multiple short leaves have been utilized to keep the pressure in the module in a manageable level.[39] Spiral-wound modules were used in a number of early artificial kidney designs, but were fully developed for industrial membrane separations. While spiral wound modules are most common and standardized, there may be some limitations for highly polluted waters.

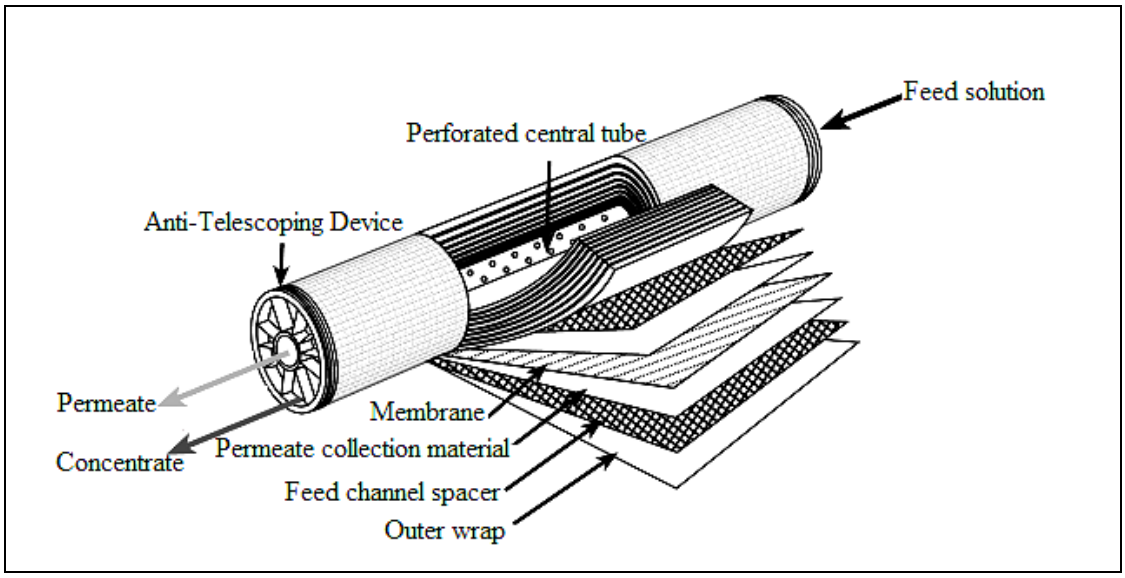

Figure 2.6: Spiral wound membrane module.[32]

2.6.3 Tubular

While the previously described two membrane module types required flat sheet membrane material for their preparation, special membrane configurations are needed for the preparation of the tubular, capillary, and hollow fibre modules. Tubular membranes are usually made from stainless steel and PVC although some have also been produced from CA, PVDF, ceramic, PSO and thin films.[32] A schematic of the tubular module design is given in Figure 2.7.Tubular modules have a high resistance to fouling due to good fluid hydrodynamics.[2] Plugging of the membrane module is avoided even with feed solutions that have very high concentration of solid matter and thus high viscosity. [35] The disadvantage of the tubular module design is the low surface area, that can be installed in a given unit volume, and the very high costs. Therefore, tubular membrane modules are generally only applied in applications where feed solutions with high solid content and high viscosity have to be treated and other module concepts fail due to membrane fouling and module plugging. This is the case in certain applications in the food and pharmaceutical industries and in the treatment of certain industrial

effluents.[37] Research institutions also love tubular membrane modules because they make it simpler to calculate the Reynolds number and to make theories about mass transfer coefficients.

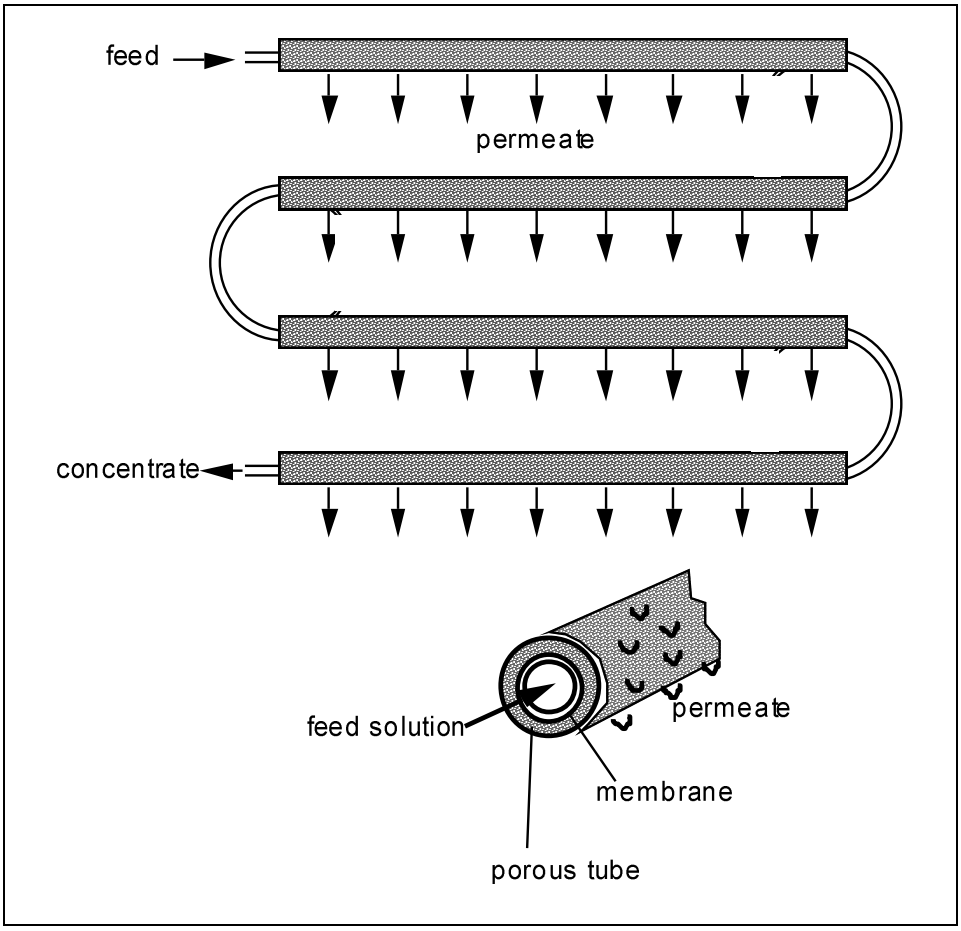

Figure 2.7: **Schematic of the tubular module.**[37]

2.6.4 The capillary membrane module

The capillary membrane module, which is shown schematically in Figure 2.8, consists of a large number of membrane capillaries. These are arranged in parallel as a bundle in a shell tube and both ends are potted into a head plate.[37, 40] The feed solution is passed down the center of the membrane capillary and the filtrate, which permeates the capillary wall and is collected in the shell tube.[37] The capillary membrane module provides a high membrane area per module volume.[40] The production costs are very low and concentration polarization and membrane fouling can effectively be controlled by the proper feed flow and back-flushing of the permeate in certain time intervals. The main disadvantage of the capillary membrane module is the required low operating pressure.[37] Because of the limited stability of the capillary membranes operating pressures generally can not exceed 4 to 6 bars.[37] Therefore, the capillary membrane is used in applications where low trans-membrane pressures are applied, such as in dialysis, microfiltration, and low pressure ultrafiltration. The most significant application of the capillary membrane module is an artificial kidney. The capillary membrane module

is the most appropriate configuration in the applications on a commercial scale since it is both compact and easily manufactured.

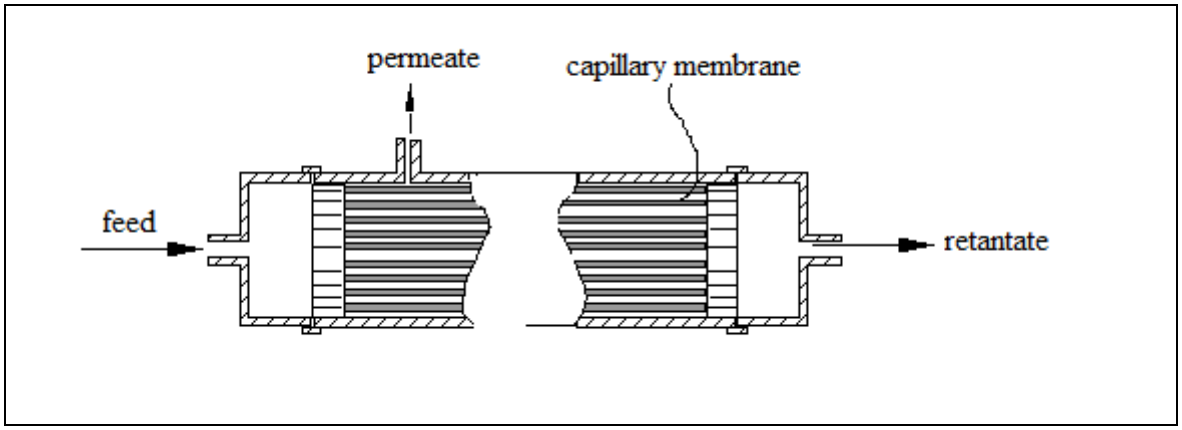

Figure 2.8: Schematic diagram showing a capillary membrane module.[37]

2.6.5 The hollow fibre membrane module

Hollow fibre membranes are prepared the same way as tubular and capillary module. They have an outer diameter of 50 to 100 µm. In hollow fibre membranes, the selective layer is on the outside of the fibres, which are installed as a bundle of several thousand fibres in a half loop with the free ends potted with an epoxy resin in a pressure tube as indicated in Figure 2.9. The filtrate passes through the fibre walls and flows up the bore to the open end of the fibres at the epoxy head.[37] The hollow fibre membrane module has the highest packing density of all module types available on the market today.[37] Its production is very cost effective and hollow fibre membrane modules can be operated at pressures in excess of 100 bars. The main disadvantage of the hollow fibre membrane module is the difficult control of concentration polarization and membrane fouling. When operated with liquid solutions the modules do not tolerate materials that may easily precipitate at the membrane surface. Therefore, an extensive pretreatment is required when hollow fibre membranes are used for the treatment of liquid mixtures. The main application of the hollow fibre module today is in reverse osmosis desalination of sea water and in gas separation. Both applications require high operating pressures and low cost membranes which have a long useful life. In reverse osmosis, of sea water an extensive pretreatment of the sea water is required.

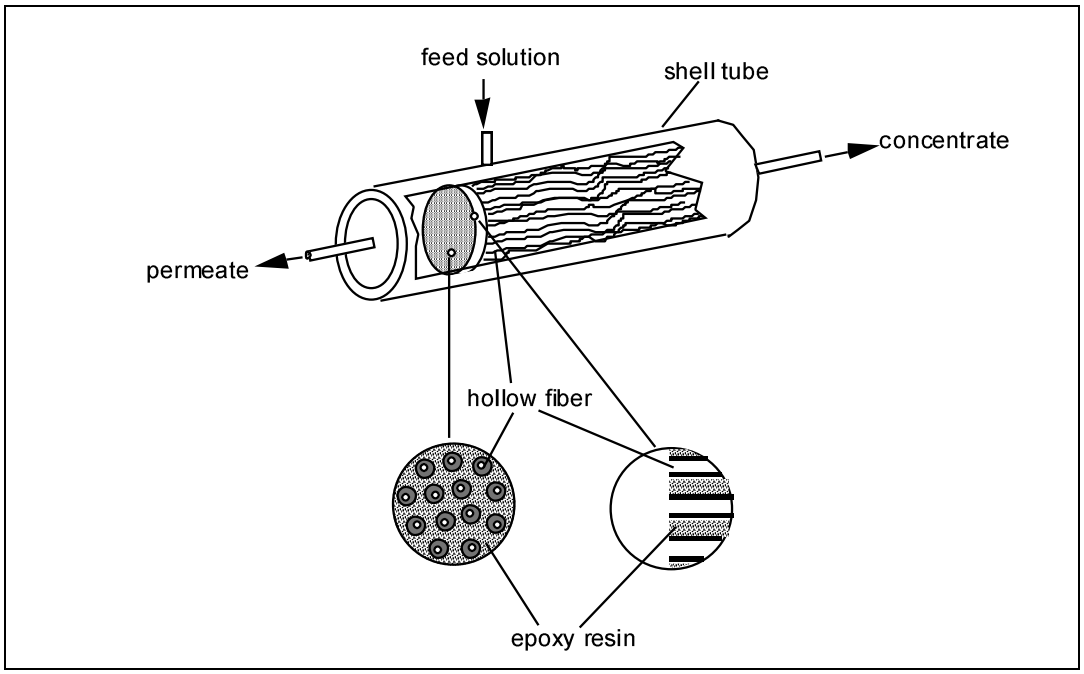

Figure 2.9: Schematic drawing illustrating the hollow fibre module.[37]

2.7 Membrane fouling

Membrane fouling can be defined as the reduction of permeate flux through the membrane, as a result of increased flow resistance due to concentration polarization, pore blocking and cake formation. Various factors, such as membrane pore size, membrane material, solute loading and size distribution, and operational conditions, influence the effect of each fouling mechanism on the flux decline.[41] Membrane fouling is the most serious problem affecting system performance and becomes the bottleneck of its development.[42] The immediate effect of fouling on membranes is a reduction in permeate flux, due to reduction in pore diameters. Long term fouling can result in irreversible fouling causing the reduction of the membrane lifetime.[43] Sources of membrane fouling can be subdivided into four principal categories as highlighted in Table 2.3.[44, 45] This subdivision among the fouling components is however only an operational definition and different types of fouling often occur simultaneously and may interact.[46] This work focuses on membrane biofouling, which can be defined as the accumulation of microorganisms such as bacteria, fungi and algae on the membrane surfaces, with the subsequent formation of harmful biofilms and operational problems.[47]

Table 2.3: Types of fouling

Type	**Causes**
Scaling/inorganic	Precipitation of inorganic salts
Silting	Suspended particulates such as organic colloids, corrosion products, precipitated iron hydroxide
Biofouling	attachment of microorganisms on membrane surfaces
Organic fouling	Attachment of organic materials such as oil or grease on membrane surfaces

2.7.1 Membrane biofouling

Microbial growth during membrane separation processes is a constant concern, especially in aqueous streams which provide optimum conditions for the growth of microorganisms.[48] In the natural setting, most bacterial mass exist in biofilms and attached on surfaces.[49] There are a number of reasons associated with this and they include the fact that nutrients tend to adsorb on the surfaces making these surfaces nutrient rich. Adhesion also protects the microorganisms from being swept into unfavorable conditions. Additionally, in the biofilm state, the microorganisms are less prone to being attacked by antibiotics.[49] A lot of research has been dedicated to study the mechanisms of bacterial attachment to surfaces and biofilm formation leading to biofouling. Apart from hydrophobic interaction between bacteria and membrane polymers, researchers have also suggested that extracellular polymeric substances (EPS) secreted by the bacteria play a vital role in strengthening bacterial attachment and biofilm formation on membranes.[50] A biofilm can be defined as a community of bacteria, algae, fungi and protozoa encapsulated in a matrix consisting of a mixture of polysaccharides, generally referred to as extracellular polymeric substance (EPS).[51] Some of the main factors influencing biofilm growth are, cell surface hydrophobicity, the presence of fimbriae and flagella and the degree of EPS production. According to Vu and co-workers, there are three types of forces which contribute to the overall stability of biofilm matrices and these are electrostatic interactions, hydrogen bonds and London dispersion forces.[51]

2.7.2 The process of biofouling

Although a variety of environmental signals including temperature, pH, iron availability and oxygen tension, can trigger the development of microorganisms from planktonic growth to biofilm mode.[52] The stages of biofilm development appear to be conserved among a wide range of bacteria.[53] According to Flemming and Schaule, the process of biofouling can be divided into several phases.[54] To fully understand the biofouling process, one has to consider a system of three components: bacteria, surface and liquid. Figure 2.10 illustrates the processes from primary colonization on a membrane surface to the time of full biofilm maturation. The presence of organic matter facilitates the formation of a conditioning film of adsorbed components on the membrane surface prior to microbial invasion. Microorganisms are transported to the surface through sedimentation, active transport and diffusion. This marks the beginning of the biofouling mechanism. Initial microbial adhesion takes place when planktonic cells come into contact with surfaces, the production of EPS and unfolding cell surface structures strengthen this process.[55] Growth and metabolism of the attached cells continue with EPS production and film development also takes place. This is possible due to a process known as quorum sensing, this is merely a communication between the cells. As the number of cells in the biofilms increase, there is a decline in the growth rates as a result of nutrient and oxygen limitations coupled with an increase in levels of organic acids. This eventually leads to stationary biofilm development where adhesion and growth counterbalance detachment.[56] The growing biofilm can then

spread to uncolonised areas or cells can detach from the biofilm and re-enter the planktonic mode of growth, and repeat the cycle all over again.[57, 58]

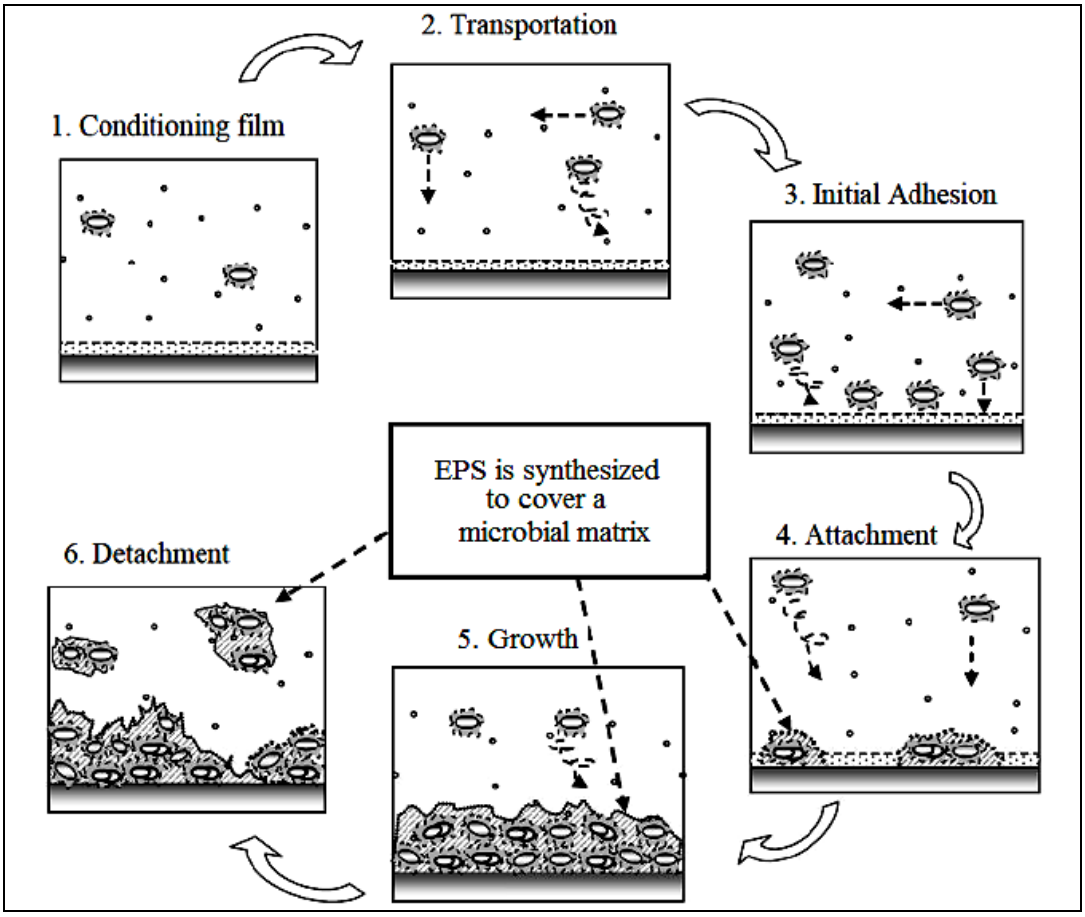

Figure 2.10: Sequential stages in biofilm formation.[56]

2.7.3 Problems caused by biofouling

All industrial systems with the exception of those operating under sterile conditions are susceptible to biofilm formation.[59, 60] This causes hygienic and functional problems to many types of devices and equipment, resulting in significant financial losses worldwide, annually. Metals and their alloys are very susceptible to microbial colonization resulting in corrosion, fouling and ultimately material failure.[61, 62] Interactions between metal surfaces, abiotic corrosion products and the diverse microbial populations and their metabolites result in biocorrosion.[63] These interactions can take place in diverse environments that vary in temperatures, nutrient content, pH and pressure and is not limited to submerged conditions but also takes place in humid conditions.[59] One of the major challenges in drinking water systems is the maintenance of the hygienic and aesthetic quality of water while it is being transported.[64, 65] The development of biofilms in water transport systems is mainly due to the traces of nutrients present in the water supply[65] and the right conditions (temperature, pH etc) for growth.[66]

Biofouling on membrane systems can result in the decline in membrane flux due to the formation of a film of low permeability on the membrane surface. It can also cause biodegradation of the membrane, which is as a result of acidic by-products produced by microorganisms concentrated at the membrane surface and which cause damage to the membrane.[67] Biofouling in RO membrane systems reduces the turbulent flow which in turn leads to the accumulation of dissolved ions at the membrane surface, increasing the degree of concentration polarization. This increases the passage of salt through the membrane and reduces the quality of the water product.[44, 67]

Additionally, biofouling increases the differential pressure and feed pressure. This is because formation of biofilms lowers the permeability of the membrane and the differential and feed pressure has to be increased in order to maintain the same production rate. If the operating pressure exceeds the manufacturer recommendations, the membrane element can be damaged. Energy requirements increase due to the higher pressure requirements.[67] Table 2.4 highlights some of the detrimental effects of biofouling on surfaces in other industries other than drinking water pipelines.

Table 2.4: Biofouling occurrences in different industrial systems.

Industry	**Problem**	**References**
Cooling towers and heat exchangers	Inhibits heat transfer by cohesive transport thus decreasing heat exchanger efficiency.	58, 68-71
Food and milk industry	Spoilage of food products, hygienic problems, cross-contamination, post-processing contamination, corrosion of equipment, obstruction of pipelines and equipment down-time.	72-74
Paper mills	Corrosion of the paper mill surfaces, the reduction of water flow in pipelines, production of explosive gasses such as methane, blockage of filters, valves and nozzles and financial losses due to equipment downtime. It also can cause paper defects such as stains and holes and leads to bad odours on the paper and in the mill.	75-78
Clinical industry	Biofilm forming bacteria are very resistant to antibiotics compared to planktonic ones. They are also responsible for serious problems like clinical biofilm infections, growth on surgical implants, catheters and other medical devices. Antibodies can not recognise the bacteria in biofilms which makes it hard to control them.	76, 79-84 82, 85-89

2.8 Biofouling control and cleaning

To start with, it is necessary to state that there is some confusion in the literature between the words 'clean' and 'control'. In general, the former refers to off-line removal of deposits, whereas 'control' refers to attempts to prevent or restrict deposit formation.[58] Evidence of biofilm control technologies has been available for centuries with the most significant ones being, the discovery of chlorine as a disinfectant in 1810 and its application in water treatment in 1902 (Belgium).[90] Important milestones in water treatment are outlined in Table 2.5.

Table 2.5: Major milestones in water treatment.[90]

Year	Milestone (s)
1804	First municipal water treatment plant (Scotland, sand filtering technology)
1810	Discovery of chlorine as a disinfectant (H. Davy)
1852	Formulation of the metropolis water act (London)
1879	Formulation of the germ theory (L. Pasteur)
1902	Use of chlorine (calcium hypochlorite) as a disinfectant in water (Belgium)
1906	Use of ozone as disinfectant (France)
1908	Use of chlorine (calcium hypochlorite) as a disinfectant in municipal water supply (New Jersey, USA)
1914	Federal regulation of drinking water supply
1916	Use of UV in municipal water supply
1935	Discovery of synthetic ion exchange resin (B.A. Adams, E.L. Holmes)
1965	World's first reverse osmosis plant launched
1974	First reports on role of carcinogenic by-products of water disinfection with chlorine Formulation of the Safe Drinking Water Act (United States Environmental Protection Agency)
1975	Development of carbon black for drinking water purification
1998	Drinking water directive applied in EU
2000	Adoption of the Millennium Declaration during the UN millennium summit
2007	Launch of noble metal nanoparticle-based domestic water purifier. (T. Pradeep, A.S. Nair, Eureka Forbes)

2.8.1 Biofilm control

Due to economic losses associated with the deleterious effects of biofouling, different methods have been used for minimizing the accumulation of biofilms on surfaces. Biofilm control agents typically include oxidizing biocides which inactivate or inhibit biofilm forming bacteria, mechanical methods that displace the biofilm biomass and use of dispersing agents, surfactants or chelating agents that are aimed at destabilizing the biofilm structure.[61, 91-93] The sequence of events that leads to the accumulation of biofilm may influence the method of control that is adopted. For example, if deposition of microorganisms is the primary factor in the development of a biofilm, it would be important to concentrate the control technology in the liquid phase. On the other hand, if it is reproduction and growth of the biofilm itself that is the essence of the problem, it would be imperative that this is where the control technique should be applied. Thus, biofouling control can be done either chemically or physically.[58]

2.8.1.1 Chemical control of biofouling

The use of chemicals to control microbial activity has been employed for many years but particularly over the recent past, considerable research has been carried out in the development of improved techniques to meet the changing needs of industry and society at large.[58, 69] The term biocide is often loosely used to include all chemicals that are employed to control biofilm formation and growth. The word ‘biocide’ is derived from the Latin ‘bio’ (which means life) and ‘cida’ (which means killer). In strict terms therefore, ‘biocide’ refers to a substance that is toxic to microbial life forms.[58]

Chemical control technology may be grouped into three broad sectors, i.e. biocides that kill microorganisms, biostats that interfere with metabolism and surface active agents that restrict adhesion to surfaces. The interactions of biocides with microorganisms can also be considered to be as a result of a sequence of three events which are; (i) absorption on the cell wall; (ii) penetration of the biocide into the cell and ultimately (iii) damage to the cell structure and its functions leading to cell lysis. Chemical biocides can be divided into oxidising and non-oxidizing. The different ways in which biocides can affect microorganisms are summarized in Table 2.6.

Table 2.6: Damaging effects of biocides [58, 94]

Target	Damaging effect	Result
Wall	• Abnormal morphology and construction. Initiation of autolysis.	• Lysis (cell death)
Membrane	• Inhibition of membrane • Increase in permeability of some ions. • Loss of structural integrity	• Restriction of respiratory chain and energy transfer. • Interference with normal chemical activity • Leakage of intercellular material. Initiation of lysis.

[1] Oxidizing biocides

Oxidizing biocides include chlorine,[95, 96] chlorine dioxide,[97] bromine,[98, 99] iodine,[58]hydrogen peroxide[92, 100]and ozone[10, 99]to mention but a few. These biocides target the thiol group present in polypeptides and this consequently result in the oxidation of various proteins, carbohydrates, lipids and nucleic acids.[91, 101, 102] These reactions lead to the loss of cell structure and the loss of the essential functions of these compounds, including unfolding, fragmentation and cross reaction with oxidized groups. The loss of coherent structure and function is sufficient to produce loss of viability.[58]

Chlorine is the most reported oxidizing biocide and has been used effectively for many years. The usual application has been in connection with cooling water particularly in electric power production. When chlorine comes into contact with water, it hydrates to form hypochlorous and hydrochloric acids.[58] Hypochlorous acid is a powerful oxidising agent, which has the ability to diffuse through the cell wall of microorganisms to react with the cytoplasm. This produces chemically stable nitrogen-chlorine bonds with cell proteins resulting in cell death. Hypochlorite ion is much less effective.

The use of chlorine as a biocide for many years has created a wide range of experience in its use for many different applications.[103] However, the use of chlorine has diminished in recent times due to increasing legislation in respect of chlorine use and public opinion against its continued application where chlorinated water is discharged to the environment. This has stimulated interest in alternative biocides that do not present environmental hazards. Many such biocides have been developed and marketed over the last few years. Ozone use has been explored and found more effective than chlorine.[76, 93, 104] However, it is more expensive and has a short lifespan.[10] Other oxidizing biocides such as bromine and hydrogen peroxide are not as effective in removing bacteria.[105]

[2] Non oxidizing biocides

Non oxidizing biocides include aldehydes,[76] quaternary ammonium compounds,[106] isothiazolones,[107] organosulphers[58] and detachment promoting agents like surfactants.[108, 109] Toxic organic and inorganic

metal compounds may also be classified as non-oxidising biocides.[58] These disturb bacterial cell wall permeability and interfere with the respiration and metabolic activity in bacterial cells.[110] Of these, isothiazolones have been used in a number of industrial water treatment systems for biofilm control.[107] Non oxidising biocides are usually not manufactured with the aim of biofilm removal and there are several problems associated with their use.[96] Bacteria also develop some resistance against them which reduces biocidal efficiency with every subsequent treatment.[111]

The use of coagulants and surfactants has been reported largely in literature. AlMalack and Anderson reported that the addition of coagulants can cause the molecules or particles to form larger particles which are readily swept off the membrane surface.[112] They explored the effect of using alum, polyaluminium silicate sulphate and lime as coagulants. Using these coagulants enhanced the crossflow of domestic wastewater through a woven polyester membrane.[112] A 1.5 fold initial and a 2 fold long term flux increase were obtained with coagulant over those without coagulant. The improvement of crossflow microfiltration with addition of coagulants was also reported by other researchers.[113-116]

Jonsson investigated the effect of different surfactants on ultrafiltration membranes.[117] Triton X-100, potassium oleate and hexadecyltrimethylammonium bromide which are nonionic, anionic and cationic surfactants respectively were used in these experiments. The membranes polysulfone (PSF) and poly(vinylidene) fluoride (PVDF) were used. The flux reductions of the hydrophobic membranes were higher than the flux variations of the hydrophilic membranes. Styrene divinyl benzene based ion exchange membranes were also modified for electrodialysis of aqueous solutions with high molecular mass surfactants. The filtration results showed that no membrane fouling occurred in the presence of humic acid and dodecylbenzenesulphonate.[118]

2.8.1.2 Physical methods of controlling biofouling

The use of physical methods in controlling biofouling eliminate the use of chemicals and thus avoiding potential problems associated with their use, such as cost and environmental hazards. An additional incentive to investigate the opportunities of physical control is the possibility of increased and stricter legislation concerning the development and use of biocides.

[1] Backflushing and backwashing

One of the earliest techniques to combat the accumulation of microorganisms on the surfaces of industrial process equipment is reversal of flow.[58] Backflushing, which is also referred to as periodic reverse filtration back through the membrane, has been widely applied in the control of membrane fouling. Backflushing in a crossflow microfiltration unit recorded up to 3-fold higher fluxes than in a case where there was no backflushing.[119] A combination of backflushing and relaxation was also used to mitigate fouling in a membrane bioreactor, this resulted in even improved flux increases.[120]

[2] Pulsing

Pulsed flow is another relatively simple method used to control biofouling.[58] The associated rapid changes in velocity impose removal forces on the biofilm. A difficulty however, is to ensure that the changes in velocity are rapid enough to be effective. Over relatively long distances therefore, the effectiveness is likely to be reduced. Backpulsing has also attracted a lot of interest among researchers in recent years. [121-124] Backpulsing can be defined as a variation of backflushing in which the back pressure is applied in an extremely rapid pulse (pulse duration generally less than a second) every few seconds throughout the process.[125] This reversal results in hydraulic cleaning of the membrane by forcing permeate back through the membrane in the reverse direction. Foulants are lifted off the membrane by the backpulses and then swept to the filter exit by crossflow. Crossflow filtration with rapid backpulsing has been studied extensively and has been reported as an effective technology for controlling fouling and improving permeate flux for non adhesive foulants exhibiting reversible fouling.[121-124] Up to 25 times permeate flux improvement was reported by Ramirez and Davis for filtration of dilute oil-in-water dispersions.[126]

Periodic gas backpulsing, also known by other researchers as gas injection is another method that has been extensively explored by researchers in the past two decades.[127-130] This technique combines backpulsing with periodic gas injection into the feed stream to enhance membrane flux in crossflow microfiltration experiments. The injected gas forms complex hydrodynamic conditions inside the MF module which increases the wall shear stress. This then prevents membrane fouling and enhances MF mass transfer.[58] Using this technique has been reported to result in up to 5-fold improvements in permeate flux. Periodic gas backpulsing however, can not work in the case of a membrane whose fouling is not exclusively on the surface of the membrane.[128, 131]

[3] Ultrasonic waves

The use of ultrasonic waves has been reported to reduce fouling caused by natural organic matter and subsequently by bacteria. Studies carried out using an ultrasonic probe system to prevent fouling of ceramic membranes with polypropylene support rings reported an increased permeate flux by up to 4-fold when compared to the system without the ultrasound.[132] The ultrasound process also had no negative impact on the membrane in the sense that even after several repetitions of the process, the membrane surface was not damaged. Matsumoto obtained four to six times higher steady state flux than that without ultrasonic waves.[133]

[4] Crossflushing

Crossflushing is another method of reducing/ removing foulants in membrane systems. It is however a much weaker cleaning technique than backpulsing or backflushing. It involves periodic stoppage of permeate flow while maintaining crossflow over the membrane surface. In the absence of permeate

flow, the cake layer may be partially removed by the crossflow. This removal increases the subsequent permeate flux .[125, 134] Crossflushing to increase permeate flux in crossflow microfiltration experiments using yeast as a foulant was reported.[134, 135] Crossflushing was accomplished by maintaining flow over the membrane while periodically stopping the permeate flow, thereby eliminating the pressure drop across the membrane and allowing the shear exerted by the crossflow to erode the foulant layer. Crossflushing has also been reported to improve the effectiveness of backwashing.[136]

[5] Coating of Surfaces

The adhesion of microorganisms to surfaces is affected by the quality of the surface both in terms of its physicochemical properties and the roughness of the surface. Both these characteristics can be modified by the application of a suitable coating but surface modification by coating is a relatively modern technology. It is particularly relevant to the control of biofouling. The use of polymer based antimicrobial coatings e.g. polytetrafluoroethylene (PTFE), to control biofilms in industrial settings is on the rise. Permeation studies reveal an increase in hydrophilicity and hence flux which then decreases fouling in coated membranes.[137] Although most of the research in this area especially for application in the water industry is still in the developmental stage, major milestones on its effectivity have been reached. Most researchers have introduced antimicrobial properties either by direct sputtering of antimicrobial agents on surfaces or by surface-tethering.[138, 139] Titanium and silver-based coatings have been largely explored and in most cases resulted in massive decrease in fouling intensities.[138, 140] Surface-tethering using coatings has also been explored and satisfactory reductions in biofouling on membranes has been achieved.[140] The use of polymer based coatings, e.g. could facilitate application of the technology. It has to be appreciated however, that a surface treatment may be vulnerable to mechanical off-line cleaning procedures. Dickson developed an interfacial polymerization technique to coat the internal surface of a polypropylene (PP) membrane.[137]

[6] Surface modification

Microfiltration and ultrafiltration membranes are usually made from structurally rigid polymers in order to withstand chemical treatment and elevated temperatures during cleaning, but their pronounced hydrophobicity typically encourages solute adsorption.[141] Moreover, the interfacial characteristics of membranes can rarely be achieved by bulk modifications of the membrane forming polymer without complicating the membrane fabrication processes. It is generally acknowledged that hydrophilic surfaces do not adsorb proteins and other foulants to the same degree as do hydrophobic surfaces.[142-144] According to Norde, at constant temperature and pressure, irrespective of the mechanism, particle-surface interactions are determined by changes in the Gibbs energy, $\Delta_{ad} G$, of the system i.e. particles will adhere spontaneously if $\Delta_{ad} G < 0$. Factors which contribute to $\Delta_{ad} G$ include electrostatic, hydrophobic and dispersion forces. Steric forces also become contributers to $\Delta_{ad} G$ if the surfaces are soft and not rigid.[49] A lot of research has been done in this area and several functional groups with the

ability to inhibit non-specific adsorption of proteins from solutions can be grafted or incorporated into surfaces. These functional groups as reported by Ostuni exhibit the following characteristics; they are hydrophilic and include hydrogen-bond acceptors (no hydrogen-bond donors).[145] They also have a neutral overall electrical charge. A few studies where surfaces have been successfully modified by changing the membrane surface chemistry are discussed in the subsequent sections.

[i] Covalent binding of hydrophilic polymers on the membrane using heat curing; an example of this technique was a type of ultrafiltration membrane consisting of a polyethersulfone support membrane and a thin polyurea/polyurethane was prepared by surface coating of hydrophilic phase inversion membranes. It was found that the surface hydrophilicity of the membranes as well as flux were significantly enhanced.[146]

[ii] Grafting monomers to the membrane using electron-beam irradiation is another well referenced method for reducing fouling on membrane systems. Kim and co-workers introduced an alcoholic hydroxyl or diol group into a porous PE hollow fibre membrane by electron beam radiation-induced grafting of vinyl acetate followed by saponification or acid hydrolysis.[147] This hydrophilization significantly reduced fouling of the PE membrane. Another electron beam induced membrane surface modification was reported by Keszler and his team who prepared asymmetric polyethersulfone ultrafiltration membranes and modified them using beam irradiation in various environments. Significant changes were observed in the modified membranes at certain combinations of experimental parameters, both water flux and solute retention were improved compared with the untreated membrane.[148] Grafting of surfaces using oligomers and polymer brushes also demonstrated protein inhibition on a study carried out by Norde.[49]

[iii] Lithiation chemistry has also been reported as an effective method for increasing the hydrophilicity of membrane systems and subsequently improving permeation flux.b In a study carried out by Guiver, PSF membranes were activated with a lithiating reagent and the lithiated intermediates were covered by the addition of suitable electrophiles. The introduction of hydrophilic groups enhanced water flux and decreased fouling.[149]

[iv] Photografting monomers onto the membrane using ultra violet irradiation has been reported by many researchers. [150-157] An example is a study whereby cellulose acetate (CA) membranes and polyamide membranes were modified using acrylamide and acrylic monomers respectively, followed by UV irradiation.[158] Ulbricht and co- workers also used a simultaneous UV grafting method for grafting acrylic acid (AA) onto polyacrylonitrile (PAN) ultrafiltration membranes and for grafting AA and 2-hydroxyethyl methacrylate (HEMA) onto PAN membranes.[157, 159, 160]

Hydrophobic PSF ultrafiltration membranes were also modified with UV irradiation and hydrophilicity increasing agents which resulted in flux increases of up to 400%.[161]

2.8.2 Cleaning

Cleaning as defined in Section 0 refers to off-line removal of biofilms deposits. Available cleaning techniques include manual cleaning, which may be carried out 'dry' or 'wet'. Manual cleaning is a relatively simple and familiar technique involving wiping, brushing, and scraping.[58] Because of its labour-intensive nature the cost of manual cleaning could be high. Another method used in cleaning biofouled membranes is jetting that may involve the use of high pressure water, air or steam lances. Access may be a difficulty with this method. Drilling and rodding is a possibility for tenacious deposits but this is not usually the case with biofouling. The drilling may be accompanied by the inclusion of compressed air or a water supply to take away the deposit. The technique is particularly relevant to the inside of tubular equipment, such as shell and tube heat exchangers.[58]

High temperature sterilisation or heat shock often referred to as 'steam soaking' is another method used in biofilm removal. It involves the admission of steam into the membrane to be cleaned which results in killing of the microorganisms and subsequent removal by water flushing. However, there is the possibility that large volumes of dead material and other debris may present difficulties of removal, thereby causing blockage, partial or complete, that may necessitate a shutdown of the process. Increased frequency of cleaning is most likely the best solution to overcome this particular problem. Osmotic shock that upsets the metabolic processes of the microorganisms and results in lysis of the cells, is a means of controlling biofouling but it may also be employed for cleaning purposes.[58]

2.9 Advances in membrane technology through nanotechnology

Nanotechnology is the discipline of manipulating matter at the nanoscale (1-100 nm), yielding nanoparticles or materials that often possess novel biological, physical or chemical properties.[162] Over the last two decades, a lot of progress progress has been made in the study and discovery of new organic and inorganic membranes. Many academic and industrial research projects in this area are underway. The use of nanostructured materials, such as mesoporous media, nanoparticles, carbon nanotubes and nanofibres in membrane systems has also increased.[163] Among these materials, nanofibres offer a number of attractive features compared to the other nanostructures.[164] Research and development of nanofibres has gained significant prominence in recent years due to the increased awareness of their ability to enhance performance of various filter media. Nanofibres have a high surface area which favous higher adsorption rate of various trace organics and bacteria for improving water quality. They also have higher acid/basic and temperature resistance. Additionally, nanofibres are environmentally friendly and have longer membrane life spans as well as possess a flexible

property which enables the membrane to be formed into various membrane modules for larger commercial applications.[165]

2.9.1 Production of nanofibres

There are a number of methods that can be used to produce nanofibres. These include, among others, drawing, template synthesis, phase separation, self assembly and electrospinning.[166] The choice of process for producing nanofibres is dependant on the the fibrous materials to be produced, the type of alignment needed, the production scale and investment cost. Table 2.7 highlights methods of fabricating nanofibres and gives advantages and disadvantages of each technique. The electrospinning process was used in this study for reasons well outlined in the following sections.

Table 2.7: Different methods of producing nanofibres.

Process	Description	Advantages	Disadvantages	References
Drawing	Similar to dry spinning in fibre industry.	Can make very long nanofibres.	Only a viscoelastic material can be used to make fibres	164, 167
Template synthesis	A nanoporous membrane is used as a template to make nanofibres of solid or hollow shape.	Nanofibres of various raw materials e.g. polymers, metals, semiconductors and carbons can be fabricated.	This method can not make continuous nanofibres.	164, 168
Phase separation	Consists of dissolution, gelation, and extraction using a different solvent, freezing, and drying resulting in nanoscale porous foam.	It is a relatively convenient process	The process takes relatively long period of time to transfer the solid polymer into the nano-porous form.	169
Self assembly	Individual, pre-existing components organize themselves into desired patterns and functions.	It is easy to manipulate.	Time-consuming in processing continuous polymer nanofibres.	170
Electrospinning	It uses electrostatic forces to produce continuous fibres.	Process can be upscaled.	Needs trained personnel to operate.	166

2.9.2 Electrospinning

Electrospinning (ES) has recieved the most attention not only because of its simplicity, but also because it can produce nanofibres composed of different materials. In the 1628, William Gilbert described the behaviour of the magnetic and electrostatic phenomena. In his experiments, he observed that when a suitable electrically charged piece of amber was brought in close proximity to a droplet of

water, a cone shape would form and small droplets would be jet out from the tip of the cone: this is the first recorded observation of electrospraying. Electrospinning as a process was first patented by J.F Cooley in February 1902 and by W.J. Morton in July 1902.[171] The behaviour of liquid droplets at the tip of metal capillaries was also reported by John Zeleny in 1914.[172] His effort began the attempt to mathematically model the behaviour of fluids under electrostatic forces. However, these formerly developed methods offered no feasible devices for collection of the produced threads, making them incapable for manufacture.[171]

Between 1934 and 1944 Formhals published a series of patents with innovative set-ups for the generation of polymeric fibres including the classic spinning setup with one spinneret, needle-less and multi-spinneret devices.[171] Drawbacks of these previous inventions were the incomplete drying and sticking of the fibres to each other due to the applied short distance between the spinneret and the collecting device as well as that no compact form of the fibre webs could be gained. Nevertheless, many of the recent electrospinning constructions can be traced back to these early inventions. Over the following decade, only few further investigations were pursued and electrospinning generally attracted very little attention. In the 1960s, Taylor studied the formation of a jet at the nozzle induced by the electrical field. He observed a deformation of the droplet at the end of the tip into a conical shape after application of the electrical field, now known as a Taylor cone.[173] Larrando and Mandley reported in 1981 the electrospinning of fibres from polymeric melts (polyethylene and polypropylene).[174] With increasing interest in nanotechnology and therewith arising application potential of nanofibres, the electrospinning technique has gained interest during the last decade. The real potential of electrospinning was demonstrated by the work of Doshi and Reneker.[175]

Nowadays, a wide variety of pure and blended, natural and synthetic, organic as well as inorganic polymers have already been successfully electrospun into fibres allowing the production of tailored nanofibrous webs for multiple applications, e.g. in filtration, catalysis, (bio-)medicine, protective or smart clothing, optical devices, membranes, sensors and as reinforcements in composite materials. ES has been demonstrated to be an extremely versatile technology able to produce fibres with diameters ranging from few nanometers to several microns, from over two hundred synthetic and natural polymers, in the form of plain fibres, blends and organic-inorganic composite fibres.[164, 176] Another advantage is the simplicity of the process that does not require any sophisticated and expensive equipment and that can be easily scaled-up for mass production.

2.9.2.1 The process of electrospinning

ES involves the application of a high voltage difference between a positively charged metallic needle, ejecting the polymeric solution, and a negatively charged grounded collector as shown in Figure 2.11. When the electrostatic force overcomes the cohesive force of the solution an electrically charged jet emerges from the capillary. The fluid jet is accelerated and stretched by the external electric field and

thins dramatically while travelling towards the collector (theory of jet modeling) leading to the formation of nanometer-sized fibres which are collected on the target as a non-woven fibre web. A summary of the parameters affecting the electrospinning process is given in Table 2.8.[171]

Table 2.8: Parameters affecting the process of electrospinning

Parameter	Examples
Process	electric field strength, feeding rate, needle geometry
System	concentration, viscosity, solvent, surface tension, conductivity, temperature
Environmental	humidity, temperature, air velocity

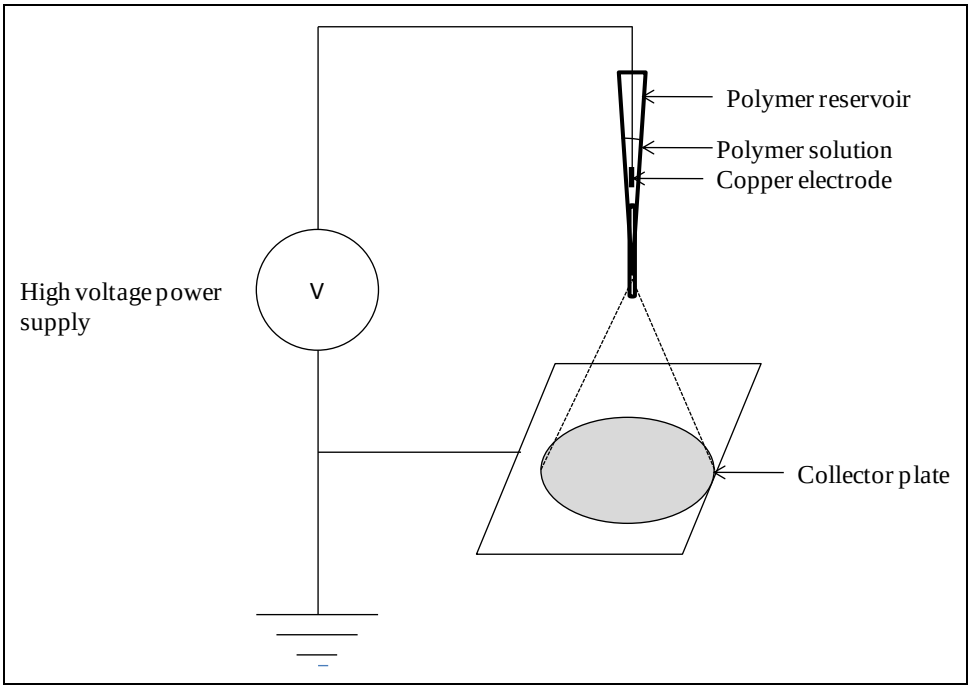

Figure 2.11: Basic ES set-up.

While the ES technique is very simple, the spinning mechanism is rather complicated due to the instabilities of the jet on its way to the collector. The theory behind these instabilities is known as jet modeling. The jet modeling mechanism generally takes place in three stages known as initiation, thinning and solidification of the jet.[171] Under the influence of a strong electrostatic field, charges are induced in the solution and the charged polymer is accelerated towards the grounded metal collector.[177] At low electrostatic field strength, the pendant drop emerging from the tip of the pipette becomes highly electrified and Coulomb forces are exerted from the external electric field, this marks the beginning of the initiation state. Inside the droplet, the surface tension minimizes the surface area and to hold the droplet form spherically. As the intensity of the electric field is increased, the induced charges on the liquid surface repel each other and create shear stresses. These repulsive forces act in a direction opposite to the surface tension which results in the extension of the pendant drop into a conical shape (Taylor cone) and serves as an initiating surface (Figure 2.12).[177, 178] When the critical

voltage is reached, the equilibrium of the forces is disturbed and a charged jet emanates from the tip of the conical drop.[177] While moving, the jet undergoes instability due to repulsing forces between the electrical charges inside the jet. This bending instability is mainly responsible for thinning of jet diameter into the nanometre scale.[171] The last stage which is jet solidification depends on the solvent vapour pressure and on the evaporation rate of the solvent as well as on the available time for the solvent to evaporate and is directly affected by the distance between spinneret and target.

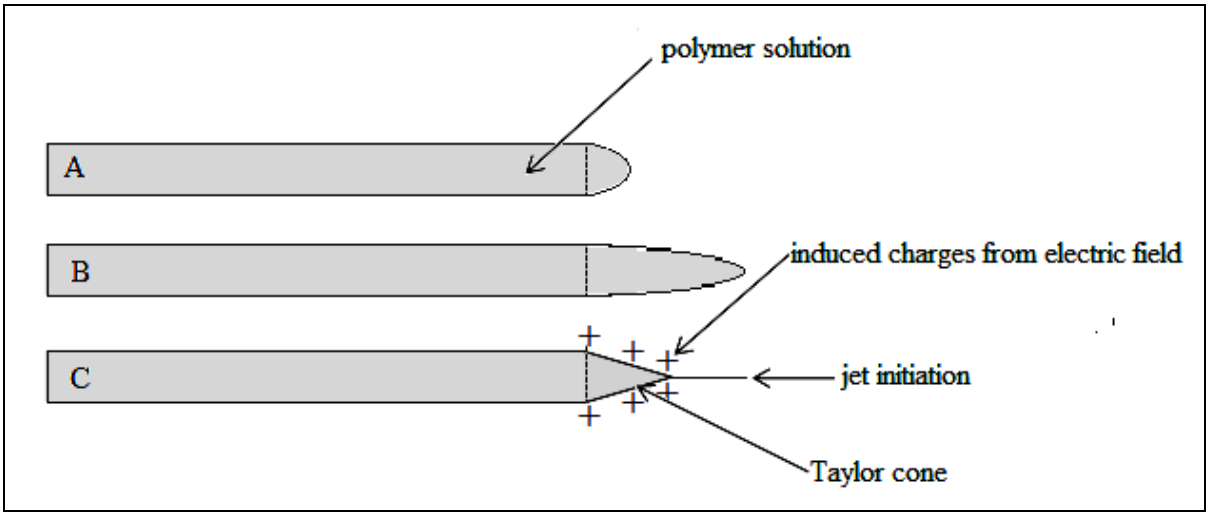

Figure 2.12: Taylor cone formation (A) Surface charges induced in the polymer solution due to the electric field. (B) Elongation of the pendant drop. (C) Deformation of the pendant drop to the form the Taylor cone due to the charge-charge repulsion. A fine jet initiates from the cone.[177]

2.9.3 Uses of electrospun nanofibres

The use of electrospun nanofibres for commercial filter media is widespread and has been around for many years. Advantages of electrospun filter media over more traditional filter media include the longer filter life, high filtration efficiency, ease to maintenance and lower weights for ease in didstribution.[164] Other applications of electrospun polymer nanofibres have been steadily increasing especially in recent years. According to the US patent records, most applications are in the field of filtration systems and medical prostheses. Other applications include tissue templates, electromagnetic shielding, composite delamination resistance, and liquid crystal devices.[164, 177]

A summary of these patent applications is shown in Figure 2.13 and the extended application areas are summarized in Figure 2.14. Most of these applications are still being investigated and developed, they have not reached the industry level as yet. Their promising potential is attracting attentions and investments from academia, governments, and industry all over the world.[164, 179] Potential medical applications include nanofibre scaffolds for nerves, tissues, skin and bone.[180] Research findings have already proven that bioactive surfaces are enhanced when covered by a mesh of biopolymer nanofibres.[164, 180] In these cases cell adhesion and proliferation have been promoted. Nanofibre

membranes are also studied for sensors, polymer batteries, polymer electrolyte membrane fuel cells and photovoltaic cells.[164, 177]

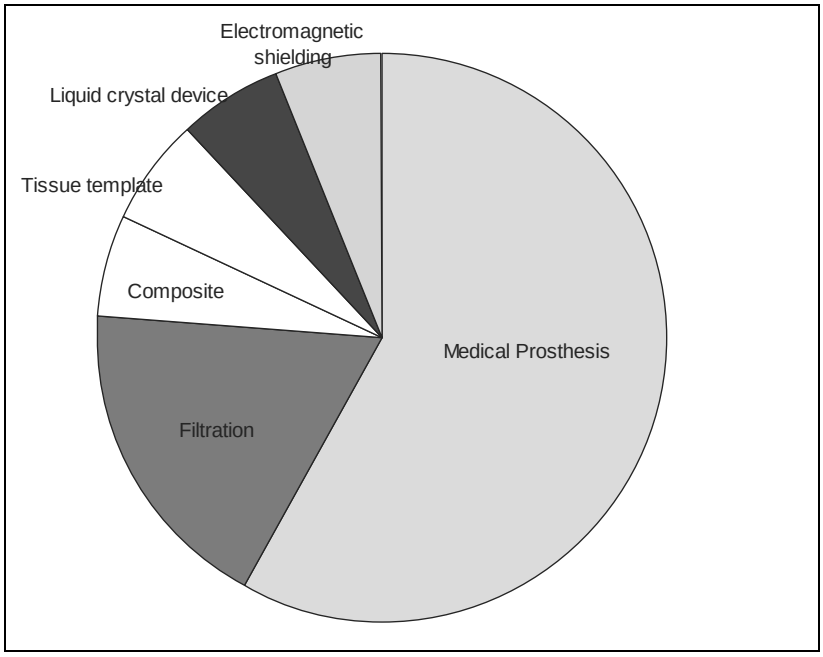

Figure 2.13: **Application fields targeted by US patents on electrospun nanofibres.**[164]

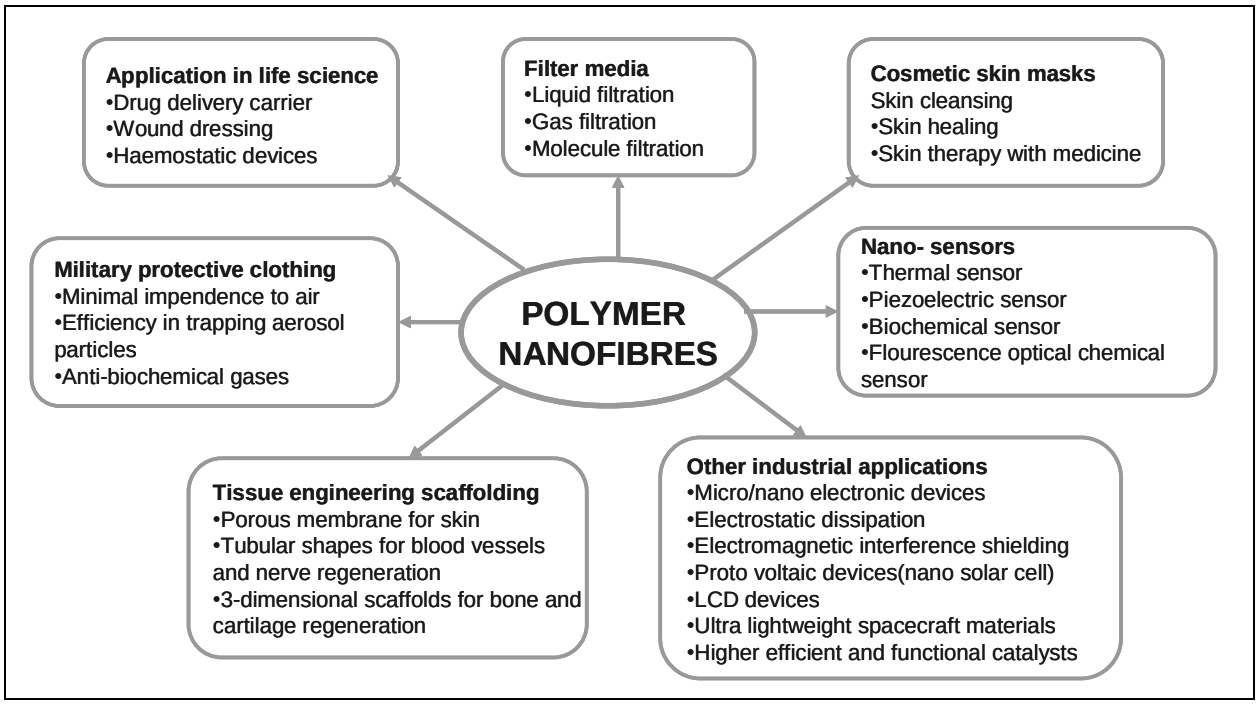

Figure 2.14: Potential applications of electrospun polymer nanofibres.[164]

2.9.4 Nanofibres for filter media

Recent times have seen an increase in the use of nanostructured materials, such as mesoporous media, nanoparticles, carbon nanotubes and nanofibres in filter media.[163] Among these materials, electrospun nanofibres offer a number of attractive features compared to the other nanostructures in filter media applications.[164] Electrospun nanofibres have an advantage over mesoporous media by relieving the mass transfer limitation of substrates/products due to their reduced thickness. Additionally, it is easier to recover and reuse nanofibres than nanoparticles or carbon nanotubes since electrospinning can generate long nanofibres, which can also be further processed into various structures such as non-woven mats, well aligned arrays, or membranes.[163] Nanofibres also posses high surface to volume ratios, high acid/basic and temperature resistance, light weight, longer membrane life spans as well as high flexibility which enables nanofibre membranes to be formed into various membrane modules for larger commercial applications.[164] The use of nanofibres in filter media has received a lot of attention from researchers wordwide.[181] Research on the use of nanofibre membranes in filter media has given rise to a new era of high technology and efficient media for filtering various compounds in all the three states of matter. A few prototype applications of nanofibrous filter media were summarized by Barhate and Ramakrishna (Table 2.9)

Table 2.9: Specialty filtration applications of nanofibrous media.[181]

No.	Filtering media
1.	Air filtering media for engine air filtration, cabin air filtration and self cleaning air intake for gas turbines
2.	Filter media for pulse clean cartridges in dust collection
3.	Penetrating aerosol particulate filtering media
4.	High efficiency air filtering media
5.	Cigarette filter for filtration of smoke
6.	Adsorptive catalytic gas filter for respirators
7.	Layer composite material for protective apparels
8.	Filtering media for catalytic cracking and high temperature filtration
9.	Particulate filtering media for liquid filtration
10.	High flux ultrafiltration media
11.	Water-in-oil emulsion separation media or coalescence promoting filtering media
12.	Filter media for hemodialysis
13.	Filter media for wound dressing
14.	Antimicrobial and antimycotic biocompatible filter for wound healing application
15.	Biocatalytic filtering media
16.	Affinity filtering media for highly selective separation and diagnostics
17.	Ion-exchange filtering media

2.9.5 Functionalization of nanofibres

Surfaces-modifications of degradable and non-degradable synthetic nanofibres have been carried out using bioactive molecules for advanced applications.[182] Synthetic polymers when compared to natural polymers are easier to process for electrospinning and offer a more flexible nanofibrous morphology. Due to the processing benefits of synthetic polymers, a wide variety of functional groups as well as other compounds can be immobilized onto the surface of synthetic polymers without compromising bulk properties. The modification of polymer surfaces is a research field that has received much attention, mainly because of the lack of some specific surface properties needed in a number of applications, such as adhesion, biomaterials and protective coatings, although the polymers might possess excellent bulk properties.[183] Various surface modification techniques have been explored for

functionalizing nanofibres and these include physical coating, plasma treatment, chemical modifications using wet treatment, surface grafting polymerization and co-electrospinning.

2.9.5.1 Physical coating

Buldum and co-workers demonstrated physical coating of nanofibres through sputtering or deposition.[184] They successfully coated fibres with films of copper, aluminum, titanium, zirconium, and aluminum nitride by using a plasma-enhanced physical vapor deposition sputtering process.[185] Kim also covalently bound enzymes to poly (styrene-co-maleic anhydride) nanofibres through coating and these fibres were stable and highly active.[163]

2.9.5.2 Plasma treatment

Plasma treatment of polymer substrates has been commonly used to achieve surface adhesion and wetting properties by modification of the surface chemical composition. The selection of an appropriate plasma source enables the introduction of various functional groups on the targeted surface. This is usually done to improve biocompatibility or to permit subsequent covalent immobilization of other molecules. Plasma treatments with oxygen, ammonia, or air can generate carboxyl groups or amine groups on the nanofibre surfaces.[182] Höcker reported the use of this technique to produce shrink resistant fibres while Ladizesky and Ward plasma-treated polyethylene fibres to reinforce them for clinical applications. In plasma treatment of nanofibrous mats, modification of nanofibres located inside thick mats is impossible due to the limited penetration depth of plasma within the nanopores.[186, 187]

2.9.5.3 Wet chemical method

A popular wet chemical method involves random chemical scission of ester linkages on the polymer backbones located on nanofibre surfaces. This results in the generation of carboxylic and hydroxyl groups from degraded water-insoluble polymer fragments.[182] Wet chemical etching methods offers flexibility for the modification of thick nanofibrous meshes. An example of this method was reported by Sun and Onebby who investigated surface modification of biodegradable polycaprolactone films via base catalysed hydrolysis in sodium hydroxide solution.[183]

2.9.5.4 Surface graft polymerization

Most synthetic polymers have hydrophobic surfaces and often require hydrophilic surface modification to achieve antifouling properties. The introduction of surface graft polymerization does not only confer surface hydrophilicity, but is also used to introduce multi-functional groups on nanofibrous mesh surfaces.[182] To initiate surface graft polymerization, Redox, plasma and UV radiation treatments are often employed to generate free radicals for the polymerization.[188] In a study by Bernstein and co-workers, redox-initiated graft polymerization of vinyl monomers resulted in RO

and NF filtration membranes with reduced concentration polarization.[189] A lot of research has been done on the fabrication of filtration membranes via plasma and UV initiated surface graft polymerization.[190-192] These studies demonstrated good fouling mitigation properties. There are two methods for chemically attaching polymer chains to a solid substrate: the "grafting to" and "grafting from" techniques and these are illustrated in Figure 2.16.[193] In the "grafting to" method, pre-formed, end-functionalized polymer chains are reacted with a chemically activated substrate.[194] One advantage of this method is that polymer chains can be characterized before being attached to the substrate.[195] The drawback, however, is that only relatively low grafting densities are obtained due to steric crowding of already attached chains on the surface, which hinder diffusion of additional chains to reactive sites. The "grafting from" method involves formation of an initiator layer on the surface of the nanofibres followed by polymerization of monomer.[194, 195]

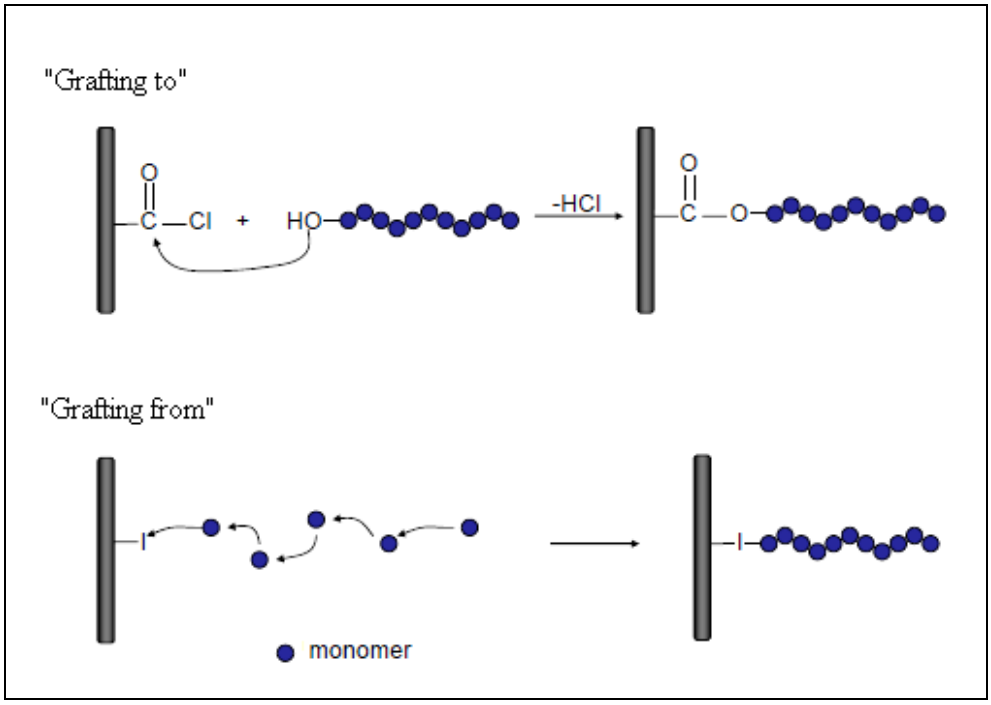

Figure 2.15: Schematic of the grafting to and grafting from approaches.[194]

2.9.5.5 Co-electrospinning of surface active agents and polymers

The previously discussed surface modification methods are intended to be used for prefabricated electrospun nanofibres. Modification of polymer solutions can also be done prior to electrospinning in what is termed co-electrospinning. The introduction of the bioactive agents to the bulk polymer solution followed by electrospinning results in functionalized nanofibrous mats which can be further modified by post electrospinning techniques.[182] An example of this is work done by Voigt and du Plessis who fabricated water-stable antimicrobial nanofibres from poly(vinyl alcohol) and polyacrylonitrile respectively by adding silver nitrate to the spinning solutions prior to the

electrospinning process.[162, 171] As mentioned earlier, new research in membrane technology focuses on surface modification of nanofibres to achieve increased hydrophobicity and improve bacterial resistance of existing nanofibre membranes. Some of the techniques discussed in this chapter were used in this study to fabricate different antimicrobial and antibiofouling membranes.

The theories and techniques discussed in this chapter will be used in subsequent chapters to meet the objectives of this study.

2.10 References

1. Wang L.K.; Chen J.P.; Hung Y-T.; Shammas N.K., *Membrane and Desalination Technologies*. Humana Press: 2011.
2. Barker RW, *Membrane Technology and Applicaions*. Wiley: 2004.
3. Ma H.; Bowman C.N.; Davis R.H. *Journal of Membrane Science* **2000,** 173, 191-200.
4. Allgeier S., Membrane filtration guidance manual. In Allgeier S., Ed. United States Environmental Protection Agency (Office of Water): 2005; Vol. EPA 815-R-06-009.
5. Vrouwenvelder H. Biofouling of spiral wound membrane systems. Delft University of Technology Delft , The Netherlands 2009.
6. Satinderpal K. Surface modification of electrospun poly(vinylidene fluoride) nanofibrous microfiltration membrane. National University of Singapore, Singapore, 2007.
7. Kang S-K; Choo K-H. *Journal of Membrane Science* **2003,** 223, 89-103.
8. Liu Q-F; Kim S-H. *Separation Science and Technology* **2008,** 43, 45-58.
9. Harrelkas F.; Azizi A.; Yaacoubi A.; Benhammou A.; Pons M.N. *Desalination* **2009,** 235, 330-339.
10. Vieira M.; Tavares C.R.; Bergamasco R.; Petrus J.C. *Journal of Membrane Science* **2001,** 194, 273–276.
11. Tavares CR, M. V. M., Petru JCC, Bortoletto EC, Ceravollo F. *Desa lination* **2002,** 144, 261-265.
12. Molinari R.; Gallo S.; Argurio P. *Water Research* **2004,** 38, 593–600.
13. Bodzek M.; Konieczny K. *Waste Management* **1992,** 12, 75-82.
14. Miao J.; Li N.; Chen G.; Gao C.; Dong S. *Chinese Journal of Chemical Engineering* **2008,** 16, (2), 209-213.
15. Chmiel H.; Kaschek M.; Blocher C.; Noronha M.; Mavrov V. *Desalination* **2002,** 152, 307–314.
16. Koyuncu I. *Desalination* **2003,** 155, 263–275.
17. Ahn KH; Song KG; Cha HY; Park ES; Yeom IT. *Desalination* **1998,** 119, 169–176.
18. Nataraj SK; Hosamani KM; Aminabhavi TM. *Desalination* **2009,** 249, 12-17.
19. Ku Y.; Lee P-L.; Wang W-Y. *Journal of Membrane Science* **2005,** 250, 159-165.
20. Satyawali Y.; Balakrishnan M. *Journal of Environmental Management* **2008,** 86, (3), 481-497.
21. Luo J.; Ding L.; Chen X.; Wan Y. *Separation and Purification Technology* **2009,** 66, 429–437.
22. Lastra A.; Gómeza D.; Romero J.; Francisco J.L.; Luque S.; Álvarez J.R. *Journal of Membrane Science* **2004,** 242, (97-105).

23. Rautenbach R.; Groschl A. *Desalination* **1990,** 77, 73-84.
24. Abdulhussain A.A.; Guo J., L. Z. P.; Pan Y.Y.; Wisaam S.A. *American journal of Applied sciences* **2009,** April.
25. Potts DE; Ahlert RC; Wang SS. *Desalination* **1981,** 36, 235-264.
26. Fritzmann C.; Löwenberg J.; Wintgens T.; Melin T. *Desalination* **2007,** 216, 1–76.
27. Cadotte JE; Petersen RJ; Larson RE; Erickson EE. *Desalination* **1980,** 32, 25-31.
28. Williams M.E. *A Review of Wastewater Treatment by Reverse Osmosis*; EET Corporation and Williams Engineering Services Company: New York, USA, 2003.
29. Wang LK; Chen JP; Hung Y-T; Shammas NK, *Membrane and Desalination Technologies*. Humana Press: 2011.
30. Savage N.; Diallo M.; Duncan J.; Street A.; Rustich R., *Nanotechnology applications for clean water*. William Andrew Inc.: Norwich, NY, 2009.
31. Kislik VS, *Liquid Membranes:Principles and Applications in Chemical Separations and Wastewater Treatment*. 1 ed.; Elsevier Great Britain, 2010.
32. Wagner J., *Membrane Filtration Handbook: Practical Tips and Hints*. Osmonics: 2001; p 129.
33. Ní Mhurchú B.E.J. Dead-end and crossflow Microfiltration of yeast and Bentonite suspensions: Experimental and modelling Studies incorporating the use of Artificial neural networks. Dublin City University, , Dublin, 2008.
34. Kwannate (Manoonpong) S. Membrane fouling studies in suspended and attached growth membrane bioreactor systems. Asian Institute of Technology School of Environment, Resources and Development, Thailand, 2007.
35. Schafer AI; Fane AG; Waite TD, *Module design and operation. In Nanofiltration: Principles and Applications*. Elsevier: Oxford, 2005.
36. Osada Y.; Nakagawa T., *Membrane Science and Technology*. Marcel Dekker, Inc: New York, 1992.
37. Strathmann H. Introduction to Membrane Science and Technology. www.colorado.edu/che/courses/chen4838 (30 June),
38. Senthilmurugan S.; Ahluwalia A.; Gupta S.K. *Desalination* **2005,** 173, 269-286.
39. Lau KK. Feed Spacer of Spiral Wound Membrane Module for Nanofiltration and Reverse Osmosis: Modelling, Simulation and Design. Universiti Sains Malaysia, Nibong Tebal, Penang, 2007.
40. van der Meer WGJ; van Dijk JC. *Desalination* **1997,** 113, (2-3), 129-146.
41. Bai R.; Leow H.F. *Seperation Purification Technology* **2002,** 29, 189-198.
42. Qiu S. Nanofibre as Flocculant or Modifier in Membrane Bioreactors for Wastewater Treatment. University of Akron, Akron, 2005.
43. Lim AL; Renbi B. *Journal of Membrane Science* **2003,** 216, 279-290.
44. Herzberg M.; Elimelech M. *Journal of Membrane Science* **2007,** 295, 11-20.

45. Van Paassen JA; Kruithof J; Bakker SM; Kegel FS. *Desa lination* **1998,** 118, 239-248.
46. Persson F.; Långmark J.; Heinicke G.; Hedberg T.; Tobiason J.; Stenström T.; Hermansson M. *Water Research* **2005,** 39, (16), 3791-3800.
47. Al-Ahmad M.; Aleem F.A.A.; Mutiri A.; Ubaisy A. *Desalination* **2000,** 132, 173-179.
48. Ridgway HF; Flemming HC, Membrane Biofouling in Water Treatment Membrane Processes. In *Water Treatment Membrane Processes*, Ridgway HF, F. H., Ed. McGraw-Hill: New York, 1996.
49. Norde W. *Z. Phys. Chem* **2007,** 221, 47-63.
50. Leslie GL; Schneider RP; Fane AG; Marshall KC; Fell CDJ. *Collodial Surfaces A: Physicochemical Engineering Aspects* **1993,** 73, 165-178.
51. Vu B.; Chen M.; Crawford R.J.; Ivanova E.P. *Molecules* **2009,** 14, 2535-2554.
52. Stanely NR; Lazazzera BA. *Molecular Microbiology* **2004,** 52, 917-924.
53. O'toole GA; Kaplan HB; Kolter R. *Annual Reviews in Microbiology* **2000,** 54, (49-79).
54. Flemming HC; Schaule G. *Desalination* **1988,** 70, 95-119.
55. Davey ME; O'Toole GA. *Microbiology and Molecular Biology Reviews* **2000,** 64, 847-867.
56. Tiranuntakul M. Evaluation of fouling in a pilot scale membrane bioreactor. James Cook University, Qeensland, Australia, 2011.
57. Monroe D. *PLoS Biology* **2007,** 5, 307.
58. Bott TR, *Industrial biofouling*. Elsevier: The Boulevard, Langford Lane, Kidlington, Oxford, UK, 2011.
59. Coester S.E.; Cloete T.E. *Clinical Reviews in Microbiology* **2005,** 31, 1466-1477.
60. Bishop PL. *Water Science Technology* **2007,** 55, 19-26.
61. Vidella HA. *International Biodeterioration and Biodegradation* **2002,** 49, 259-270.
62. deCarvallo CC. *Recent Patents in Biotechnology* **2007,** 1, 49-57.
63. Beech I.B.; Sunner J.A. *Current Opinions in Biotechnology* **2004,** 15, 181-186.
64. Flemming H.C. *Applied Microbiology and Biotechnology* **2002,** 59, 629-640.
65. Hu J.Y.; Yu B.; Feng Y.Y.; Tan X.L.; Ong S.L.; Zeng W.J.; Hoe W.C. *Biofilms* **2005,** 2, 19-25.
66. Momba M.N.B.; Kfir R.; Venter S.N.; Cloete T.E. *Water SA* **2000,** 26, 59-66.
67. Abd El Aleem FA, A.-S. K. a. A. M. *International Biodeterioration and Biodegradation* **1998,** 41, (19-23).
68. Rao TS; Kora AJ; Chandrzmohan P; Panigrahi BS; Narasimhan SV. *Biocatalysis* **2009,** 25, 581-591.
69. Bott TR. *International Journal of Chemical Engineering* **2009,** 29, 1-4.
70. Melo L.F.; Bott T.R. *Experimental Thermal and Fluid Science* **1997,** 14, 375-381.
71. Pu H.; Ding G-I.; Ma X-K.; Hu H-T.; Gao Y-F. *International Journal of Refrigeration* **2009,** 34, 1032-1040.

72. Kumar CG; Anand SK. *International Journal of Food Microbiology* **1998,** 42, 9-27.
73. Chmielewski R.A.N.; Frank J.F. *Comprehensive Reviews in Food Science and Food Safety* **2003,** 2, 22-32.
74. Sharma M.; Anand S.K. *Food Control* **2002,** 13, 469-477.
75. Vaïsänen O.M.; Weber A.; Bennasar A.; Rainey F.A.; Busse H-J.; Salkinoja-Salonen M.S. *Journal of Applied Microbiology* **1998,** 84, 1069-1084.
76. Richards M. Self immobilization of single and combinations of enzymes in spherical particles and evaluation of their anti-biofouling potential. University of Pretoria, Pretoria, South Africa, 2010.
77. Blanco M.A.; Negro C.; Gaspar I.; Tijero J. *Applied Microbiology and Biotechnology* **1996,** 46, (203-208).
78. Ludensky M. *International Biodeterioration and Biodegradation* **2003,** 51, 255-263.
79. Gilbert P.; Foley I. *Advances in Dental Research* **1997,** 11, 160-167.
80. Costerton J.W.; Veeh R.; Shirtliff M.; Pasmore M.; Post C.; Ehrlich G. *Journal of Clinical Investigation* **2003,** 112, 1466-1477.
81. Del Pozo JL; Patel P. *Clinical Pharmacology and Therapeutics* **2007,** 82, 204-209.
82. Hall-Stoodley L.; Costerton J.W.; Stoodley P. *Nature Reviews: Microbiology* **2004,** 2, 95-108.
83. Vuong C.; Kocianova S.; Voyich J.M.; Yao Y.; Fischer E.R.; DeLeo F.R.; Otto M. *Journal of Biological Chemistry* **2004,** 279, 54881-54886.
84. Costerton JW; Stewart PS; Greenberg EP. *Science* **1999,** 284, 1318-1322.
85. Cohen N.; Morisset J.; Emilie D. *Journal of Dental Research* **2004,** 83, 429-433.
86. Sun D.; Accavitti M.A.; Bryers J.D. *Clinical Diagnostic Laboratory Immunology* **2005,** 12, 93-100.
87. Van Delden C.; Inglewski B.H. *Emerging Infectious disease* **1998,** 4, 551-560.
88. Gotz F. *Molecular Microbiology* **2002,** 48, 1367-1378.
89. Donlan RM; Costerton JW. *Clinical Microbiology Reveiws* **2002,** 15, 167-193.
90. Pradeep T.; Anshup P. *Thin Solid Films* **2009,** 517, 6441-6478.
91. Chen X.; Stewart P. *Water Research* **2000,** 34, 4229-4233.
92. Stewart P.; Roe F.; Rayner J.; Elkins F.G.; Lewandowski Z.; Ochsner U.A.; Hassett D.J. *Applied and Environmental Microbiology* **2000,** 66, 836-838.
93. Meyer B. *International Biodeterioration and Biodegradation* **2003,** 51, 249-253.
94. Denyer S.P. *International Biodeterioration and Biodegradation* **1990,** 26, 89.
95. Chen X.; Stewart P.S. *Environmental Science and Technology* **1996,** 30, 2078-2083.
96. Keevil C.W.; Godfree A.; Holt D.; Dow C., *Biofilms in the aquatic environment*. The Royal Society of Chemistry: United Kingdom, 1999.
97. Veschetti E.; Cittadini B.; Maresca D.; Citti G.; Ottaviani M. *Microchemical Journal* **2005,** 79, 165-170.

98. Kramer J.F., Biofilm control with bromo-chloro-dimethylhydantion. In *Corrosion NACE International. Paper number 1277*, Houston, Texas, 2001.
99. Vidella H.A. *International Biodeterioration and Biodegradation* **2002,** 49, 259-270.
100. Presterl E.; Suchomel M.; Eder M.; Reichmann S.; Lassnigg A.; Graninger W.; Rotter M. *Journal of Antimicrobial Chemotherapy* **2007,** 60, 417-420.
101. McDonnell G.; Russell A.D. *Clinical Microbiology Reviews* **1999,** 12, 147-179.
102. Wiencek K.M.; Chapman J.S., Biocides: how do they work and should you care. In *Corrosion 99. Paper number 99308*, San Antonio, Texas, USA, 1999.
103. Freese S.D.; Noziac D.J. *Water SA* **2004,** 30, 18-24.
104. Wang Y.; Kim J-H.; Choo K-H.; Lee Y-S.; Lee C-H. *Journal of Membrane Science* **2000,** 169 269-276.
105. Mah T-F.; O'Toole G.A. *Trends in Microbiology* **2001,** 9, 34-39.
106. Langsrud S.; Sundheim G.; Borgmann-Strahsen R. *Journal of Applied Microbiology* **2003,** 95, 874-882.
107. Williams T.M., Isothiazole biocides in water treatment applications. In *Corrosion 2004, Paper number 04083*, New Orleans, Los Angeles, U.S.A., 2004.
108. Cloete TE, V. S., Brozel S, Van Holy A. *International Biodeterioration and Biodegradation* **1992,** 29, 299-341.
109. Splendidani A.; Livingston A.G.; Nicolella C. *Biotechnology and Bioengineering* **2006,** 94, 15-23.
110. Cloete TE. *International Biodeterioration and Biodegradation* **2003,** 51, 277-283.
111. Ludensky M. *Journal of Industrial Microbiology and Biotechnology* **1998,** 20, 109-115.
112. Al-Malack M.H.; Anderson G.K. *Journal of Membrane Science* **1996,** 112, 287-296.
113. Milisik V. *Filtration and separation* **1986,** 23, 347-349.
114. Peuchot MM; Ben Aim R. *Journal of Membrane Science* **1992,** 68, 241-248.
115. Zhang J.; Sun Y.; Chang Q.; Liu X.; Meng G. *Desalination* **2006,** 194, 182-191.
116. Katayon S.; Megat Mohd Noor M.J.; Kien Tat W.; Abdul Halim G.; Thamer A.M.; Badronisa Y. *Desalination* **2007,** 204, 204-212.
117. Jonsson B.; Jonsson B. *Journal of Membrane Science* **1991,** 56, 49-76.
118. Grebenyuk VD, C. R., Peters S and Linkov V. *Desa lination* **1988,** 115, 313-329.
119. Cakl J.; Bauer I.; Doleček P.; Mikulášek P. *Desalination* **2000,** 127 189-198.
120. Wu J.; Le-Clech P.; Stuetz R.M.; Fane A.G.; Chen V. *Journal of Membrane Science* **2008,** 324, 26-32.
121. Matsumoto K.; Kawahar M.; Ohya H. *Journal of fermentation technology* **1988,** 66, 199-205.
122. Nipkow JG; Zeikus P; Gephardt P. *Biotechnol. Bioeng.* **1989,** 34, 1075-1084.
123. Redkar S.; Davis R.H. *A.I.Ch.E. Journal* **1995,** 41, (3), 501-508.
124. Wenten IG. *Filtration and Separation* **1995**, 252-254.

125. Kuberkar VT; Davis RH. *Biotechnology Progress* **1999,** 15 472.
126. Ramirez JA; Davis RH. *Journal of Hazardous Materials* **1998,** 63, 179-197.
127. Cabassud A.; Laborie S.; Laine J.M. *Journal of Membrane Science* **1997,** 128, 93-101.
128. Si-Hassen D.; Ould-Dris A.; Jaffrin M.Y.; Benkahla Y.K. *Journal of Membrane Science* **1996,** 118, 185-198.
129. Su SK; Liu JC; Wiley RC. *Journal of Food Science* **1993,** 58, (3), 638-641.
130. Czekaj P.; López F.; Güell C. *Journal Food Engineering* **2001,** 49, 25-36.
131. Vera L.; Villarroel R.; Delgado S.; Elmaleh S. *Journal of Membrane Science* **2000,** 165, 47.
132. Chen D.; Weavers L.K.; Walker H.W.; Lenhart J.J. *Journal of Membrane Science* **2006,** 276, 135-144.
133. Matsumoto Y.; Miwa T.; Nakao S; Kimura S. *Journal of chemical engineering of Japan* **1996,** 29, 561-567.
134. Kuruzovich JN; Piergiovanni PR. *Journal of Membrane Science* **1996,** 112, 241-247.
135. Tanaka S.; Numata K.; Kuzumoto H.; Sekino M. *Desalination* **1994,** 96, 191-199.
136. Kennedy M.; Kim S-M.; Mutenyo I.; Broens L.; Schippers J. *Desalination* **1998,** 118, 175-187.
137. Dickson J.M.; Childs R.F.; McCarry B.E.; Gragnon D.R. *Journal of Membrane Science* **1998,** 148, 25-46.
138. Kelly P.J.; Li H.; Whitehead K.A.; Verran J.; Arnell R.D.; Iordanova I. *Surface & Coatings Technology* **2009,** 204, 1137-1140.
139. Gao G.; Lange D.; Hilpert K.; Kindrachuk J.; Zou Y.; Cheng J.T.J.; Kazemzadeh-Narbat M.; Yu K.; Wang R.; Straus S.K.; Brooks D.E.; Chew B.H.; Hancock R.E.W.; Kizhakkedathu J.N. *Biomaterials* **2011,** 32, 3899-3909.
140. Mauter M.S.; Wang Y.; Okemgbo K.C.; Osuji C.O.; Giannelis E.P.; Elimelech M. *ACS Applied Materials & Interfaces* **2011,** 3, 2861-2868.
141. Brash J.L.; Horbett T.A. In *Proteins at interfaces: current issues and future prospects*, Proteins at Interfaces II, ACS Symposium Series 602, Washington DC, 1995; Brash J L, H. T. A., Ed. American Chemical Society: Washington DC, 1995; pp 1-23.
142. Fane AG; Fell CD. *Desalination* **1987,** 62, 117-136.
143. Nystrom M. *Journal of Membrane Science* **1989,** 44, 183-186.
144. Hanemaaijer J.H.; Robbertsen T.; van den Boomgaard T.H.; Gunnink J.W. *Journal of Membrane Science* **1989,** 40, 199-217.
145. Ostuni E.; Chapman R.G.; Holmlin R.E.; Takayama S.; Whitesides G.M. *Langmuir* **2001,** 17, 5605-5620.
146. Stengaard F.F. *Desalination* **1988,** 70, 207-224.
147. Kim K.J.; Fane A.G.; Fell C.J.D. *Desalination* **1988,** 70, 229-249.

148. Keszler G.; Kovacs A.; Toth I.; Bertoti M.; Hegyi. *Journal of Membrane Science* **1991,** 62, 201- 210.

149. Guiver M.D; Black P.; Tam C.M.; Deslandes Y. *Journal of Applied Polymer Science* **1993,** 48, 1597-1606.

150. Uchida E.; Uyama Y.; Ikada Y. *Journal of Applied Polymer Science* **1993,** 47, 417-424.

151. Yamagishi H.; Crivello J.V.; Belfort G. *Journal of Membrane Science* **1995,** 105, 237-247.

152. Oster G.; Shibata O. *Journal of Membrane Science* **1957,** 26, 233.

153. Ranby B.; Gao Z.M.; Zhang P.Y. *Polym Am Prep Chem Soc* **1988,** 27, 38.

154. Zhang P.; Ranby B. *Journal of Applied Polymer Science* **1990,** 41, 1469-1478.

155. Yang W.; Ranby B. *Journal of Applied Polymer Science* **1996,** 62, 533-543.

156. Ogiwara Y.; Kanda M.; Takumi M.; Kubota H. *Journal of Membrane Science, Polymer letter edition* **1981,** 19, 457-462.

157. Ulbricht M; Matuschewski H; Oechel A; Hicke HG. *Journal of Membrane Science* **1996,** 115, 31-47.

158. Yan W.; Yang P.; Wang Y. *Shuichuli Jishu* **1988,** 14, 213-222.

159. Ulbricht M.; Belfort G. *Journal of Applied Polymer Science* **1995,** 56, 325-343.

160. Ulbricht M; Belfort G. *Journal of Membrane Science* **1995,** 111, 193-215.

161. Nystrom M; Jarvinen P. *Journal of Membrane Science* **1991,** 60 275-296.

162. du Plessis D.M. Fabrication and characterization of anti-microbial and biofouling resistant nanofibers with silver nanoparticles and immobilized enzymes for application in water filtration. University of Stellenbosh, Stellenbosch, South Africa, 2011.

163. Kim B.J.; Nair S.; Kim J.; Kwak J.H.; Grate J.W.; Kim S.H.; M.B., G. *Nanotechnology* **2005,** 16, S382-S388.

164. Huang Z-M.; Zhang Y-Z.; Kotaki M.; Ramakrishna S. *Composites Science and Technology* **2003,** 63, 2223-2253.

165. Wertz J.; Schneiders I. *Filtration and Separation* **2009,** July/ August.

166. Ramakrishna S.; Fujihara K.; Teo W-E.; Lim T-C.; Ma Z., *An Introduction to Electrospinning and Nanofibres*. World Scientific Publishing Co. Pte. Ltd.: Toh Tuck Link, Singapore, 2005.

167. Ondarcuhu T.; Joachim C. *Europhysics Letters* **1998,** 42, 215-220.

168. Feng L.; Li S.; Li H.; Zhai J.; Song Y.; Jiang L. *Angew Chem Int Ed* **2002,** 41, 1221-1223.

169. Ma P.X.; Zhang R. *J Biomed Mat Res* **1999,** 46, 60-72.

170. Li W.J.; Laurencin C.T.; Caterson E.J.; Tuan R.S.; Ko F.K. *Jounal of Biomedical Materials Research* **2002**, (60), 613-621.

171. Voigt W.V. Water stable, antimicrobial active nanofibres generated by electrospinning from aqueous spinning solutions. RWTH Aachen University, Munich, 2009.

172. Zeleny J. *Physical Review* **1914,** 3, 69-91.

173. Taylor B., *Electrically driven jets*. Proc. Roy. Soc: London 1969.

174. Subbiah T.; Bhat G.S.; Tock R.W.; Parameswaran S.; Ramkumar S.S. *Journal of Applied Polymer Science* **2005,** 96, 557-569.
175. Doshi J.; Reneker D.H. *J Electrostat* **1995,** 35, 151-160.
176. Theron A.; Zussman E.; Yarin A.L. *Nanotechnology* **2001,** 12, 384-390.
177. Baji A.; Mai Y-W.; Wong S-C.; Abtahi M.; Chen P. *Composites Science and Technology* **2010,** 70, 703-718.
178. Taylor G.I., *Disintegration of water drops in an electric field.* Proc Roy Soc Lond Ser A: 1969; p 313:453.
179. Teo W.E.; Ramakrishna S. *Nanotechnology* **2006,** 17, 89-106.
180. Koyal Garg K.; Bowlin G.L. *Biomicrofluidics* **2011,** doi: 10.1063/1.3567097.
181. Barhate R.S.; Ramakrishna S. *Nanofibrous filtering media: Filtration problems and solutions from tiny materials* **2007,** 296, 1-8.
182. Yoo H.S.; Kim T.G.; Park T.G. *Advanced Drug Delivery Reviews* **2009,** 61, 1033-1042.
183. Sun H.; Onebby S. *Polymer International* **2006,** 55, 1336–1340.
184. Buldum A.; Clemons C.B.; Dill L.H.; Kreider K.L.; Young G.W.; Zheng X.; Evans E.A.; Zhang G.; Hariharan S.I. *Journal of Applied Physics* **2005,** 98, 044304.
185. Buldum A.; Busuladzic I.; Clemons C.B.; Dill L.H.; Kreider K.L.; Young G.W.; Evans E.A.; Zhang G.; Hariharan S.I.; Kiefer W. *Journal of Applied Physics* **2005,** 98, 044303.
186. Höcker H. *Pure Applied Chemistry* **2002,** 74, 423-427.
187. Ladizesky N.H.; Ward I.M. *Journal of Materials Science: Materials in Medicine* **1995** 6, 497-504.
188. Deng J.; Wang L.; Liu L.; Yang W. *Progress in Polymer Science* **2009,** 34, 156-193.
189. Bernstein R.; Belfer R.; Freger V. *Langmuir* **2010,** 26, 12358-12365.
190. Abu Semana M.N.; Khayet M.; Bin Ali Z.I.; Hilal N. *Journal of Membrane Science* **2010,** 355, 133-141.
191. Taniguchi M.; Kilduff J.E.; Belfort G. *Journal of Membrane Science* **2003,** 22, 59-70.
192. Chang Y.; Ko C-Y.; Shih Y-J.; Quémener D.; Deratani A.; Wei T-C.; Wang D-M.; Lai J-Y. *Journal of Membrane Science* **2009,** 345, 160-169.
193. He D.; Susanto H.; Ulbricht M. *Progress in Polymer Science* **2009,** 34, 62-98.
194. Rhodes S.M. Electrically conductive polymer composites. University of Akron, Akron, United States of America., 2007.
195. Ranjan R. Surface Modification of silica nanoparticles. University of Akron, Akron, United States of America, 2008.

Chapter 3: Fabrication and characterization of antimicrobial biocide containing poly(vinyl alcohol) nanofibres for application in filter media

3.1 Chapter summary

This chapter explores the introduction of a biocide called AquaQure as an additive to poly(vinyl alcohol) to obtain nanofibres with antimicrobial properties. The addition of the AquaQure biocide to PVA nanofibres, testing of the antimicrobial activity as well as leaching of PVA nanofibres modified with the AquaQure biocide were investigated in this study. Antimicrobial activity of the AquaQure containing PVA fibres against bioluminescent strains of *Klebsiella pneumoniae* Xen 39, *Staphylococcus aureus* Xen 36, *Escherichia coli* Xen 14, *Pseudomonas aeruginosa* Xen 5 and *Salmonella typhimurium* Xen 26 were tested using plate counting. The antimicrobial tests were confirmed with non-culture-based techniques namely bioluminescent imaging and LIVE/DEAD Baclight to determine the antimicrobial efficiency against viable but non-culturable (VNBC) cells. This was done to quantify the cells that enter a dormant state during contact with the antimicrobial fibres and to eliminate the chances of overestimating the antimicrobial efficiency of the nanofibres.

The nanofibrous mats were also chemically characterized using ATR-FTIR and EDX. Thermal characterization was done usin DSC, TGA and XRD. Since leaching out of metal ions to water supplies is as much a health hazard as it is an environmental hazard, leaching experiments were conducted to ascertain the amounts of the constituents of the biocide from the fibres. Because of the intended drinking water purification application, these figures were then compared with the South African national standards (SANS) for drinking water.

3.2 Background information

In this section, historical aspects and the chemical properties of polyvinyl alcohol qualifying it for use in liquid filter media are discussed. A brief review on antimicrobial metal nanoparticles and nanofibrenanofibres looking into their development and possible drawbacks is also given.

3.2.1 Poly(vinyl alcohol) (PVA)

Poly(vinyl alcohol) (PVA) was first prepared by Herrmann and Haehnel in 1924 via the base catalyzed alcoholysis of poly(vinyl esters). The reactions were not commercially viable as large amounts of heat were evolved, which made the reactions hazardous.[1] In 1925, the duo developed new and safe methods for the large scale production of poly(vinyl acetate), resulting in vinyl acetate (VAc) becoming the

most widely used monomer for the preparation of PVA precursor. Preparation of the first PVA fibre was proposed in 1931.[1, 2]

3.2.1.1 Properties and applications

Poly(vinyl alcohol) (PVA) is a water-soluble polymer produced industrially by hydrolysis of poly(vinyl acetate). A number of grades of PVA are commercially available, these can be divided into two types: the fully hydrolysed and the partially hydrolysed PVA depending on the fraction of acetate groups left in the backbone.[3-5] PVA also has excellent mechanical and thermal properties, excellent oxygen barrier properties, oil, grease and organic solvent resistance, low moisture permeability, high heat resistance and ultra violet and infra-red radiation stability and is non-toxic. In addition, PVA fibres have high tensile and compressive strengths; high modulus and abrasion resistance. The high chemical stability of PVA at normal temperature along with its excellent physical and mechanical properties has led to its broad practical applications.[6]

PVA has been mainly used in fibre and film products for many years.[7-9] It has also been used as paper coating, adhesives and colloid stabilizer.[2, 10, 11] In recent years, much attention has been focused on the biomedical applications of PVA hydrogels including contact lenses, artificial organs and drug delivery systems.[12, 13] Electrospinning is a highly versatile method that can produce fibres with diameters in the range of 100 nm to a few μm.[14] Ultrafine PVA fibres, which may have potential applications in filtration and biomedical engineering, can be produced through the process of electrospinning. Electrospun fibre mats have a large surface-to-volume ratio, tunable porosity, and relatively high production rates, and possess the potential for use in many technological areas.[14]

3.2.1.2 Crosslinking of PVA

Poly(vinyl alcohol) (PVA) is generally soluble in water which would compromise its use in filtration systems. However, crosslinking has provided one of the techniques to improve physical properties of PVA. Crosslinking of PVA can be done using various techniques which include irradiation, chemical and physical techniques.

i. Radiation crosslinking

Gamma rays produced by the decomposition of ^{60}Co have been used to carry out radiation crosslinking of PVA. Through radiation crosslinking, polymer networks which are not harmful when used in biomedical applications are produced because no catalysts or additives are used. The disadvantage of this technique however, is that crosslinking is often accompanied by polymer degradation.

ii.Physical crosslinking

Physical crosslinking is commonly carried out though freezing and thawing. Repeating freeze-thaw cycles of PVA solutions results in the formation of crystalline regions which remain intact in water, rendering the PVA insoluble. This technique can however be only used for crosslinking PVA solutions and not other forms like solid PVA and PVA fibrils. Another well reported physical technique is the heat treatment of PVA at temperatures above 100 °C. This method has been used to crosslink PVA nanofibres. Crosslinking using heat treatment takes short periods of time e.g. Voigt reported the crosslinking of PVA nanofibres in 10 minutes at 140 °C. This method is also environmentally friendly since no harmful catalysts or additives are used in the crosslinking.[15]

iii.Chemical crosslinking

Chemical crosslinking using multifunctional compounds is however the most commonly reported technique for crosslinking PVA. The general mechanism involves the reaction of the complimentary functional group of the crosslinking agent with the O-H group of PVA. Commonly used crosslinking agents include dialdehydes, dicarboxylic acids, dianhydrides and diisocyanates. PVA undergoes esterification with dicarboxylic acids and dianhydrides, acetalization with dialdehydes (in the presence of Lewis or Brønsted acid catalysts) and carbamate (urethane) linkages are formed with diisocyanates.[6] This renders the fibres insoluble in water and also significantly preserves fibre structure and properties. An example of this type of crosslinking which was used in this study is crosslinking using glyoxal.

The general mechanism for crosslinking of PVA with dialdehydes involves hemiacetal and acetal formation, as illustrated in Scheme 3.1. In the presence of a Brønsted acid catalyst the carbonyl oxygen of the glyoxal (step **1**) is first protonated. This is then followed by nucleophilic attack of the electron deficient carbonyl carbon atom by the PVA hydroxyl group, resulting in a hemiacetal as shown in step **3**. In the presence of excess acid the hemiacetal undergoes an intramolecular nucleophilic addition reaction with a second hydroxyl group resulting in an acetal (step **4)**. The unreacted carbonyl group in step **3** can also undergo an intermolecular nucleophilic addition reaction with an hydroxyl group of PVA resulting in a dihemiacetal as shown in step **5**. The unreacted carbonyl group in step **4** and the hemiacetal groups in step **5** can then undergo a series of protonations, followed by nucleophilic addition reactions with PVA hydroxyl groups, resulting in a diacetal (step **7)** as the final product. Acetalization was important as it minimized the solubility of the PVA fibres in the aqueous media in which they were modified.

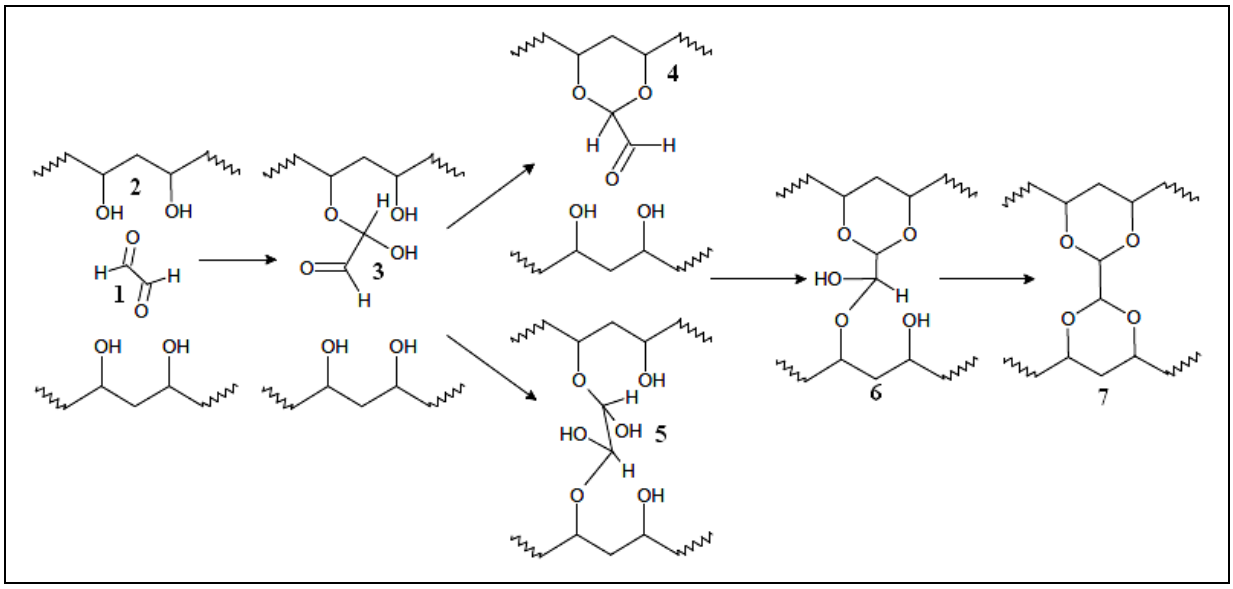

Scheme 3.1: Crosslinking of PVA with glyoxal.[1]

3.2.2 Development of antimicrobial nanofibres

Over the past 10 years, electrospun nanofibres and their applications have received a lot of interest among researchers.[16] With the rising demands for microbiologically safe drinking water, membrane systems globally are being upgraded.[17] Research on antifouling and antimicrobial polymer composites and nanofibres has received a lot of interest from researchers in the past decade. Surface modification and blending of polymers with metal particles and nanoparticles to attain bactericidal properties has been vastly explored. The chemistry of noble metal nanoparticles has a substantial amount of scientific history and their application in water purification is widely reported.[18] The uses of metal nanoparticles in water treatment include the removal and detection of severely toxic contaminants which can be pesticides, halogenated organics, heavy metals, and micro-organisms found in drinking water.[18] Antimicrobial properties of copper and zinc have been reported.[19-24] The mechanism by which these metal ions distort pathogens is still not very clear. There has been research which generated a lot of viable theories on how this happens and these include the ions causing (i) leakage of potassium glutamate through the outer membrane of bacteria, (ii) disturbance of osmotic balance, (iii) binding to proteins that do not require copper or zinc, and (iv) oxidative stress by generating hydrogen peroxide.[19] Bokow and Gabbay also reported that copper exerts its toxicity to pathogens through a series of parallel mechanisms, which can lead to cell death within minutes of contact.[23] These mechanisms include damage to the microorganisms envelope, which was also confirmed by Nan Li and co-workers.[23, 24] Cu^{2+} specifically, affects the fatty acid composition in the microorganism's membrane and tampers with its permeability causing membrane disruption.[25]

3.2.3 Impact of PVA/AquaQurenanofibres and possible drawbacks in filter applications

The development of biocide-containing nanofibres has great potential in filter media especially in point of use water filtration systems to provide safe drinking water for the world's developing regions and other air filtration applications for controlling airborne infections. This development however, also poses serious health risks should the biocide leach into the filtered water. Health hazards associated with copper in drinking water include cirrhoses, gastrointestinal illnesses and liver failure.[26] The tendency of bacteria to become resistant to current antibiotics is a serious problem in industrial and clinical settings.[27] The introduction of any antimicrobial material therefore needs to be investigated and weighed against this drawback. The use of the multi-ion biocidal system, however could mitigate the problem of resistance since different metal ions use different pathways for distorting different strains of bacteria.[28]

3.3 Objective

This study focused on the fabrication of antimicrobial PVA nanofibres through the electrospinning process, which provides a simple and versatile method for generation of nanofibres as described in Section 2.9.2. This was done by directly doping the spinning solution with AquaQure which is an aqueous biocide prior to electrospinning. AquaQure is a biocide containing mainly Cu^{2+} and Zn^{2+} among other metal ions and is commercially available from AquaQure Water Solutions, South Africa. It is used for killing bacteria to provide safe drinking water to people without access to safe water supplies i.e. 2 drops of AquaQure per liter of water kills up to 99.999 % of all bacteria. It has also been successfully used to eliminate algal blooms in dams as well as kill mosquito larvae that cause malaria.

3.4 Experimental materials and methods

For the experiments, poly(vinyl alcohol) (PVA), (Mw 146000-186000, 87-89% hydrolyzed) was obtained from Sigma Aldrich, South Africa and used without further purification. Distilled water was used as the solvent. AquaQure biocide was obtained from AquaQure water solutions, South Africa. The crosslinking agent glyoxal and concentrated hydrochloric acid were also obtained from Sigma Aldrich, South Africa. The experimental methods are summarized in the chart in Figure 3.1.

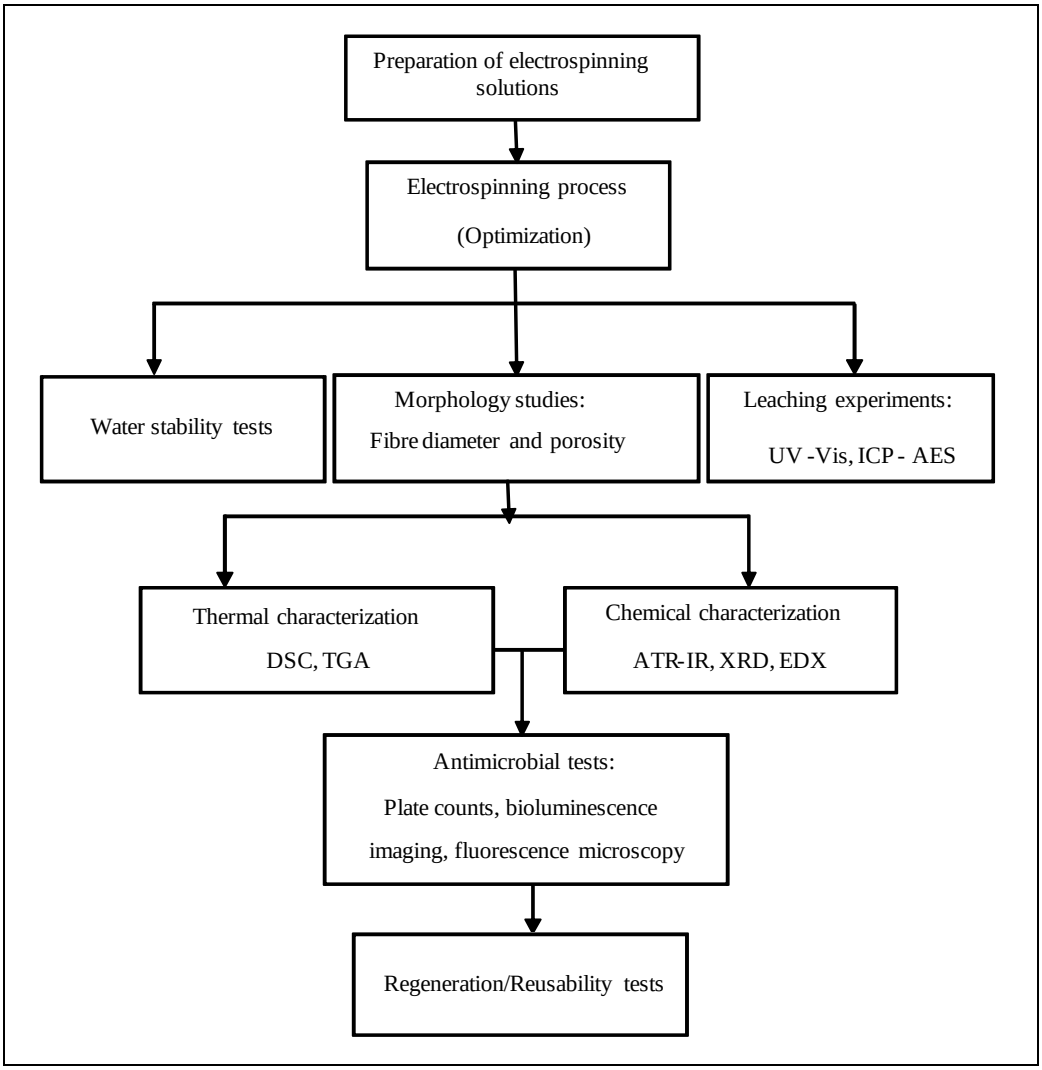

Figure 3.1: Experimental methods

3.4.1 Electrospinning

The conventional needle electrospinning technique was used to electrospin polymer/biocide solutions. Preparation of electrospinning solutions and conditions used during the electrospinning process are reported in subsequent sections.

3.4.1.1 Preparation of electrospinning solution mixtures

Poly(vinyl alcohol), was dissolved in distilled water. The aqueous biocide solution, AquaQure (5 % vol/vol) was added while stirring. About 5 minutes before the polymer was spun, a cross-linking agent, glyoxal, (8% vol/vol) was stirred into the PVA solution until dissolved and concentrated HCl (0.025% vol/vol) was added to lower the pH to 3(±1).[29] The viscosity measurements were taken using a RHEOPLUS/32 V2.62 rheometer (Anton Paar), provided with cone-plate geometry, in which the rotating cone was 0.049 mm in diameter.

3.4.1.2 The electrospinning process

The basic needle electrospinning process was adopted for fabricating nanofibres from polymer solutions. The setup consisted of a high voltage positive DC power supply between two electrodes (one of which acts as a grounded electrode) and a pipette with a capillary tip opening of approximately 0.1 mm which was the polymer reservoir.[30] A copper wire electrode was inserted into the nose of the pipette to about 5 mm from the end. All spinning was conducted inside a fume-hood (without the extraction fan operating) and both temperature and relative humidity were monitored. All fibres were spun from a 45° angle to prevent droplets on the spun mat and to minimize wastage through dripping. The grounded electrode was attached to an aluminium foil which acted as the collector plate.

Another crucial factor influencing the electrospinning process is the field created as a result of the high applied voltage. Conducting materials such as stands, clamps etc. used during electrospinning influence the electromagnetic field and hence the morphology of the produced nanofibres. Furthermore, these conductors build up static electricity that can be very dangerous. For this reason, great care was taken to ensure safety and non-conductors were used as far as possible. PVC piping was used to build a rig to hold the glass pipette that acted as the solution reservoir and polystyrene was also used to insulate all other conducting material. All samples were then heat treated in an oven at 60°C for 72 hours to enhance crosslinking and to remove any residual solvent prior to any analysis.

3.4.2 Scanning electron microscopy (SEM)

The morphology of crosslinked electrospun PVA/AquaQure fibres was observed with scanning electron microscopy (SEM). Analyses were performed at the University of Stellenbosch Microscopy Unit on a Leo® 1430VP and a Cambridge S200 scanning electron microscope after gold sputter coating was applied. The conditions for image acquisition were an accelerating voltage of 7 kV and a probe current of 150 pico amperes (pA) for the former and an accelerating voltage of 10 kV and a probe current of 50 pA for the latter. For determination of fibre diameters the SEM-Img-studio software which runs using the National Instruments LVRunTime Engine, version 1.1.0 was used. Energy dispersive X-ray spectroscopy (EDX) which is a chemical microanalysis technique used in conjunction with SEM was also performed to confirm the incorporation of AquaQure in the fibres.

3.4.2.1 Fibre diameter

For purposes of fibre diameter measurements, electrospun PVA and PVA/AquaQure fibre mats were viewed under the SEM at a magnification of between 1000 to 5000X depending on the spinning conditions and thus fibre diameters. This magnification range was chosen such that up to 50 fibres were included in the image. Each image was then processed using *SEM_Img_Studio* Software. A minimum of 15 measurements was taken and the highest and lowest values discarded prior to calculating the average. Solvent beaded and clumped fibres were ignored.

3.4.2.2 Fibre roughness and porosity

The porosity of nanofibre mats is a very important parameter especially because it determines the air and water permeability through the fibre mat.[31] To measure pore sizes, area light intensity scans were performed using the *Scanning Probe Image Processor* (SPIP) Image Metrology A/S, version 5.1.3 s*oftware*. This software uses SEM images to calculate fibre mat porosity.

3.4.3 X-ray diffraction (XRD)

The chemical composition of the electrospun material was also determined using X-ray diffraction (XRD). The XRD measurements were performed on a PANalytical X'Pert PRO MPD diffractometer with X'Celerator detector and fixed divergence slits using filtered CuKα radiation. The diffraction patterns were recorded at a pulse count rate of 1000 cps in an angular interval of 5°–40°.

3.4.4 Attenuated total reflectance-Fourier transform infra-red spectroscopy (ATR/FTIR)

A Nexus FT-IR provided by Nicolet Thermo equipped with a FTIR gas analyser was used for ATR-FTIR studies. The spectrometer was fitted with a diamond crystal and measurements were taken in the 600 cm^{-1} to 4000 cm^{-1} infra-red range at a resolution of 6 cm^{-1}. The spectra were based on a total of 32 scans per sample. The ATR-IR spectra were used to compare the molecular finger prints of PVA only and PVA/AquaQure nanofibres.

3.4.5 Thermogravimetric analysis (TGA)

Thermogravimetric analysis of the crosslinked PVA and PVA/AquaQure nanofibres was performed on a Q500 thermogravimetric analyser in air at 10°C.min^{-1} to determine their stability as well as to establish the effect of AquaQure on the stability of the fibres. This instrument determines changes in weight in relation to change in temperature, which translates to the ability of the material to withstand high temperatures. Weight loss in % was used over the temperature range 0-900°C.

3.4.6 Differential scanning calorimetry (DSC)

To investigate the crystallinity of the fibres, differential scanning calorimetry studies were carried out. All DSC thermograms were recorded on Q100 thermogravimetric analyser in nitrogen gas at a heating rate of 10°C.min^{-1}. Heat flow over a temperature range of 0-300°C was recorded.

3.4.7 Antimicrobial characterization

To determine the antimicrobial efficiency of the nanofibres, the basic plate counting technique was adopted. The antimicrobial tests were confirmed with bioluminescent imaging and LIVE/DEAD Baclight to determine the antimicrobial efficiency against viable but non-culturable (VNBC) cells.

This was done to quantify the cells that enter a dormant state during contact with the antimicrobial fibres and to eliminate the changes of overestimating the antimicrobial efficiency of the nanofibres.

3.4.7.1 Plate counts

Klebsiella pneumoniae Xen 39, *Staphylococcus aureus* Xen 36, *Escherichia coli* Xen 14, *Pseudomonas aeruginosa* Xen 5 and *Salmonella typhimurium* Xen 26 (Caliper Life Sciences, Hopkinton, MA) are pathogenic bacterial strains genetically modified with the *luxABCDE* operon so that they bioluminesce when metabolically active. Each pathogen was cultured in 10 mL Brain Heart Infusion (BHI) broth (Biolab Diagnostics) along with the appropriate antibiotics overnight on a rotating wheel at 37˚C. For each strain, cells were pelleted by 10 min centrifugation at 3000 rpm, and washed 3 times with physiological water. Spiked water samples were prepared by inoculating 10^6 CFU/mL of each strain into 500 mL sterile physiological water. Several control (cell viability) experiments (not reported here) were carried out to determine if osmotic lysing which is common when cells (especially gram negative) are removed from rich media into physiological water did not occur. The CFU/ml were measured using a Biorad smart spec™ plus spectrophotometer.

The spiked water was then filtered through pristine PVA (control) or PVA/AquaQure fibre coated 0.22 µm nanofibres as illustrated in Figure 3.2. Thenanofibres were then rinsed several times using 10 mL physiological water to wash off all remaining bacterial cells and the wash-off water was plated out on BHI agar plates to determine living cells. This was done after specific contact periods to determine cell death as a function of time. After incubating the plates overnight at 37˚C, colony counting was used to determine the antimicrobial effect of the filters. The experiment was performed for each pathogen and each specific contact period in triplicate. In order to mimic a real life scenario where bacteria species co-exist, 20µL of each pathogen was inoculated into the same tube containing 10mL BHI broth to make a cocktail of the strains and antimicrobial tests were conducted as described previously. Immediately following filtration, some of the samples were fixed in 2.5% (v/v) gluteraldehyde in PBS at 4°C for 4 hours and followed by air drying in preparation for SEM imaging

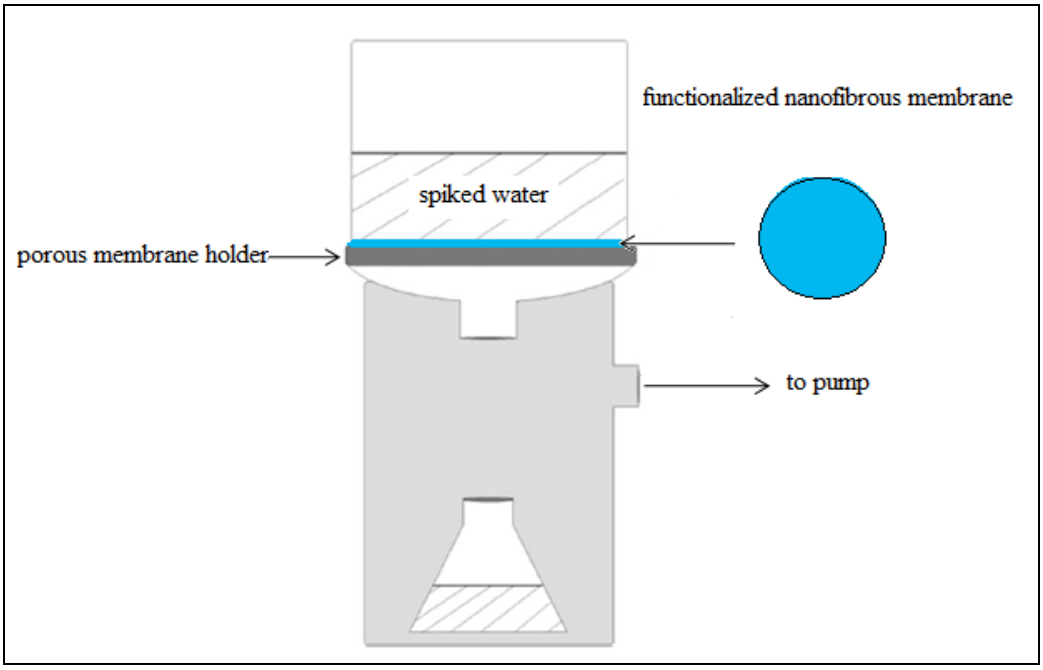

Figure 3.2: **Flow through filtration set-up for determining pathogen removal with electrospun nanofibres.**[32]

3.4.7.2 Bioluminescent imaging (BLI)

Bioluminescent imaging (BLI) is a relatively new development which uses the light emitted from living organisms as a tool for molecular imaging in small laboratory animals. BLI offers a method that is sensitive and innocuous and only allows live or viable cells to be detected. This technique measures cell viability by quantifying total photons emitted by the cells. To use bioluminescence imaging, microorganisms are genetically modified with the *luxABCDE* operon to produce the enzyme luciferase which emits photons in the presence of ATP and oxygen. These photons indicate metabolic activity in the pathogens. Research on BLI corresponded with plate counting data with a correlation efficiency of about 0.98.[33] The same procedure as described in section 3.3.6.1 was used but instead of washing out the filter and plating out, the filter was placed in a XENOGEN VIVO VISION In Vivo Imaging Lumina System (IVIS) supplied by Caliper Life Science and the Living image ® 3.1 Software was used to process them. Imaging was performed immediately after filtering the spiked water through the fibre coatednanofibres and also after 10 minutes exposure to monitor level of bioluminescence emitted by the strains.

3.4.8 Fluorescence experiments

Fluorescence imaging of nanofibres after exposure to spiked water was done to demonstrate the bactericidal effects of the nanofibrenanofibres on viable cells of *K. pneumoniae* Xen 39, *S.aureus* Xen 36, *E.coli* Xen 14, *P. aeruginosa* Xen 5 and *S. typhimurium* Xen 26.

3.4.8.1 Sample preparation

Fibres (10 mg) were exposed to the pathogen cocktail described in section 2.4 along with the appropriate antibiotics overnight on a rotating wheel at 37˚C. After that the fibres were taken out of the media using forceps and rinsed lightly using physiological water.

3.4.8.2 Fluorescent staining

The LIVE/DEAD BacLight kit with SYTO 9 and propidium iodide fluorescent dyes were used (Molecular Probes Inc.). SYTO 9 stains all cells green, while propidium iodide penetrates cells whose cell membrane has been damaged and stains them red. Both reagents are contained in a solution of anhydrous dimethylsulfoxide (DMSO). Viable and total counts can be obtained in one staining step. The intensity of fluorescence is high, with a strong contrast between the red and green cells and background fluorescence is minimal. Staining was done by incubation of samples with 6.5 μM dye at room temperature for 10 min.

3.4.8.3 Microscopy

These samples were then observed on an Olympus Cell^R system attached to an IX-81 inverted fluorescence microscope equipped with a F-view-II cooled CCD camera (Soft Imaging Systems). Using a Xenon-Arc burner (Olympus Biosystems GMBH) as light source, images were excited with the 472 nm or 572 nm excitation filter. Emission was collected using a UBG triple- bandpass emission filter cube. For the image frame acquisition, an Olympus Plan Apo N 60x/1.4 Oil objective and the Cell^R imaging software were used. Images were processed and background-subtracted using the Cell^R software.

3.4.8.4 Regeneration tests

The reusability of a membrane prior to it being replaced is a very important factor in filtration systems. To establish the number of times PVA/AquaQure nanofibres could be used before losing their antimicrobial efficiency, regeneration tests were conducted. This was done by rinsing the fibres with sterile de-mineralised water three times followed by rinsing with physiological water and irradiation with ultra violet light. Thesenanofibres were then reused to filter spiked water as described in previous sections and their antimicrobial effectiveness was measured over six cycles. Morphological changes on the nanofibres were monitored using SEM imaging.

3.4.9 Testing of water stability

In order to determine stability of the electrospun fibres in liquid media, weighed quantities (0.025 g) of the PVA and PVA/AquaQure nanofibre mats were immersed in distilled water at room temperature for 4 hours. These fibres were then blotted dry with tissue paper and weighed to obtain the wet weight

(m_2).[34] The fibres were also left immersed in water for 48 hours, weighed and then viewed under the SEM to observe morphological changes. The water absorbency (Q_{H_2O}) was calculated as follows:

$$Q_{H_2O} = \frac{m_2 - m_1}{m_1} \qquad \textit{Equation 3.1}$$

where Q_{H_2O} is the water absorbency and m_1 and m_2 were the masses of the dry and the wet fibres respectively. Q_{H_2O} was expressed in grams of water per gram of fibres.

3.4.10 Leaching experiments

Studies on the extent of leaching of the constituents of AquaQure were conducted. Nanofibres (100 mg) were immersed in 10 mL distilled water for periods of 1, 6, 12 and 24 hours. The leachates were then analysed using Inductive Coupled Plasma –Atomic Emission Spectroscopy (ICP-AES) on a Varian Radial ICP-AES as well as ultra violet visible (UV-Vis) spectroscopy. The Varian radial ICP-AES and Perkin Elmer Lambda 20 UV-Vis Spectrometer were used to do the analysis. A sample (100 mg) was obtained by electrospinning about 3 mL solution and the concentrations of the leachates were compared to the concentrations of individual ions in Table 3.1. The concentrations of the metal ions leaching out were then compared to the recommended limit for drinking water according to the South African national standards (SANS) shown in Table 3.2.

Table 3.1: Concentrations of individual ions in leachates from three nanofibres with different AquaQure concentration.

Concentration AquaQure (%)	Amount µg/L					
	Cu	**Zn**	**K**	**Ca**	**Na**	**Fe**
5	571	192	0.360	0.386	0.151	0.383
10	1140	384	0.720	0.772	0.302	0.766
15	1710	576	1.08	1.16	0.453	1.15

Table 3.2: Recommended limits for the constituents AquaQure in drinking water (Annexure 1: SANS 241: 2005 drinking water specification).[35]

Determinant	K^+	Ca^{2+}	Cu^{2+}	Zn^{2+}	Fe^{3+}	Na^+
Recommended limit (mg/L)	<50	<150	<1000	<5	<200	<200

3.4.11 The effect of electrospinning variables

To establish the right conditions for the electrospinning process, several parameters which have an effect on the electrospinning process and resultant nanofibre webs were investigated. The following sections describe how each of the parameters were investigated.

3.4.11.1 The effect of biocide concentration

Addition of the biocide solution made the PVA solution visibly less viscous compared to the unmodified control. This triggered an interest to study the effect of the AquaQure ions on the viscosity of the PVA/AquaQure electrospinning mixtures. Therefore, different concentrations (5-15% vol/vol) of AquaQure were added to PVA samples. The viscosity of the samples was then monitored over a period of 15 minutes.

3.4.11.2 The effect of tip-collector distance

The effect of the distance between the tip of the needle and the collector was studied using fibres electrospun from 5% v/v AquaQure, 8% vol/vol glyoxal and 10% wt/v PVA solution. The distances investigated were 10, 15 and 20 cm.

3.4.11.3 The effect of applied voltage

A series of experiments were also carried out to establish whether changing the voltage had any impact on fibre diameter. The electrospun solution had 10% w/w PVA with 8% v/v glyoxal and 5 % v/v AquaQure spun at a distance of 15 cm. The applied voltage was varied from 10 to 20 kV and the tip to target distance was maintained at 15 cm.

3.4.11.4 The effect of crosslinking agent

The concentration of the crosslinking agent present in a polymer is the major parameter of the degree of crosslinking in the resultant polymer matrix. Over crosslinked polymer nanofibres give a smudgy morphology and this has an effect on the surface area and thus the filtration efficiency of the nanofibre mat. The effect of the amount of crosslinking agent (glyoxal) on the fibre diameter and morphology was studied. The time between the addition of glyoxal and the start of electrospinning was varied (1, 3 and 5 minutes) and the resultant fibres were compared. There was no significant difference in the morphology of the fibres and the intermediate time (3 minute) was used for further experiments. Solutions of PVA/AquaQure with different amounts of glyoxal (0.04M PVA/AquaQure: 0.01M glyoxal; 0.04M PVA/AquaQure: 0.002M glyoxal and 0.04M PVA/AquaQure: 0.004M glyoxal) were prepared and electrospun to investigate the effect of varying the OH groups available for crosslinking with glyoxal. The polymer concentrations were in excess to the crosslinking agent and this resulted in ease of the crosslinking reaction between the PVA hydroxyl group and the carbonyl oxygen in the glyoxal.

3.4.11.5 The effect of crosslinking on fibre stability and strength

The effect of crosslinking on the morphological stability of PVA/AquaQure fibres was investigated. The fibre mat was immersed in distilled water for an hour, it was then removed from the water using forceps and pat dried using a paper wipe to remove just enough water to stop dripping (no squashing of fibre mat). The fibre mat was then oven dried for 2 hours at 60°C and gold coated to enhance viewing under the SEM.

3.5 Results and discussion

This section outlines findings of the study and either supports or refutes them based on relevant literature. Results on the optimization of the electrospinning process, morphology of the fibres are discussed in this section. Additionally, chemical, antimicrobial and mechanical results are reported and discussed. Findings on the stability of the fibres in liquid media and their extent of leaching are also reported.

3.5.1 Morphology of the fibres

In this section, findings on the surface morphology of the fibres are reported. This was investigated using SEM and the *SEM_Img_Studio* and *SPIS* softwares.

3.5.1.1 Fibre diameter

Fibre diameter was measured from SEM images using the *SEM_Img_Studio* software. From Figure 3.3A, it is noted that PVA/AquaQure nanofibrous mats had fibres in the 100 to 300 nm diameter range. Although there is no specific diameter range for nanofibrous materials in filter applications, according to the filtration theory, smaller fibre sizes give better filtration efficiency.[36] The smaller fibre result in high surface to volume ratios which are advantageous for filtration application. This was a good property since it increased the surface area for water filtration.

3.5.1.2 Mat porosity

SEM images were also analysed using the SPIS software to determine the pore sizes between the fibres. The average distribution was taken from 10 images for four different ranges (5-50, 51-100, 101-150 and 151-200 nm^2) as illustrated in Figure 3.3B. As shown by this figure, about 70% of the pores were in the 5-50 nm^2 range. The sizes of the mat pores were very important for this study since, for accuracy in measuring antimicrobial efficacy, the pores had to be smaller than the sizes of the studied bacteria strains. The recorded pore sizes were all less than 250 nm^2 and therefore appropriate for further tests.

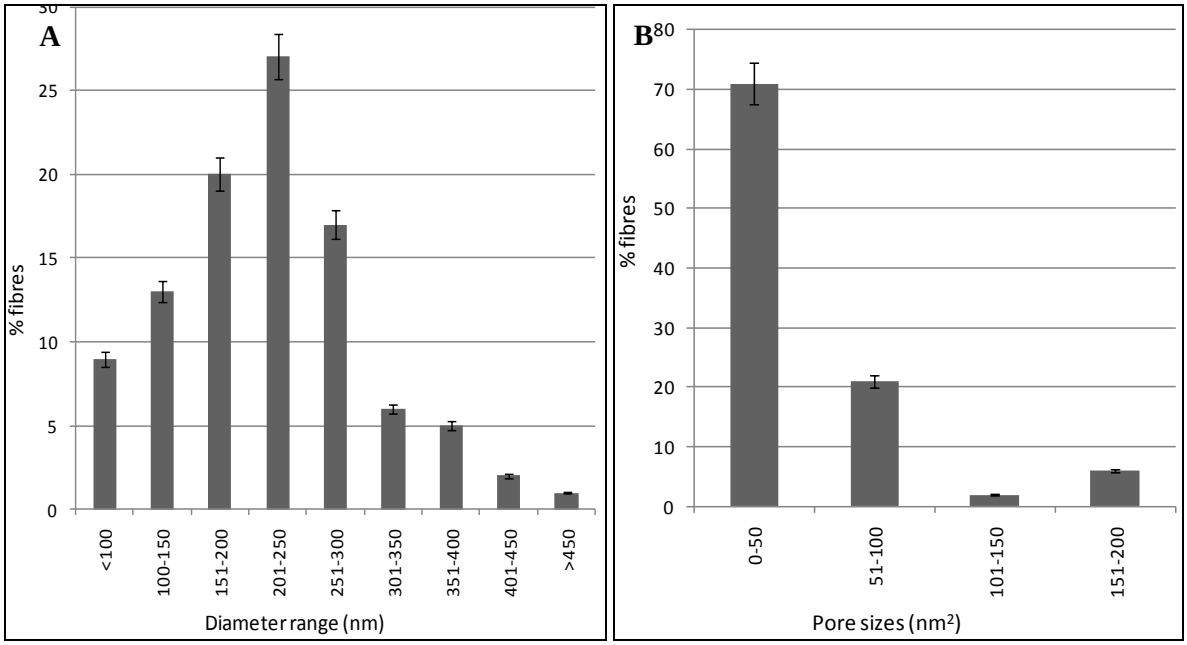

Figure 3.3: Fibre diameters (A) and pore size distribution (B) on PVA/AquaQure nanofibrous mats [10 % wt/vol PVA, 5 % vol/vol AquaQure, 8 % vol/vol glyoxal].

3.5.2 The effect of spinning variables

This section discusses findings on the effects of biocide concentration, voltage, tip-collector distance and the applied voltage on the electrospinning process as well as the morphology of the resultant fibres.

3.5.2.1 The Effect of biocide concentration

It was noted that the viscosity of the polymer solutions with AquaQure decreased with time(Figure 3.4). Another observation made was that viscosity decreases with an increase in the amount of ionic species in solution. This was clearly demonstrated by the low viscosity measurements obtained with the solutions containing 15% vol/vol of AquaQure compared to those containing 5 and 10% vol/vol. After 15 minutes, all the solutions had such a low viscosity that the electrospinning process was not possible and instead of forming a fibre jet from the needle, the polymeric solution was dripping. .

The decrease in viscosity as a result of the presence of multivalent ions in the solution shown by the rheological data can be attributed to chelation. This data agrees with research performed by Moneva and Ivanova who were exploring the feasibility of making PVA/Cu gels.[37] They used 0.01, 0.025, 0.05 and 0.1 molar ratios and obtained the same decrease in viscosity with an increase in salt concentration. The samples were electrospun after 5 minutes and the resultant fibre diameters were compared to observe how ion concentration affects the morphology of the resultant fibres. The graph in Figure 3.5A illustrates that as the concentration of AquaQure increases, the viscosity and fibre diameter decreases.

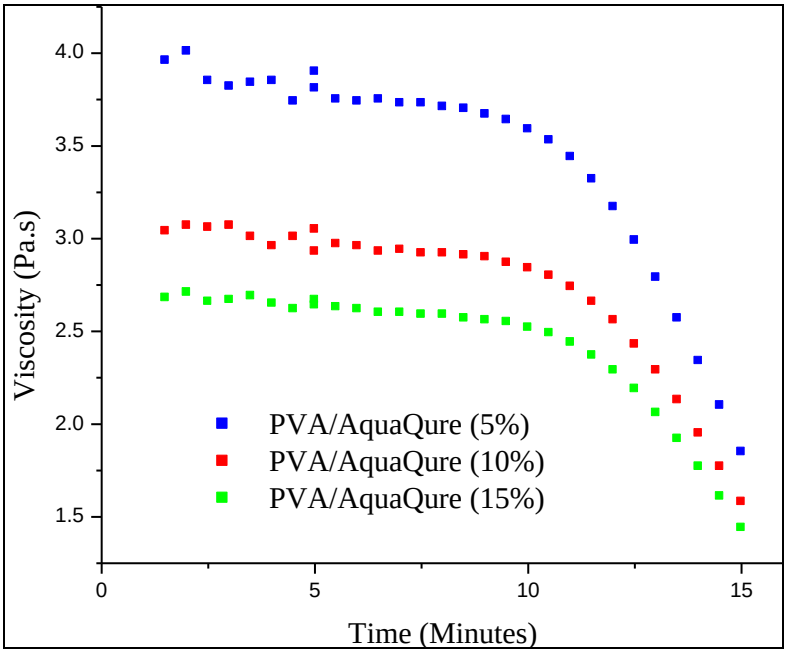

Figure 3.4: Plots of viscosity of PVA/AquaQure electrospinning solutions [10% wt/vol PVA, varying AquaQure concentrations, no glyoxal]

3.5.2.2 The effect of tip-collector distance

The results obtained showed no linear relationship between the tip-collector distance (field strength) and the fibre diameter as illustrated in Figure 3.5B. It is worth mentioning that, when the tip-collector distance is short, the fibres tend to form beads due to the very short solvent evaporation distance, this has also been reported by other researchers.[38, 39]

3.5.2.3 The effect of the applied voltage on fibre diameter

The results in Figure 3.5C indicate that with an increase in the applied voltage there was a slight decreasing tendency in the fibre diameter. This condition was consistent only if extreme care was taken to ensure that the conditions are stable and repeatable, including humidity, temperature and the size of the spinneret orifice. This is also illustrated by the images in Figure 3.6, where an increase in the applied voltage resulted in smaller diameters on the nanofibrous webs. Similar findings on different polymer nanofibres have been reported in literature by other researchers.[40-42]

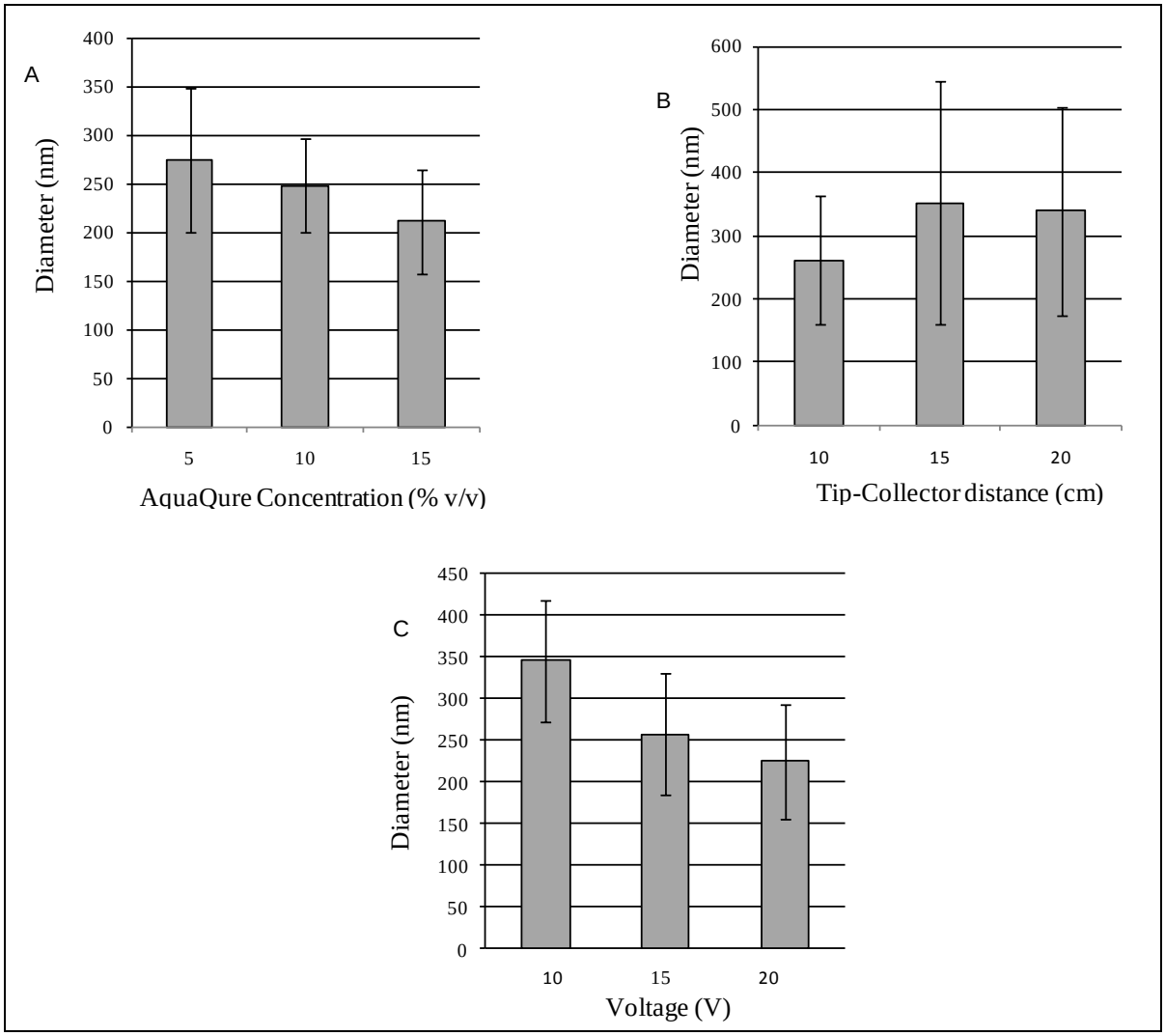

Figure 3.5: Effect of different spinning parameters on fibre diameter (nm) including the AquaQure concentration (% vol/vol) (A), tip-collector distance (cm) (B), and voltage (V) (C).

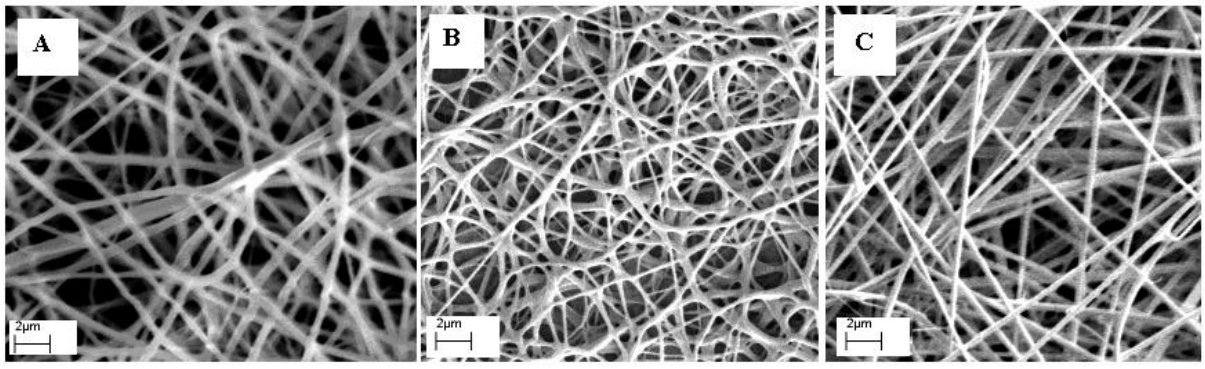

Figure 3.6: PVA/AquaQure fibres electrospun at 10 kV (A), 15 kV (B) and 20 kV (C).

3.5.2.4 The effect of the crosslinking agent

As illustrated in Figure 3.7A, fibres obtained when 0.004M glyoxal was added to the polymeric solution lost their integrity which could mean that the high concentration of glyoxal also made the

solution less viscous thus the solvent (water) did not evaporate enough before hitting the collector. Another explanation for this could be that the crosslinking was already taking place before the electrospinning process began due to the amount of crosslinking agent present in solution and because of this, the whipping action in the region of instability was not enough giving thick fibres.[30]

A decrease in the amount of glyoxal used to crosslink the fibres from 0.004M to 0.002M resulted in well separated fibres with diameters between 200 nm and 800 nm (Figure 3.7B). With only 0.001M glyoxal added the fibres had diameters between 90 and 180 nm. This shows that an increase in the crosslinking agent results in an increase in the diameter of the resultant fibres. This increase in the degree of crosslinking with an increase in the glyoxal concentration was primarily due to the increase in the availability of glyoxal molecules in the vicinity of the PVA chains.[6]

Figure 3.8 shows the effect of the crosslinking agent on the viscosity of the spinning solution as a function of time. Pristine PVA samples had constant viscosities averaging around 3.2 Pa.s. With the addition of the AquaQure, the viscosity went down to about 3.0 and was constant until after 10 minutes where there was a notable decline in the viscosity and the solution mixture became less viscous and after 12 minutes the solution viscosity was around 2.3 Pa.s and could not be electrospun but just dripped from the electrospinning needle. Adding glyoxal (0.001M) on its own increased the viscosity of PVA gradually but when hydrochloric acid was added to enhance the crosslinking process (lower pH) the viscosity of the mixture increased and within about 6 minutes formed a gel and could not be electrospun. From these experiments it was gathered that the polymeric solutions could only be electrospun between 2.5 and 6 Pa.s and this range is marked as elecrospinnable (Figure 3.8).

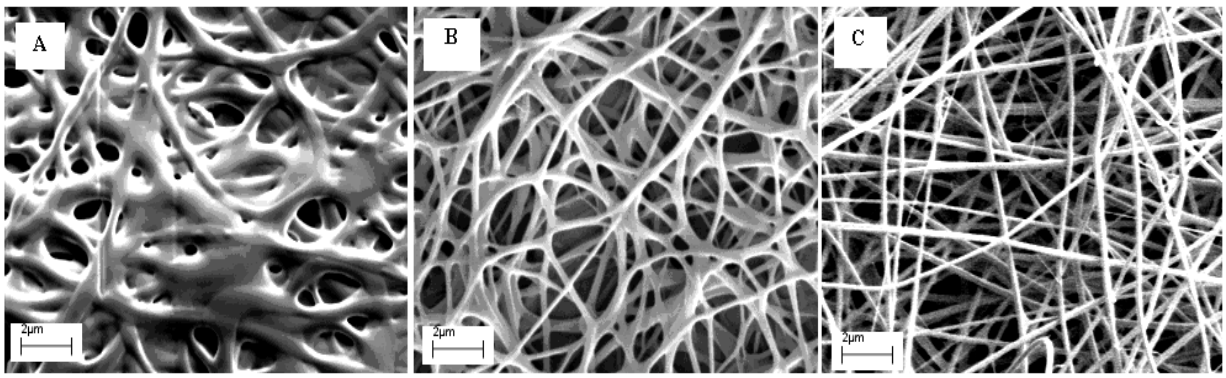

Figure 3.7: Effect of varying the amount of crosslinking agent on the fibre diameter; A: 0.004M glyoxal, B: 0.002M glyoxal and C: 0.001M glyoxal.

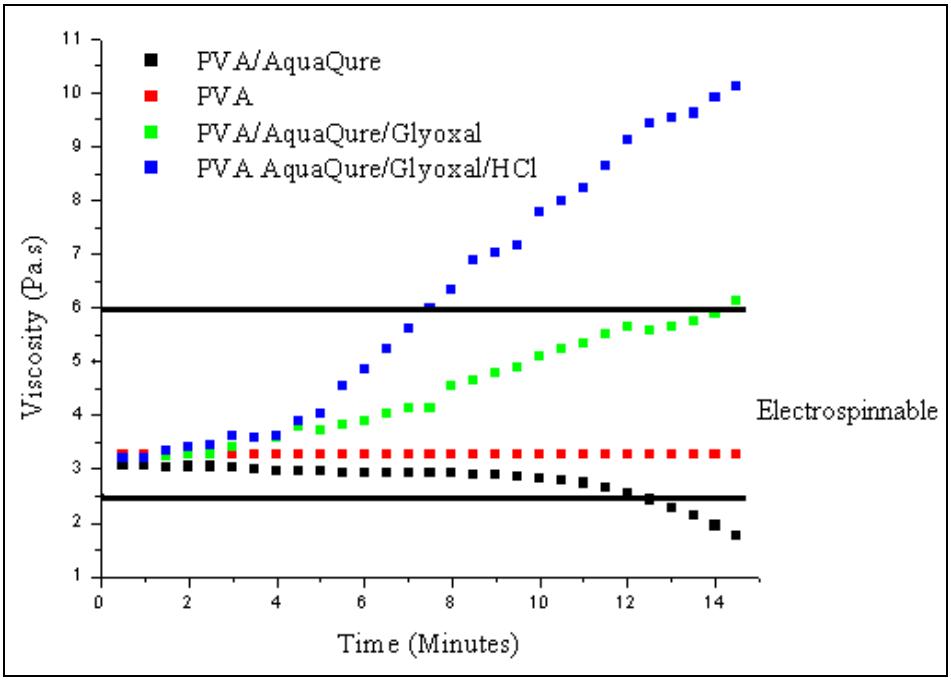

Figure 3.8: Effect of glyoxal on viscosity of PVA/AquaQure mixtures.

3.5.3 Chemical analysis and stability of the electrospun fibres

Chemical analysis and stability tests were carried out on fibres electrospun from the solution with 10% wt/vol PVA, 8% vol/vol glyoxal and 5% vol/vol AquaQure.

3.5.3.1 The effect of crosslinking on fibre stability and strength

Figure 3.9A to D show the morphological differences on the PVA fibres before and after crosslinking. Figure 3.9A illustrates the morphology of the fibres before crosslinking. These fibres were well separated (individual fibres distinct) and quite wide in diameter (average 250-320 nm) compared to its crosslinked counterparts (Figure 3.9C). In Figure 3.9B is an image of the non crosslinked fibres after immersion in water. The fibres show an unstable morphology in that they adopt a ribbon-like morphology and stick together which decreases the porosity of the nanofibre mats to a large extent. Figure 3.9C shows crosslinked PVA/AquaQure nanofibres before submersion in water and Figure 3.9D shows the same fibres after submersion in water. Figure 3.9D indicates that even though the crosslinked nanofibres swell, they do not lose their intact morphology, which leaves the nanofibre sufficiently porous. From these results the crosslinked PVA/AquaQure nanofibres demonstrated stable mechanical properties in liquid media which makes their application in filtration a viable option.

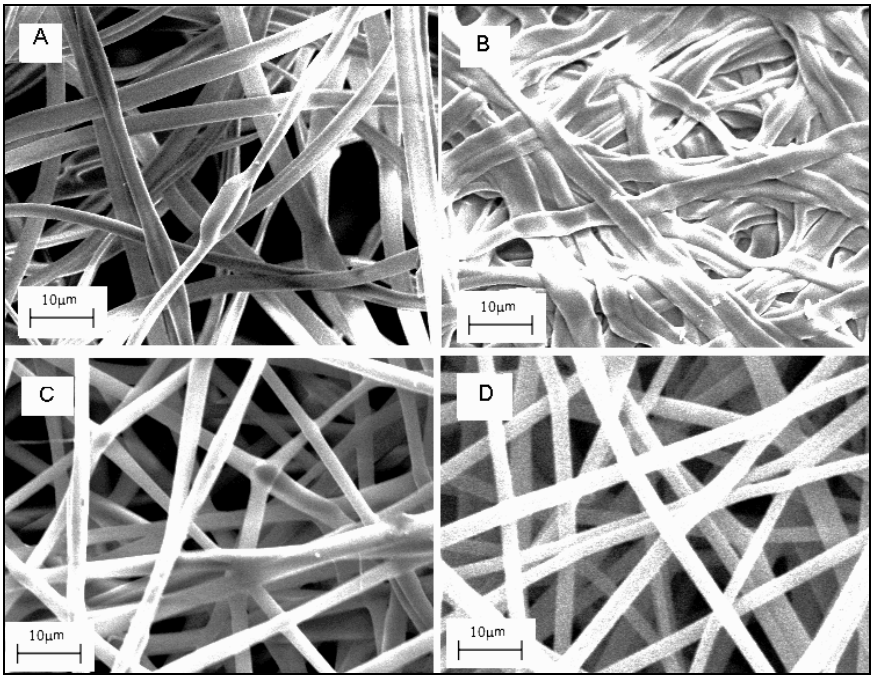

Figure 3.9: **Effect of crosslinking; A: non-crosslinked fibres, B: non crosslinked fibres after submerging in water, C: crosslinked fibres and D: crosslinked fibres after submersion in water.**

3.5.3.2 Energy dispersive X-ray analysis (EDX)

The presence of the constituents of AquaQure on the fibres was demonstrated by EDX (Figure 3.10). This figure shows peaks of Cu, Zn and Fe are present in the spectra. Quantitative EDX results of these ions showed percentage abundances as follows; Cu (17 ±1.43), Zn (11.2 ±1.82) and Fe (6.79 ±3.44). This indicated that these metal ions were successfully incorporated onto the fibres.

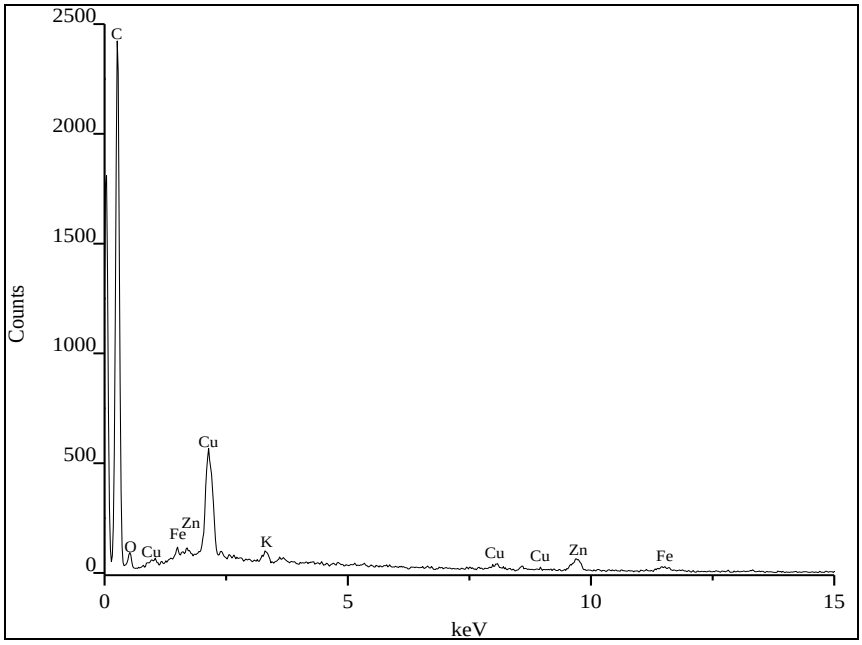

Figure 3.10: **EDX spectrum of PVA/AquaQure fibres.**

3.5.3.3 Attenuated total reflectance infra red spectroscopy (ATR-IR) and X-Ray diffraction (XRD)

In the IR spectra of PVA a broad band at 3,317 cm^{-1} is from hydroxyl groups in PVA (Figure 3.11). Absorptions of asymmetrical and symmetrical stretching of C-H in the PVA backbone are at 2,941 and 2,907 cm^{-1}, respectively. The two peaks at 1,426 and 1,330 cm^{-1} are from the secondary OH in-plane bending and C-H wagging vibrations. Finally, the C-C-C stretching band is presented at 1,144 cm^{-1}. The band centered at 1,094 cm^{-1} represents the C-O stretching vibration of PVA. There are also two carbonyl bands at 1,708 cm^{-1} and at 1,735 cm^{-1}. The shoulder at 1,735 cm^{-1} is from carbonyl group of acetate ion and the band at 1,708 cm^{-1} is from hydroxyl associated carbonyl group of unhydrolyzed acetate. Both signals are not changed by the introduction of AquaQure on the fibres. Of interest is the shift of the O-H broad band from 3,317 cm^{-1} in the case of PVA only to 3,207 cm^{-1} in PVA/AquaQure fibres. This is an indication of the interaction of the PVA with the metal ions in AquaQure.[42]

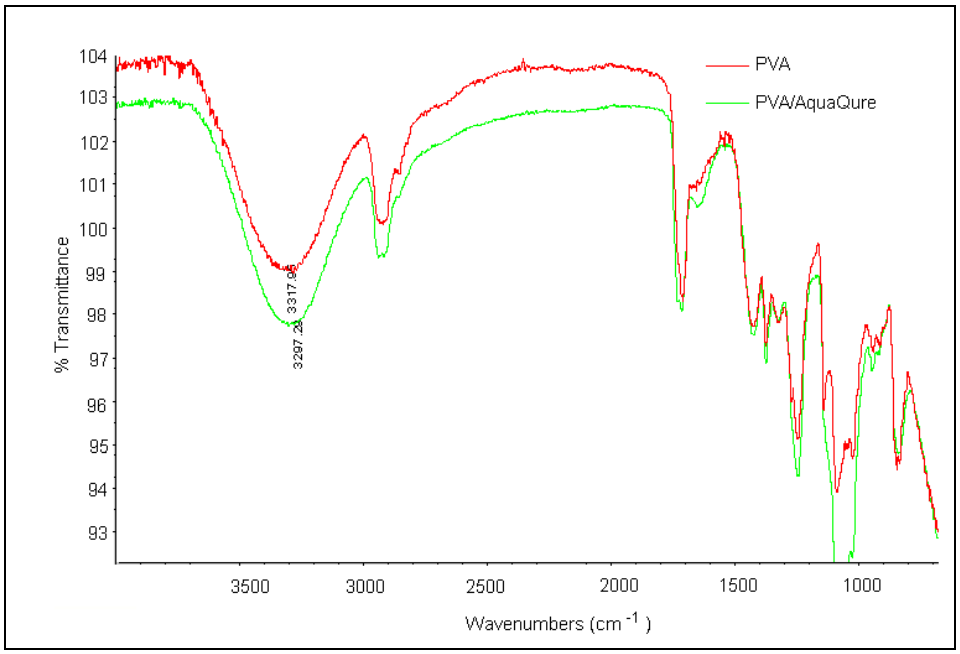

Figure 3.11: ATR-IR spectra of PVA only and PVA/AquaQure nanofibres.

3.5.3.3.1 Thermogravimetric Analysis (TGA) and Differential Scanning calorimetry (DSC)

Thermogravimetric analysis of the crosslinked PVA and PVA/AquaQure nanofibres was performed on a Q500 thermogravimetric analyser to determine their stability as well as to establish the effect of AquaQure on the stability of the fibres. This instrument determines changes in weight in relation to change in temperature, which translates to the ability of the material to withstand high temperatures. Weight loss in % was used over the temperature range 0-900°C. The thermal decomposition of PVA occurs via two steps (Figure 3.12A). The mass loss observed at about 100°C was attributed to moisture loss. The PVA and PVA/AquaQure TGA thermograms show that the same mechanism was involved

in the thermal degradation of both samples. The PVA (unmodified) fibres and PVA/AquaQure fibres both lost a bulk of their weight around 400°C (Figure 3.12A). This indicates that the addition of AquaQure to PVA did not compromise the thermal stability of the fibres.

The DSC thermogram shows a similar trend in heat flow for both the PVA and PVA/AquaQure samples until around 180°C. After 180°C there was a decrease in heat flow for the PVA/AquaQure fibres which could be attributable to the polar interactions of the metal ions in AquaQure with PVA (Figure 3.12B).

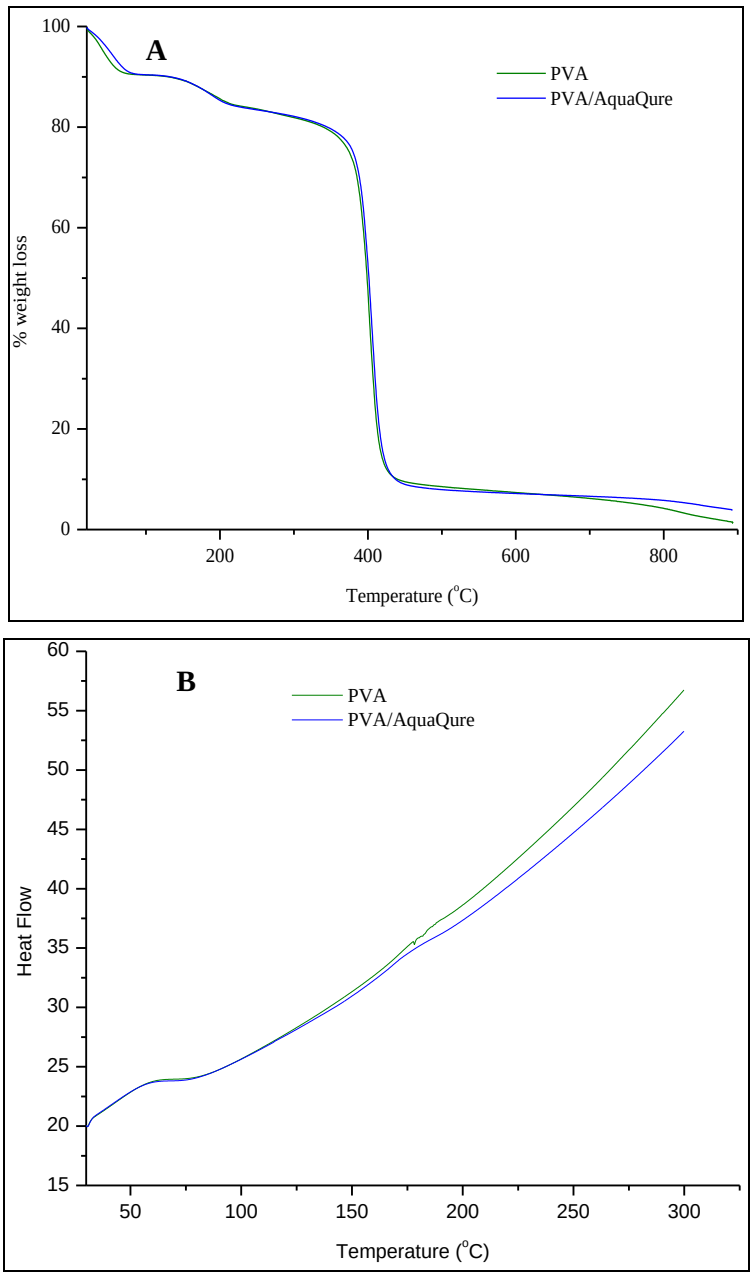

Figure 3.12: **TGA (A) and DSC (B) thermograms comparing stability of PVA only and PVA/AquaQure nanofibres**.

3.5.3.4 X-ray diffraction (XRD)

The X-ray diffraction patterns of PVA and PVA/AquaQure fibres are demonstrated in Figure 3.13. The peaks at 2θ = 17.6° and 23.4° respectively correspond to the (101) and (200) plane of crystalline PVA.[42] The weak peak at 38° corresponds to Cu_2O and matches well with the standard values (JCPDS 78-3288).

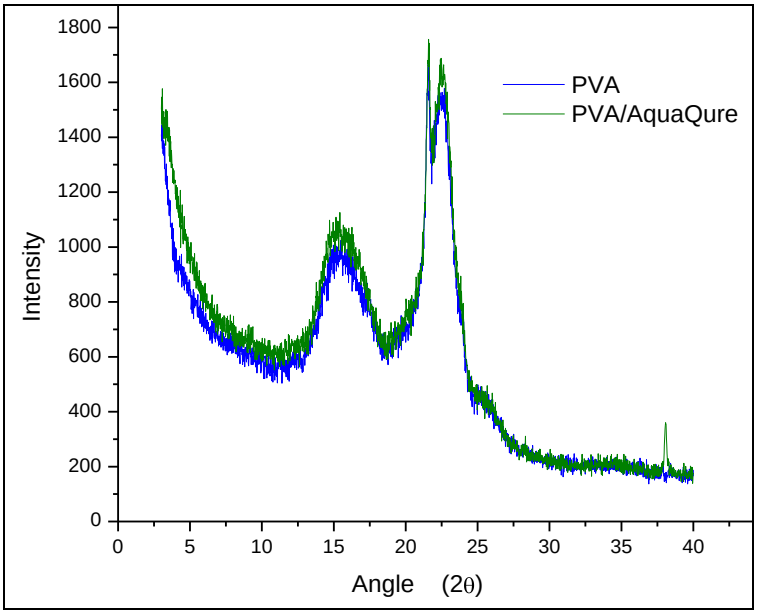

Figure 3.13: XRD spectrum of PVA/AquaQure fibres

3.5.4 Antimicrobial characterization

In this section the findings on antimicrobial characterization are reported. Results from the plate counting, bioluminescence imaging and fluorescence imaging are reported and discussed.

3.5.4.1 Plate counts

The fibres were antimicrobial against the Gram-positive strain *S. aureus* Xen 36 and Gram-negative strains *E. coli* Xen 14, *S. tymphimurium* Xen 26, *P. aeruginosa* Xen 5 and *K. pneumoniae* Xen 39. From Figure 3.14 it is noted that within the first 5 minutes of contact with the PVA/AquaQure fibres, up to 5 log reduction on *E coli* cells took place and at least 4 log reductions was observed on all other strains. After five minutes there was a gradual decrease in cell numbers and after 30 minutes of exposure to the AquaQure treated fibres, *E. coli* Xen 14 was reduced by up to 6 log and all the other strains by more than 5 log. The control experiments performed with PVA only fibres show an almost constant number of cells for all the strains with a few minor fluctuations attributable to cell death due to change of environment and experimental error. These results showed increased antimicrobial efficiency compared to research done on Zn and Cu individually. Grace and co-researchers reported the antimicrobial efficiency of Zn loaded cotton fibres as almost negligible. Reports on the antimicrobial nature of Cu^{2+} have shown up to 3 log reduction in *E. coli* populations.[21, 22] The

PVA/AquaQure nanofibres achieved up to 2 log reductions on mixed cell populations in viable cell counts as illustrated in Figure 3.15. The loss of antimicrobial activity of the strain cocktail compared to individual strains is suspected to be due to the inclusion of *E. coli* and *S. typhimurium* in the mixed culture as reported that this could result in loss of activity.[43]

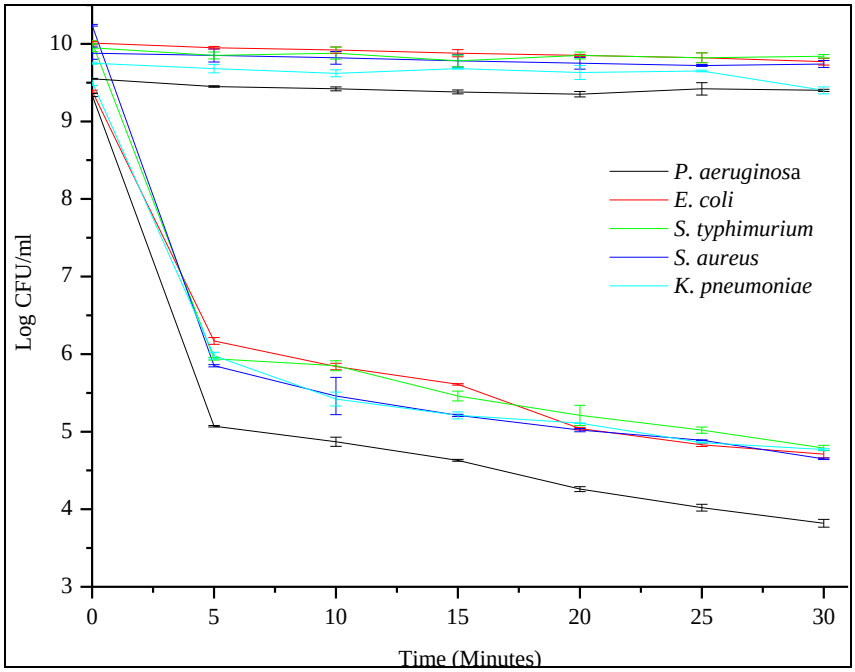

Figure 3.14: Pathogen viability (expressed in CFU/mL) on treated (PVA/AquaQure) and non-treated (controls) nanofibres for individual strains.

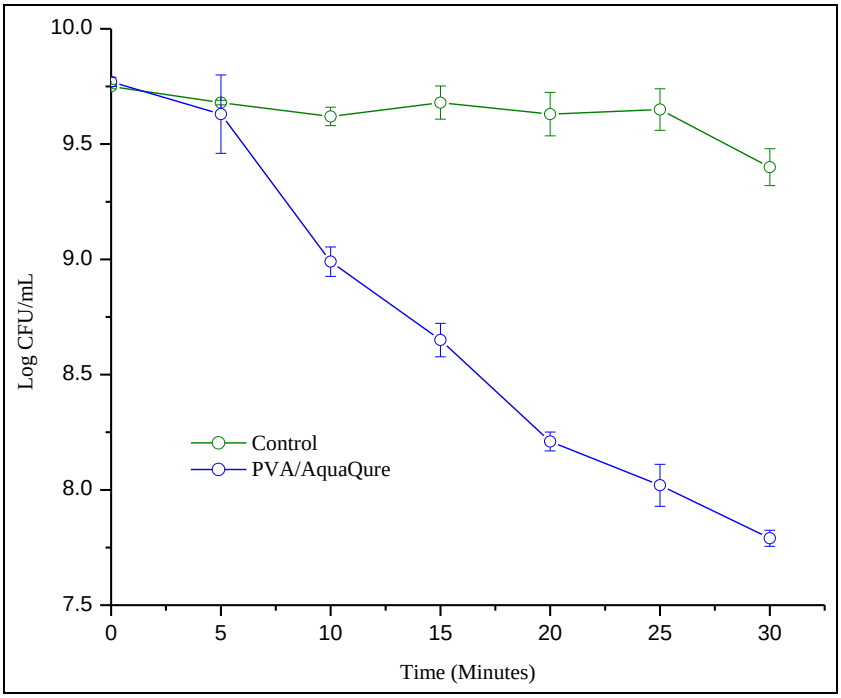

Figure 3.15: Cell viability (expressed in CFU/mL) on treated (PVA/AquaQure) and control (Pristine PVA) nanofibres for strain cocktail.

3.5.4.2 Bioluminescence imaging (BLI)

The results obtained from bioluminescence imaging correlated with the plate counts as shown by the images in Table 3.3. From these results it is noted that that the fibres are indeed antimicrobial. The control experiments done with unmodified PVA fibres did not show any reduction in viable bacterial cells even after 10 minutes of exposure. On the other hand, PVA/AquaQure fibres instantly (1 minute) show reduction in viable cells and further reductions after 10 minutes exposure. *S. tymphimurium* Xen 26 showed more cell bioluminescence (metabolic activity) after 10 minutes compared to the other strains.

Table 3.3: Antimicrobial activity of PVA/AquaQure fibres demonstrated by IVIS imaging.

Strain	PVA		PVA/AquaQure	
	1 minute	10 minutes	1 minute	10 minutes
Pseudomonas aeruginosa (Xen 5)	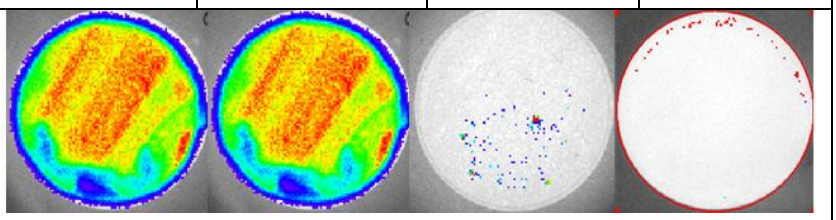			
Escherichia coli (Xen 14)	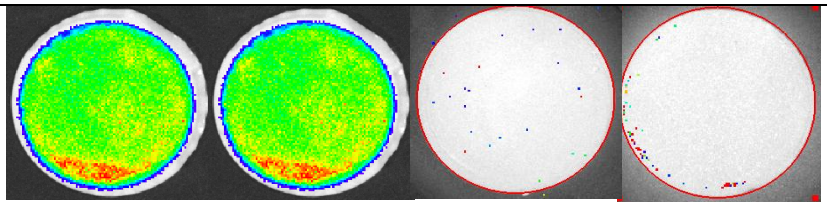			
Salmonella typhimurium (Xen 26)	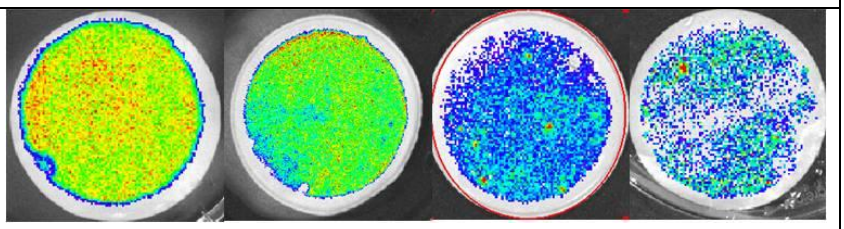			
Staphylococcus aureus (Xen 36)	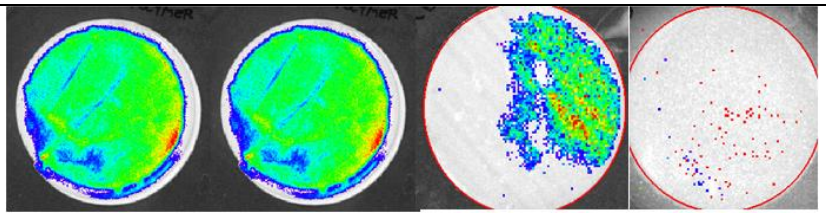			
Klebsiella pneumoniae (Xen 39)	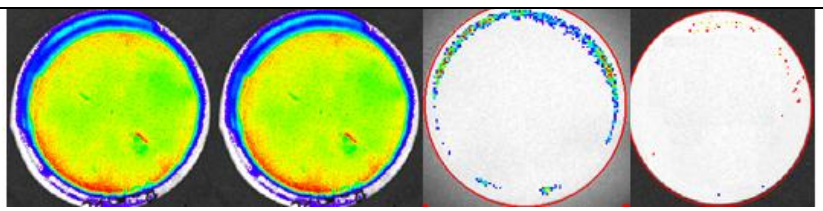			

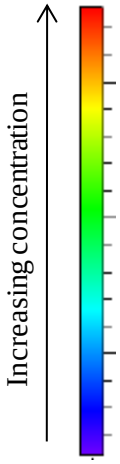

3.5.4.3 Fluorescence microscopy

The results from fluorescence microscopy further confirmed the antimicrobial capability of the AquaQure treated fibres (Figure 3.16). It needs to be stressed that the fibres absorb some of the dyes as well. Colonies are the brightly coloured dots appearing over the surface of the fibres. The control fibres showed numerous attached colonies (A) which did not absorb propidium iodide (B) indicating that they were alive. Whereas in the case of AquaQure treated fibres, the colonies observed in C almost all absorbed propidium iodide showing that their cell membranes were damaged as shown in D. This is a good indication of the antimicrobial effectiveness of AquaQure containing fibres in decreasing bacteria colonies on fouled surfaces.

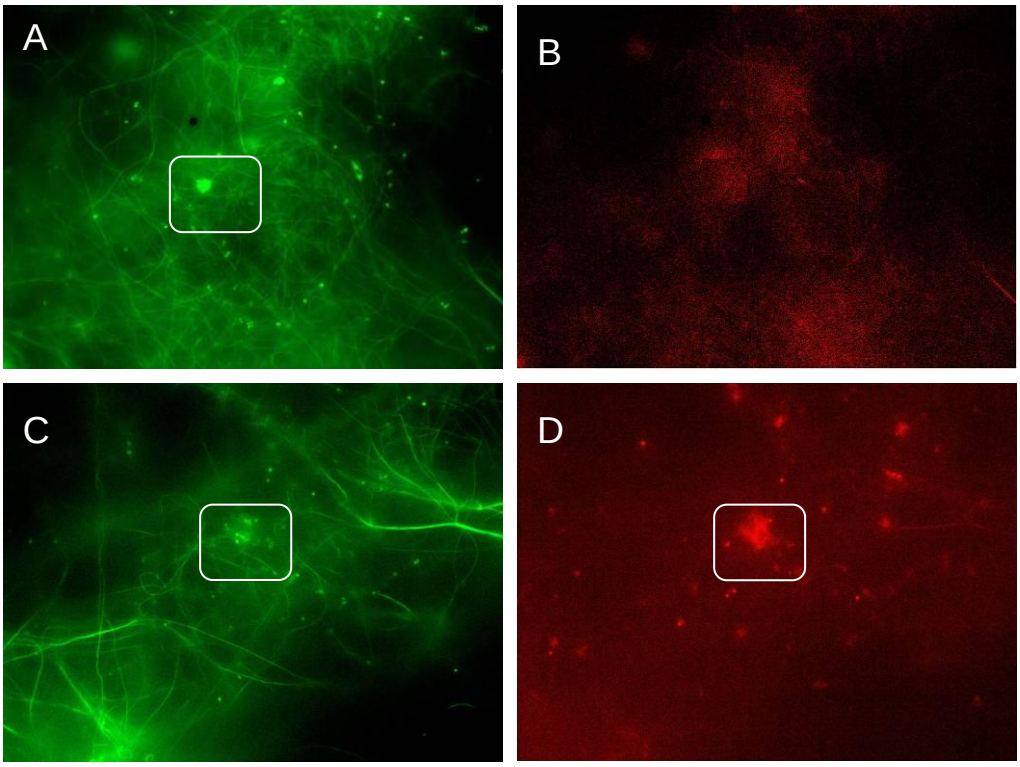

Figure 3.16: Fluorescence Microscopy images showing (A) total number of colonies in control fibres (PVA only); (B) Dead colonies (none) in control fibres; (C) total number of colonies in AquaQure treated fibres and (D) Dead colonies (almost all dead) in AquaQure treated fibres.

** The fibres also absorb some of the dye

3.5.5 Scanning electron microscopy (SEM)

The fibres were also viewed under the SEM to ascertain the morphology of the bacterial strains after contact with the treated fibres. SEM imaging confirmed the damaged (collapsed) cell membranes as predicted by fluorescence microscopy results (Figure 3.17). This collapse in cell membrane integrity could be due to reduction in osmotic pressure as reported also by Sheikh and co researchers .[19]

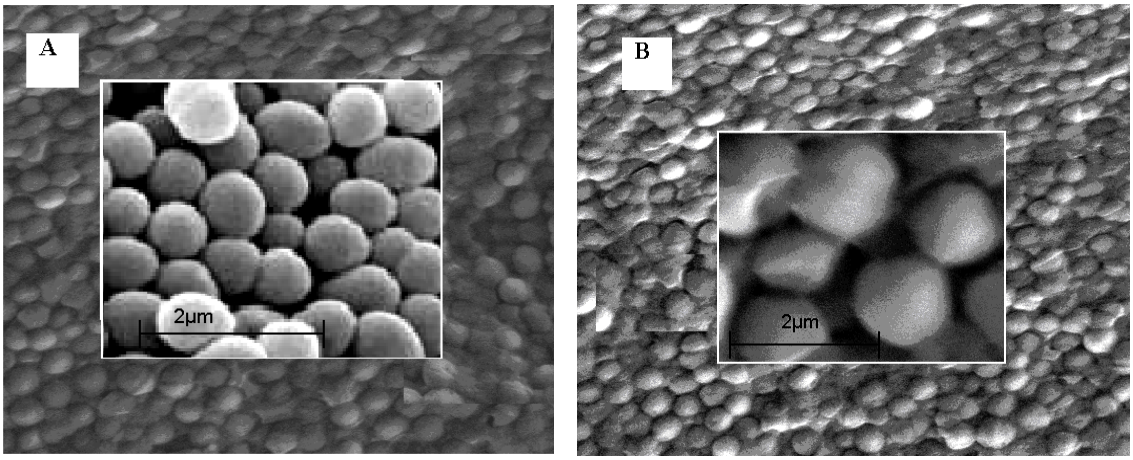

Figure 3.17: SEM image showing intact (A) cells in contact with pristine PVA fibres and damaged bacterial cell walls (B) in contact with AquaQure treated fibres.

3.5.6 Regeneration studies

PVA/AquaQure nanofibres showed a decline in antimicrobial activity from almost 5 log reduction in the first cycle to around 2.5 log reductions in the second. This 2 log decrease was sustained over the third cycle. The fibres then gradually lost antimicrobial activity as well as their morphological integrity over subsequent cycles. There were 10 times less bacteria cells (1 log reduction) after 6 cycles compared to 100 000 times less after the first cycle. These results demonstrate that the current nanofibres can only be used once for reducing bacteria to acceptable drinking water levels. Figure 3.18 shows the antimicrobial effectiveness of the nanofibres over the 6 cycles and Figure 3.19 shows morphological differences between PVA/AquaQure nanofibres before the first cycle and after the sixth cycle.

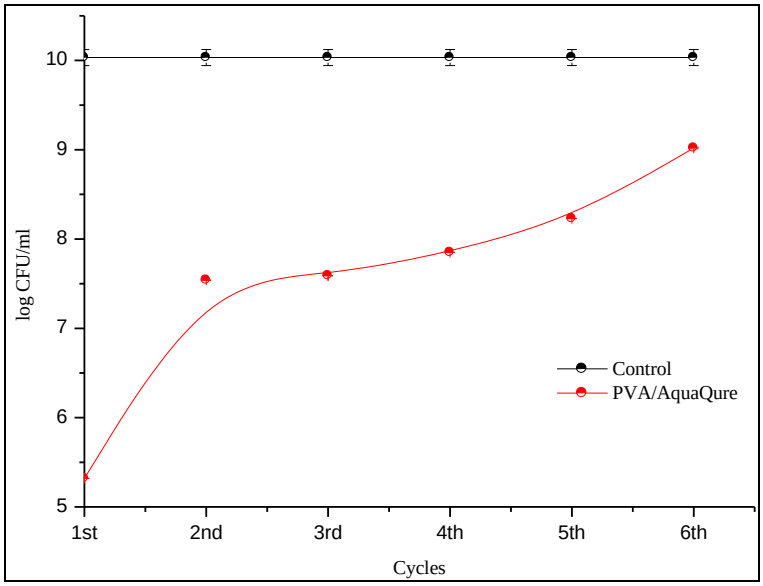

Figure 3.18: Antimicrobial effectiveness of PVA/AquaQure nanofibres over six cycles.

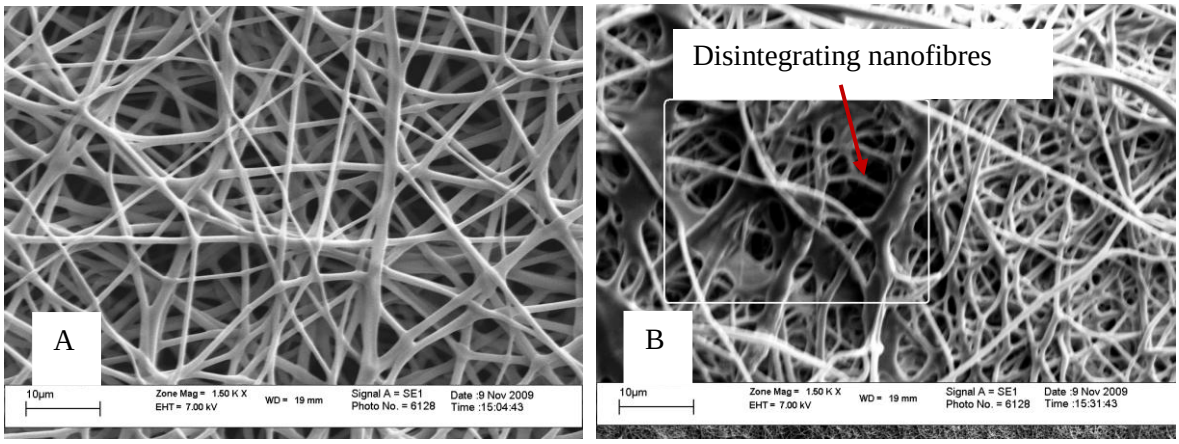

Figure 3.19: Morphology of nanofibres before (A) and after (B) antimicrobial tests.

3.5.7 Water Stability

Water stabilities of the unmodified and PVA/AquaQure nanofibres were studied using SEM after drying at 60˚C. The unmodified fibres showed up to 184 % swelling degree and remained stable even after 48 hours of immersion. Modification of the fibres with AquaQure did not alter the stability of the fibres in water and this was evidenced by the 189 % swelling degree even after 48 hours of exposure (Table 3.4). Figure 3.20 shows SEM images of the fibres before and after being exposed to water for 48 hours. The control fibres (PVA only) did not increase too much in diameter but became more round whereas the PVA/AquaQure nanofibres showed a slight increase in diameter as well as the more rounded morphology. Both PVA and PVA/AquaQure fibres retained their morphology after 48 hours of exposure to water. Improvements on the crosslinking of thesenanofibres is also necessary to eliminate the swelling behavior which could compromise the membrane lifecycle in water filtration applications.

Table 3.4: Properties of unmodified PVA and PVA/AquaQure nanofibres after water immersion.

Sample	**Dry mass**	**Wet mass**	**absorbed H_2O**	**Q_{water} (g/g)**	**SD %**
Unmodified PVA	0.0251±0.0002	0.0714±0.001	0.0463±0.001	1.84±0.01	184±1
PVA/AquaQure	0.0252±0.0002	0.0728±0.001	0.0476±0.001	1.89±0.015	189±1.5

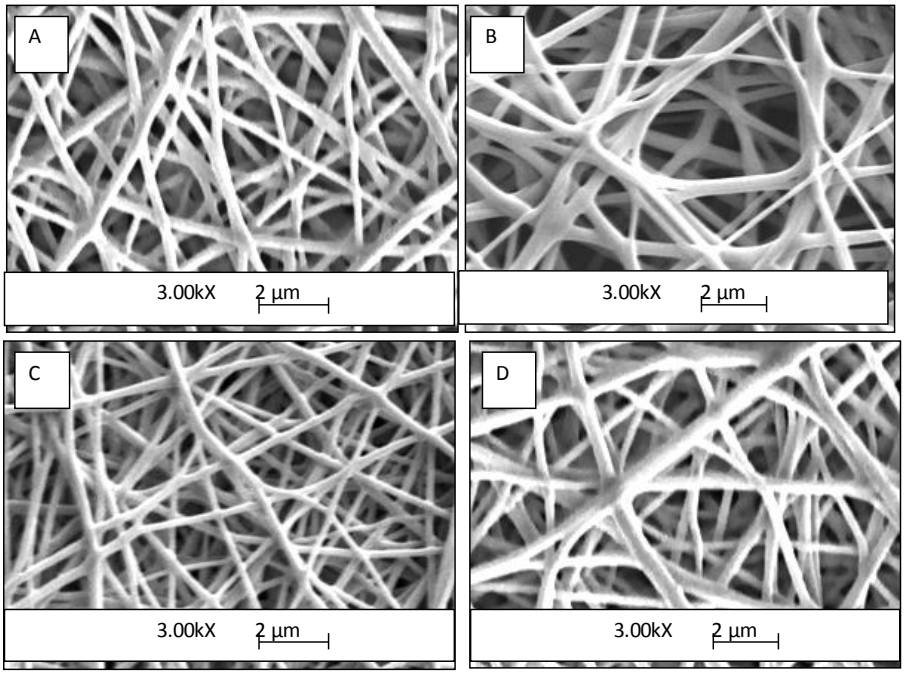

Figure 3.20: SEM images of the fibres: A, PVA only before water absorption; B, PVA only after water absorption; C. PVA/AquaQure before water absorption D, PVA/AquaQure after water absorption.

3.5.8 Leaching experiments

The ICP-AES results showed very low amounts of the metal ions Cu^{2+}, Zn^{2+},Ca^{2+}, K^{+}, Fe^{3+} and, Na^{+} ions which ranged between 0 to $1.1x10^{-4}$ g/L which equals 0.01 to 0.03% for all the metal ions. Figure 3.21 shows a steady increase in the concentration of the ionic species leaching into the water which stabilized after 10 hours. The leaching of the biocide to filtered water was negligible. With the dangers associated with metal ions in drinking water, the minimal leaching of the constituents of AquaQure was a pointer in the right direction. This makes the PVA/AquaQure fibres safe to use in filter media without fear of AquaQure leaching out into the water. The measured concentrations adhere to the SANS guidelines for drinking water.[35]

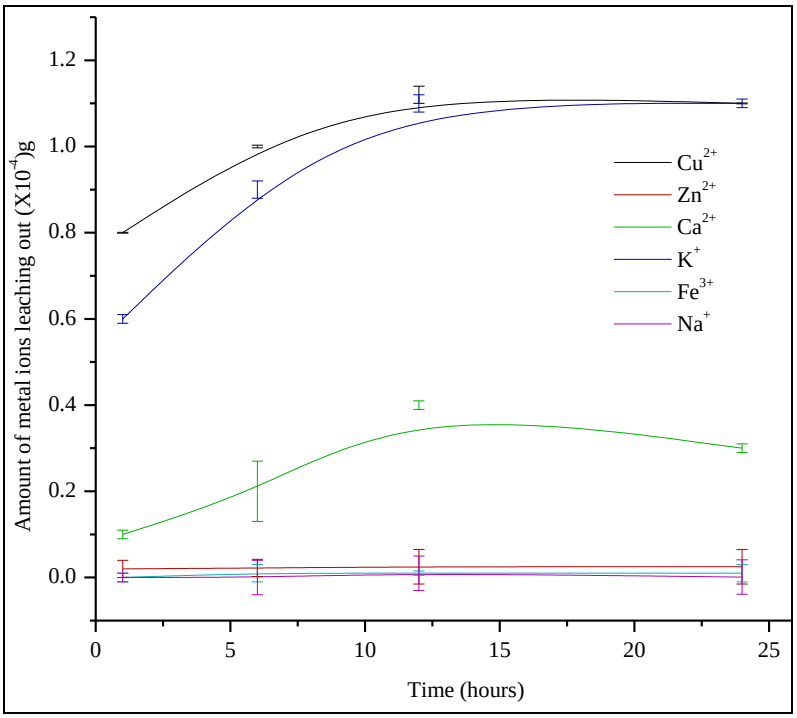

Figure 3.21: Leaching intensities of ions.

The ICP-AES results were further confirmed by UV-Vis results which showed an absorption band at 300 nm for AquaQure and none of the leachates exhibited the band. This suggests that the metal ions in AquaQure were most likely complexed to the OH bonds of PVA (Figure 3.22).[37]

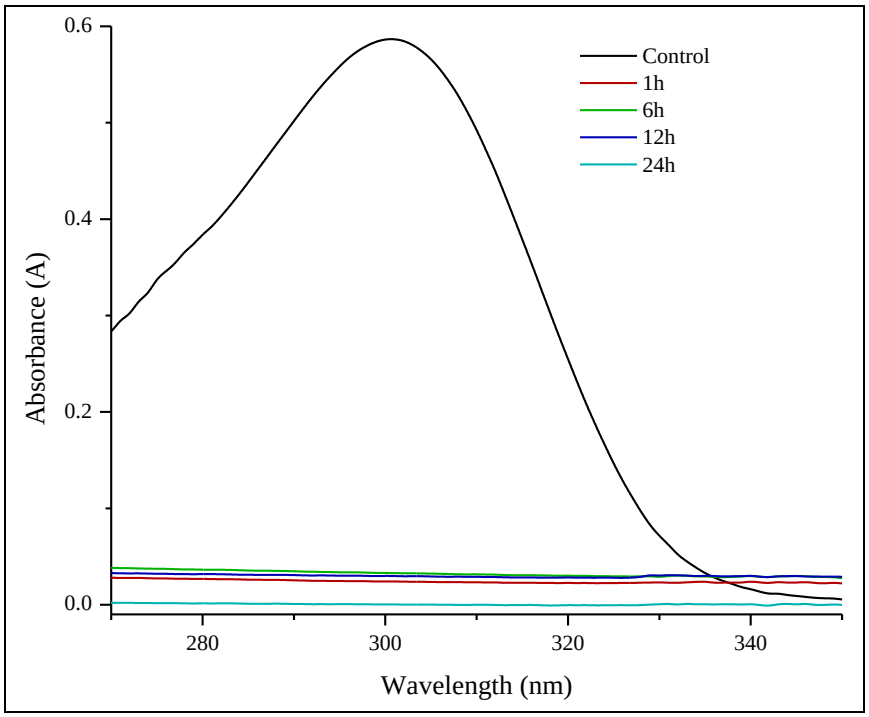

Figure 3.22: UV-VIS Spectra of leachates.

3.6 Conclusions

PVA/AquaQure fibres were successfully produced using the electrospinning technique. It was observed that under controlled conditions there is a linear relationship between the voltage and the fibre diameter as well as between concentration of AquaQure and fibre diameter. There is however no linear relationship between the spinning distances (field strength) and the fibre diameter. From the PVA/AquaQure fibres evaluated in this study, the fibre diameter reaches a maximum at a spinning distance of 15 cm. About 90% of the nanofibres had diameters less than 300 nm and about 70% of the pores were in the 5-50 nm^2 range. Successful incorporation of the biocide was ascertained by the existence of the constituents of AquaQure on surfaces of the nanofibres which was shown by EDX studies. Crosslinking improves the water resistance of PVA/AquaQure fibres without compromising the thermal and chemical stability of the PVA/AquaQure nanofibres. The non-crosslinked PVA/AquaQure fibres dissolved in water and resulted in dramatic loss in porosity of the nanofibres and morphology change. With crosslinking however, insolubility in water was achieved. This water-insoluble property would give PVA/AquaQure fibres good potential for water filtration applications.

Antimicrobial tests on the fibres against the Gram-positive strain *S. aureus* Xen 36 and Gram-negative strains *E. coli* Xen 14, S. *typhimurium* Xen 26, *P. aeruginosa* Xen 5 and *K. pneumoniae* Xen 39 showed up to 5 log reductions in bacteria populations when compared with unmodified PVA fibres. The antimicrobial tests were confirmed with bioluminescent imaging and LIVE/DEAD Baclight to determine the antimicrobial efficiency against viable but non-culturable (VNBC) cells. This was done to quantify the cells that enter a dormant state during contact with the antimicrobial fibres and to eliminate the changes of overestimating the antimicrobial efficiency of the nanofibres. These techniques further confirmed the results obtained by plate counting. The fibres also demonstrated stability in water and only up to about 190% absorption of water without disintegration even after 48 hours. Leaching experiments showed leachate concentrations between 0 to $1.1x10^{-4}$ g/ml for all the ions after 24 hours of exposure.

From the findings of this study, the concept of incorporating biocides in nanofibres showed potential for application in filter media. For application in filtration media, these nanofibres still need improvents in their mechanical properties to eliminate swelling which could lead to shorter membrane life should the nanofibres be used in membrane filtration. Further studies on the immobilization of the metal ions on the surface of the nanofibres are also necessary to completely eliminate leaching and possibly give permanent antimicrobial efficacy over many cycles.

References

1. Chirowodza H. Synthesis and characterization of cationically and anionically modified poly(vinyl alcohol) microfibrils. Stellenbosch University, Stellenbosch, 2009.
2. Finch C.A., *Polyvinyl Alcohol: Properties and applications*. John Willey and Sons: London 1973.
3. Liou E.J.; Wang Y.J. *Journal of Applied Polymer Science* **1996,** 59, 1395-1403.
4. Choi J.H.; Cho Y.W.; Ha W.S.; Lyoo W.S.; Lee C.J.; Ji B.C.; Han S.S.; Yoon W.S. *Polymer International* **1998,** 47, 237-242.
5. Chen C.; Wang F.; Mao C. *Journal of Applied Polymer Science* **2007,** 105, 1086-1092.
6. Chirowodza H.; Sanderson R.D. *Macromolecular Materials and Engineering* **2010,** 295, 1009-1016.
7. Garrett P.D.; Grubb D.T. *Polymer Communications* **1988,** 29, 60.
8. Su J.; Wang Q.; Wang K.; Zhang Q.; Fu Q. *Journal of Applied Polymer Science* **2008,** 107, 4070-4075.
9. Lee Y.J.; Shin D.S.; Kwon O.W.; Park W.H.; Choi H.G.; Lee Y.R.; Han S.S; Noh S.K.; Lyoo W.S. *Journal of Applied Polymer Science* **2007,** 106, 1337-1342.
10. Reisa E.F.; Campmposa F.S.; Lagea A.P.; Leitea R.C.; Heneineb L.G.; Vasconcelosc W.L.; Lobatoa Z.I.; Mansurc H.S. *Materials Research Bulletin* **2005,** 9, 185-191.
11. Finch C.A., *Polyvinyl Alcohol: Developments*. John Willey and Sons: London 1992.
12. Ruiz J.; Mantecón A.; Cádiz V. *Polymer* **2001,** 42, 6347- 6354.
13. Kumeta K.; Nagashima I.; Matsui S.; Mizoguchi K. *Journal of Applied Polymer Science* **2003,** 90, 2420-2427.
14. Liu S.; Sun G. *Carbohydrate Polymers* **2008,** 71, 614-625.
15. Voigt W.V. Water stable, antimicrobial active nanofibres generated by electrospinning from aqueous spinning solutions. RWTH Aachen University, Munich, 2009.
16. Ramakrishna S.; Fujihara K.; Teo T.; Yong Z.; Ma R.R. *Materials Today* **2006,** 9, 40-50.
17. Lufrano G.; Brown J. *Total Environment* **2010,** 408, 5254-5264.
18. Anshup T.P. *Thin Solid Films* **2009,** 517, 6441-6478.
19. Sheikh F.A.; Kanjwal M.A.; Saran S.; Chung W-J.; Kim H. *Applied Surface Science* **2011,** 257, 3020-3026.
20. Wang H.; Lu X.; Zhao Y.; Wang C. *Materials Letters* **2006,** 60, 2253-2253.
21. Grace M.; Chand N.; Bajpai S.K. *Journal of Macromolecular Science Part A* **2008,** 45, 795-803.
22. Grace M.; Chand N.; Bajpai S.K. *Journal of Engineered Fibers and Fabrics* **2009,** 4, 24-35.
23. Borkow G.; Gabbay J. *Current Chemical Biology* **2009,** 3, 272-278.

24. Nan L.; Liu Y.; Lu M.; Yang K. *Journal of Materials Science: Materials in Medicine* **2008,** 19, 3057-3062.
25. Ohsumi Y.; Kitamoto K.; Anraku Y. *Journal of Bacteriology* **1988,** 170, 2676-2682.
26. Potera C. *Environmental Health Perspectives* **2004,** 112, A568-A569.
27. Singh M.; Singh S.; Gambhir P.S. *Digest Journal of Nanomaterials and Biostructures* **2008,** 3, 115 - 122.
28. Osman D.; Cavet J.S. *Advances in Microbial Physiology* **2011,** 58, 175-232.
29. Zhang Y.; Zhu P.C.; Edgren D. *Journal of Polymer Research* **2009**, 1-6.
30. Ramakrishna S.; Fujihara K.; Teo W-E.; Lim T-C.; Ma Z., *An Introduction to Electrospinning and Nanofibres*. World Scientific Publishing Co. Pte. Ltd.: Toh Tuck Link, Singapore, 2005.
31. Aydilek A. *Journal of Computation in Civil Engineering* **2002**, 280-290.
32. Daels N.; De Vrieze S.; Sampers I.; Decostere B.; Westbroek P.; Dumoulin A.; Dejans P.; De Clerck K.; Van Hulle S.W.H. *Desalination* **2011**.
33. Francis D.L.; Visvikis D.; Costa D.C. *European Journal of Nuclea and Medical Molecular Imaging* **2003,** 30, 988-994.
34. Liu Z.X.; Miao Y.G.; Wang Z.Y.; Yin G.H. *Polymer* **2009,** 77, 131-135.
35. SANS 241, *South African National Standards-Drinking Water*. 6th ed.; ISBN 0-626-17752-9: South Africa, 2005.
36. Yun K.M.; Suryamas A.B.; Iskandara F.; Bao F.L.; Niinuma H.; Okuyama K. *Separation and Purification Technology* **2010,** 75, 340-345.
37. Moneva L.I.; Ivanova K.H. *Polymer Science USSR* **1990,** 32, 2054-206.
38. Bölgen N.; Menceloglu Y.Z.; Acatay K.; Vargel I.; Piskin E. *Journal of Biomaterial Science* **2005,** 16, 1537-1555.
39. Deitzel J.M.; Kleinmeyer J.; Harris D.; Beck Tan N. *Polymer* **2001,** 42, 261-272.
40. Demir M.M.; Yilgor I.; Yilgor E.; Erman B. *Polymer* **2002,** 43, 3303-309.
41. Ding B.; Kim H.Y.; Lee S.C.; Shao C.L. *Journal of Poymer Science. Part B: Polymer Physics* **2004,** 40, 1261-268.
42. Xu J.; Cui X-J.; Zhang J.; Liang H-W.; Wang H-Y.; Li J-F. *Bulletin of Materials Science* **2008,** 31, 189-192.
43. Fukuda T.; Yamamo S.; Morita H. *World Journal of Microbiological Biotechnology* **2008,** 241, 893-1899.

Chapter 4: The fabrication and characterization of antimicrobial copper functionalized nanofibres from poly(vinyl alcohol) and poly(styrene-co-maleic anhydride) via bubble electrospinning

4.1 Chapter Summary

The bactericidal effects of copper and its compounds have been known for centuries and the incorporation of copper compounds on various materials has been widely reported.[1-3] Most of these works however focused on the use of copper in wound dressing and other medical applications as well as its use in agricultural settings.[4-6] However, very few reports are available on the immobilization of copper compounds on surfaces with the aim of the purification of water supplies.[7] In this chapter, the fabrication and functionalization of nanofibre mats from poly(vinyl alcohol) (PVA) and poly(styrene-co-maleic anhydride) (SMA) are reported. These nanofibre mats were fabricated through blending of bactericidal copper salts to spinning solutions and electrospinning them to produce fibres in the nanometer range using bubble electrospinning. Bubble electrospinning is a high-throughput version of the conventional needle based electrospinning technique.

The effects of the modification of the polymers, electrospinning, antimicrobial tests as well as leaching of copper ions are presented in this chapter. The antimicrobial activities of copper containing PVA and SMA against bioluminescent strains of *Klebsiella pneumoniae* Xen 39, *Staphylococcus aureus* Xen 36, *Escherichia coli* Xen 14, *Pseudomonas aeruginosa* Xen 5 and *Salmonella typhimurium* Xen 26 were obtained through plate counting. To determine the antimicrobial efficiency against viable but non-culturable (VNBC) cells (that enter a dormant state during contact with the antimicrobial fibres), bioluminescent imaging and LIVE/DEAD Baclight were used in order to eliminate the chances of overestimating the antimicrobial efficiency of the nanofibres. Leaching experiments were conducted to ascertain the amounts of the constituents of the biocide from the fibres. For purposes of the intended application of these nanofibres (drinking water), these figures were then compared with the South African national standards (SANS) for drinking water.

4.2 Introduction

Preparation of metal ions and nanoparticles dispersed in polymer nanofibres has drawn great attention because these kinds of nanocomposites combine the unique properties of metal particles with the outstanding characteristics of polymer nanofibres which include among others, the high specific surface area and high interpenetrating capacity available to other materials.[8] The metal/polymer nanocomposites are expected to provide potential applications as catalysts, photonic and electronic

sensors, filters, and artificial tissue.[9] The inclusion of metal salts in electrospun fibres has been reported by a number of researchers.[10-22] The antimicrobial nature of transition element metal salts is well researched. [9] Modification of nanofibres using metal salts like silver, copper, zinc has received a lot of attention over the past decade due to their bactericidal properties. The focus on these studies however has been directed towards medical applications. In this study, the bactericidal nature of copper was evaluated for applicability in filter media. The following subsections discuss historical background, antimicrobial properties of copper and its compounds as well as some theory on the blending of polymers with copper ions.

4.2.1 Antimicrobial properties of Copper

The antimicrobial nature of copper is not a new phenomenon, copper has been used as a biocide for centuries.[2, 4] In ancient Egypt (2000 BC), copper was used to sterilize water and wounds. The ancient Greeks in the time of Hippocrates (400 BC) prescribed copper for pulmonary diseases and for purifying drinking water.[2] The antifungal properties of copper are also well documented and date back to 1761, when it was discovered that copper sulphate inhibited seed-borne fungi.[2] These attributes have triggered the interest of many researchers around the globe to come up with copper-based polymeric materials applicable in various applications such as antibacterial and antifungal agents. Copper and its compounds have also been coated onto or incorporated into various materials for various applications including filter media (Figure 4.1).[1, 2, 23-26]

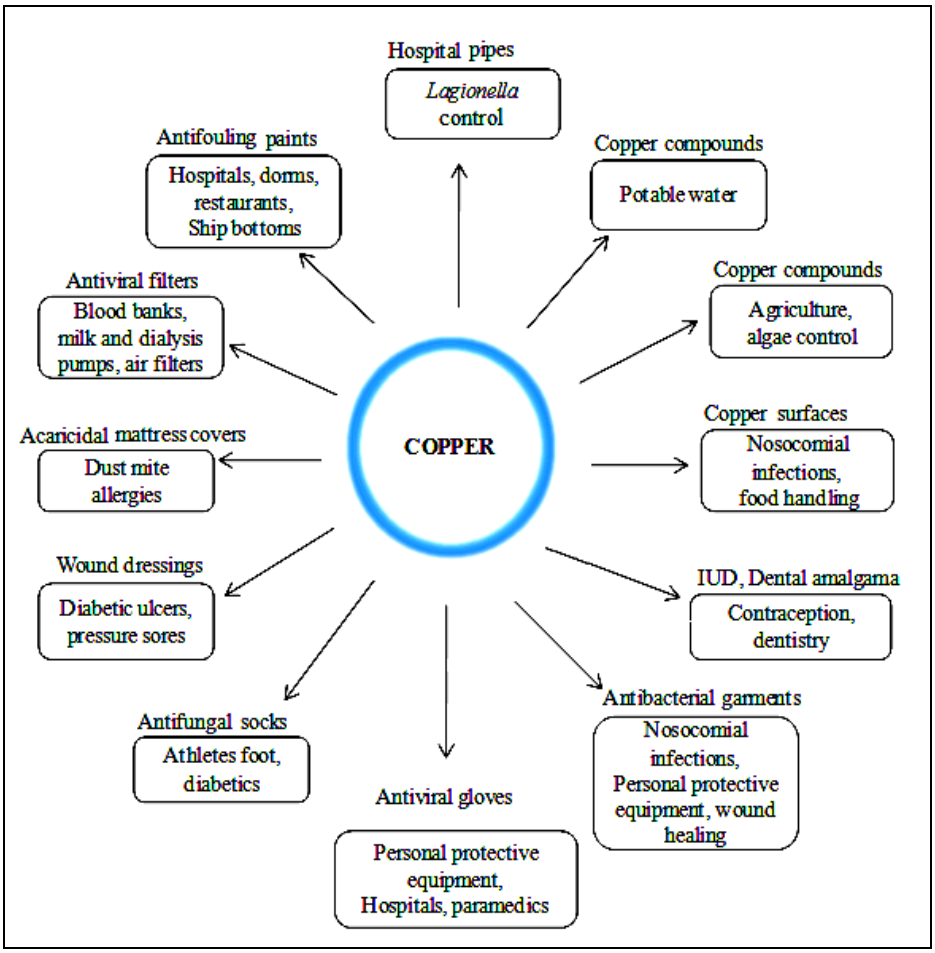

Figure 4.1: Current and future potential applications of copper and copper compounds in different areas, which are based on copper's biocidal properties (Modified from [2]).

4.2.2 Metal ion blends with polymers

In the last few years, the prevention of microbial colonization of polymeric surfaces has been mainly pursued by the release of antimicrobial agents incorporated into polymers.[27] Transition metal ions are well known for their broad-spectrum antimicrobial activity against bacterial and fungal agents together with their lack of cross resistance with antibiotics. The ability of transition metal ions to be blended with various polymers has been extensively explored.[9, 28] This is because the development of polymeric materials having high thermal and mechanical performances with specific functional properties is a new direction in polymer synthesis, due to the increasing requirements of the high technology industries.[29] More than a hundred polymers have been blended with metal ions and electrospun into fibres for various applications. These polymers include polyamide (PA), cellulose acetate (CA), poly(vinyl pyrrolidone) (PVP), polyvinylchloride (PVC), polyacrylamide (PAAm), polycaprolactone (PCL), poly(vinylidene fluoride) (PVDF), polyether imide (PEI), polyethylene glycol (PEG), nylon-4,6 (PA-4,6), polyacrylonitrile (PAN), poly(vinyl alcohol) and many more.[9, 28, 30] The blending of copper ions into polymers is an exciting area, not only because of the ability to form

conductive blends but also because of the antimicrobial potential of copper-functionalized polymer composites.[1, 2, 24] Among these copper complexes, attention has been mainly focused on the copper(II) polymer complexes due to their high nucleolytic efficiency, anti-tumor, antifungal, and antimicrobial activities.[31]

4.2.3 Metal ion attachment to polymers

Antimicrobial metal ions and nanoparticles can either be dispersed throughout the nanofibre (inside and outside) as illustrated in Figure 4.2A or immobilized (coated) on nanofibre surfaces (Figure 4.2B).[23, 32] Immobilization of antimicrobial agents (metal ions) on surfaces allows direct contact of the bactericidal metal ion or any biocide with the intended target thus increasing the effectiveness of the nanofibre whilst using less material compared to its counterparts where the antimicrobial agent is embedded on the inside and cannot have direct contact with the targeted microorganisms. The antimicrobial efficacy of copper ions coated or incorporated into various materials has been reported.[1, 33]

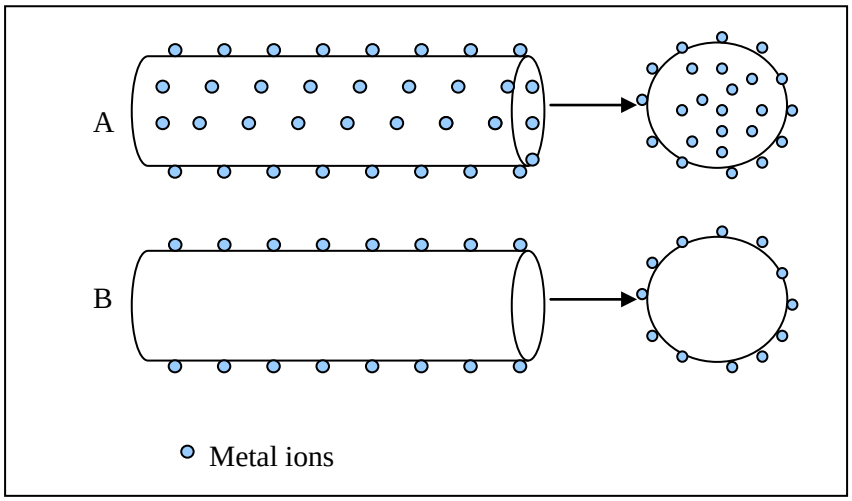

Figure 4.2: Orientations of metal ion attachment to nanofibres.

4.2.4 Impact of Cu-doped nanofibres

From an economic perspective, the development of copper-doped nanofibres for filtration studies instead of biocide-doped nanofibres is relatively cheap since copper in readily available at a lower cost compared to the biocide. Microbial resistance and leaching of copper into the filtered water however could pose serious problems.

4.3 Objective

In the previous chapter, the antimicrobial efficacy of PVA nanofibres which were fabricated from blends of PVA with a Cu^{2+} rich biocide called AquaQure was investigated. The main objective of this

part of the study was to determine if nanofibrenanofibres from blends of PVA and poly(styrene-co-maleic anhydride) (SMA) with Cu^{2+} ions could achieve similar bactericidal effects.

4.4 Polymers used in this study

Poly(vinyl alcohol) (PVA) and poly(styrene-co-maleic anhydride) copolymer (SMA) were used in this study. PVA is a well-accepted polymer because of its environmental friendliness and solvent free properties. SMA on the other hand has not been reported in liquid filter media applications because of its brittle nature. The investigation of copper doped SMA in this study was to ascertain if the incorporation of copper did not improve the properties of SMA and if the SMA backbone had the capacity to retain polar bonds with Cu^{2+} ions for sustained antimicrobial activity. These polymers were blended with Cu^{2+} ions and the solutions were electrospun. This was followed by characterization of the nanofibres for changes in chemical, crystalline structure, morphology and thermal properties. Antimicrobial tests were also carried out. The next subsections briefly describe the PVA and SMA, their synthetic routes as well as desirable properties which make them suitable for use in liquid filter media.

4.4.1 Poly(vinyl alcohol) (PVA)

The solvent free properties of PVA make it a lucrative alternative in various industrial settings in that it is easier to work with and also environmentally friendly. In order to impart the desired properties for advanced applications PVA can be modified by pre- or post-polymerization techniques. The former involves copolymerization of the vinyl ester monomer i.e. vinyl acetate, with a monomer of required functionality, followed by saponification. The latter involves secondary reactions of the hydroxyl groups (Figure 4.3), or grafting.[34-36] Post polymerization modification and electrospinning of PVA was investigated in this study. In comparison to other polymeric nanofibres which can only be generated from organic solutions, nanofibres generated from poly(vinyl alcohol)-aqueous solutions occupy higher environmental acceptability and are easier to use for industrial purposes.[37] PVA nanofibres can be electrospun from aqueous spinning solutions which is advantageous for ease in handling and facile, safe usage in industrial settings. The use of PVA fibres in liquid filter media however is not widespread due to its poor mechanical properties. Crosslinking PVA nanofibres improves its mechanical properties. The use of in situ heat treatment and aldehydes like glutaraldehyde and glyoxal to improve water stability of PVA fibres has been reported by researchers.

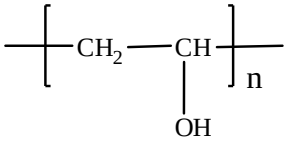

Figure 4.3: Structure of poly(vinyl alcohol).

4.4.1.1 Poly(styrene-co-maleic anhydride) copolymer (SMA)

SMA has been synthesized for the past decades using conventional radical polymerization as well as controlled/living free radical polymerization methods such as nitroxide mediated polymerization (NMP) and reversible addition-fragmentation chain transfer polymerization (RAFT).[38] The importance of SMA copolymers is attributed to their usage in a number of areas for various purposes. Its applications comprise of additives that are used to upgrade properties of styrenic polymeric material, coating additives, binder application, additives for building materials, microcapsules, blend compatibilizer, adhesion promoter for polyolefin coatings on metals and medical and pharmaceutical applications.[38-42] SMA copolymer is also regarded as a functional or reactive polymer.[38] The functionality is brought about by the maleic anhydride in the backbone of the copolymer as illustrated in Figure 4.4. The maleic anhydride in the backbone of SMA is reactive towards nucleophilic reagents (H_2O, alcohols, thiols, ammonia, amines, etc). Introduction of nucleophilic compounds enables the synthesis of new materials.[38, 43]

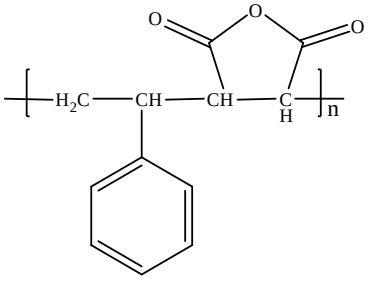

Figure 4.4: Structure of poly(styrene-co-maleic anhydride) copolymer.

4.5 Experimental materials and methods

In this section, the description of the materials and methods (experimental and characterization) used in this study is given. The experimental methods employed on this part of the study are similar to those in Section 3.4 unless specified.

4.5.1 Materials

The polymers PVA (Mw 146 000-186 000, 87-89% hydrolyzed) and SMA (Mw 23 000) were obtained from Sigma Aldrich, South Africa and were used without any further purification. Distilled water was used as the solvent in the case of PVA whilst ethanol and methanol in the case of SMA. Ethanol and methanol as well as copper sulphate pentahydrate ($CuSO_4.H_2O$) were also purchased from Sigma Aldrich and used as received.

4.5.2 Electrospun solution parameters

Preparation of the electrospinning solutions for both PVA/Cu and SMA/Cu nanofibres is described in the following subsections.

4.5.2.1 PVA/ Cu

Poly(vinyl alcohol) was dissolved in distilled water with continuous stirring at room temperature forming a 10 % wt/vol solution. This was followed by addition of $CuSO_4.5H_2O$ (6 mM) to obtain a pale blue solution. Control PVA nanofibre mats were prepared from the unmodified 10 % wt/vol solutions.

4.5.2.2 SMA/Cu

A 10 % wt/vol solution of SMA copolymer was prepared by dissolving SMA in a 1:1 mixture of methanol and ethanol with stirring until a clear homogenous solution was formed. After that, 6 mM $CuSO_4.5H_2O$ was added with continuous stirring at room temperature until the salt was completely dissolved forming a green solution. For control experiments, pristine SMA nanofibres were prepared from 10 % wt/vol solution of SMA solutions.

4.5.3 Electrospinning

The electrospinning technique is well referenced for its effectiveness in the production of nano-sized polymer fibres. A number of techniques based on the conventional needle electrospinning model have been developed and patented over the past two decades and these include among others bubble electrospinning and coaxial electrospinning. Bubble electrospinning was tested for its potential to produce nano-sized fibres of PVA/Cu and SMA/Cu as well as its ability to upscale nanofibre production. The bubble spinning technique and the method used to produce nanofibre mats through this technique are described in the following sections.

4.5.3.1 Electrospinning technique (Bubble electrospinning)

A variation of conventional needle-based electrospinning, known as bubble electrospinning was used for this study. Bubble electrospinning allows production of nanofibres on a large scale. This process has been used by other researchers.[44-46] In bubble electrospinning, the same concept as in the needle based electrospinning is used, but it involves the formation of multiple electrostatically driven jets of polymer from a charged bubble of polymer solution.[46] Also, an electric field of a much higher voltage than used in conventional needle spinning is necessary, and fibres generated from polymer jets are collected on a negatively charged metallic collector plate positioned above the bubble widget (Figure 4.5).

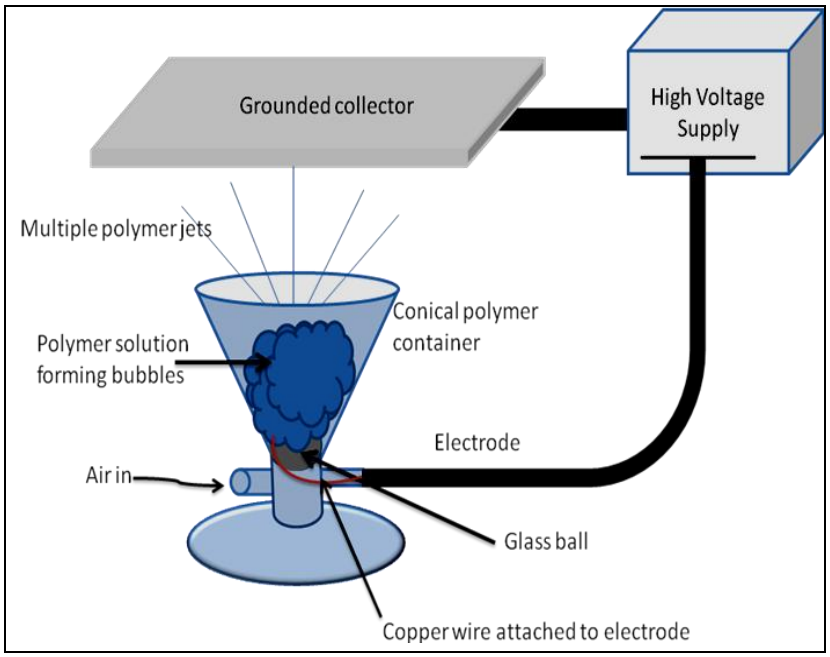

Figure 4.5: Bubble spinning set-up.

4.5.3.2 Method

The polymer solution (3 ml) was poured into the well of the bubble spinning widget (conical polymer container). A copper wire attached to the positive electrode of a high voltage power supply was inserted into the polymer solution, while the negative electrode was attached to a tinfoil collector plate suspended above the widget. Air was pumped into the polymer widget using a syringe to form bubbles and a voltage of 50 kV was applied. The use of non-conducting material became even more crucial when using this electrospinning set-up because of the high voltage used. All the polymer solutions were electrospun at room temperature but other conditions like widget-collector distance and relative humidity differed for each of them (Table 4.1). Widget-collector distances of between 15-35 cm and relative humidity between 30-70% were studied to ascertain which condition would produce nanofibres with well defined diameters. The nanofibrous mats were crosslinked by heat treatment at 140°C for 15 minutes in the case of PVA and PVA/Cu. SMA and SMA/Cu nanofibres were crosslinked at 120°C for 1 hour. Similar characterization techniques as described in Figure 3.1 and described in subsequent sections were employed for these nanofibres unless otherwise stated.

Table 4.1: Electrospinning conditions for the polymers

Polymer	Widget-collector distance (cm)	Relative humidity (%)
PVA	20	below 45 % RH
SMA	25	45-55 %RH

4.6 Results and discussion

This section outlines findings of the study and supports them based on relevant literature. Results on the chemical, antimicrobial and mechanical results are reported and discussed. Findings on the stability of the fibres in liquid media and their extent of leaching are also reported.

4.6.1 Properties of electrospun PVA/Cu and SMA/Cu solutions

The decrease in viscosity as a result of the presence of Cu^{2+} ions in the solution shown by the rheological results was attributed to chelation (Figure 4.6A and Figure 4.6B). This trait has been reported by other researchers as well. Figure 4.6A indicates that PVA/Cu solutions experienced a decrease in viscosity which was sustained over 10 minutes followed by a sharp decrease after 10 minutes. Fibres obtained from solutions electrospun after 10 minutes exhibited solvent beads and poor bubble formation was experienced. The same decrease in viscosity was observed in the case of SMA/Cu^{2+} (Figure 4.6B). Addition of Cu^{2+} to SMA resulted in a viscosity decrease from 3.43 to about 2.96 Pa.s. This was followed by gradual drop in viscosity over 15 minutes eventually recording a viscosity of 2.7 Pa.s after 15 minutes.

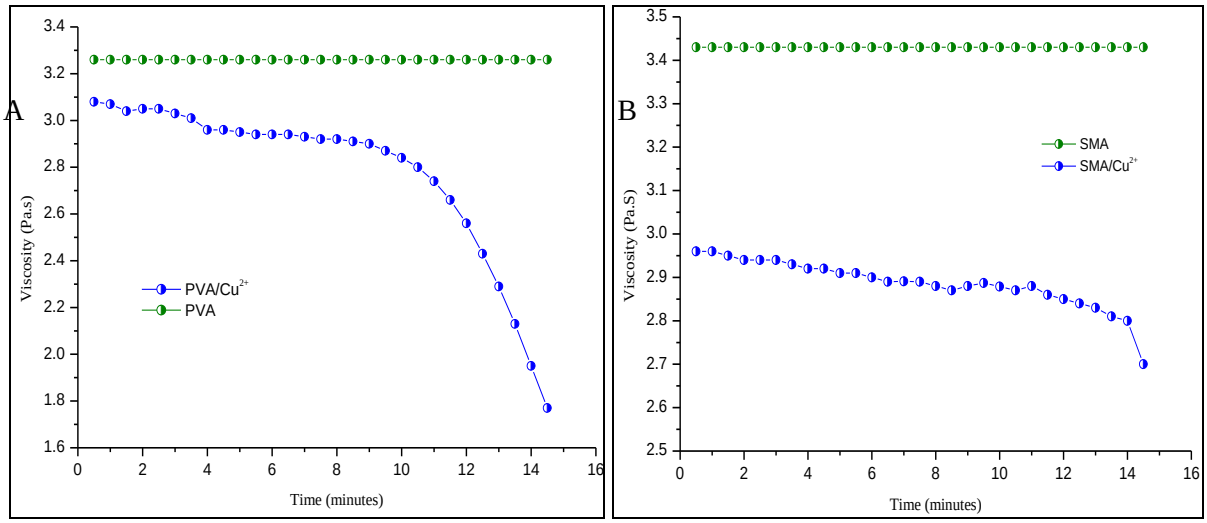

Figure 4.6: Changes in viscosity of PVA/Cu (A) and SMA/Cu (B) electrospinning solutions monitored over 15 minutes

4.6.2 Morphology studies of electrospun PVA/Cu and SMA/Cu nanofibre mats

Bubble electrospinning of the polymer solutions generated well aligned nanofibres. SEM images generated from the SEM demonstrated this. One observation made however was that these nanofibres had a wide diameter range compared to needle spun nanofibres. The following sections discuss the findings and differences between the PVA/Cu and SMA/Cu nanofibres.

4.6.2.1 Nanofibre mat porosity of PVA/ Cu and SMA/Cu nanofibres

Mat porosity analysis was achieved by taking area light intensity scans from SEM images of the electrospun nanofibres. These results revealed that the pore sizes of 73±0.26% of the pores on the PVA/Cu mats were less than 50 nm^2. SMA/Cu mats had about 91±0.67 % of the pores in the 30 nm^2-150 nm^2 size range (Figure 4.7A and Figure 4.7 B). The narrow pore sizes demonstrated by these nanofibrous mats are good properties especially for filter applications.

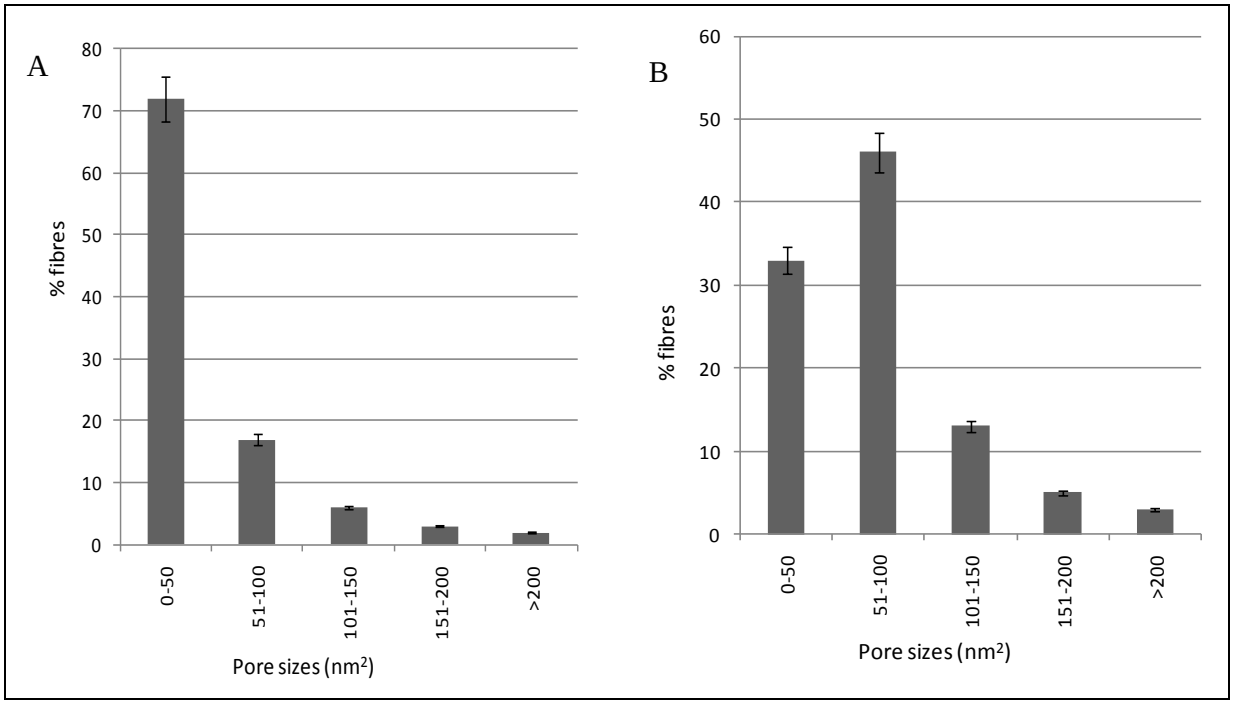

Figure 4.7: PVA/Cu (A) and SMA/Cu (B) nanofibre pore sizes.

4.6.2.2 Nanofibre diameters of PVA/ Cu and SMA/Cu nanofibres

About 68±0.8% of the nanofibres generated from the PVA/Cu solution had diameters between 150nm and 300 nm. About 18±1% had diameters less than 150 nm and only 14±0.3% were distributed between 300 and 450 nm. This is illustrated in Figure 4.8A. SMA/Cu nanofibres on the other hand had much thinner diameters when viewed under the SEM (Figure 4.8B). The nanofibres also showed some traces of the metal ions on the surfaces. A bulk (77±0.1%) of them had diameters between 150 nm and 350 nm with only 16±0.95% and 7±0.63% of the generated nanofibres below 150 nm and above 350 nm respectively. The narrow diameters recorded for these nanofibres qualify them as viable materials for filter applications due to their high surface to volume ratios which is important for filter media applications.[47]

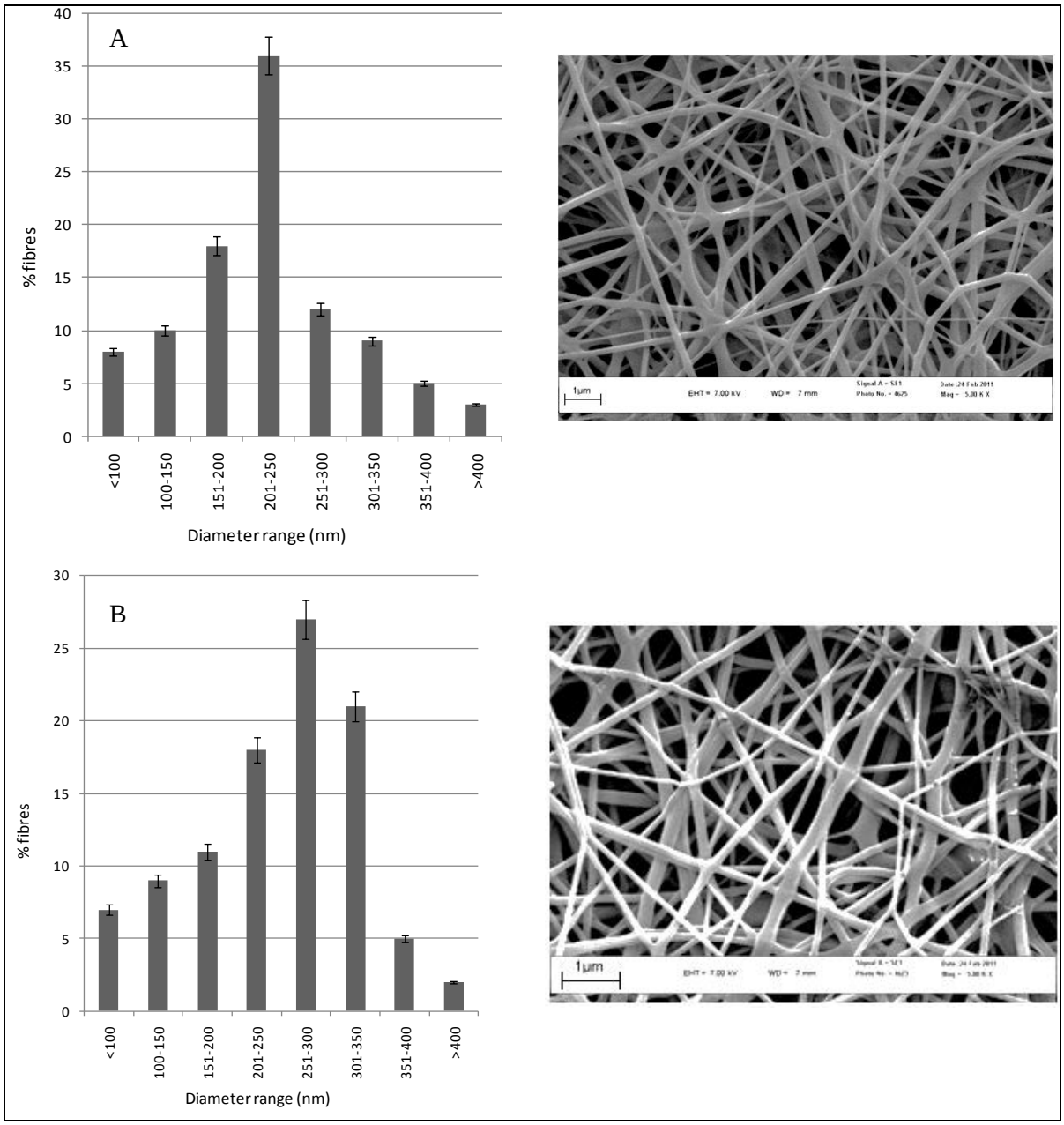

Figure 4.8: PVA/Cu (A) and SMA/Cu (B) nanofibre diameters.

4.6.3 Energy dispersive x-ray analysis (EDX)

Energy dispersive X-ray analysis (EDX) confirmed the presence of the Cu^{2+} ions on the surfaces of both SMA/Cu and PVA/Cu. SMA/Cu nanofibres mats had more Cu^{2+} traces on the surface compared to PVA/Cu nanofibres. This was confirmed by quantitative EDX results where by 12 ±1.43% Cu was detected on PVA/Cu nanofibre surfaces and 18.79 ±3.44% on SMA/Cu nanofibrous mat surfaces. This is also seen on the EDX spectra where SMA/Cu nanofibres had more detections of Cu compared to PVA/Cu (Figure 4.9B). (The unlabelled peaks were either Au from gold sputtering or C-O from polymer backbone).

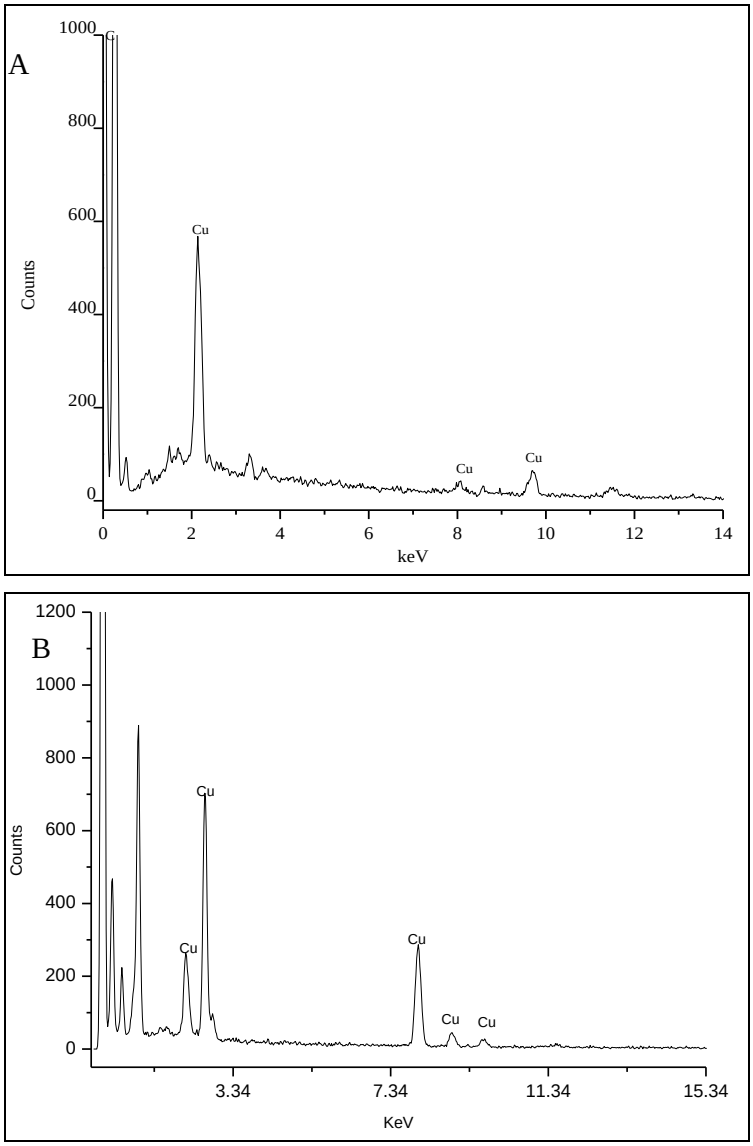

Figure 4.9: EDX traces of PVA/Cu (A) and SMA/Cu (B).

4.6.4 Thermogravimetric analysis

As shown in Figure 4.10A, both pristine PVA and PVA/Cu nanofibres mats lost the bulk of their weight at around 400°C. From this figure it is also noted that the thermal decomposition of PVA took place via two steps. The initial mass loss around 100°C was due to moisture loss. This is the same case with PVA/Cu TGA thermograms which indicates that the same mechanism was involved in the thermal degradation of both samples. This indicates that the presence of copper did not alter the thermal stability of the fibres. Figure 4.10B indicates that the addition of Cu^{2+} on SMA nanofibres also did to cause major changes in the thermal stability of SMA.

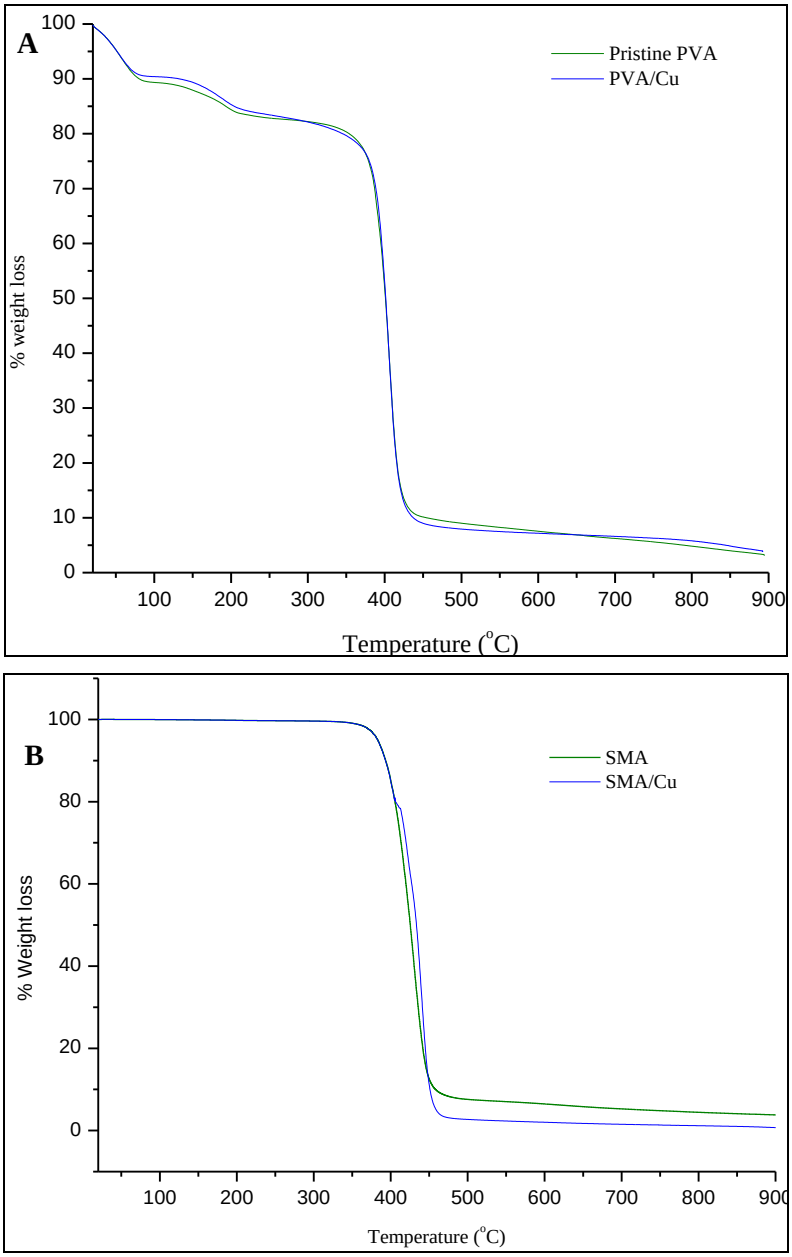

Figure 4.10: TGA thermograms of PVA, PVA/Cu (A) and SMA, SMA/Cu (B).

4.6.5 Differential scanning calorimetry (DSC)

PVA nanofibres had a glass transition temperature (T_g) value of 85°C while PVA/Cu had a T_g value of 100°C (Figure 4.11A). The introduction of Cu^{2+} to PVA increased the packing efficiency and the steric effect of the O-H groups. As a result, the lateral forces in the bulk state increase leading to a shift in T_g value towards high temperature region. SMA/Cu nanofibres also had a higher T_g value compared to pristine SMA nanofibres. SMA/Cu nanofibres also demonstrate the same behavior in which SMA has a T_g of about 150°C and SMA/Cu a T_g of about 170°C (Figure 4.11B).

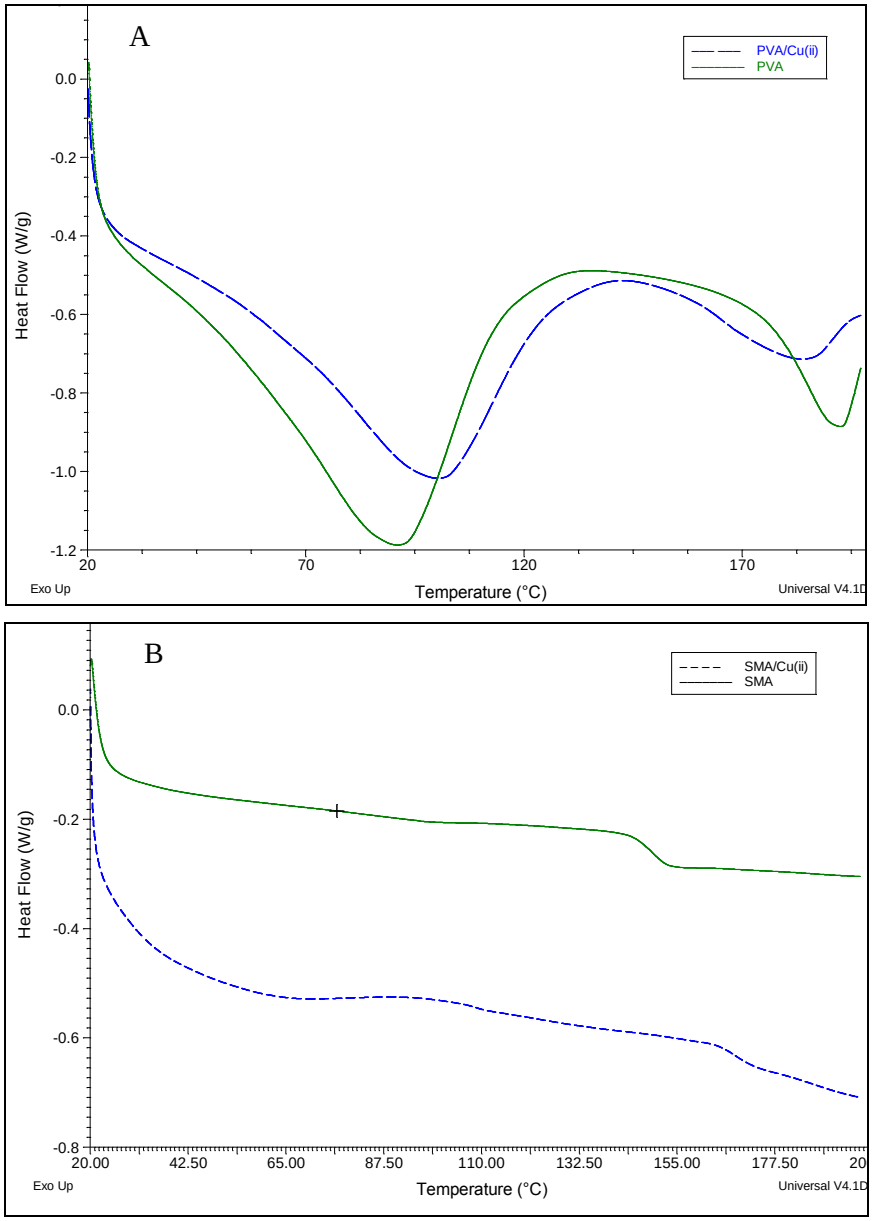

Figure 4.11: PVA/Cu (A) and SMA/Cu DSC (B) thermograms.

4.6.6 Attenuated Total Reflectance Infra Red spectroscopy (ATR-IR)

The ATR-IR spectra of PVA and PVA/Cu showed similar bands described in Section 3.5.3.3 (Figure 3.11), the only differences are indicated in Figure 4.12A. In this figure, region 1 indicates the broadening of the O-H band of PVA whilst region 2 shows the disappearance of the C-H band in the backbone of PVA. These were attributable to the polar interactions between PVA and the Cu^{2+} ions. The ATR-IR spectrum of SMA copolymer shows bands at 1853 cm^{-1} and 1773 cm^{-1} which are assigned to the cyclic anhydride (C=O) and 1222 cm^{-1} is due to the cyclic ring ether (C-O-C) (Figure 4.12B). The band at 1495 cm^{-1} is a styrenic band. Aromatic C-C stretching vibrations appear at 1454 cm^{-1} and 1157 cm^{-1}. The SMA/Cu spectrum has similar bands to the one of the SMA copolymer except for the shrinking of the maleic anhydride bands marked as Region 1. In Region 2, the aromatic

C-C stretching vibrations both disappear. The band that appears at 900 cm^{-1} marked as region 3 is characteristic for the interactions of metal ions with SMA. It is generally known that reactions of SMA with alcohols result in hemi esterification of SMA because of the high reactivity of the anhydride group of SMA.[48] The extent of anhydride conversion depends strongly on the nature of the alcohol and reaction temperature. At high temperatures, reversible hemi-esterification is shifted back to the anhydride side.[49-51] This behaviour shows that during heat treatment of SMA nanofibres, the anhydride ring closed again. This explains why ATR/FTIR spectra did not indicate ring opening of the cyclic anhydride peaks (C=O).

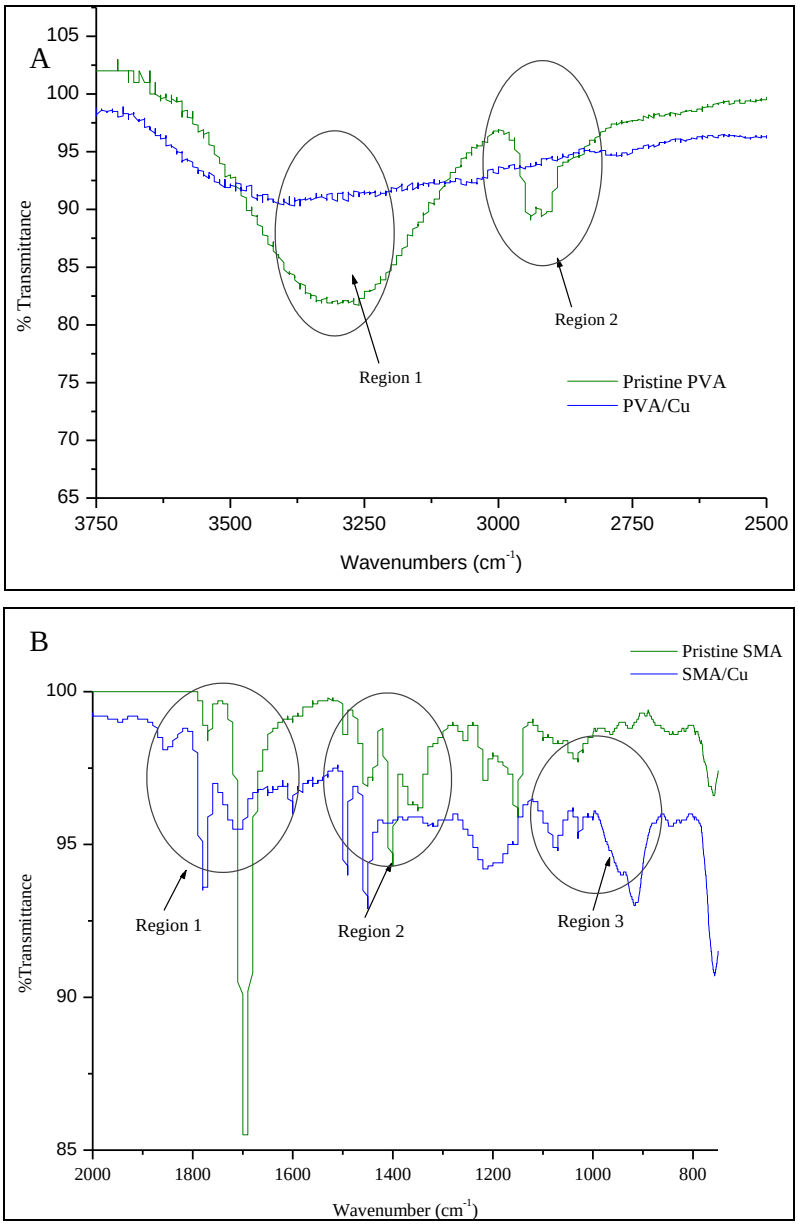

Figure 4.12: ATR-FTIR spectra of PVA, PVA/Cu (A) and SMA, SMA/Cu (B).

4.6.7 Antimicrobial characterization results

This section reports results on the antimicrobial potential of PVA/Cu^{2+} and SMA/Cu^{2+} nanofibres. Antimicrobial characterization was achieved through plate counts, bioluminescence imaging as well as fluorescence imaging.

4.6.7.1 Plate counts

PVA/Cu nanofibres reduced the populations of *P. eudomonas aeruginosa* Xen 5 by up to 5 logs and those of *E. coli* Xen 14, *S. typhimurium* Xen 26, *S. aureus* Xen 36 and *K. pneumoniae* Xen 39 by up to 4 logs after 30 minutes of exposure (Figure 4.13A). These fibres demonstrated their bactericidal effects after just 5 minutes where all the strains showed population declines of at least 3 logs and after 15 minutes up to 4 log reductions were recorded on all the strains. This was followed by a gradual decline in pathogen numbers leading to all the strains being reduced by at least 4.5 logs after 30 minutes.

SMA/Cu nanofibres achieved high reductions in the numbers of viable bacteria after 5 minutes of contact (Figure 4.13B). *E. coli* Xen 14 recorded about 5 log reduction in just 5 minutes while *S. typhimurium* Xen 26 and *K. pneumoniae* Xen 39 recorded reductions of over 4 logs. *S. aureus* Xen 36 on the other hand showed reduction of just over 3 logs after 5 minutes. This was followed by a steady decrease in cell numbers resulting in *E. coli* Xen 14, *S. typhimurium* Xen 26 and *K. pneumoniae* Xen 39 having above 5 log reductions and *S. aureus* Xen 36 having about 3.5 log after 30 minutes.

Both PVA/Cu and SMA/Cu demonstrated up to 4 log reduction in pathogen numbers on the mixed strain culture (Figure 4.14). PVA/Cu nanofibres recorded up to almost 3 log reduction compared to SMA/Cu which demonstrated just over 2 log declines in population numbers. After 15 minutes of exposure however, SMA/Cu nanofibres had reduced pathogen numbers by almost the same number as PVA/Cu nanofibres and after 20 minutes of exposure the SMA/Cu nanofibres had reduced pathogen numbers by more than 0.5 log higher than PVA/Cu nanofibres. A gradual increase in the antimicrobial activity of both the nanofibres resulted in more than 4 log reductions for both sets of fibres after 30 minutes of exposure.

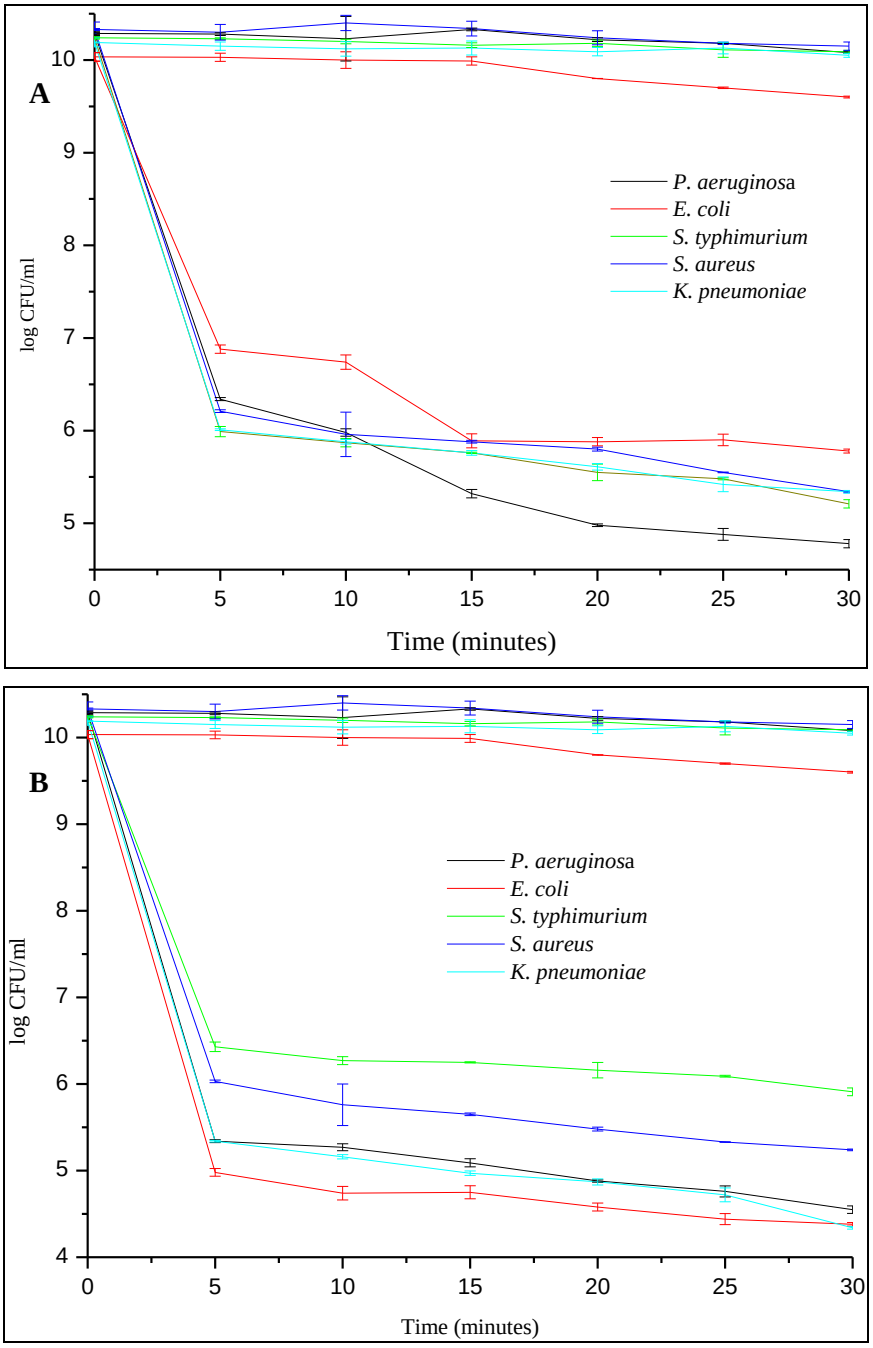

Figure 4.13: Pathogen viability (expressed in log CFU/mL) over 30 minutes of direct contact with PVA/Cu (A) and SMA/Cu nanofibres.

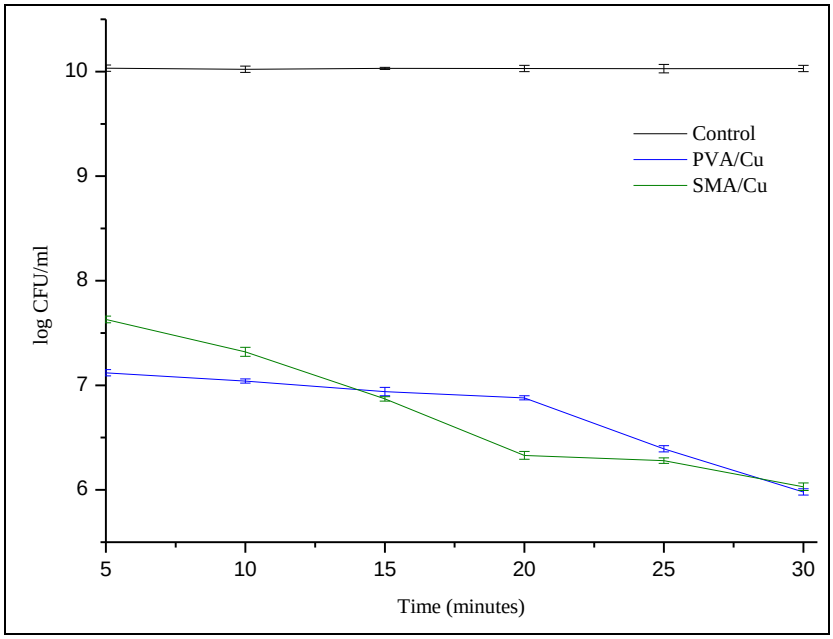

Figure 4.14: Antimicrobial activity demonstrated by PVA/Cu and SMA/Cu on mixed-culture cells.

4.6.7.2 Bioluminescence Imaging

In vivo imaging *Pseudomonas aeruginosa* Xen 5, *Escherichia coli* Xen 14, *Salmonella typhimurium* Xen 26, *Staphylococcus aureus* Xen 36 and *Klebsiella pneumoniae* Xen 39 on PVA/Cu and SMA/Cu nanofibres confirmed some of the results obtained from plate counting. PVA/Cu demonstrated high inactivation of *Pseudomonas aeruginosa* Xen 5, *Staphylococcus aureus* Xen 36 and *Salmonella typhimurium* Xen 26 (Table 4.2), this is indicated by the decrease in the number of photons emitted by these strains especially after 10 minutes of being exposed to the nanofibres. *Escherichia coli* Xen 14 and *Klebsiella pneumoniae* Xen 39 on the other hand showed some resistance to the bactericidal Cu^{2+}. These findings were in agreement with those obtained from the plate counting technique (Figure 4.13 A).

SMA/Cu nanofibres also showed reduction in the number of photon emissions by the bacteria (Table 4.2). An instant reduction in metabolically active *Escherichia coli* Xen 14 cells was observed. *Pseudomonas aeruginosa* Xen 5 cells were also significantly reduced after 10 minutes of exposure to the SMA/Cu nanofibres. *Salmonella typhimurium* Xen 26, *Staphylococcus aureus* Xen 36 and *Klebsiella pneumoniae* Xen 39 all had their numbers reduced as depicted from the photon emissions. The results from *in vivo* imaging suggest that *Escherichia coli* Xen 14 and *Klebsiella pneumoniae* Xen 39 develop some dormancy on getting into contact with PVA/Cu nanofibres. This assumption comes about as a result of the amount of metabolically active (photon emitting) cells observed on the *in vivo* images compared to the high (up to 4 log) reductions obtained from plate counting. The same assumption goes for the case of *Salmonella typhimurium* Xen 26, *Staphylococcus aureus* Xen 36 and *Klebsiella pneumoniae* Xen 39 in SMA/Cu nanofibre nanofibres.

Table 4.2A: *In vivo* images to illustrate antimicrobial activity of PVA/Cu nanofibres.

Strains	Control (Pristine PVA)		PVA/Cu	
	1minute	10 minutes	1 minutes	10 minutes
Pseudomonas aeruginosa (Xen 5)	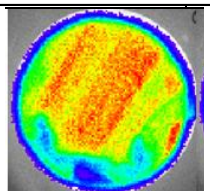	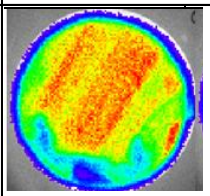	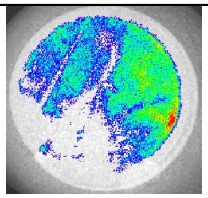	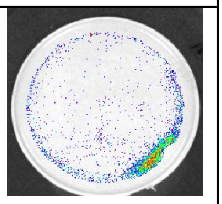
Escherichia coli (Xen 14)	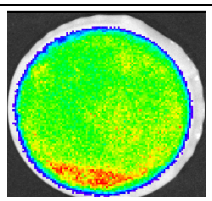	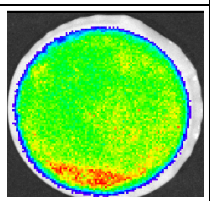	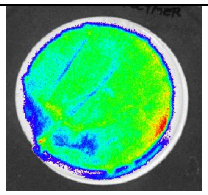	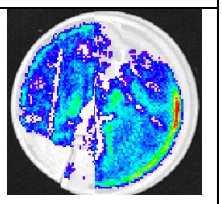
Salmonella typhimurium (Xen 26)	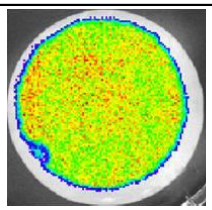	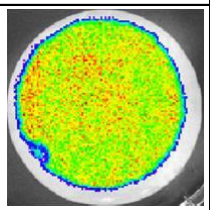	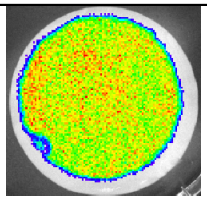	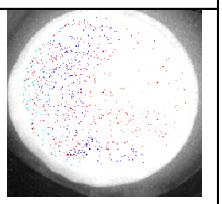
Staphylococcus aureus (Xen 36)	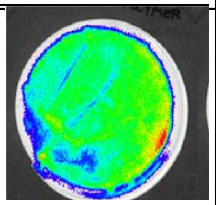	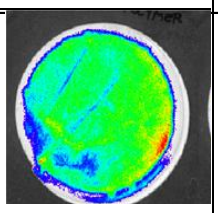	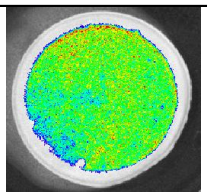	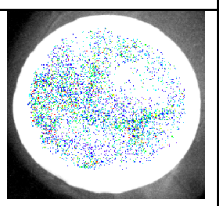
Klebsiella pneumoniae (Xen 39)	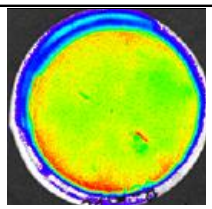	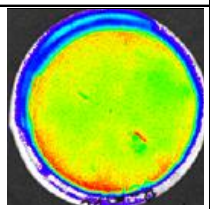	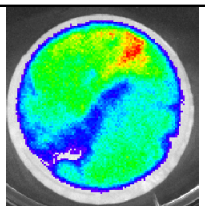	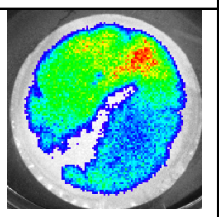

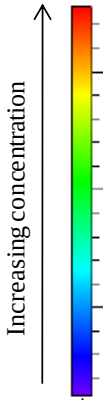

Table 4.3b: *In vivo* images to illustrate antimicrobial activity of SMA/Cu nanofibres.

Strains	Control (Pristine SMA)		SMA/Cu	
	1minute	10 minutes	1 minutes	10 minutes
Pseudomonas aeruginosa (Xen 5)	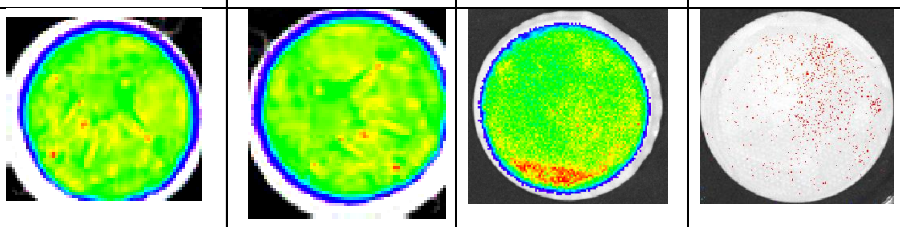			
Escherichia coli (Xen 14)	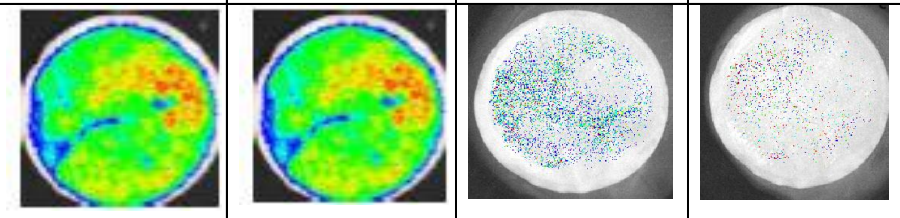			
Salmonella typhimurium (Xen 26)	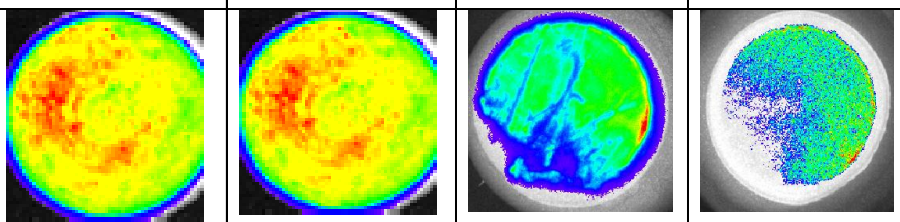			
Staphylococcus aureus (Xen 36)	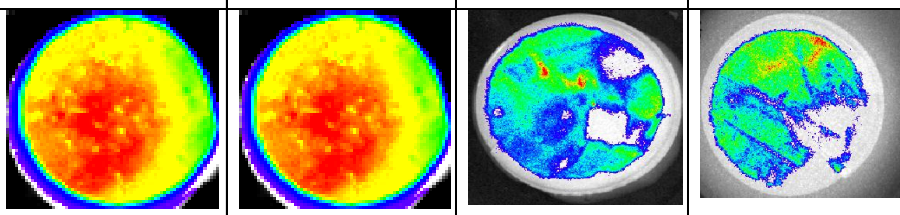			
Klebsiella pneumoniae (Xen 39)	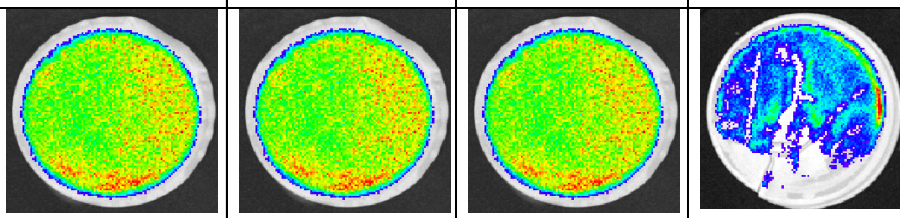			

4.6.7.3 Fluorescence Microscopy

From the control PVA and SMA micrographs most of the attached colonies of bacteria did not absorb propidium iodide (red) dye which would indicate cell death (Figure 4.15 A_1, A_2, A_3 and Figure 4.15 B_1, B_2, B_3). The few cells which absorbed the dye might have lost their viability due to change of environment prior to fluorescence imaging. PVA/Cu nanofibres demonstrated cell deactivation in that almost all the cells exposed to these fibres absorbed the red dye indicating cell death Figure 4.15(C_1, C_2, C_3). The same behavior is seen with SMA/Cu nanofibres which demonstrated bactericidal effects

on the bacteria colonies which were attached to them Figure 4.15 (D_1, D_2, D_3). These results further confirm the antimicrobial nature of PVA/Cu and SMA/Cu nanofibres.

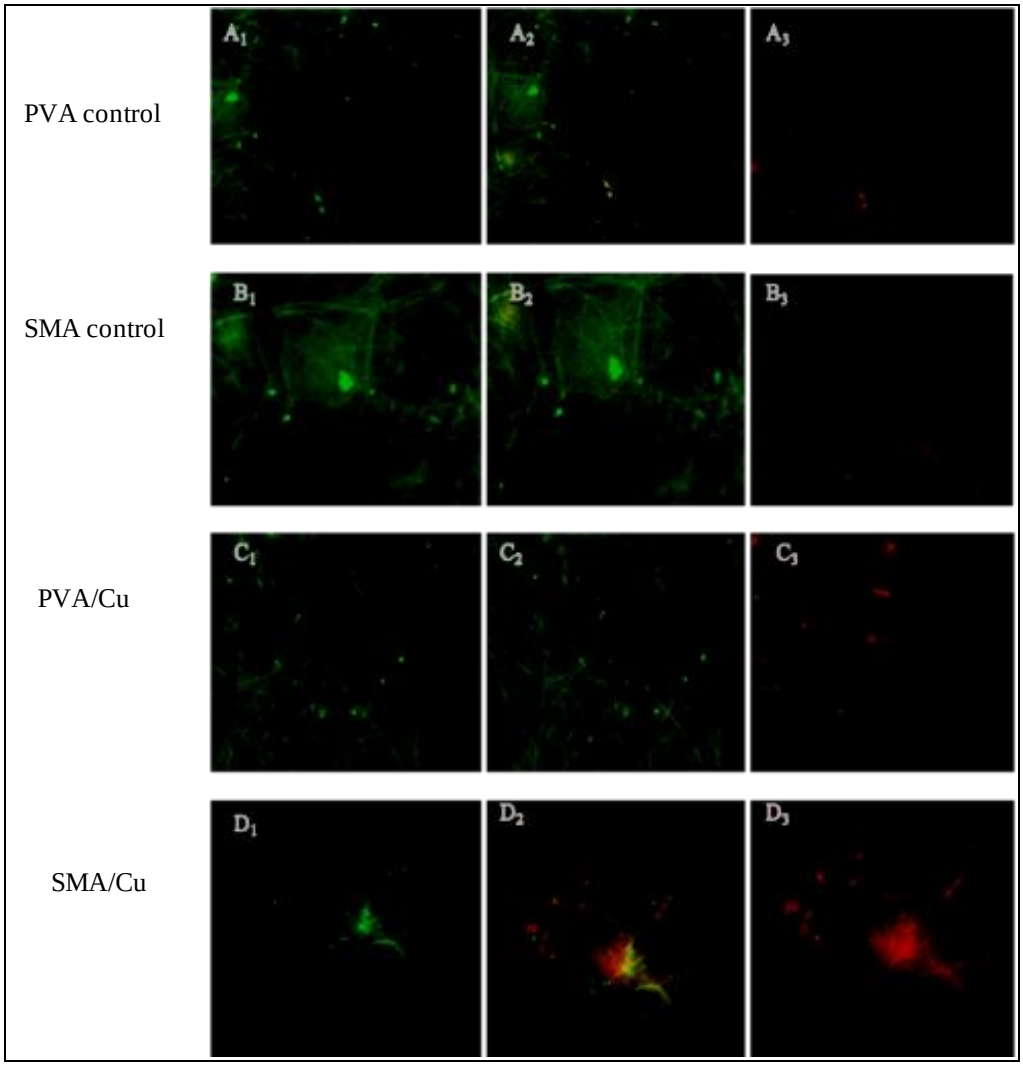

Figure 4.15: Fluorescence Microscopy images showing bacteria on pristine PVA nanofibres (A), pristine SMA nanofibres, PVA/Cu nanofibres (B) and SMA/Cu nanofibres.

4.6.8 Regeneration studies

PVA/Cu nanofibres had sustained antimicrobial effectiveness of 3 log reduction over the first three cycles. A decrease however followed on the fourth cycle resulting in a 2 log reduction over 6 cycles. SMA/Cu nanofibres on the other hand gradually lost antimicrobial activity from 3.8 log reduction in bacteria populations to a 3 log reductions after 6 cycles (Figure 4.16). SMA/Cu nanofibres became brittle and thinner after contact with water (Figure 4.17). This suggests that further investigations on the improvement of the mechanical properties of SMA are necessary for it to be suitable for water filtration properties. These results indicate an improvement in the retainance of antimicrobial effectivity of the heat-treated nanofibres compared to chemically crosslinked nanofibres in previous

sections. The heat-crosslinked PVA/Cu nanofibres also showed minimal swelling compared to previously studied glyoxal-crosslinked PVA/AquaQure nanofibres.

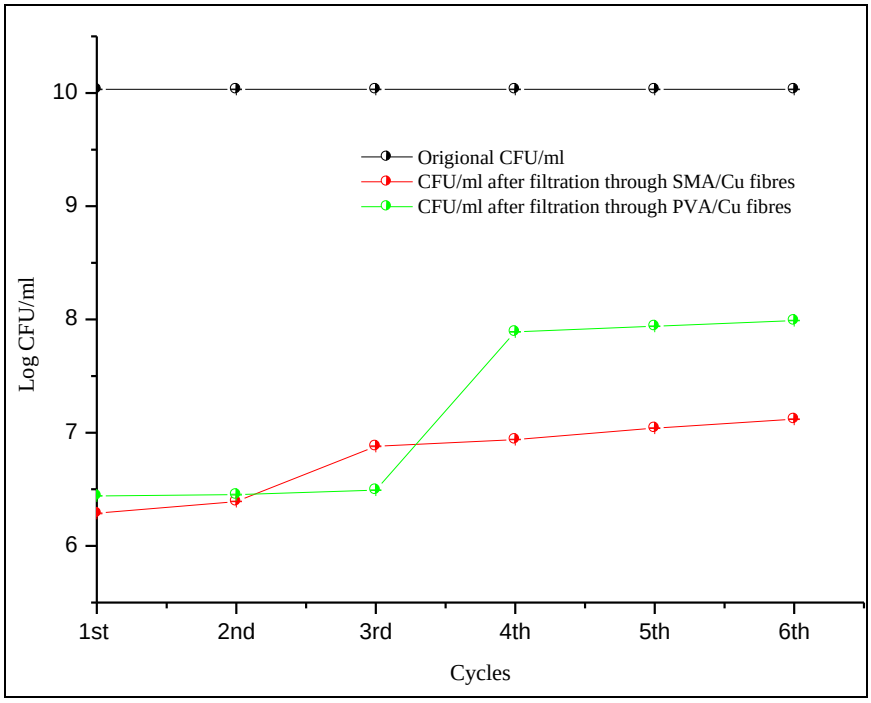

Figure 4.16: Antimicrobial effectiveness of PVA/Cu and SMA/Cu over six cycles

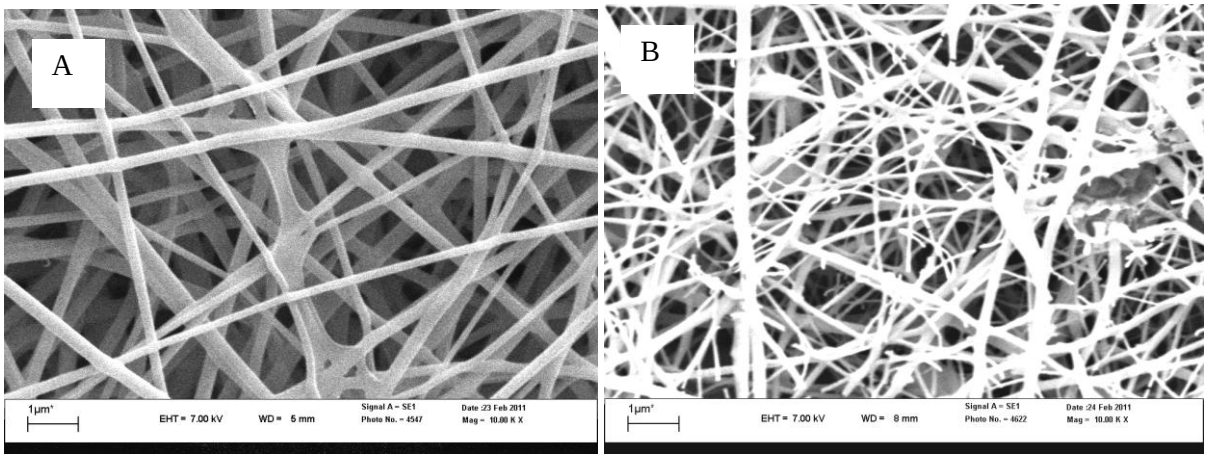

Figure 4.17: Morphological changes on PVA/Cu (A) and SMA/Cu nanofibre mats after six cycles.

4.6.9 Leaching experiments

The ICP-AES results showed very low Cu^{2+} leaching intensities for both PVA/Cu and SMA/Cu nanofibres over 24 hours of water exposure. A steady increase in the amount of Cu^{2+} detected in the water was observed (Figure 4.18). After 12 hours only about 1.62 µg/µl and 1.31 µg/µl of Cu^{2+} ions had leached into the water and even after 24 hours the amount of Cu^{2+} in the water had not increased. Quantitative EDX analysis of the used nanofibres further confirmed these results. More than 90% of

the initially detected Cu was still detectable on surfaces both PVA/Cu and SMA/Cu nanofibrous mats after water filtration. This attribute of the PVA/Cu and SMA/Cu renders these nanofibres environmentally friendly and safe to be used in liquid filter media since it adheres to the SANS guidelines for drinking water.

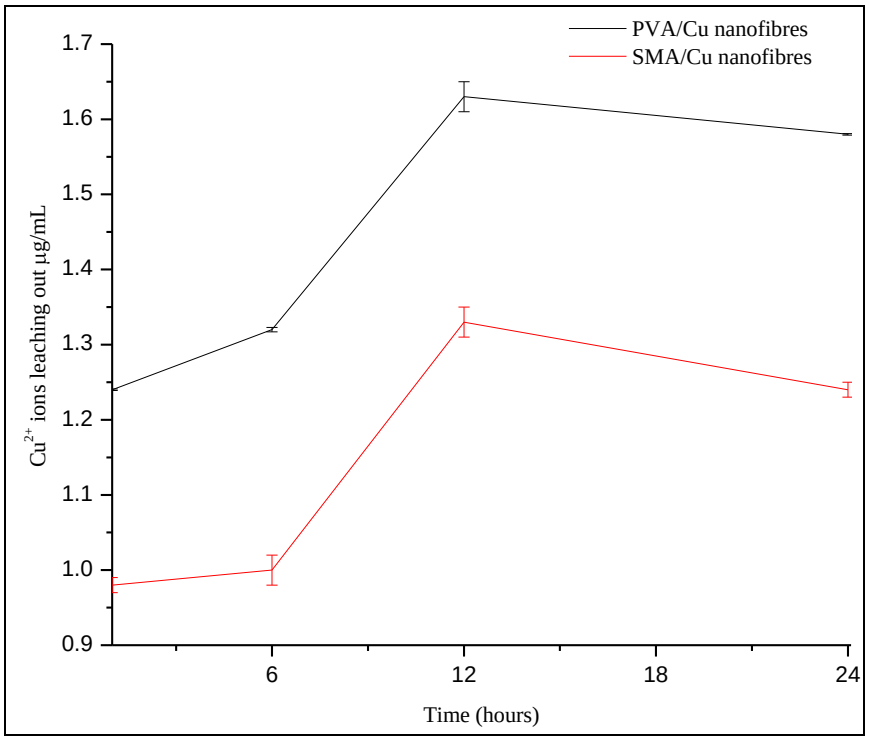

Figure 4.18: Leaching of Cu^{2+} ions from PVA/Cu and SMA/Cu nanofibres over 24 hours.

4.6.10 Water stability tests

Both pristine PVA and PVA/Cu nanofibre mats demonstrated good water stability properties in that even after 48 hours of being exposed to water, their morphology remained intact. The pristine and copper modified PVA nanofibres absorbed water with swelling degrees of 176±1 and 166±1.5% respectively (Table 4.3). This shows that modifying these nanofibres with copper does not affect the stability of the fibres in water. Pristine SMA and SMA/Cu nanofibres on the other hand also showed good stability in water with limited swelling (34±1.5 and 31±1.5% respectively). The SMA and SMA/Cu nanofibres however became hard and brittle after water exposure. SEM images indicated that these nanofibres became thinner in diameter (Figure 4.19).

Table 4.4: Properties of pristine and Cu^{2+} modified PVA and SMA nanofibres after water immersion.

Sample	Dry mass	Wet mass	absorbed H_2O	Q_{water} (g/g)	SD %
Pristine PVA	0.0251±0.0002	0.0694±0.001	0.0443±0.001	1.76±0.01	176±1
PVA/Cu	0.0252±0.0002	0.0671±0.001	0.0419±0.001	1.66±0.015	166±1.5
Pristine SMA	0.0252±0.0002	0.0329±0.001	0.0077±0.001	0.31±0.015	31±1.5
SMA/Cu	0.0252±0.0002	0.0338±0.001	0.0086±0.001	0.34±0.015	34±1.5

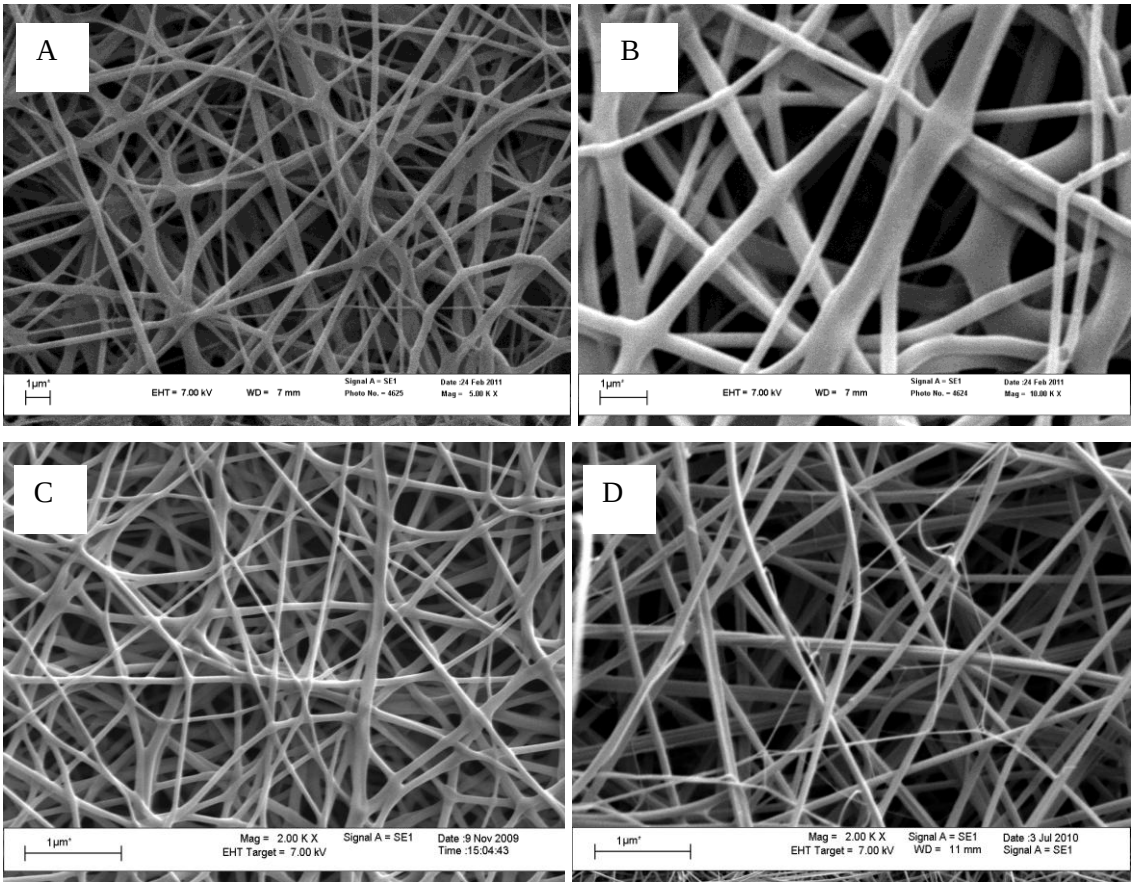

Figure 4.19: PVA/Cu nanofibres before (A) and after (B) water immersion. SMA/Cu nanofibres before (C) and after (D) water immersion.

4.7 Conclusions

PVA/Cu and SMA/Cu nanofibres were fabricated from Cu^{2+}-polymer blends using the bubble electrospinning technique. The presence of Cu^{2+} in the nanofibres was confirmed using EDX. Thermogravimetric analysis indicated that the inclusion of Cu^{2+} to both PVA/Cu^{2+} and SMA/Cu^{2+} nanofibres did not affect the thermal stability of the nanofibres. Increases in the T_g values from 85°C in pristine PVA nanofibres to about 100°C in the case of PVA/Cu^{2+} and 150°C (pristine SMA nanofibres) to 170°C for SMA/Cu^{2+} were recorded through differential scanning calorimetry.

PVA/Cu nanofibres reduced the populations of *P. aeruginosa* Xen 5 by up to 5 logs and those of *E. coli* Xen 14, *S. typhimurium* Xen 26, *S. aureus* Xen 36 and *K. pneumoniae* Xen 39 by up to 4 logs after 30 minutes of exposure. SMA/Cu nanofibres on the other hand, achieved high reductions in the numbers of viable bacteria after 30 minutes of contact. *E. coli* Xen 14, *S. typhimurium* Xen 26 and *K. pneumoniae* Xen 39 were reduced by more than 5 log and *S. aureus* Xen 36 by about 3.5 log. Both PVA/Cu and SMA/Cu demonstrated up to 4 log reduction in pathogen numbers on the mixed strain culture.

Bioluminescence imaging confirmed some of the results obtained through plate counting for both PVA/Cu^{2+} and SMA/Cu^{2+} nanofibres. The *in vivo* images also suggested some metabolic activity (photon emissions) in more cells than revealed by plate counting suggesting that some of the strains develop dormancy on contact with Cu^{2+} containing nanofibres. The antimicrobial activity of copper containing PVA and SMA nanofibres was also confirmed through fluorescence microscopy. Regeneration results indicated that PVA/Cu^{2+} had sustained activity with more than 3 log reductions over 3 cycles followed by loss in activity but still exhibited more than 2 log reductions after 6 cycles. SMA/Cu^{2+} nanofibres on the other hand showed minor losses in antimicrobial effectiveness after 6 cycles and still achieved up to 3.8 log reductions in populations of the mixed strain culture (*P. aeruginosa* Xen 5, *E. coli* Xen 14, *S. typhimurium* Xen 26, *S.aureus* Xen 36 and *K. pneumoniae* Xen 39).

SMA/Cu nanofibres however became brittle and thin after contact with liquid media. This led to the assumption that the gradual loss of activity could be due to some fibres breaking thus increasing the pores on the nanofibre mat allowing some bacteria to pass through. From the leaching experiments PVA/Cu and SMA/Cu nanofibres showed leaching of 1.62 and 1.31 µg/ml of Cu^{2+} respectively and further quantitalive EDX confirmed these results. Further improvements on the mechanical properties of SMA in order for it to be usable in filtration media especially liquid media.

4.8 References

1. Sheikh F.A.; Kanjwal M.A.; Saran S.; Chung W-J.; Kim H. *Applied Surface Science* **2011,** 257, 3020-3026.
2. Borkow G.; Gabbay J. *Current Chemical Biology* **2009,** 3, 272-278.
3. Borkow G.; Gabbay J. *FASEB Journal* **2004,** 18, 1728-1730.
4. Dollwet H.H.A.; Sorenson J.R.J. *Trace Elements Medicine* **2001,** 2, 80-87.
5. Scigliano J.A.; Grubb T.C.; Shay D.E. *Journal of American Pharmeutical Association* **1950,** 39, 673-676.
6. Belli N.; Marin S.; Sanchis V.; Ramos A.J. *Food Addition: Contamination* **2006,** 23, 1021-1029.
7. Botes M.; Cloete T.E. *Critical Reviews in Microbiology* **2010,** 36, 68-81.
8. Ramakrishna S.; Fujihara K.; Teo W-E.; Lim T-C.; Ma Z., *An Introduction to Electrospinning and Nanofibres*. World Scientific Publishing Co. Pte. Ltd.: Toh Tuck Link, Singapore, 2005.
9. Greyling C.J. Electrospinning of polyacrylonitrile nanofibres with additive: Study of orientation and crystalinity. Stellenbosch University, Stellenbosch, 2010.
10. Wang Y.; Aponte M.; Leon N.; Ramos I.; Furlan R.; Evoy S.; Santiago-Avil´e J. *Materials Letters* **2005,** 59, 3046-3049.
11. Melaiye A. *Journal of the American Chemical Society* **2005,** 127, 2285-2291.
12. Patel A.C.; Li S.; Wang C.; Zhang W.; Wei Y. *Chemical Materials* **2007,** 19, 1231-1238.
13. Yuh J. *Materials Letters* **2005,** 59, 3645-3647.
14. Guan H.; Shao X.; Chen B.; Gong J.; Yang X. *Inorganic Chemistry Communications* **2003,** 6, (1409-1411).
15. Guan H. *Gaodeng Xuexiao Huaxue Xuebao* **2004,** 25, 1413-1415.
16. Guan H. *Inorganic Chemistry Communications* **2003,** 6, 1302-1303.
17. Ma J. *Journal of Physical Chemistry B* **2001,** 105, 11994-12002.
18. Viswanathamurthi P. *Nanotechnology* **2004,** 15, 320-323.
19. Viswanathamurthi P.; Bhattarai N.; Kim H.; Lee D. *Scripta Materialia* **2003,** 49, 577-581.
20. Viswanathamurthi P.; Bhattarai N.; Kim H.; Lee D.R.; Kim S.; Morris M.A. *Chemical Physics Letters* **2003,** 374, 79-84.
21. Demir M.M. *Macromolecules* **2004,** 37, 1787-1792.
22. Choi B.K. *Materials Science and Engineering B* **2005,** 119, 177-181.
23. Ruparelia J.P.; Chatterjee A.K.; Duttagupta S.P.; Mukherji S. *Acta Biomaterials* **2008,** 4 707-716.
24. Grace M.; Chand N.; Bajpai S.K. *Journal of Macromolecular Science Part A* **2008,** 45, 795-803.
25. Grace M.; Chand N.; Bajpai S.K. *Journal of Engineered Fibers and Fabrics* **2009,** 4, 24-35.

26. Daels N.; De Vrieze S.; Sampers I.; Decostere B.; Westbroek P.; Dumoulin A.; Dejans P.; De Clerck K.; Van Hulle S.W.H. *Desalination* **2011**.
27. Francolini I.; Ruggeri V.; Martinelli A.; D'Ilario L.; Piozzi A. *Macromolecular Rapid Communications* **2006,** 27, 233-237.
28. Voigt W.V. Water stable, antimicrobial active nanofibres generated by electrospinning from aqueous spinning solutions. RWTH Aachen University, Munich, 2009.
29. Hulubei C.; Hamciuc E.; Bruma M.; Ignat M. *IEEE* **2008**, 275-278.
30. Lu X.; Wang C.; Wei Y. *Small* **2009,** 5, 2349-2370.
31. Chatzinikolaou I.; Hanna H.; Graviss L.; Chaiban G.; Perego C.; Arbuckle R.; Champlin R.; Darouiche R.; Samonis G.; Raad I. *Infect. Control Hosp. Epidemiol.* **2003,** 24, 961-963.
32. Xing X.; Lu D.; Wang X.; Liu Z. *Journal of Macromolecular Science Part A: Pure and Applied Chemistry* **2009,** 46, 560-565.
33. Staniìc V.; Dimitrijeviˇıc S.; Antiˇıc-Stankoviˇıc J.; Mitriˇıc M., J. ı. B.; Pleˇıcaˇs I.B.; Raìceviìc S. *Applied Surface Science* **2010,** 256, 6083-6089.
34. Moritani T.; Yamauchi J. *Polymer* **1998,** 39, 559-572.
35. Mukherjee G.S.; Shukla N.; Singh R.K.; Mathur G.N. *Journal of Scientific Industrial Research* **2004,** 63, 596-602.
36. Chirowodza H. Synthesis and characterization of cationically and anionically modified poly(vinyl alcohol) microfibrils. Stellenbosch University, Stellenbosch, 2009.
37. Chirowodza H.; Sanderson R.D. *Macromolecular Materials and Engineering* **2010,** 295, 1009-1016.
38. Mpitso K. Synthesis and characterization of styrene – maleic anhydride copolymer derivatives. Stellenbosch University, Stellenbosch, 2009.
39. Brouwer H.D.; Schellekens M.A.J.; Klumperman B.; Monteiro M.J.; German A.L. *Journal of Polymer Science Part A: Polymer Chemistry* **2000,** 38, 3596-3603.
40. Edgren D.; Wong P.S.L.; Theeuwes F. US Patent 4587117. 1986.
41. Guha S.K. US Patent 5488075 1996.
42. Bellettini A.G.; Bellettini R.J. US Patent 6210653. 2001.
43. Saad G.R.; Morsi R.E.; Mohammady S.Z.; Elsabee M.Z.J. *Polymer Research* **2008,** 15, 115-123.
44. Varabhas J.S.; Tripatanasuwan S.; Chase G.G.; Reneker D.H. *Journal of Engineered Fibers and Fabrics* **2009,** 4, 46-50.
45. Liu Y.; He J-H. *International Journal of Nonlinear Sciences and Numerical Simulation* **2007,** 8, 393-396.
46. Liu Y.; He J-H.; Yu J-Y. *Journal of Physics: Conference Series 012001* **2008,** 96, 1-4.
47. Yun K.M.; Suryamas A.B.; Iskandara F.; Bao F.L.; Niinuma H.; Okuyama K. *Separation and Purification Technology* **2010,** 75, 340-345.

48. Bruch M.; Mader D.; Bauers F.; Loontjens T.; Mulhaupt R. *Journal of Polymer Science: Part A: Polymer Chemistry* **2000,** 38, 1222-1231.

49. Lambla M.; Druz J.; Mazeres F. *Plastic and Rubber Process Applications* **1990,** 13, 75-79.

50. Hu G.H.; Lindt J.T. *Journal of Polymer Science Part A: Polymer Chemistry* **1993,** 31, 691-700.

51. Aoyagi J.; Shinohara I. *Journal of Applied Polymer Science* **1972,** 16, 449-460.

Chapter 5: An investigation into the use of furanone derivatives as antibiofouling agents in filter media

5.1 Chapter summary

The 3(2H) furanone derivative 2,5-dimethyl-4-hydroxy-3(2H)-furanone (DMHF) was investigated for its biofilm-inhibiting properties against biofilms of *Klebsiella pneumoniae* Xen 39, *Staphylococcus aureus* Xen 36, *Escherichia coli* Xen 14, *Pseudomonas aeruginosa* Xen 5 and *Salmonella typhimurium* Xen 26. The free furanone as well as nanofibres emanating from blends of 2,5-dimethyl-4-hydroxy-3(2H)-furanone and PVA which were electrospun to produce PVA/DMHF nanofibres were tested for their ability to inhibit adherence of bacteria on their surfaces.

This furanone was also used to synthesize two other furanone derivatives (5(2H) and 3(2H)) which were also tested for their ability to inhibit surface colonization by the above mentioned strains. The two synthesized furanones were covalently immobilized onto poly(styrene-co-maleic anhydride) (SMA) and electrospun into nanofibres which were also tested for inhibition of biofilm formation. Nuclear magnetic resonance, electron spray (ES) mass spectroscopy and attenuated total reflectance-infrared spectroscopy were used to confirm the structures of the synthesized furanones as well as their successful immobilization on SMA. To ascertain if the compounds leach into filtered water, samples of filtered water were analyzed using gas chromatography coupled with mass spectroscopy (GC-MS). Various techniques were also used to characterize the electrospun nanofibres and these include SEM, ATR-IR, TGA and DSC.

5.2 Introduction

The therapeutic efficacy of antibiotics collates closely with their bactericidal and bacteriostatic effects. Bacteria can however adapt to the selective pressure from antibiotics through genetic alteration leading to the development of antibiotic resistance.[1] Other means of controlling biofilms and their consequences thereof can be environmentally hazardous and costly especially in membrane systems. This has led to a need to develop other means of controlling or destroying biofilms apart from using chemical orientated measures.

As discussed in previous sections, membrane filtration is a promising technology in water purification. This technology is however limited as a result of biofilm attachment to membranes which is also referred to as biofouling. Biofouling of membranes demands costly periodic cleaning and membrane replacement. A sustainable and environmentally friendly solution for which inhibits attachment of biofilms on membrane surfaces is currently not available and would be of great interest for many

purposes. In this chapter, surface functionalization of nanofibres using furanone derivatives as well as coating surfaces with free (unimmobilized) furanones was investigated as a solution to prevent bacteria attachment. Complex biofilm formation by environmental strains which is the major cause of biofouling and biofilm formation is in most cases controlled by *N*-acyl homoserine lactone (AHL)-mediated Quorum Sensing (QS). A brief review of existing literature on QS, which is a language bacteria use to assess their population densities, is given. The role of quorum sensing in biofilm formation was discussed as well as mechanisms which inhibit QS. Furthermore, furanones which are derivatives of homoserine lactones and appear to interfere with QS and subsequently biofilm formation are reviewed using relevant literature. A discussion on naturally occurring and synthetic furanones which have shown effectiveness against bacteria is given.

5.3 Quorum sensing (QS)

Bacteria use the language of low-molecular weight ligands to communicate amongst each other and to assess their population sizes in a process called quorum sensing (QS). The first evidence of cooperative behaviour among bacteria was reported by Tomasz in 1965.[2] The biology of light producing organelles, through a cell-density-dependent reaction was then studied by Nealson and coresearchers.[3] Over the following decades this population-dependent phenomenon was termed "quorum-sensing".[4, 5] Over the past few years, large amounts of literature and data have been available on bacterial QS and interest among researchers in modulating quorum sensing using different approaches has increased. QS is not necessary for bacterial survival but helps in coordinating the community-based bacterial behaviour, therefore, the inhibition of QS only interrupts the desired phenotype. Therefore, interference with QS may not bring about a universally beneficial effect but makes the bacteria more susceptible to control/destruction by traditional means.

5.3.1 The role of QS in biofilm formation

Microorganisms prefer living in surface-attached colonies rather than in the planktonic state and as individual cells.[6] These communities of bacterial cells referred to as a biofilms are almost always enclosed in self-produced polymeric matrix and adherent to either inert or living surfaces.[6] Cell to cell signaling between the bacteria, which results in changes in gene and protein expression is necessary for biofilm formation and this is known as quorum sensing.[7] Biofilms are highly resistant to antibiotics and disinfection treatments and this results in persistent human infections and detrimental corrosion and equipment failure in industrial settings.[8] Modification of surfaces and new inhibitor designs have been investigated for the control of biofilm formation in industrial settings. [9-12] Biofilm formation in filtration membranes is one of the major limitations associated with membrane technology. [13] This reduces the quality and quantity of water in water purification systems and consequently results in higher treatment costs.

5.3.2 Quorum Sensing Inhibitors (QSI)

An interference with this cell density-dependent communication mechanism, Quorum Quenching (QQ) has been suggested to be a promising strategy to control their coordinated behavior.[13] Reduction of biofilms has been achieved by inhibition of quorum sensing due to changes in the LuxR family protein receptor for AHL signal molecules.[13, 14] Several chemicals and enzymes that target the key components of bacterial quorum sensing systems have been identified as Quorum Sensing Inhibitors (QSI) in recent years.[13, 15] A QSI system used by the marine algae *Delisea pulchra* has gained much interest. [13] These furanones are found in vesicles on the algae surface and prevent fouling of the algae surfaces by marine organisms.

5.4 Furanones

Furanones are analogs of homoserine lactones that appear to interfere with the development of typical biofilm structure, leaving these organisms more susceptible to treatment with natural biocides. Furanones are derivatives of furan as illustrated in Figure 5.1. The furanone moiety is the structural feature of a large number of biologically active compounds such as alkaloids, lignans, and pheromones and γ-alkylidene furanones constitute an important subclass of the furanone family with a wide range of biological activity.[16] Many natural products contain the core 3(*2H*)-furanone structure, which has been found to have various medicinal properties, such as anticancer, antifungal, and anti-inflammatory properties. These compounds do occur naturally in the marine environment and can also be chemically synthesized. There are several reported ways of producing this diverse group of compounds. Some have even been modified and some even flavored e.g. the strawberry flavored furanone and hazel flavored reported by Perez et al.[17]

furan 3(*2H*)-furanone

Figure 5.1: Basic structures of furan and 3(*2H*)-furanone.

5.5 How furanones inhibit QS

Furanones act by mimicking the AHL signal, they do this by occupying the binding site on the putative regulatory protein, making it highly unstable and accelerating its turnover rate. This results in the disruption of QS-mediated gene regulation.[18] Defoirdt et al. investigated the mechanism of action of furanones isolated from the marine algae *Delisea pulchra* at molecular level and found three QS pathways, AI-1, AI-2, and CAI-1, in *V. harveyi*. From his findings, *Delisea pulchra* inhibited QS by

decreasing the DNA-binding activity of the master transcriptional regulator protein LuxRvh in *V. harveyi*.[19] The following sections describe naturally occurring and synthetic furanones which have been used in controlling biofouling. This model has been extensively experimented and a lot of evidence confirming it has been accumulated in recent years. Furanones have been found to (a) repress AHL-dependent expression of *V. fischeri* bioluminescence, (b) inhibit AHL controlled virulence factor production and pathogenesis in *P. aeruginosa*, (c) inhibit QS-controlled luminescence and virulence of the black tiger prawn pathogen *Vibrio harveyi*, and (d) inhibit QS-controlled virulence of *E. carotovora* .[14, 20-22 23]

5.5.1 Naturally occurring furanones

Naturally occurring furanones have been isolated from red marine algae (*Delisea pulchra*) which produces them as secondary metabolites known as halogenated furanones.[24] This algae attracted the attention of marine biologists because unlike all other marine flora, it was devoid of surface colonization. The furanone derivatives are found in vesicles in a specialised gland both in the interior and surface of the plant. The algae uses these compounds to prevent fouling by micro and macro foulers found in the marine environment as well as pathogenic bacteria.[25] The algae produces a range of halogenated furanones and demonstrates antibiofouling and antimicrobial properties.[26] The halogenated furanones bind to *LuxR* proteins without activating them thus inhibiting bacterial adhesion and biofilm development through quorum sensing pathways in Gram-negative and Gram-positive bacteria, including human pathogens.[14, 27 2] Ren et al. established that the natural furanone compound from *Delisea pulchra* could also inhibit the AI-2-mediated QS in *V. harveyi* and *E. coli.* [19]

5.5.2 Synthetic furanones

Several furanone-based structural analogues have been synthesized and analyzed for their ability to inhibit QS. Synthetic furanones demonstrated equal activity against biofilm bacteria and planktonic cells in similar concentrations, despite the profoundly different modes of growth. Researchers have demonstrated antifouling properties of furanone compounds against Gram-positive and Gram-negative bacteria. Most of these studies have focused on the efficacy of the furanone compounds against *S. aureus* and *E. coli*.[28, 29] Some synthetic furanones have been reported to not only inhibit quorum sensing but also act as antimicrobial agents. On a study carried out by Khan and Husain, 3-arylidene-5-(biphenyl-4-yl)-2(3H)-furanones were reported to be effective as antimicrobial agents against *S. aureus* and *E. coli* with a MIC ranging from 10–100 µg/ml. Additionally, there is also evidence of growth inhibition of *Bacillus subtilis* by these furanone compounds. To date, there have been few reports of furanone activity against *S. epidermidis*, which is the most commonly isolated pathogen from medical device infections.[30, 31] Baveja et al. investigated the use of furanones as potential anti-bacterial coatings on biomaterials. Bacterial load on all furanone coated materials was significantly

reduced as was slime production. [30] Wu *et al*. reported that synthetic furanones inhibited several bacterial quorum sensing and simultaneously reduced the severity of the lung infection.[32]

5.6 Objectives

The main objective of this study was to produce nanofibres with the ability to inhibit biofouling and this was divided into minor objectives which were;

- To test the antifouling potential of free 2,5-dimethyl-4-hydroxy-3(2H)-furanone
- To fabricate nanofibres from blends of poly(vinyl alcohol)/2,5-dimethyl-4-hydroxy-3(2H)-furanone solutions (PVA/DMHF).
- To synthesize a 3(2H) and a 5(2H) furanone derivative from 2,5-dimethyl-4-hydroxy-3(2H)-furanone.
- Test the antibiofouling efficiencies of the synthesized furanones in their free form
- Covalently bind the synthesized furanone derivatives on SMA.
- Test the antifouling potential of the bound furanones.

5.7 Impact of furanone-modified nanofibres

The use of furanon- modified nanofibres in filtration applications has not been explored much. Research on biofouling inhibition especially on medical devices is widespread. The application of these for biofouling inhibition could be beneficial especially because it does not use the same pathway as many antibiotics and the risks of bacterial resistance are completely eliminated.[30, 33] Toxicity of halogenated furanones is well reported and thus for this study, only non-halogenated furanone derivatives were used.

5.8 Experimental materials and methods

In this section the materials and methods used to carry out the objectives of this study are given. Some methods have already been used in previous sections in which case reference is made to those sections.

5.8.1 Materials

The furanone compound 2,5-dimethyl-4-hydroxy-3(2H)-furanone, butadiene monoxide, acryloyl chloride 2,2-(aminoethoxy)ethanol and sodium hydride (NaH) were obtained from Sigma Aldrich, South Africa and used without further purification. Boc oxide $(Boc)_2$, iodine (I_2), Grubbs (ii) catalyst, sodium hydrogen carbonate ($NaHCO_3$) and sodium thiosulfate ($Na_2S_2O_3$) were obtained from Merk chemicals. The solvents and acids (tetrahydrofuran (THF), diethyl ether, dichloromethane (DCM), p-toluenesulfonic acid, phosphoric acid (H_3PO_4) and toluene) used in this study were all purchased from Sigma Aldrich.

5.8.2 Antibiofouling characterization

Tests of the antibiofouling capacity of the free furanones, PVA/DMHF and SMA immobilized furanones were carried out as outlined in Figure 5.2. Biofilm attachment on surfaces marks the initial stages of biofilm attachment. This method uses the assumption that without surface attachment, biofilm formation has been inhibited. To quantify inhibition efficiency, similar techniques as in antimicrobial characterization were used with the assumption that if any attachment took place, the cells would still be in the planktonic stage allowing plate counting. Other techniques were also used to characterize the nanofibres in order to confirm plate counting results. A description of the method is given in Section 5.8.2.1. Real biofilm development and biofilm architecture was not studied and future studies on these nanofibres will explore these details.

5.8.2.1 Method

Serial dilutions of the furanone derivatives up to 10^{-5} were prepared and on each of the dilutions, a 0.22 µm Millipore filter was soaked for an hour. This was followed by pat drying of the filters and subsequent culturing in BHI (10 mL) media containing inoculums of *E. coli* Xen 14, *S. tymphimurium* Xen 26, *P. aeruginosa* Xen 5, *K. pneumoniae* Xen 39 and *S. aureus* Xen 36. After culturing these strains overnight, the filters were removed from the culture media and rinsed in physiological water to remove unattached colonies. This was then followed by plate counting, bioluminescence imaging and fluorescence imaging techniques to ascertain the degree of attachment inhibition by the furanone derivatives. The same procedure was used for antibiofouling characterization of PVA and SMA furanone modified nanofibrous mats. In this case weighed furanone modified nanofibrous mats were used instead of Millipore filters.

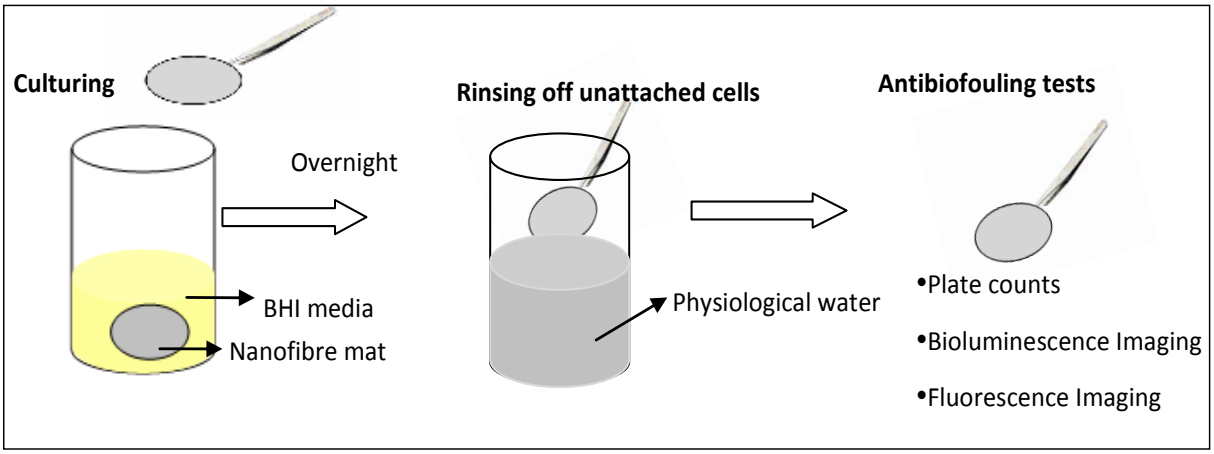

Figure 5.2: Antibiofouling characterization outline

5.8.3 Synthesis of furanone derivatives

Brominated furanones as well as 2(3H) and 2(5H) furanone derivatives have been reported to inhibit microbial growth on surfaces.[34, 35] Furanone compounds with 2(3H) and 2(5H) cores were synthesized from 2,5 dimethyl-4-hydroxy-3(2H)-furanone. The following sections describe the synthetic routes undertaken to prepare these compounds.

5.8.3.1 2(5H) furanone derivative

To a magnetically stirred mixture of 2-(2-(aminoethoxy) ethanol (1 mmol) **1** and $(Boc)_2O$ (1 mmol), a catalytic amount of iodine (10 mol %) was added under solvent-free conditions at room temperature. After stirring the reaction mixture for 3 hours, diethyl ether (10 mL) was added. The reaction mixture was washed with $Na_2S_2O_3$ (5%, 5 mL) and saturated $NaHCO_3$, dried over Na_2SO_4 and the solvent was evaporated under reduced pressure. The product was further purified using silica gel chromatography using ethyl acetate and triethylamine (7:1) as solvent system and vacuum evaporation to remove any residual solvent resulting in the desired boc protected 2-(2-(aminoethoxy) ethanol **2**. Tetrahydrofuran (THF)(20 mL) was gradually added to product **2** while stirring followed by NaH (1.2 equivalent). The reaction temperature was lowered to -20°C using the HAAKE Thermo DC5-K75 cryostat. When the temperature reached -20°C and the hydrogen gas had completely evolved, butadiene monoxide (also called 3,4 epoxy butene) was added to the reaction mixture and stirred for a further 1 hour. The reaction was then stirred for a further 16 hours at room temperature. Water (20 mL) was then added slowly with stirring until H_2 evolution ceased. The organic layer was separated using DCM, washed with H_2O and dried using Na_2SO_4.This was followed by ring closing metathesis through the nucleophilic attack of the O-H group at butadiene monoxide resulting in product **3**. The alcohol **3** was ringclosed by using Grubbs' second-generation catalyst towards a boc protected 5-(2-(2-aminoethoxy)ethoxy)methyl)-2(5H)furanone (**4**)which after deprotection yielded 84 % product (**5**). This reaction is illustrated in Scheme 5.1.

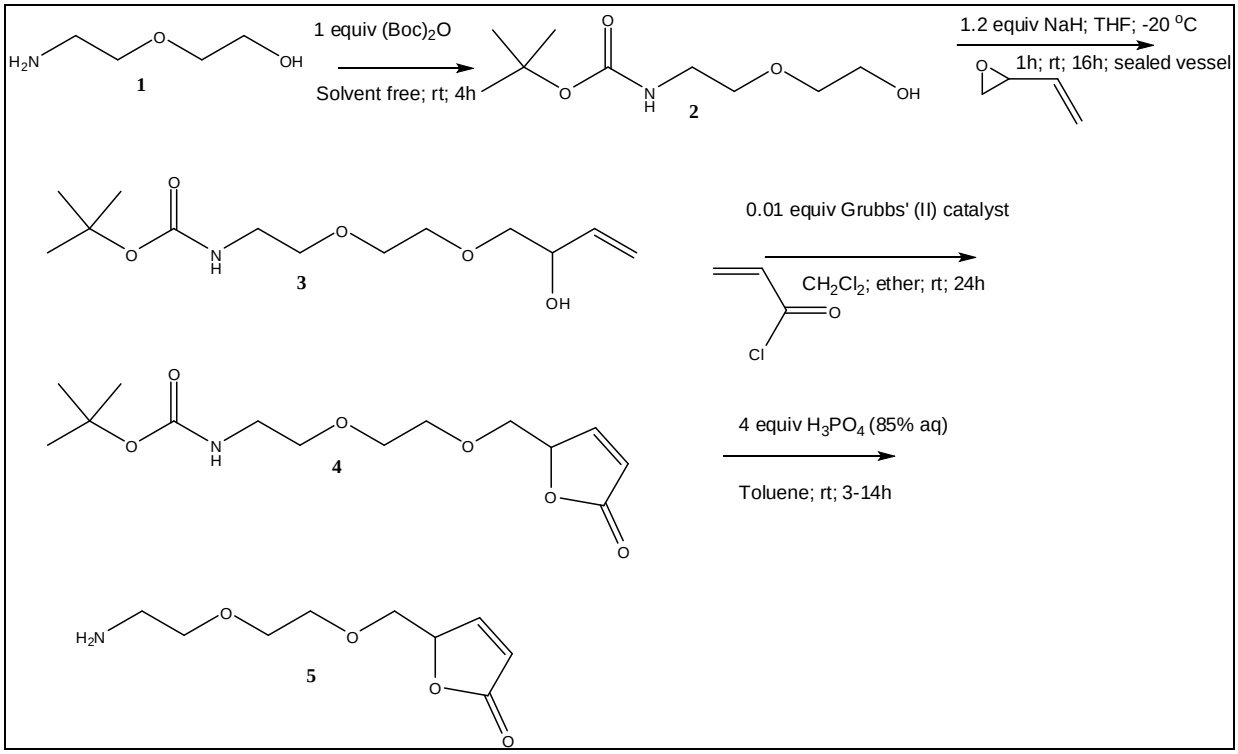

Scheme 5.1: Synthesis of 5-(2-(2-aminoethoxy)ethoxy)methyl)-2(5H)furanone.

5.8.3.2 3(2H) furanone derivative

The amine group in 2-(2-aminoethoxy)ethanol was boc-protected as described in Section 5.8.3.1 and the resultant boc-protected product was reacted with 2,5-dimethyl-4-hydroxy-3-(2H)-furanone (2.0 g) in a 250 mL round bottom flask in the presence of p-toluenesulfonic acid (100 mg). A drying tube was attached to the top of the reflux condenser, and the mixture refluxed for 6 hours. The mixture was then cooled, shaken with solid $NaHCO_3$ (5 g), and filtered through a 2 mm layer of $NaHCO_3$ to remove the acid catalyst. The product contained both the starting material and the boc-protected product, possibly because the p-toluenesulfonic acid deprotected 2-(2-aminoethoxy)ethanol. Column chromatography was used to purify the boc- protected 4-(2-(2-aminoethoxy)-2,5-dimethyl-3(2H)-furanone. This was followed by deprotection using 4 equiv H_3PO_4 in the presence of toluene as the solvent giving a 78% yield (Scheme 5.2).

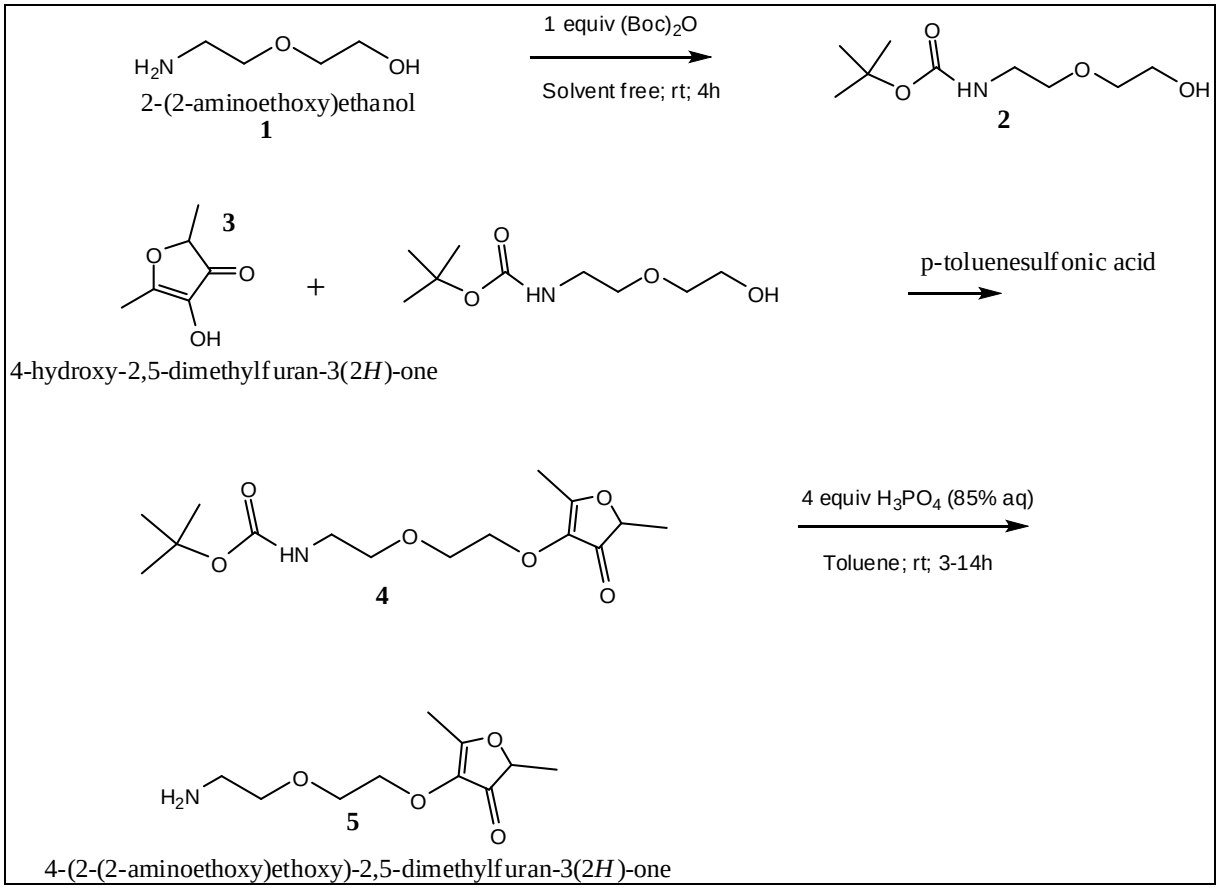

Scheme 5.2: Synthesis of 4-(2-(2-aminoethoxy)-2,5-dimethyl-3(2H)-furanone

5.8.4 Immobilization of furanone derivatives on SMA

In a three necked round bottomed flask equipped with a stirrer, SMA (0.5 g, 0.0051 mol MAnh) was placed and dimethyl formamide (DMF) (20 mL) was added as a solvent. Then the solution was stirred at 70°C. After complete dissolution of SMA, 4-(2-(2-aminoethoxy)-2,5-dimethyl-3(2H)-furanone (1 g, 0.0051 mol) was added dropwise with continuous stirring. This resulted in gelation of the reactants, vigorous stirring as well as increasing the temperature to 150°C resulting in a clear gold solution. This solution was then dehydrated and dried to give the final product in a yield of 61% after purification (Scheme 5.3). In the case of 5-(2-(2-aminoethoxy)ethoxy)methyl)-2(5H)furanone, 1.069 g, 0.0051 mol of MAnh and 0.534 g, 0.0051 mol 5-(2-(2-aminoethoxy)ethoxy)methyl)-2(5H)furanone were used.

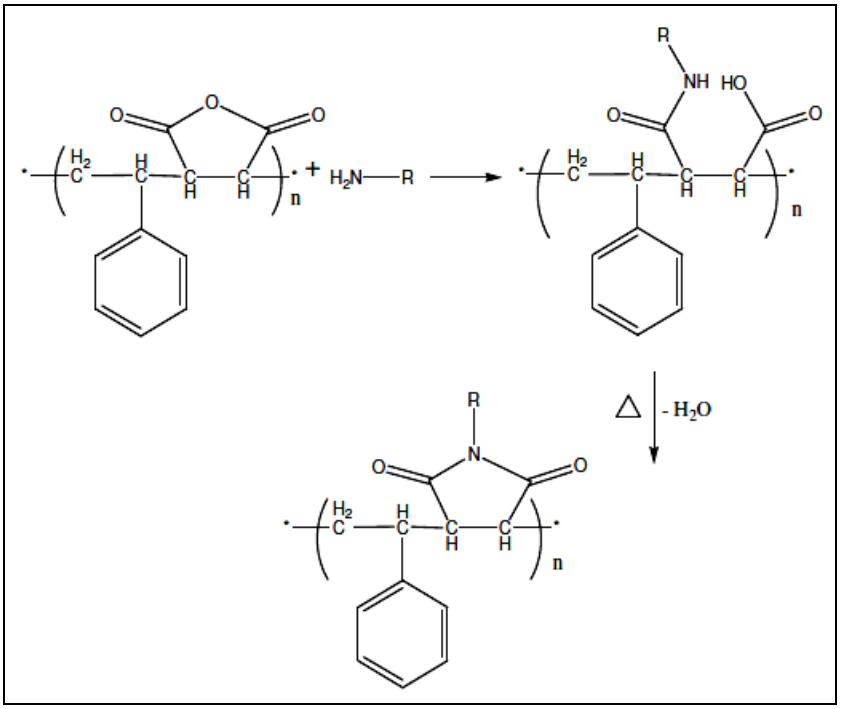

Scheme 5.3: Immobilization of furanone derivatives on SMA copolymer backbone. [36, 37]

5.8.5 Characterization of synthesized furanones

This section describes the techniques used to characterize the synthesized furanones which have not been described in previous sections.

5.8.5.1 Nuclear Magnetic Resonance (NMR) Spectroscopy

NMR spectroscopy was used to elucidate the chemical structures of the synthesized compounds and to determine their purity. One dimensional ^{1}H spectra were acquired with a Varian Unity Inova 600MHz NMR spectrometer with 5 mm broad band probe at 293 K in deuterated chloroform ($CDCl_3$) unless specified otherwise. Relaxation delays of 1 second and frequencies of 600 MHz were used for the ^{1}H NMR. Spectra were internally referenced to TMS. All peaks are reported downfield of TMS.

5.8.5.2 Electron spray (ES) mass spectroscopy

Electron spray mass spectroscopy (ES-MS) was carried out using a Waters API Q-TOF Ultima equipped with a Waters UPLC. 3. The sample (3 µL) was injected at a capillary voltage of 3.5 kV, cone voltage of 35 V and RFI value of 50. The source temperature was maintained at 80ºC and the desolvation temperature at 350ºC. The desolvation gas was set at 350 L/h and the cone gas at 50 L/h. Scans between 100 and 2000 were taken per sample.

5.8.5.3 Gas chromatograph coupled mass spectroscopy (GC-MS)

Gas Chromatograph coupled Mass Spectroscopy (GC-MS) was performed using a Waters GCT spectrometer equipped with CTC CombiPAL Autosampler a DB_XLB column (30 m, 0.25 mm ID, 0.1 μm film thickness) was utilized. The instrument settings were as outlined in Appendix A. Solid phase microextraction (SPME) vials were used in the analysis and the headspace of the samples were analysed following the CTC PAL method described Appendix A.

5.8.6 Preparation of electrospinning solutions and electrospinning conditions

Polymer/furanone blends of PVA (10% wt/vol) and 2,5 dimethyl-4-hydroxy-3(2H)-furanone (5% vol per volume of dissolved polymer) were prepared and electrospun into ultra fine nanofibre mats. SMA/5-(2-(2-aminoethoxy)ethoxy)methyl)-2(5H)furanone (SMA/Furanone 1) and SMA/4-(2-(2-aminoethoxy)-2,5-dimethyl-3(2H)-furanone (SMA/Furanone 2) were dissolved in (1:1) mixtures of ethanol and methanol to form 10% wt/vol electrospinning solutions. The conditions used to electrospin each of these solutions are given in Table 5.1.

5.8.6.1 PVA/DMHF

Polymer/furanone blends of PVA (10% wt/vol) and 2,5 dimethyl-4-hydroxy-3(2H)-furanone (5% vol per volume of dissolved polymer) were prepared and electrospun into ultra fine nanofibre mats which were then used instead of the Millipore filters.

5.8.6.2 SMA/Furanone

For SMA, the polymer could not form electrospinnable blends with the furanone derivatives but instead it formed gels. To achieve this, furanone derivatives from 2,5 dimethyl-4-hydroxy-3(2H)-furanone were synthesized in the lab and covalently bound to poly(styrene-co-maleic anhydride) (SMA).

Table 5.1: Electrospinning conditions

Polymer/blend	% relative humidity	Tip-collector distance (cm)	Applied voltage (kV)	Flow rate (μL/min)
PVA	40-45	25	15	15
PVA/DMHF	40-45	25-30	15	15
SMA	45-60	17	10	10
SMA/Furanone 1	45-60	17-20	10-12	10
SMA/Furanone 2	45-60	17-20	10-12	10

5.9 Results and discussions

In this section, the findings of this study are reported and discussed using relevant literature. Results on antimicrobial and antibiofouling tests on nanofibres emanating from blends of PVA with 2,5 dimethyl-4-hydroxy-3(2H)-furanone are given and discussed. Additionally, the synthesis of furanone derivatives and their immobilization on SMA copolymer backbone are reported. Chemical characterization and antibiofouling tests as well as leaching of the immobilized furanones are reported.

5.9.1 Nuclear Magnetic Resonance (NMR)

Synthesis of 5-(2-(2-aminoethoxy)ethoxy)methyl)-2(5H)furanone and 4-(2-(2-aminoethoxy)-2,5-dimethyl-3(2H)-furanone was successful. Their structures and molar masses were confirmed using ^{1}H NMR and electron spray mass spectroscopy. Figure 5.3 and Figure 5.4 outline the synthetic routes of the furanone derivatives giving the relevant ^{1}NMR spectrum for each step. Product yields of 81% and 63 % for 5-(2-(2-aminoethoxy)ethoxy)methyl)-2(5H)furanone and 4-(2-(2-aminoethoxy)-2,5-dimethyl-3(2H)-furanone respectively were obtained. Further purification by column chromatography on silica was dismissed due to losses in product yields when these were repeatedly columned.

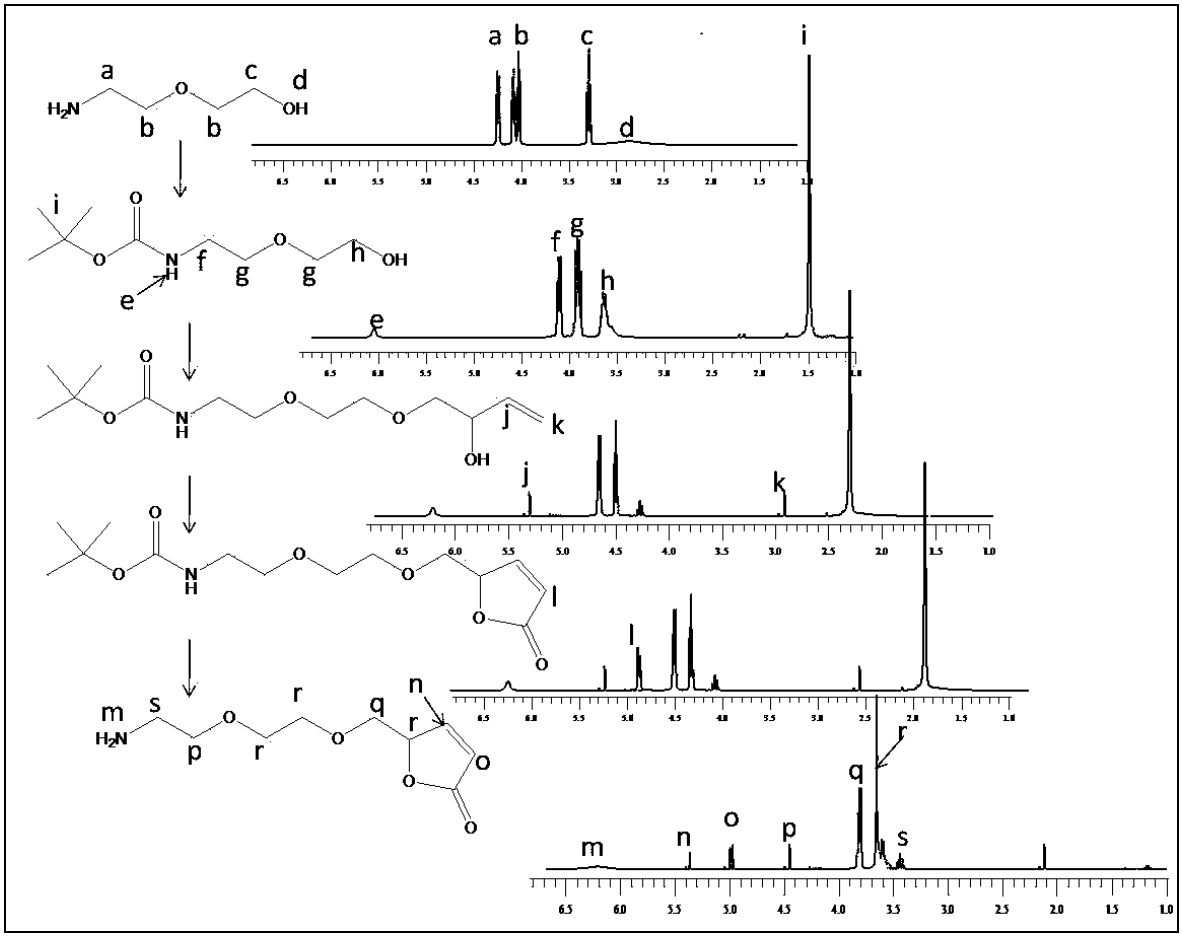

Figure 5.3: ^{1}HNMR spectra for the synthesis of 5-(2-(2-aminoethoxy)ethoxy)methyl)-2(5H)furanone.

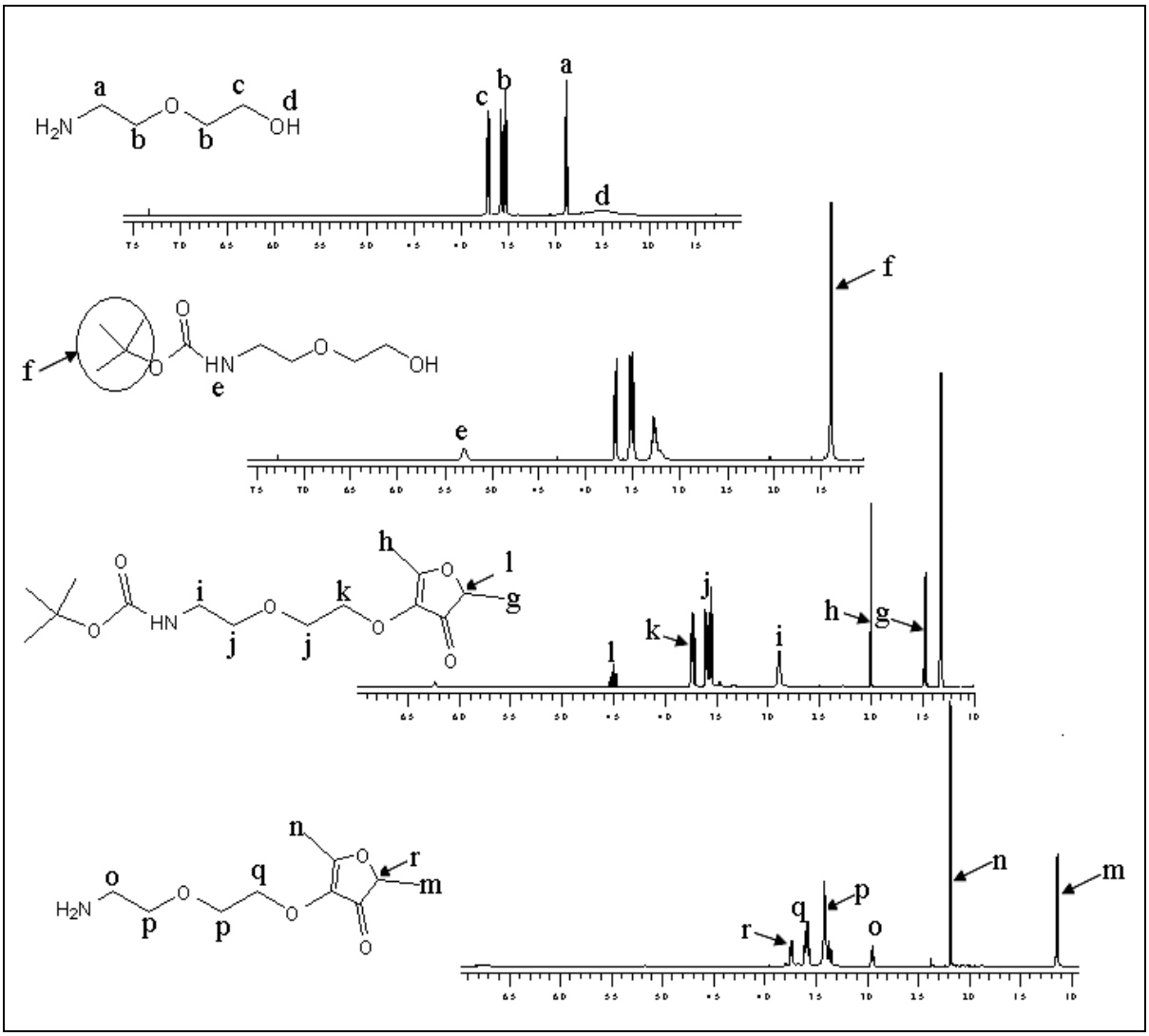

Figure 5.4: ^{1}HNMR spectra for the synthesis of 4-(2-(2-aminoethoxy)-2,5-dimethyl-3(2H)-furanone

5.9.2 Electron Spray Mass spectroscopy (ES-MS)

The molar masses of 5-(2-(2-aminoethoxy)ethoxy)methyl)-2(5H)furanone and 4-(2-(2-aminoethoxy)-2,5-dimethyl-3(2H)-furanone were confirmed by electron spray mass spectroscopy. The ES-MS spectra given in Figure 5.5 confirmed the molar masses of 5-(2-(2-aminoethoxy)ethoxy)methyl)-2(5H)furanone and 4-(2-(2-aminoethoxy)-2,5-dimethyl-3(2H)-furanone to be m/z 215.01 and m/z 201.1 respectively. This corresponds to calculated molar masses of 215.101 g for 5-(2-(2-aminoethoxy)ethoxy)methyl)-2(5H)furanone and 201.110 g for 4-(2-(2-aminoethoxy)-2,5-dimethyl-3(2H)-furanone.

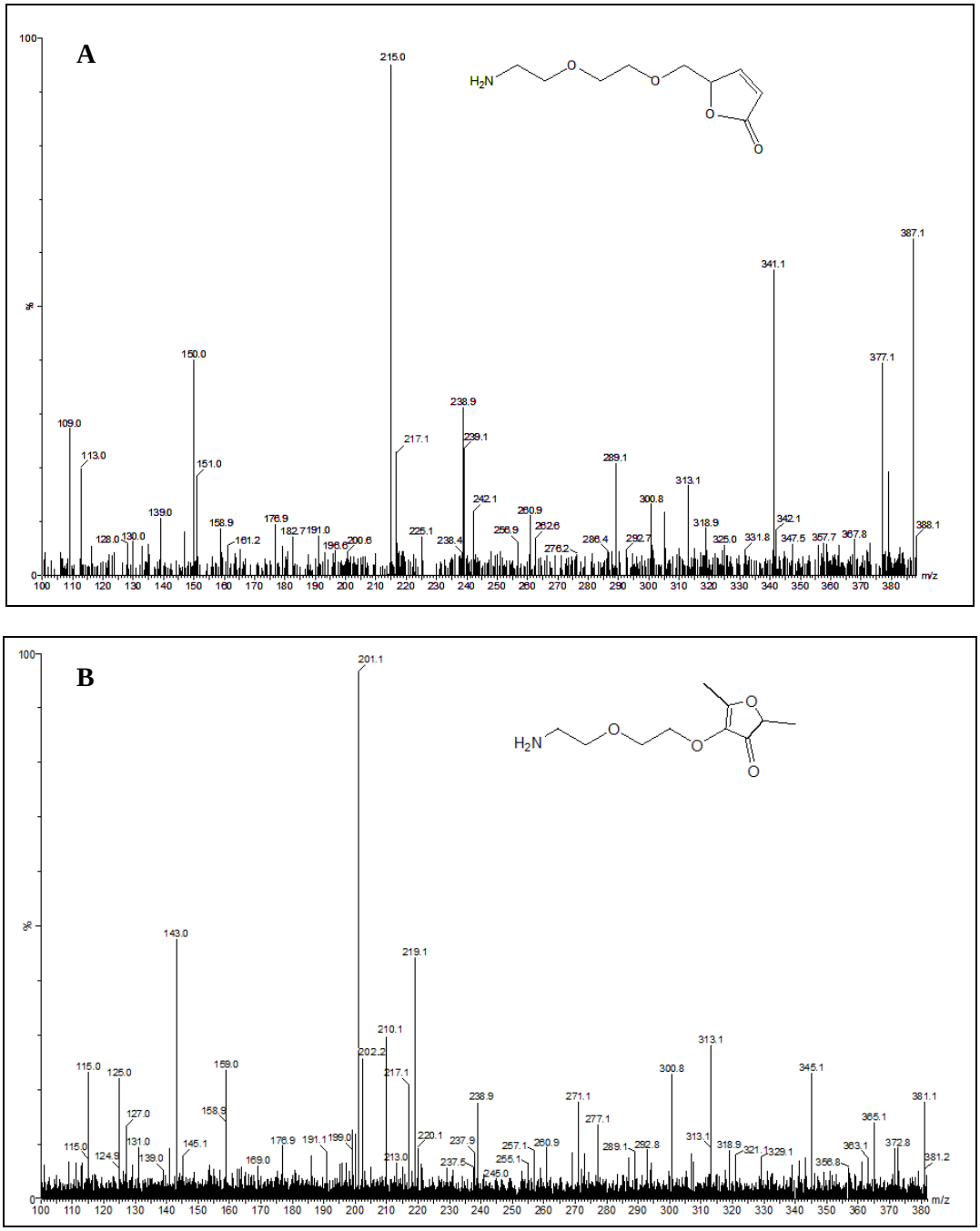

Figure 5.5: Electron spray-mass spectra of 5-(2-(2-aminoethoxy)ethoxy)methyl)-2(5H)furanone (A) and 4-(2-(2-aminoethoxy)-2,5-dimethyl-3(2H)-furanone (B).

5.9.3 Morphology of the nanofibres

In this section, morphological features including fibre diameters and pore sizes of the nanofibres are discussed.

5.9.3.1 Nanofibre diameters

About 63% of the nanofibres obtained from PVA/DMHF blends had diameters between 150-300nm, with a majority of these (29%) in the 200 and 250 nm range (Figure 5.6A). Nanofibres making up SMA/Furanone 1 nanofibres had smaller diameters with about 83% between 50-250 nm and more than 40% had diameters between 100 and 200 nm (Figure 5.6B). About 88% SMA/Furanone 2 nanofibres had diameters between 50 and 300 nm (Figure 5.6C). These diameter ranges are acceptable for filter media applications as discussed in previous sections.

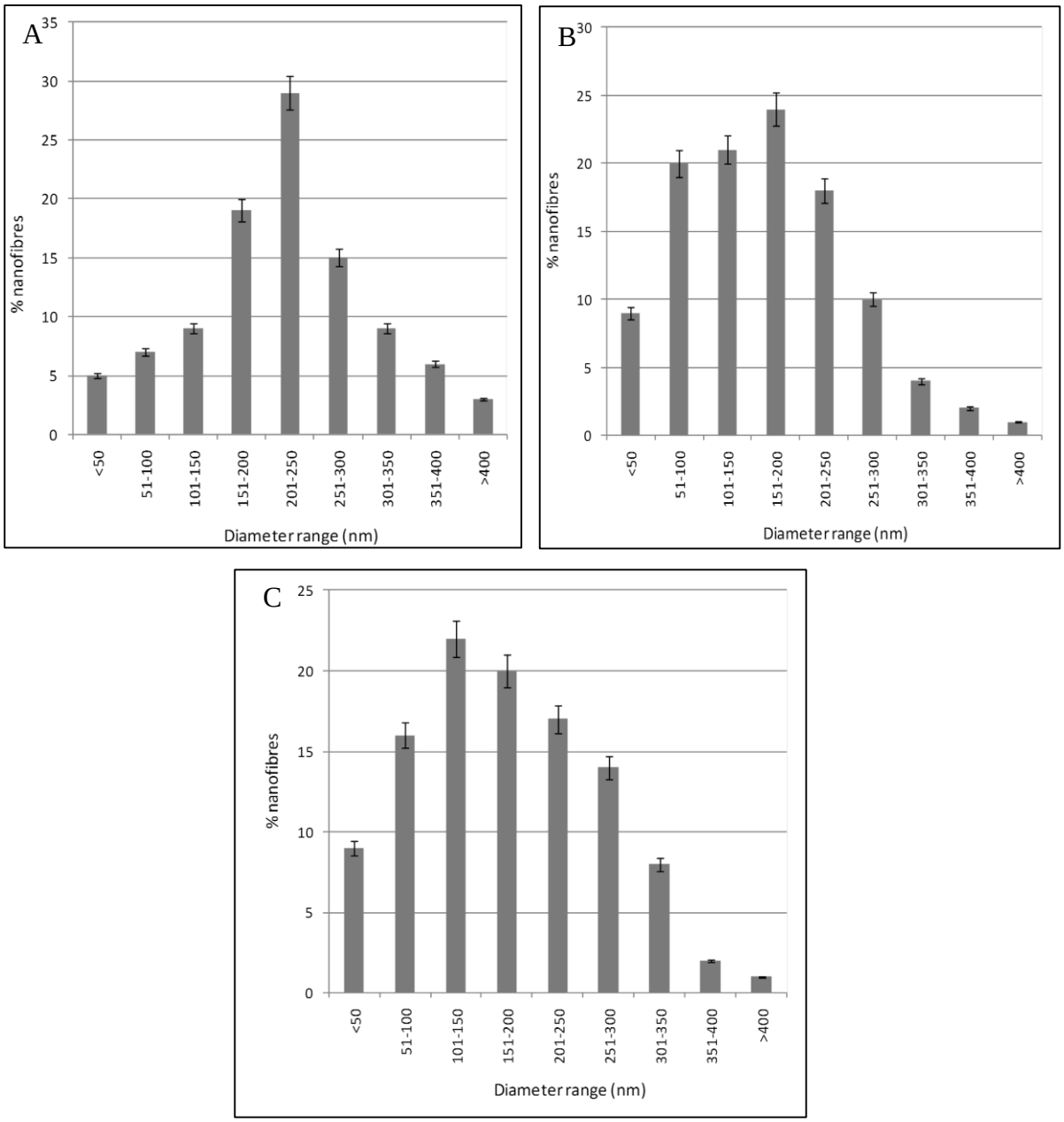

Figure 5.6: Nanofibre diameters of PVA/DMHF (A), SMA/Furanone 1 (B) and SMA/Furanone 2 (C).

5.9.3.2 Mat porosity

More than 80% of the pores on PVA/DMHF nanofibre mats had sizes of less than 100nm^2 with a majority of these pores in the 50-100 nm^2 range (Figure 5.7 A to C). About 70% of pores on SMA/Furanone 1 nanofibres mats had sizes less than 100nm^2 whilst SMA/Furanone 2 mats had a majority (about 70%) of their pores in the 100-150 nm^2 range.

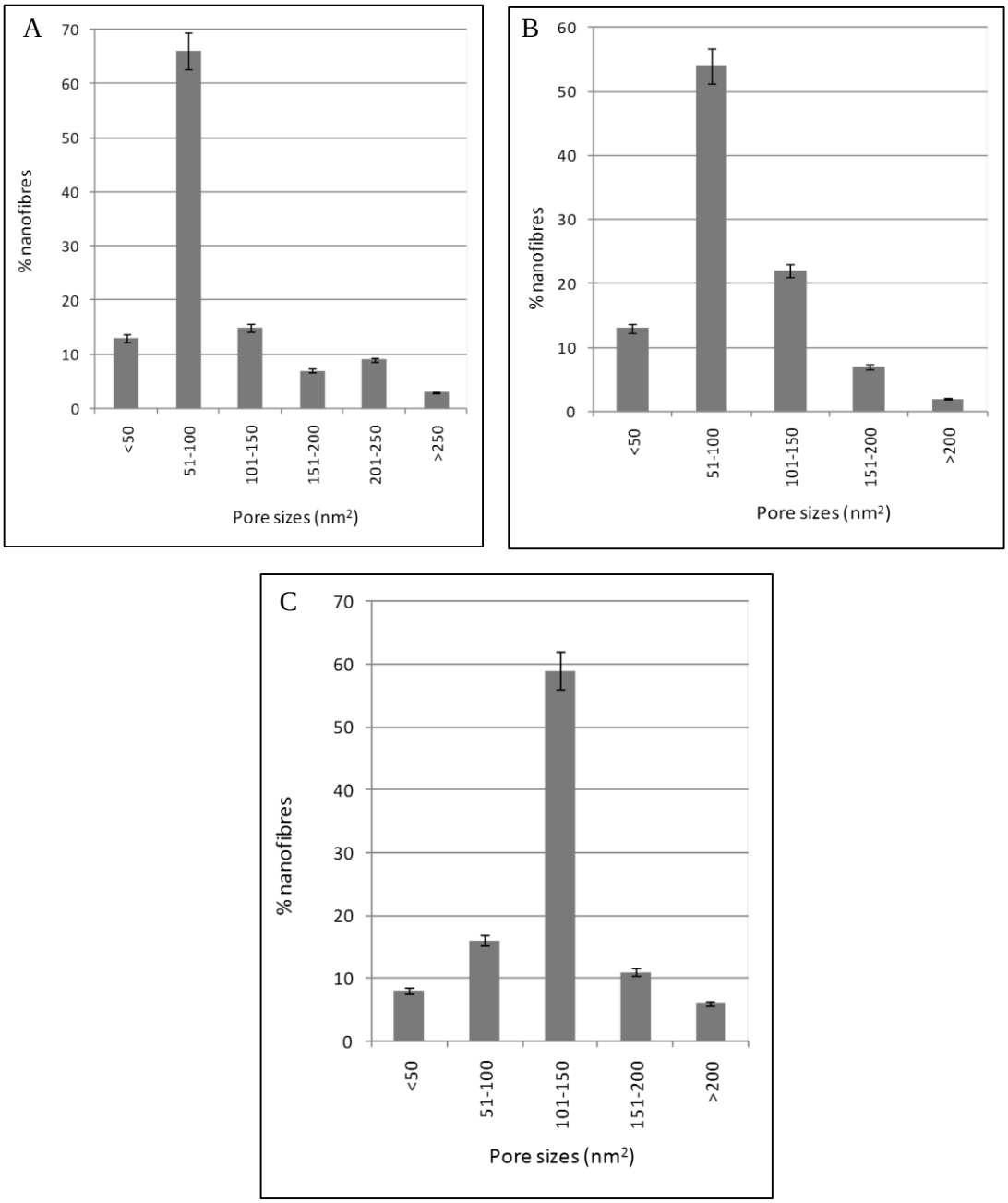

Figure 5.7: Pore sizes on PVA/DMHF (A), SMA/Furanone 1 (B) and SMA/Furanone 2 (C) nanofibre mats.

5.9.4 Attenuated total reflectance –infra red spectroscopy (ATR-FTIR)

From the ATR-FTIR spectra it is noted that the addition of 2,5-dimethyl-4-hydroxy-3(2H)-furanone to PVA introduced peaks characteristic of the furanone moiety on the PVA nanofibres (Figure 5.8). Evidence of this is shown by the peaks at 995, 920, 850 and 810 cm^{-1} (**region 1**) which are all characteristic of 2,5-dimethyl-4-hydroxy-3(2H)-furanone. PVA/DMHF also shows a new peak (**region 2**) at around 700 cm^{-1} which indicates formation of a new compound. In the ATR/FTIR spectrum of SMA copolymer (Figure 5.9 A and B), the bands at 1853 cm^{-1} and 1773 cm^{-1} are assigned to the cyclic anhydride (C=O) and 1222 cm^{-1} is due cyclic ring ether (C-O-C). The band at 1495 cm^{-1} is a styrenic band. Aromatic C-C stretching vibrations appear at 1454 cm^{-1} and 1157 cm^{-1}. The ATR/FTIR spectra of SMA/Furanones (1 and 2) nanofibres have similar bands to the one of the SMA copolymer except for the broadening of the peaks at around 3000 cm^{-1}. The maleic anhydride bands at 1853 (**1**)and 1600 (**2**) also disappear and new peaks (**3** and **4**) appear in the place of the C-C stretching vibrations around 1100 cm^{-1}. A new peak around 940 appears and was identified to be characteristic of the furanone moiety.

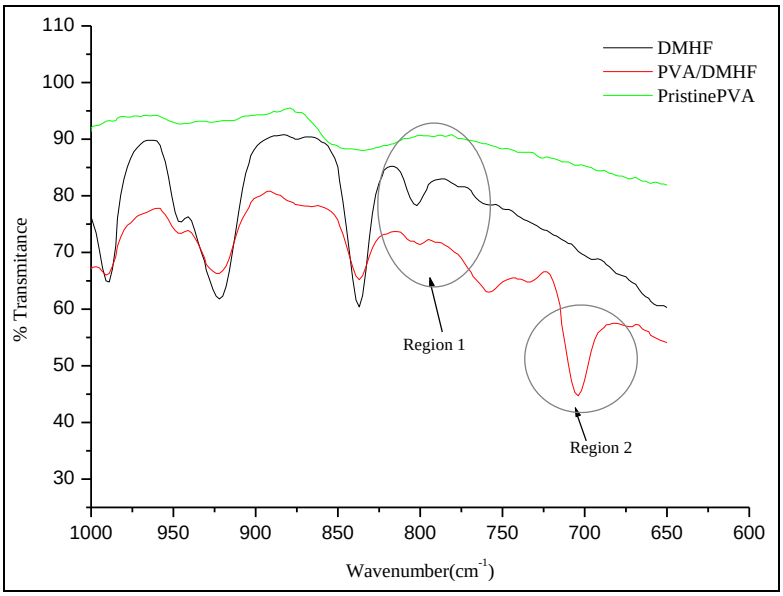

Figure 5.8: ATR-FTIR spectra of PVA/DMHF nanofibres.

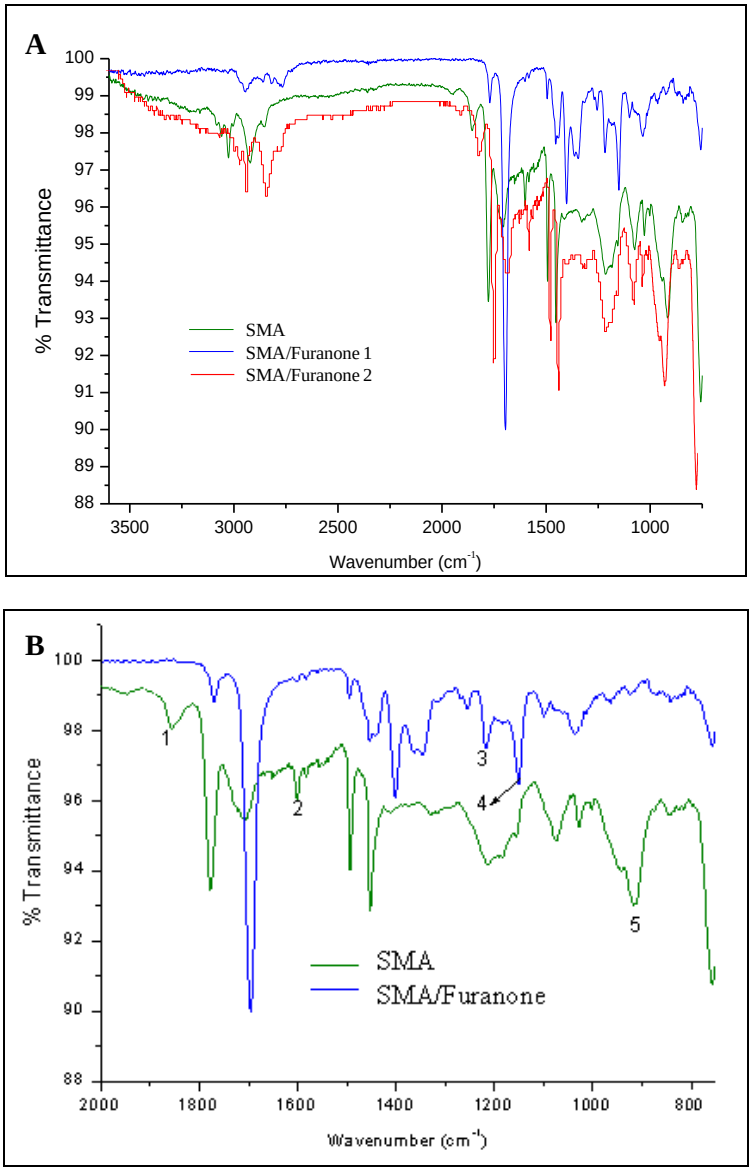

Figure 5.9: ATR-FTIR of SMA/Furanone.

5.9.5 Thermogravimetric analysis (TGA)

The degradation patterns of pristine PVA and PVA/DMHF nanofibres were similar and proceeded in three stages, which were the initial weight losses around 100°C and 200°C which are attributable to dehydration (Figure 5.10A). This was followed by the major weight loss at around 400°C. SMA/Furanone (both 1 and 2) nanofibres mats demonstrated a major weight loss in the temperature range between 250-300°C which was not shown by pristine SMA nanofibres (Figure 5.10B). No such weight loss is observed in SMA over this temperature range.[38] Weight loss in the temperature range 250–420°C is observed in both SMA and SMA/Furanone, which is attributed to decarboxylation reaction. A similar study by Switala-Zeliazkow on thermal degradation study of SMA and hydrolyzed SMA also showed a similar trend in degradation behavior of SMA and hydrolysed SMA.[39] This is an

indication that the modification of SMA with furanone compounds has some effects on the decomposition pattern of SMA nanofibres.

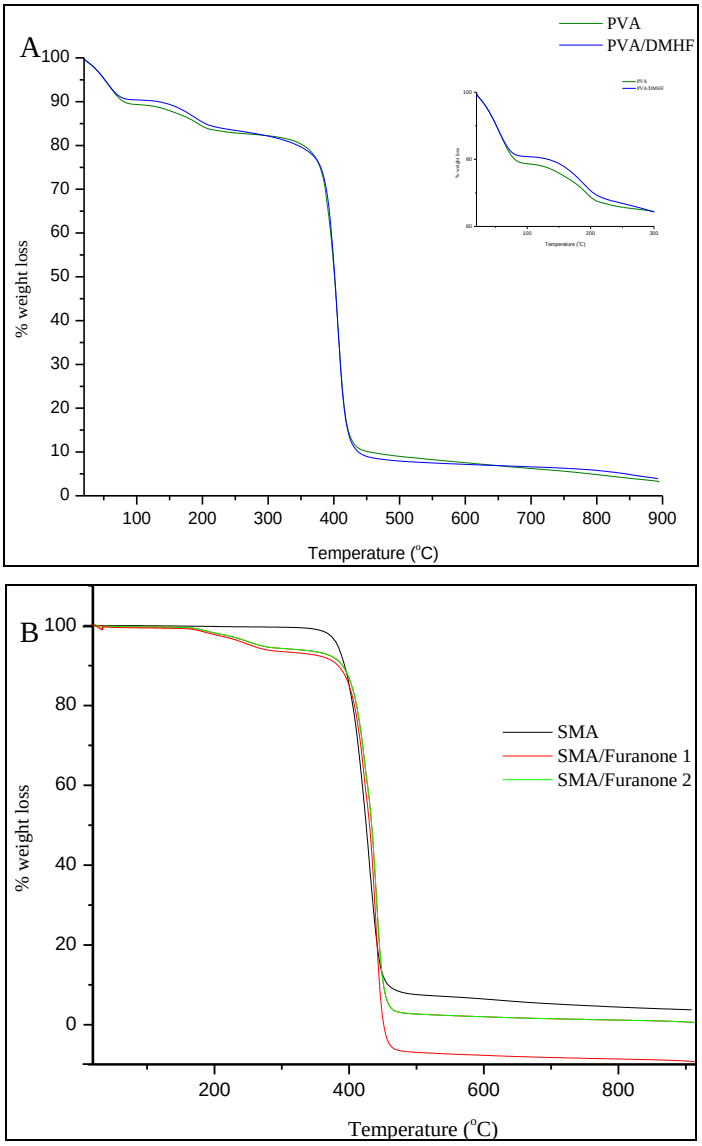

Figure 5.10: TGA thermograms of PVA/DMHF (A) and SMA/Furanone (B).

5.9.6 Differential scanning calorimetry (DSC)

By introducing DMHF to pristine PVA, the glass transition temperature decreased from 90°C to 82°C (Figure 5.11A). This could be due to the interactions of DMHF with the O-H groups in the PVA backbone.[40] There is no significant difference in the T_g values of SMA and SMA/Furanone 1 (Figure 5.11B). The only notable differences were an increased heat flow in the case of SMA/Furanone 1 compared to pristine SMA and the change in the zigzag structure of SMA to a more planar structure of SMA/Furanone 1. SMA/Furanone 2 on the other hand had a higher glass transition temperature of about 170°C compared to the 140°C shown by pristine SMA (Figure 5.11C).

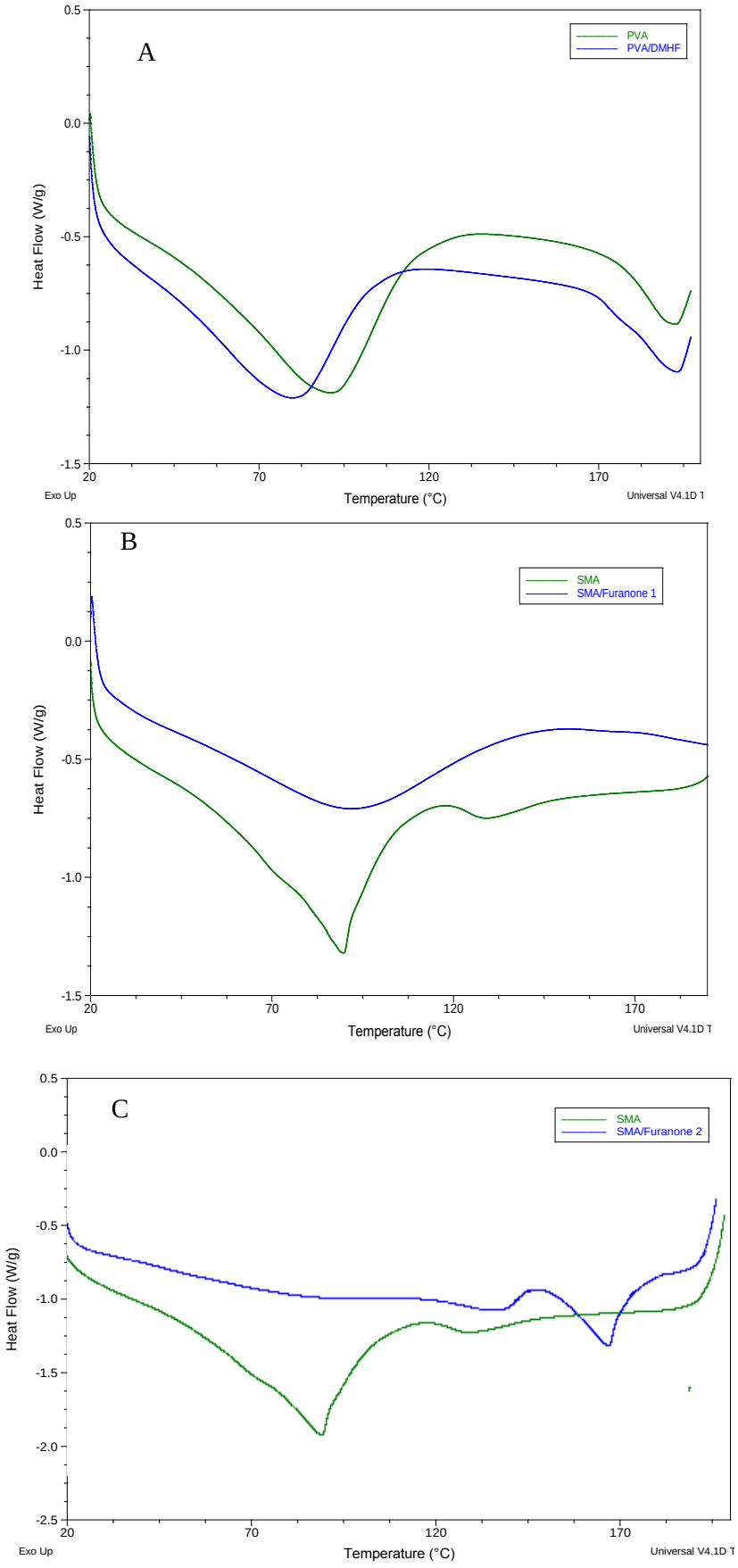

Figure 5.11:DSC themograms of PVA/DMHF (A), SMA/Furanone 1 (B) and SMA/Furanone 2 (C).

5.9.7 Antimicrobial and antibiofouling determination

In this section the antimicrobial and antibiofouling potentials of the free furanone compounds coated on Millipore filters as well as immobilized on polymer nanofibres is reported. Results on plate counting, bioluminescence imaging and fluorescence microscopy are discussed and supported using relevant literature. Control experiments were conducted on uncoated Millipore filters in the case of free furanones and unmodified nanofibres (pristine PVA and pristine SMA) in the case of furanone-modified nanofibres.

5.9.7.1 Free furanones

Millipore filters (0.22 µm sized) coated with 2,5 dimethyl-4-hydroxy-3-(2H)-furanones (DMHF) demonstrated up to 4 log reductions in populations of *S. aureus* Xen 36 cells and 2 log reductions on cells of *P. aeruginosa* Xen 5, *E. coli* Xen 14, *S. typhimurium* Xen 26, and *K. pneumoniae* Xen 39 after 30 minutes (Figure 5.12A). Almost 3 log reductions in *S. aureus* Xen 36 cells were achieved within 5 minutes of contact with the coated filters. These coated filters also inhibited biofilm formation by more than 3 log for all the strains (Figure 5.12B). *P. aeruginosa* Xen 5, *E. coli* Xen 14 and *S. aureus* Xen 36 recorded almost 5 log biofilm inhibitions after 36 hours.

Filters coated with 5-(2-(2-aminoethoxy)ethoxy)methyl)-2(5H)furanone achieved up to 2 log reductions in populations of *P. aeruginosa* Xen 5, *E. coli* Xen 14, *S. typhimurium* Xen 26, *S. aureus* Xen 36 and *K. pneumoniae* Xen 39 after 30 minutes of exposure. The antimicrobial activity exhibited by this furanone compound was low after the first 5 minutes for all the strains and gradually increased thus achieving up to 2 log after 30 minutes of exposure (Figure 5.13A). This furanone also inhibited biofilm formation by strains of *P. aeruginosa* Xen 5, *E. coli* Xen 14, *S. typhimurium* Xen 26, *S. aureus* Xen 36 and *K. pneumoniae* Xen 39 by at least 1.5 log after 36 hours (Figure 5.13B).

Filters coated with 4-(2-(2-aminoethoxy)-2,5-dimethyl-3(2H)-furanone on the other hand demonstrated up to 5.5 log reductions in populations of *P. aeruginosa* Xen 5 and *S.typhimurium* Xen 26 after 30 minutes of exposure (Figure 5.14A). Up to 4.5 log reductions were achieved for *E. coli* Xen 14, *S. aureus* Xen 36 and *K. pneumoniae* Xen 39. All the strains were reduced by more than 4 log after the first 5 minutes of exposure. These 4-(2-(2-aminoethoxy)-2,5-dimethyl-3(2H)-furanone coated filterss also inhibited surface colonization by biofilms of *P.aeruginosa* Xen 5, *E. coli* Xen 14, *S. typhimurium* Xen 26, *S. aureus* Xen 36 and *K. pneumoniae* Xen 39 by almost 3 log after 36 hours (Figure 5.14B).

Sung and co-workers also obtained satisfactory antimicrobial efficacy of DMHF on strains of *P.aeruginosa, S. aureus, E coli* and *Enterococci.* The antimicrobial efficacy and quorum sensing

inhibition by other 3(2H) and 5(2H) furanones has been reported in literature.[30, 41-43] Sindhu Ramachandran and Sreekumar reported antimicrobial activity of a 2(5H) furanone (4-dibromo-5-hydroxy-2(*5H*)-furanone) against strains of *Escherichia coli*, *Proteus vulgaris*, *Pseudomonas aeruginosa* and *Staphylococcus aureus* using the zone inhibition technique. Even though most of these studies do not quantify the number of cells (or colonies) inhibited, the concept of inhibition is well demonstrated.

To mimic a real life scenario, where microorganisms co-exist, the furanone-coated Millipore filters were tested on a mixed strain culture containing *P. aeruginosa* Xen 5, *E. coli* Xen 14, *S. typhimurium* Xen 26, *S. aureus* Xen 36 and *K. pneumoniae* Xen 39 cells. As noted in Figure 5.15A, 2,5-dimethyl-4-hydroxy-(3(2H)-furanone coated nanofibres demonstrated high antimicrobial efficiency (up to 4 log after 30 minutes) compared to those coated with 5-(2-(2-aminoethoxy)ethoxy)methyl)-2(5H)furanone and 4-(2-(2-aminoethoxy)-2,5-dimethyl-3(2H)-furanone which achieved reductions of 1.5 and 3 log respectively. Antibiofouling characterization revealed that the filters coated with 4-(2-(2-aminoethoxy)-2,5-dimethyl-3(2H)-furanone showed higher inhibition efficiency (4.2 log) compared to those coated with 2,5-dimethyl-4-hydroxy-(3(2H)-furanone and 5-(2-(2-aminoethoxy)ethoxy)methyl)-2(5H)furanone which demonstrated inhibition of 3.6 and 2.4 log inhibitions respectively (Figure 5.15B).

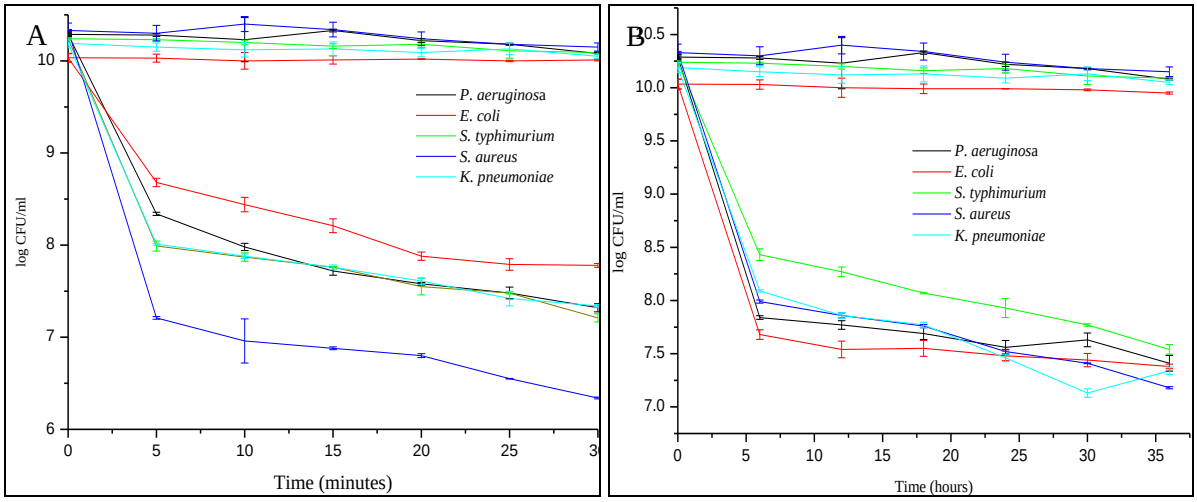

Figure 5.12: Antimicrobial (A) and antifouling (B) potential of free 2,5-dimethyl-4-hydroxy-3(2H)-furanone over 30 minutes and 36 hours respectively.

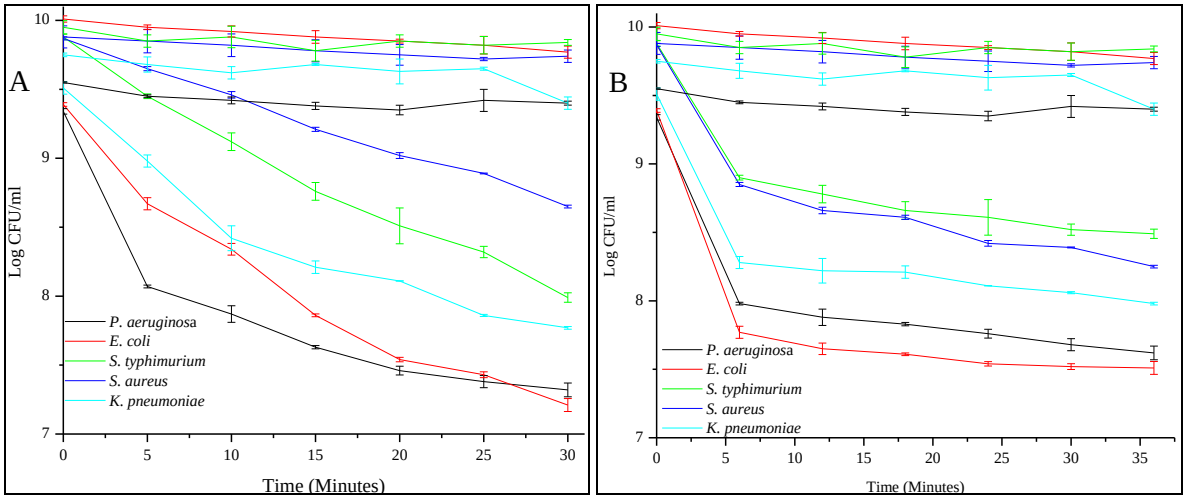

Figure 5.13: Antimicrobial (A) and antifouling (B) potential of free 5-(2-(2-aminoethoxy)ethoxy)methyl)-2(5H)furanone over 30 minutes and 36 hours respectively.

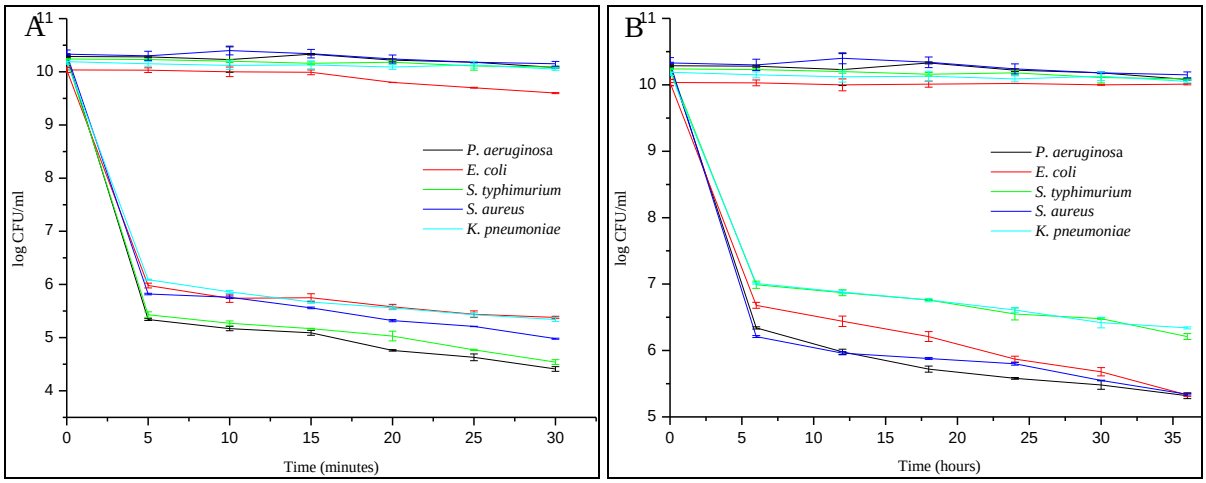

Figure 5.14: Antimicrobial (A) and antifouling (B) potential of free 4-(2-(2-aminoethoxy)-2,5-dimethyl-3(2H)-furanone over 30 minutes and 36 hours respectively.

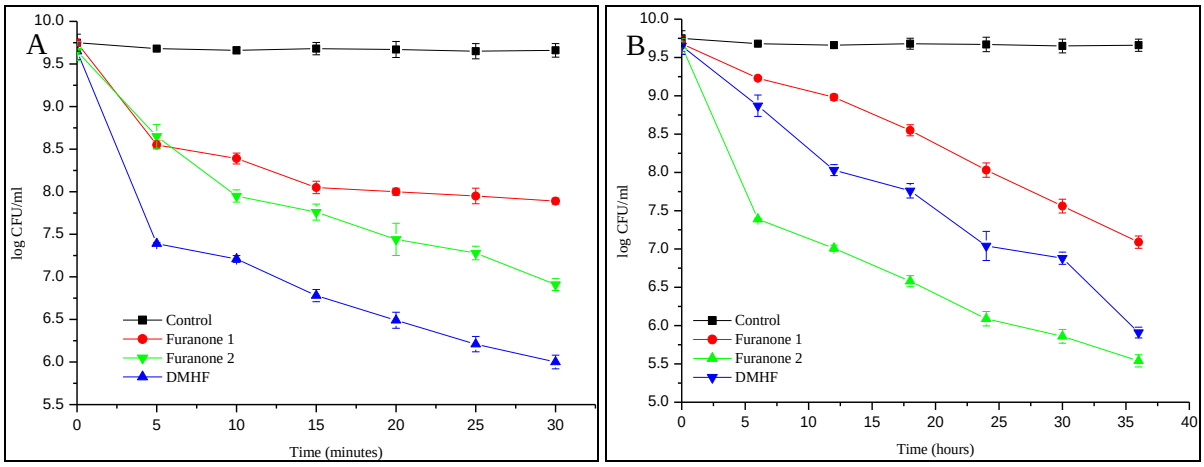

Figure 5.15: Antimicrobial and antifouling potential of free furanones on mixed cultures

5.9.7.2 Polymer/Furanone nanofibres

In this section, results on the antimicrobial and colonization inhibition efficiencies demonstrated by the furanone derivatives immobilized on SMA and blended with PVA are reported.

[1] PVA/DMHF

As illustrated in Figure 5.16A, nanofibres emanating from blends of PVA with 2,5 dimethyl-4-hydroxy-3-(2H)-furanones (DMHF) demonstrated up to 3.5 log reductions in populations of *P. aeruginosa* Xen 5 and *E. coli* Xen 14 cells and about 2.2 log reductions on *S. aureus* Xen 36 , cells of *S. typhimurium* Xen 26, and *K. pneumoniae* Xen 39 after 30 minutes. Figure 5.17 B also demonstrates that these coated filters also inhibited biofilm formation by more than 3 log for all the strains. *Pseudomonas aeruginosa* Xen 5, *E. coli* Xen 14 and *S. aureus* Xen 36 recorded up to 4.3 log biofilm inhibitions after 36 hours. Figure 5.17A demonstrates that, up to 4 log microbial population reductions were achieved by these nanofibres on mixed strain cultures over 30 minutes of exposure. Antibiofouling efficiencies of up to 2.5 log were achieved after 36 hours as shown in Figure 5.17B.

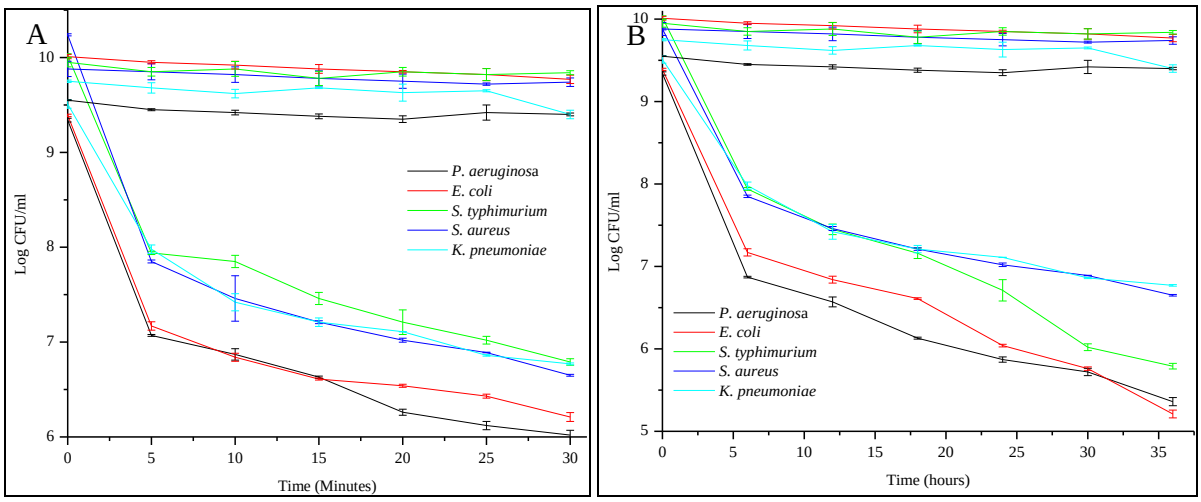

Figure 5.16: Antimicrobial (A) and antifouling (B) potential of PVA/DMHF nanofibres over 30 minutes and 36 hours respectively.

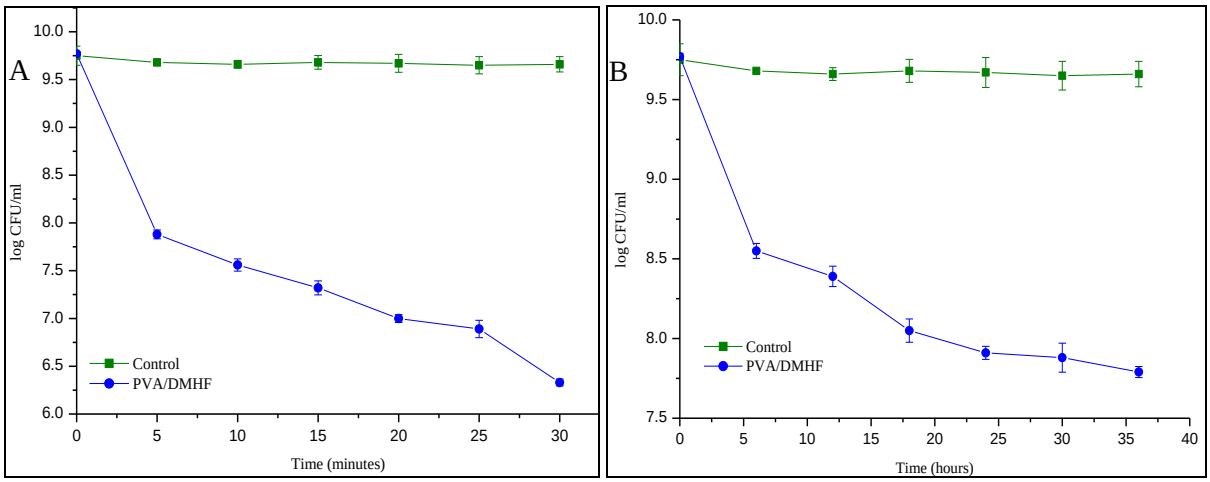

Figure 5.17: Antimicrobial (A) and antifouling (B) potential of PVA/DMHF nanofibres on mixed cultures over 30 minutes and 36 hours respectively.

[2] SMA/5-(2-(2-aminoethoxy)ethoxy)methyl)-2(5H)furanone

SMA/5-(2-(2-aminoethoxy)ethoxy)methyl)-2(5H)furanone nanofibres showed up to 1.1 log reductions in populations of *P. aeruginosa* Xen 5, *E. coli* Xen 14, *S. typhimurium* Xen 26, *S. aureus* Xen 36 and *K. pneumoniae* Xen 39 after 30 minutes of exposure (Figure 5.18A). The antimicrobial activity shown by these nanofibres after the first 15 minutes was about 0.5 log for all the strains and gradually increased thus achieving at least 1 log reductions after 30 minutes of exposure. These nanofibres also inhibited biofilm formation by strains of *P. aeruginosa* Xen 5, *E. coli* Xen 14, *S.typhimurium* Xen 26, *S. aureus* Xen 36 and *K. pneumoniae* Xen 39 by at least 2.5 log after 36 hours (Figure 5.18B).

Nanofibres made from SMA/4-(2-(2-aminoethoxy)-2,5-dimethyl-3(2H)-furanone showed up to 4 log reductions in populations of *P. aeruginosa* Xen 5, closely followed by *S. typhimurium* Xen 26 which was reduced by up to 3.4 log after 30 minutes of exposure (Figure 5.19B). *E.coli* Xen 14, *S. aureus* Xen 36 and *K. pneumoniae* Xen 39 were all reduced by at least 2.5 log after 30 minutes of exposure. All the strains were reduced by more than 2 log after the first 5 minutes. The SMA/Furanone 2 nanofibres also inhibited biofilm attachment by up to 3 log for all the strains over 36 hours of exposure (Figure 5.19B).

From Figure 5.20A, it is noted the SMA nanofibres containing 4-(2-(2-aminoethoxy)-2,5-dimethyl-3(2H)-furanone achieved antimicrobial activity of up to 3.75 log after 30 minutes of exposure to a mixed strain culture containing *P. aeruginosa* Xen 5, *E. coli* Xen 14, *S. typhimurium* Xen 26, *S. aureus* Xen 36 and *K. pneumoniae* Xen 39 cells. Those modified with 5-(2-(2-aminoethoxy)ethoxy)methyl)-2(5H)furanone on the other hand achieved about 2 log reductions. Figure 5.20B illustrates that, the nanofibres derived from 4-(2-(2-aminoethoxy)-2,5-dimethyl-3(2H)-

furanone modified SMA showed higher inhibition efficiency (3 log) compared to those from 5-(2-(2-aminoethoxy)ethoxy)methyl)-2(5H)furanone which demonstrated inhibition of 1.2 log.

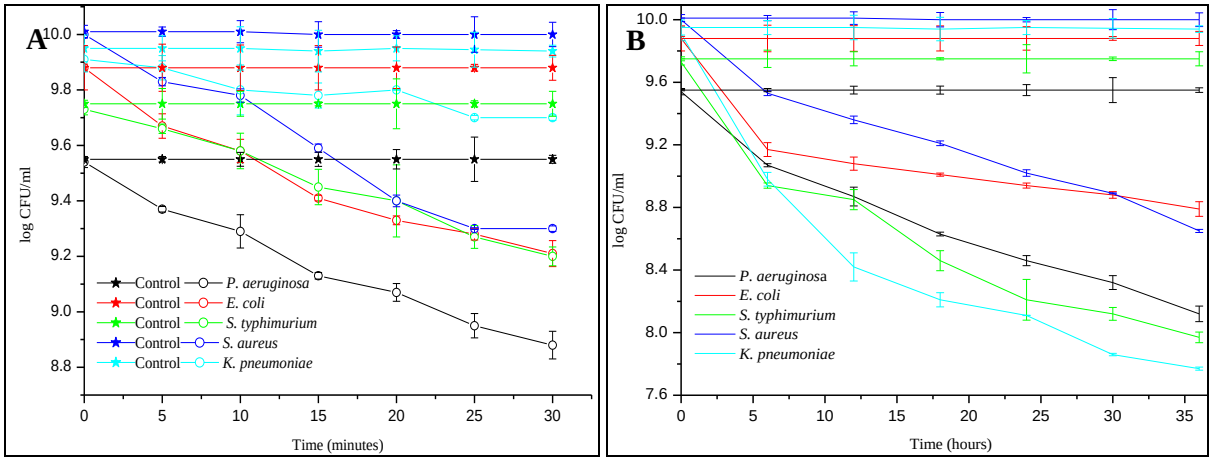

Figure 5.18: Antimicrobial (A) and antifouling (B) potential of SMA/Furanone 1 nanofibres over 30 minutes and 36 hours respectively.

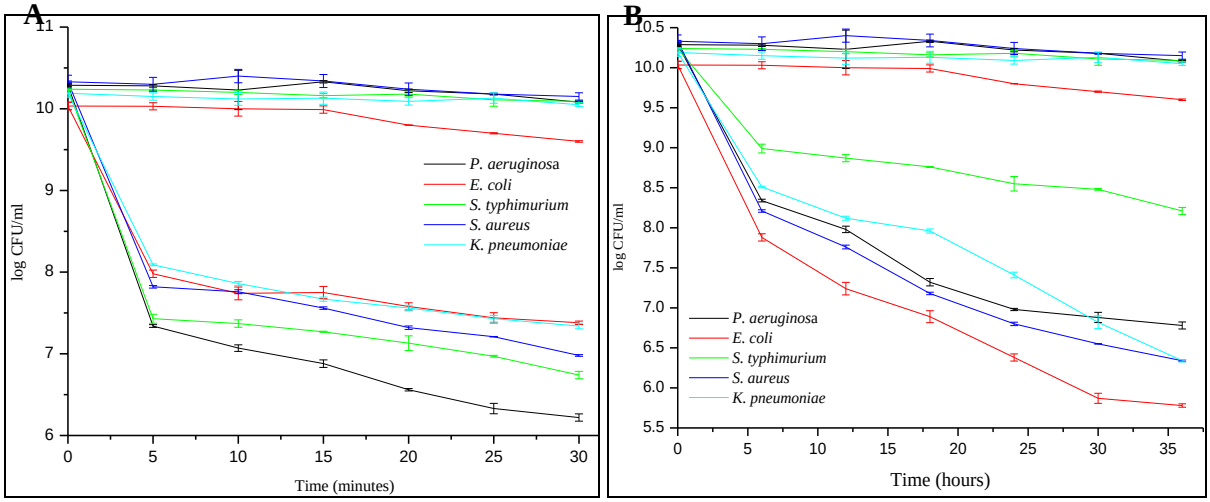

Figure 5.19: Antimicrobial (A) and antifouling (B) potential of SMA/Furanone 2 nanofibres over 30 minutes and 36 hours respectively.

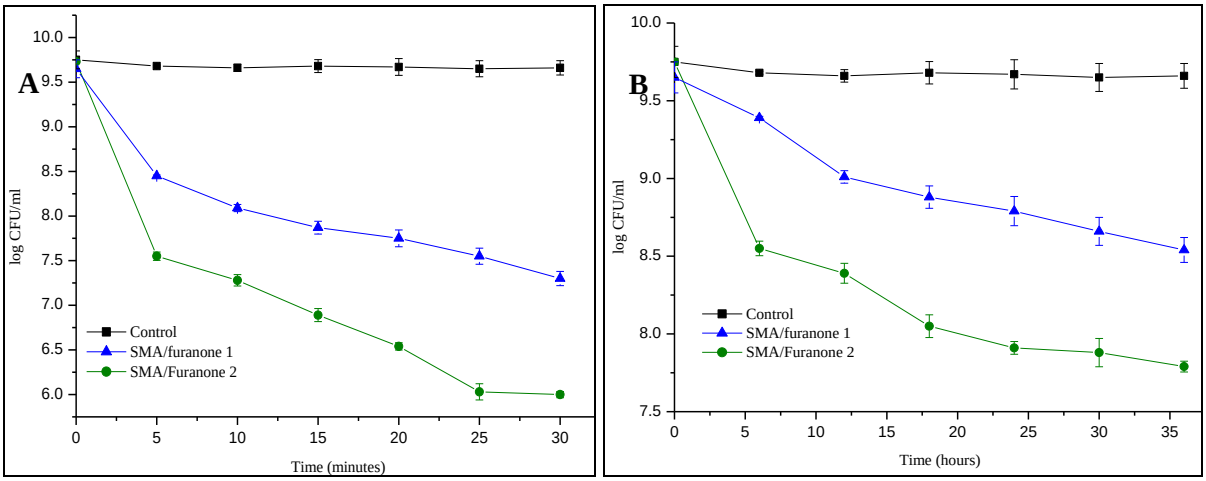

Figure 5.20: Antimicrobial (A) and inhibition (B) tests of immobilized furanones.

5.9.8 Bioluminescence Imaging

In vivo imaging of the mixed strain culture of *P. aeruginosa* Xen 5, *E. coli* Xen 14, *S. typhimurium* Xen 26, *S. aureus* Xen 36 and *K. pneumoniae* Xen 39 on Free furanone coated filters as well as PVA/DMHF and SMA/Furanone (1 and 2) nanofibres confirmed some of the results obtained from plate counting. DMHF demonstrated high antimicrobial potential followed by 4-(2-(2-aminoethoxy)-2,5-dimethyl-3(2H)-furanone which demonstrated good antimicrobial potential (Figure 5.21). Free 5-(2-(2-aminoethoxy)ethoxy)methyl)-2(5H)furanone, demonstrated very low antimicrobial potential compared to the other furanone compounds. Nanofibres made from electrospinning SMA/Furanone 2 showed the highest antimicrobial capacity followed by those emanating from PVA/DMHF blend (Figure 5.21). The nanofibres made from electrospun SMA/Furanone 1 however showed very little antimicrobial activity (Figure 5.21). These results confirmed the results obtained from plate counting.

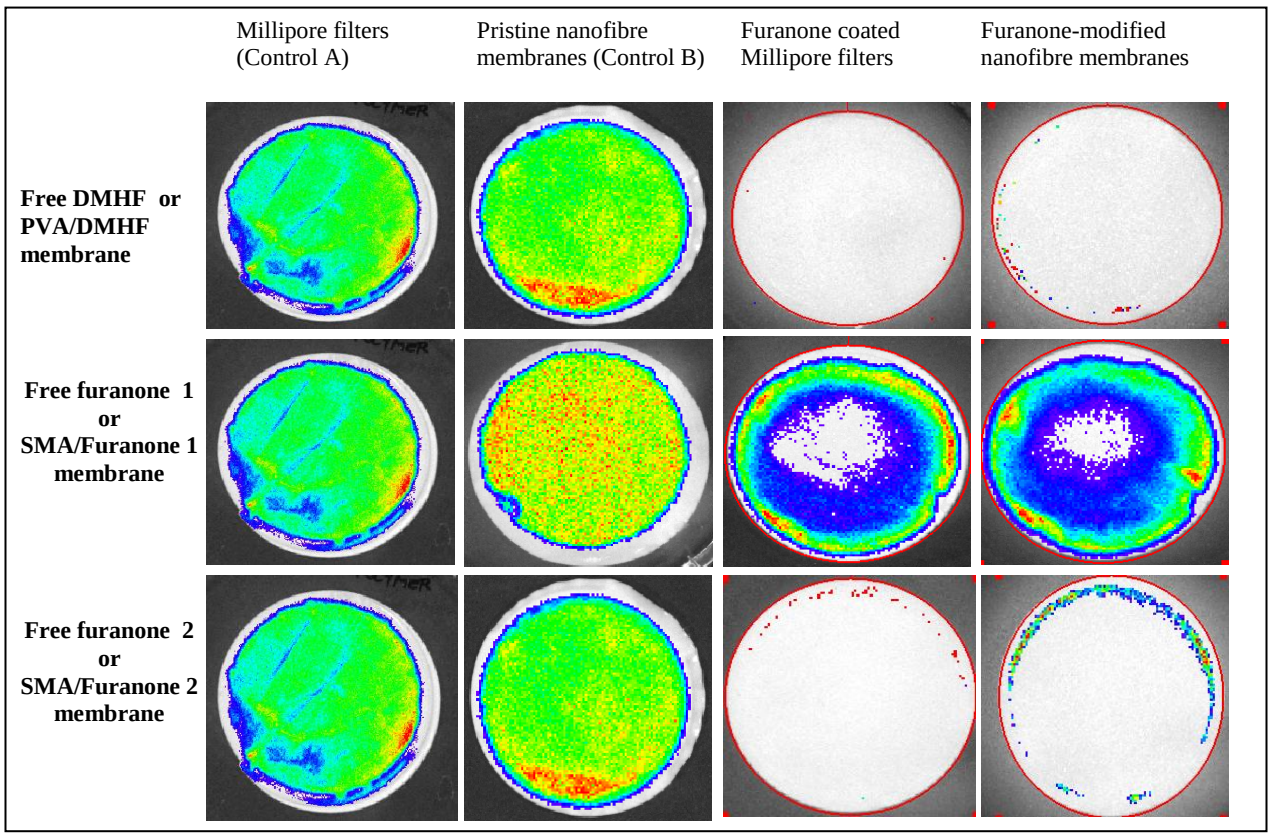

Figure 5.21: *In vivo* images

5.9.9 Fluorescence microscopy

The control PVA and SMA micrographs showed no antimicrobial or antibiofouling capability in that the colonies attached to them did not absorb propidium iodide (red) dye which would indicate cell death(Figure 5.22 A_1, A_2, A_3 and B_1, B_2, B_3). Furanone modified nanofibres demonstrated biofilm formation inhibition in that no colonization was visible (Figure 5.22 C and E). SMA/Furanone 1 nanofibres demonstrated biofilm inhibition coupled with cell deactivation. This is indicated by the colony which managed to attach to the nanofibres but was deactivated (absorbed the red dye indicating cell death) (Figure 5.22 D). These results further confirm the inhibition properties of furanone compounds and also support the antimicrobial efficacy of these nanofibres.

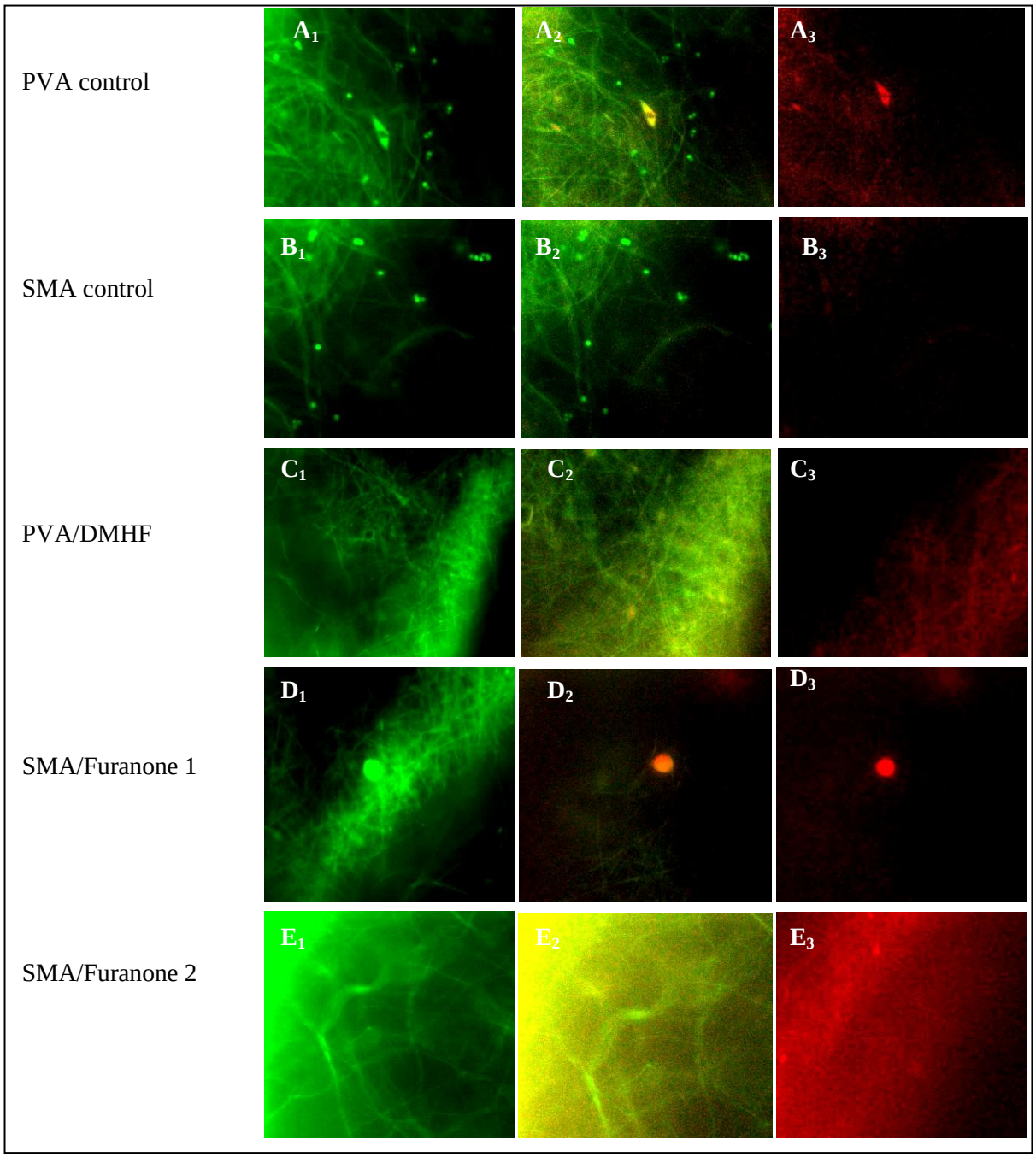

Figure 5.22: Fluorescent microscopy images.

5.9.10 Regeneration

Results from the regeneration experiments indicated that PVA/DMHF nanofibre mats reduced populations of the mixed strain culture (*E. coli* Xen 14, *S. typhimurium* Xen 26, *S. aureus* Xen 36 and *K. pneumoniae* Xen 39) by up to 2.8 log in the first cycle and by up to 1.5 log reduction was achieved after six cycles (Figure 5.23). SMA based nanofibre mats had less antimicrobial efficacy compared to PVA/DMHF. SMA/Furanone 2 nanofibre mats achieved 2 log reductions in populations of the mixed strain culture after the first cycle and about 0.98 log reductions after six cycles. SMA/Furanone 1

nanofibres demonstrated the least antimicrobial potential with less than 1.5 log reductions after the first cycle and almost nothing removed after six cycles. Colonization of SMA/Furanone 2 nanofibre mats by biofilms of the mixed strains was inhibited by up to 2.5 log after the first cycle and this was sustained over the six cycles. Biofilm inhibition by PVA/DMHF and SMA/Furanone 1 was up to 2 and 0.5 log respectively, this was sustained over the six cycles. The nanofibres also did not show signs of disintegration even after 6 cycles (Figure 5.24).

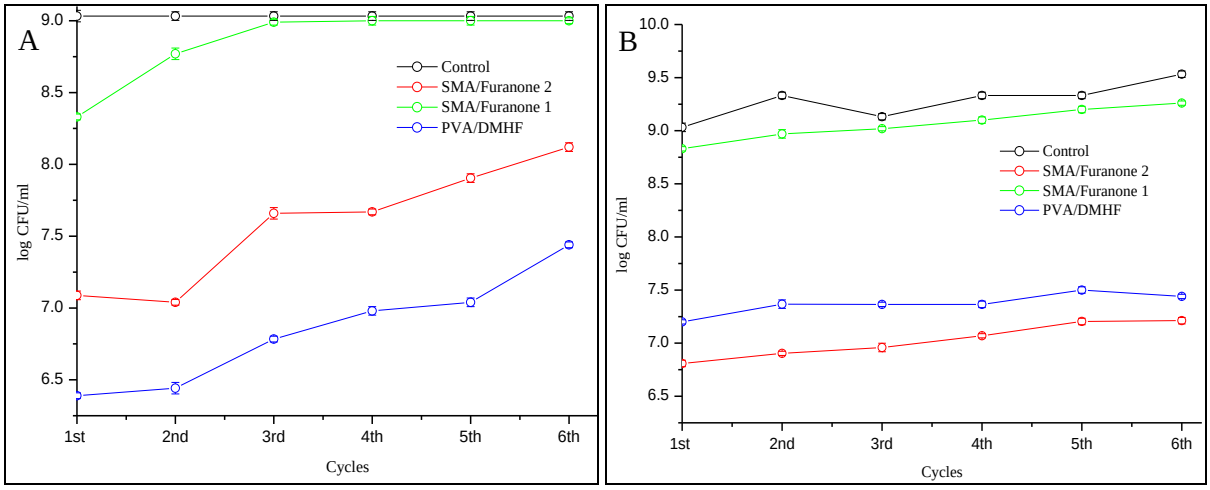

Figure 5.23: Antimicrobial (A) and colonization inhibition (B) of mixed strains on furanone containing nanofibres.

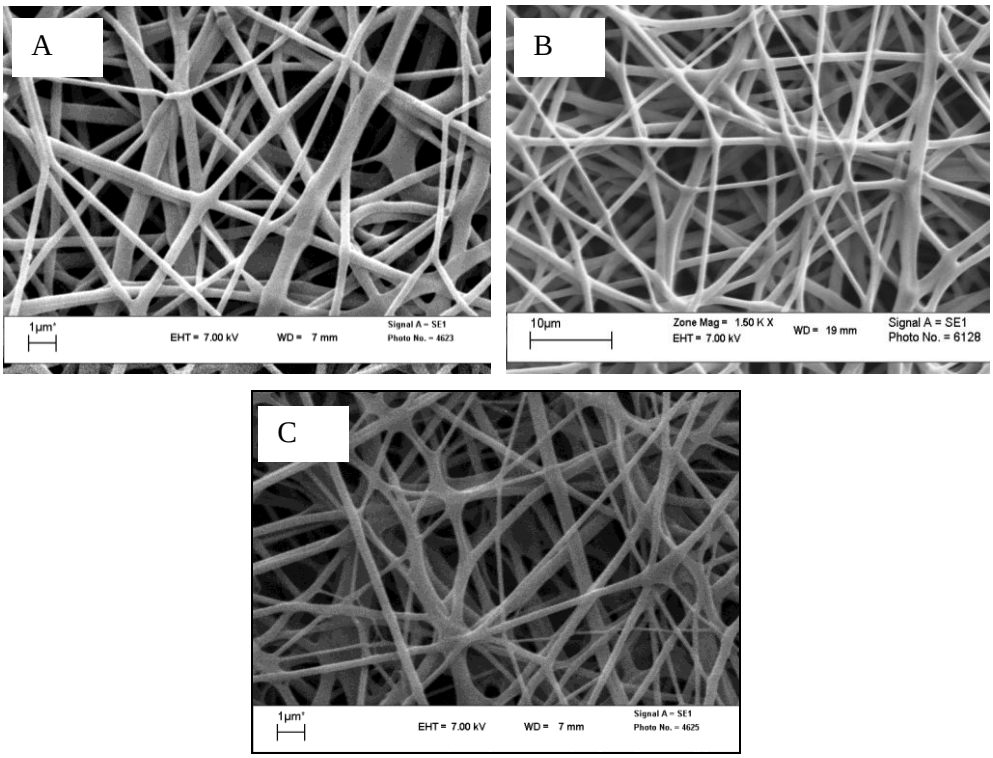

Figure 5.24: PVA/DMHF (A), SMA/Furanone 1 (B) and SMA/furanone 2 (C) nanofibres after regeneration tests.

5.9.11 Leaching experiments

The GC-MS results as illustrated by Figure 5.25 indicated that the leachates from PVA/DMHF and SMA/Furanone (1 and 2) did not contain any furanone compounds. This is because all the samples did not contain the peak at 11.59 which was only present in the furanone containing control (positive control).This indicates that the furanone compounds from both PVA/Furanone blends and immobilized on polymers did not leach into the filtered water.

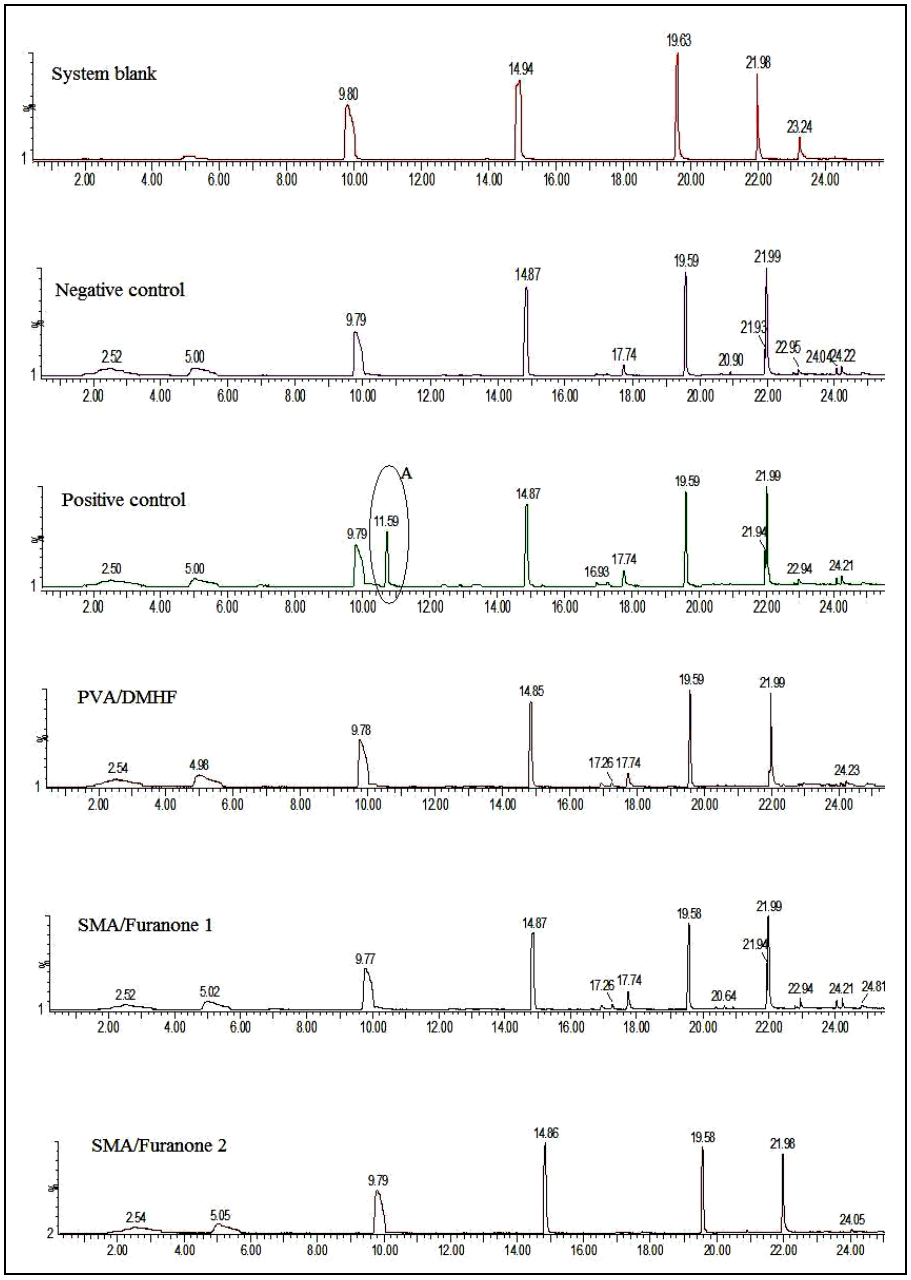

Figure 5.25: GC-MS spectra to ascertain leaching intensity of furanone compounds.

5.10 Conclusions

5.10.1 PVA/DMHF

Blends of PVA with 2,5 dimethyl-4-hydroxy-3(2H)-furanone were successfully prepared and electrospun using the electrospinning process. The nanofibres obtained had diameters between 150-300 nm, with a majority of these (29%) in the 200 and 250nm range. More than 80% of the pores on PVA/DMHF nanofibre mats had sizes of less than 100 nm^2 with a majority of these pores in the 50-100 nm^2 range. ATR-FTIR revealed that the addition of 2,5-dimethyl-4-hydroxy-3(2H)-furanone to PVA introduced peaks characteristic of the furanone moiety on the PVA nanofibres. Thermogravimetric studies indicated that there was no significant difference in the degradation patterns of PVA and PVA/DMHF nanofibres. This was further confirmed by the slight drop from 90 to 82°C in the T_g of PVA/DMHF compared to that of PVA.

Free 2,5 dimethyl-4-hydroxy-3(2H)-furanone demonstrated up to 4 log reductions in populations of *S. aureus* Xen 36 cells and about 2 log reductions on cells of *P. aeruginosa* Xen 5, *E. coli* Xen 14, *S. typhimurium* Xen 26, and *K. pneumoniae* Xen 39 after 30 minutes. This furanone also inhibited biofilm formation by up to 5 log over 36 hours of exposure. This furanone also demonstrated the highest antimicrobial efficiency on mixed-strain cultures of *P. aeruginosa* Xen 5, *E. coli* Xen 14, *S. aureus* Xen 36, *S. typhimurium* Xen 26 and *K. pneumoniae* Xen 39 when compared to the other synthesized furanone compounds.

PVA/DMHF nanofibres on the other hand achieved up to 3.5 log reductions in populations of *P. aeruginosa* Xen 5 and *E. coli* Xen 14 cells and about 2.2 log reductions on *S. aureus* Xen 36, cells of *S. typhimurium* Xen 26, and *K. pneumoniae* Xen 39 after 30 minutes. These nanofibres also demonstrated antibiofouling efficiencies of up to 2.5 log were achieved after 36 hours on all the strains. PVA/DMHF nanofibres also achieved up to 4 log microbial population reductions on mixed strain cultures over 30 minutes of exposure.

5.10.2 SMA-Furanone

Synthesis of 5-(2-(2-aminoethoxy)ethoxy)methyl)-2(5H)furanone and 4-(2-(2-aminoethoxy)-2,5-dimethyl-3(2H)-furanone from 2,5 dimethyl-4-hydroxy-3(2H)-furanone was successful. Their structures and molar masses were confirmed using ^1H NMR and ES mass spectroscopy. Product yields of 84% and 78% for 5-(2-(2-aminoethoxy)ethoxy)methyl)-2(5H)furanone and 4-(2-(2-aminoethoxy)-2,5-dimethyl-3(2H)-furanone respectively were obtained. These furanone compounds were successfully immobilized into SMA copolymer backbone. The furanone-modified SMA was electrospun to obtain nanofibres. About 83% of the nanofibres derived from 5-(2-(2-aminoethoxy)ethoxy)methyl)-2(5H)furanone modified SMA had diameters between 50-250 nm and pore sizes of less than 100 nm^2 (about 70%). About 88% of nanofibres from 4-(2-(2-aminoethoxy)-

2,5-dimethyl-3(2H)-furanone modified SMA had diameters between 50 and 300 nm and about 70% of the nanofibrous mat pores between 100-150 nm^2 in size.

SMA copolymers modified with 5-(2-(2-aminoethoxy)ethoxy)methyl)-2(5H)furanone and 4-(2-(2-aminoethoxy)-2,5-dimethyl-3(2H)-furanone demonstrated a major weight loss in the temperature range between 250-300°C which was not shown by pristine SMA nanofibres. This indicated that the modification of SMA with furanone compounds has some effects on the decomposition pattern of SMA nanofibres. There was no significant change in the T_g value of 5-(2-(2-aminoethoxy)ethoxy)methyl)-2(5H)furanone modified SMA nanofibres compared to pristine SMA copolymer. Structural changes from the zigzag structure of SMA to a more planar structure of the furanone SMA were however noted. The 4-(2-(2-aminoethoxy)-2,5-dimethyl-3(2H)-furanone modified SMA on the other hand had a higher glass transition temperature of about 170°C compared to the 140°C shown by pristine SMA.

Free 5-(2-(2-aminoethoxy)ethoxy)methyl)-2(5H)furanone achieved up to 2 log reductions in populations of *P. aeruginosa* Xen 5, *E. coli* Xen 14, *S. typhimurium* Xen 26, *S. aureus* Xen 36 and *K. pneumoniae* Xen 39 after 30 minutes of exposure. This furanone compound also inhibited biofilm formation by strains of *P. aeruginosa* Xen 5, *E. coli* Xen 14, *S. typhimurium* Xen 26, *S.aureus* Xen 36 and *K. pneumoniae* Xen 39 by at least 1.5 log after 36 hours. Reduction in viable cell populations of up to 1.5 log was achieved by this furanone in mixed-strain cultures.

Nanofibres derived from 5-(2-(2-aminoethoxy)ethoxy)methyl)-2(5H)furanone modified SMA furanone coated filters achieved up to 1.1 log reductions in populations of *P. aeruginosa* Xen 5, *E. coli* Xen 14, *S. typhimurium* Xen 26, *S. aureus* Xen 36 and *K.pneumoniae* Xen 39 after 30 minutes of exposure. This furanone also inhibited biofilm formation by strains of *P. aeruginosa* Xen 5, *E. coli* Xen 14, *S. typhimurium* Xen 26, *S. aureus* Xen 36 and *K. pneumoniae* Xen 39 at least 2.5 log after 36 hours and almost the same in mixed-strain cultures (2.4 log inhibition).

Free 4-(2-(2-aminoethoxy)-2,5-dimethyl-3(2H)-furanones recorded reductions of up to 5.5 log in populations of *P. aeruginosa* Xen 5 and *S. typhimurium* Xen 26 after 30 minutes of exposure. Up to 4.5 log reductions were achieved for *E. coli* Xen 14, *S. aureus* Xen 36 and *K. pneumoniae* Xen 39. The 4-(2-(2-aminoethoxy)-2,5-dimethyl-3(2H)-furanone also inhibited surface colonization by biofilms of *P. aeruginosa* Xen 5, *E. coli* Xen 14, *S. typhimurium* Xen 26, *S. aureus* Xen 36 and *K. pneumoniae* Xen 39 by almost 3 log after 36 hours. Antibiofouling characterization revealed that the free 4-(2-(2-aminoethoxy)-2,5-dimethyl-3(2H)-furanone showed higher inhibition efficiency (4.2 log) compared to free 2,5-dimethyl-4-hydroxy-(3(2H)-furanone and 5-(2-(2-aminoethoxy)ethoxy)methyl)-2(5H)furanone.

Nanofibres made from 4-(2-(2-aminoethoxy)-2,5-dimethyl-3(2H)-furanone modified SMA on the other hand achieved up to 4 log reductions in populations of *P. aeruginosa* Xen 5, followed by *S. typhimurium* Xen 26 which was reduced by up to 3.4 log after 30 minutes of exposure. *E. coli* Xen 14, *S. aureus* Xen 36 and *K. pneumoniae* Xen 39 were all reduced by at least 2.5 log after 30 minutes of exposure. These nanofibres also inhibited biofilm formation by up to 3 log over 36 hours of exposure to the strains. These nanofibres also showed antimicrobial activity of up to 3.75 log after 30 minutes of exposure to the mixed strain culture.

5.11 References

1. Rappai J.P.; Raman V.; Unikrishnan P.A.; Pathapan S.; Thomas S.K.; Paulose C.S. *Bioorganic and Medicinal Chemistry Letters* **2009,** 19, 764-765.
2. Ahmad A.; Ahmad F.; Pichtel J., *Microbes and Microbial Technology: Agricultural and Environmental Applications*. Springer New York Dordrecht Heidelberg London, 2011.
3. Nealson K.H.; Eberhard A.; Hastings J.W. *Proc Natl Acad Sci USA* **1972,** 69, 1073-1076.
4. Fuqua C.; Winans S.C. *Journal of Bacteriology* **1996,** 178, 435-440.
5. Fuqua W.C.; Winans S.C.; Greenberg E.P. *Journal of Bacteriology* **1994,** 176, 269-275.
6. Dunne W.M. Jr. *Clinical Microbiology Reviews* **2002,** 15, 155-166.
7. Han Y.; Hou S.; Simon K.A.; Ren D.; Luk Y-Y. *Bioorganic and Medicinal Chemistry Letters* **2008,** 18, 1006-1010.
8. Hall-Stoodley L.; Costerton J.W.; Stoodley P. *Nature Reviews: Microbiology* **2004,** 2, 95-99.
9. Alfaro J.F.; Zhang T.; Wynn D.P.; Karschner E.L.; Zhou Z.S. *Organic Letters* **2004,** 6, 3043.
10. Cheng G.; Zhang Z.; Chen S.; Bryers J.D.; Jiang S. *Biomaterials* **2007,** 28, 4192-4199.
11. Morohoshi T.; Shiono T.; Takidouchi K.; Kato M.; Kato N.; Kato J.; Ikeda T. *Applied and Environmental Microbiology* **2007,** 73, 6339-6342.
12. Hjelmgaard T.; Persson T.; Rasmussen T.B.; Givskov M.; Nielsen J. *Bioorganic and Medicinal Chemistry Letters* **2003,** 11, 3261.
13. Ponnusamy K.; Paul D.; Kim Y.S.; Kweon J.H. *Brazilian Journal of Microbiology* **2010,** 41, 227-234.
14. Manefield M.; de Nys R.; Kumar N.; Read R.; Givskov M.; Steinberg P.; Kjelleberg S. *Microbiology* **1999,** 145, 283-291.
15. Dong Y.H.; Zhang L.H. *Journal of Microbiology* **2005,** 43, 101-109.
16. Mahajan V.A.; Borate H.B.; Wakharkar R.D. *Tetrahedron* **2006,** 62, 1258-1272.
17. Pe´rez A.G.; Olı´as R.; Olı´as J.M.; Sanz C. *Journal of Agricultural Food Chemistry* **1999,** 47, 655-658.
18. Eberl L.; Molin S.; Givskov M. **1999,** 181, 1703-1712.
19. Defoirdt T.; Miyamoto C.M.; Wood T.K.; Meighen E.A.; Sorgeloos P.; Verstraete W.; Bossier P. *Environmental Microbiology* **2007,** 9, 2486-2495.
20. Manefield M.; Harris L.; Rice S.A.; De Nys R.; Kjelleberg S. *Applied Environmental Microbiology* **2000,** 66, 2079-2084.
21. Hentzer M.; Wu H.; Andersen J.B.; Riedel K.; Rasmussen T.B.; Bagge N.; Kumar N.; Schembri M.A. *EMBO J* **2003,** 22, 3803-3815.
22. Manefield M.; Rasmussen T.B.; Henzter M.; Andersen J.B.; Steinberg P.; KjellebergS.; Givskov M. *Microbiology* **2002,** 148, 1119-1127.
23. Ren D.; Sims J.J.; Wood T.K. *Environmental Microbiology* **2001,** 3, 731-736.

24. de Nys R.; Wright A.D.; Konig G.M.; Sticher O. *Tetrahedron* **1993,** 49, 11213-11220.
25. Givskov M.; de Nys R.; Manefield M.; Gram L.; Maximilien R.; Eberl L.; Molin S.; Steinberg P.D.; Kejelleberg S. *Journal of Bacteriology* **1996,** 178, 6618-6622.
26. de Nys R.; Steinberg P.; Rogers C.N.; Charlton T.S.; Duncan M.W. *Mar. Ecol. Prog. Ser.* **1996,** 130, 135-146.
27. Rasmussen T.B.; Manefield M.; Andersen J.B.; Eberl L.; Anthoni U.; Christophersen C.; Steinberg P.; Kejelleberg S.; Givskov M. *Microbiology* **2000,** 146, (3237-3244).
28. Kozminykh V.O.; Igidov N.M.; Kozminykh E.N.; Aliev ZG. *Pharmazie* **1993,** 48, 99-106.
29. Gein V.L.; Gein L.F.; Bezmaternykh E.N.; Voronina E.V. *Pharmaceutical Chemistry Journal* **2000,** 34, 254-256.
30. Baveja J.K.; Willcox M.D.P.; Hume E.B.H.; Kumar N.; Odell R.; Poole-Warren L.A. *Biomaterials* **2004,** 25, 5003-5012.
31. Khan M.S.; Husain A. *Pharmazie* **2002,** 57, 448-452.
32. Wu H.; Song Z.; Hentzer M.; Andersen J.B.; Molin S.; Givskov M.; Høiby N. *Journal of Antimicrobial Chemotherapy* **2004,** 53, 1054-1061.
33. Hume E.B.H.; Baveja J.K.; Muirf B.; Schubert T.L.; Kumar N.; Kjelleberg S.; Griesser H.J.; Thissen H.; Read R.; Poole-Warren L.A.; Schindhelm K.; M.D.P., W. *Biomaterials* **2004,** 25, 5023-5030.
34. Weber V.; Coudert P.; Rubat C.; Duroux E.; Valle´e-Goyet D.; Gardette D.; Bria M.; Albuisson E.; Leal F.; Gramain J-C.; Couqueleta J.; Madesclaire M. *Bioorganic and Medicinal Chemistry* **2002,** 10, 1647-1658.
35. Hauck T.; Bru¨hlmann F.; Schwab W. *Applied and Environmental Microbiology* **2003,** 69, 3911-3918.
36. Zschoche S.; David R.; Tavana H.; P¨oschel K.; Petong N.; Dutschk V.; Grundke K.; Neumannb A.W. *Colloids Surf.A* **2007,** 307, 53-61.
37. Mpitso K. Synthesis and characterization of styrene – maleic anhydride copolymer derivatives. Stellenbosch University, Stellenbosch, 2009.
38. Pal J.; Singh H.; Ghosh A.K. *Journal of Applied Polymer Science* **2004,** 92, 102-108.
39. S´witala-Zeliazkow M. *Polymer Degradation and Stability* **2001,** 74, 579-584.
40. Sreedhar B.; Sairam M.; Chattopadhyay D.K.; Syamala Rathnam P.A.; Mohan Rao D.V. *Journal of Applied Polymer Science* **2005,** 96, 1313-1322.
41. Winzer K.; Hardie K.R.; Burgess N.; Doherty N.; Kirke D.; Holden M.T.G.; Linforth R.; Cornell K.A.; Taylor A.J.; Hill P.J.; Williams P. *Microbiology* **2002,** 148, 909-922.
42. Kozminykh V.O.; Igidov N.M.; Kozminykh E.N.; Semenova Z.N.; Andreichikov YuS. *Pharmazie* **1992,** 47, 261-263.
43. Sindhu Ramachandran C.V.; Sreekumar P.K. *International Journal of Pharmacy and Pharmaceutical Sciences* **2011,** 3, 225-228.

Chapter 6: Conclusions and recommendations

6.1 Introduction

The main objective of this study was to develop nanofibres, with surfaces having the ability to repel microbial attachment and also inactivate any bacteria which may come into contact with it, i.e. (both antibacterial (antimicrobial) and anti-biofouling properties) for possible use in filtration media. To achieve this, the authors focused on modifying existing polymers to introduce antimicrobial properties in otherwise non-antimicrobial polymers. This was explored in two ways using different polymers. Firstly, polymer blends with biocides and or bactericidal copper ions were prepared and electrospun to fabricate nanofibres with antimicrobial properties. Secondly, blending and immobilization of furanone compounds which inhibit biofilm formation on surfaces was explored. The following sections summarize the findings of the study and also give recommendations for future studies related to the same subject.

6.2 Studied nanofibres

In this section, the main conclusions from the different nanofibres investigated in this study are given.

6.2.1 Biocide-doped nanofibres

Solutions of PVA (Mw 146000-186000, 87-89% hydrolyzed) were prepared and doped with AquaQure which is a biocide containing amongst other metal ions Cu^{2+} and Zn^{2+}. These solutions were then electrospun using the conventional needle spinning technique. The nanofibres were crosslinked using glyoxal to attain water stability of the nanofibrous mats. Various conditions which affect nanofibre stability were investigated to obtain optimal conditions for the electrospinning process. These investigations led to the following conditions: PVA (10 % wt/vol), glyoxa (8% vol/vol), AquaQure (5% vol/vol), tip-collector distance (15 cm), voltage (10-12 kV), relative humidity (40-60%) and room temperature.

About 90% of the nanofibres had diameters less than 300 nm and about 70% of the pores were in the 5-50 nm^2 range. Successful incorporation of the biocide was confirmed by the existence of the constituents of AquaQure on surfaces of the nanofibres which was shown by EDX studies. Crosslinked nanofibrous mats demonstrated good water stability. The addition of the biocide did not compromise thermal properties of the pristine nanofibres and this was proven by TGA and DSC studies. This water-insoluble property would give PVA/AquaQure fibres good potential for water filtration applications. The fibres also demonstrated stability in water and up to about 190% absorption of water without disintegration even after 48 hours of submersion.

Antimicrobial tests on the fibres against the Gram-positive strain *S. aureus* Xen 36 and Gram-negative strains *E. coli* Xen 14, S. *typhimurium* Xen 26, *P. aeruginosa* Xen 5 and *K. pneumoniae* Xen 39 showed up to 5 log reductions in bacteria populations when compared with unmodified PVA fibres. The antimicrobial tests were confirmed with bioluminescent imaging and LIVE/DEAD Baclight fluorescence imaging. Leaching experiments showed leachate concentrations of less than $1.1x10^{-4}$ µg/ml for all the ions after 24 hours of exposure. When compared to the SANS guidelines for drinking water, water filtered through these nanofibres met the requirements deeming these nanofibres safe for water filtration application.

6.2.2 Copper doped nanofibres

The antimicrobial efficacy of the nanofibres obtained from biocide doping of PVA solutions roused the interest to study the antimicrobial efficiency of metal-ion containing nanofibrous mats. Cu^{2+} was chosen because it was the main constituent of the biocide. Poly(styrene-co-maleic anhydride) copolymer (SMA) and PVA were investigated for their ability to produce antimicrobial nanofibrous mats via electrospinning of solution blends containing Cu^{2+} ions. Bubble electrospinning was evaluated to increase the production scale of nanofibres through the electrospinning process. The presence of Cu^{2+} in the nanofibres was confirmed using EDX. Thermogravimetric analysis indicated that the inclusion of Cu^{2+} to both PVA/Cu^{2+} and SMA/Cu^{2+} nanofibres did not affect the thermal stability of the nanofibres. Increases in the T_g values from 85°C in pristine PVA nanofibres to about 100°C in the case of PVA/Cu^{2+} and 150°C (pristine SMA nanofibres) to 170°C for SMA/Cu^{2+} were recorded through differential scanning calorimetry.

PVA/Cu nanofibres reduced the populations of *P. aeruginosa* Xen 5 by up to 5 logs and those of *E. coli* Xen 14, *S. typhimurium* Xen 26, *S. aureus* Xen 36 and *K. pneumoniae* Xen 39 by up to 4 logs after 30 minutes of exposure. SMA/Cu nanofibres on the other hand, achieved high reductions in the numbers of viable bacteria after 30 minutes of contact. *E. coli* Xen 14, *S. typhimurium* Xen 26 and *K. pneumoniae* Xen 39 were reduced by more than 5 log and *S. aureus* Xen 36 by about 3.5 log. Both PVA/Cu and SMA/Cu demonstrated up to 4 log reduction in pathogen numbers on the mixed strain cultures. The *in vivo* images also suggested some metabolic activity (photon emissions) in more cells than revealed by plate counting, suggesting that some of the strains develop some dormancy on contact with Cu^{2+} containing nanofibres. This led to the conclusion that even though Cu^{2+} exhibits antimicrobial efficiency, there is a tendency on the bacteria cells to develop some resistance after contact with it. This could suggest that the presence of the other ions in the biocide prevented any chances of the bacteria becoming dormant after contact with the nanofibres. The antimicrobial activity of copper containing PVA and SMA nanofibres was also confirmed through fluorescence microscopy.

Regeneration results indicated that PVA/Cu^{2+} had sustained activity over 3 cycles and SMA/Cu^{2+} nanofibres had sustained antimicrobial activity with gradual minor losses over 6 cycles. SMA/Cu nanofibres however became brittle and thin after contact with liquid media. This led to the assumption that the gradual loss of activity could be due to some fibres breaking thus increasing the pores on the nanofibre mat allowing some bacteria to pass through. From the leaching experiments PVA/Cu and SMA/Cu nanofibres showed leaching of 1.62 and 1.31 µg/ml of Cu^{2+} respectively. These figures deemed the nanofibres environmentally friendly and met the SANS standards for drinking water.

6.2.3 Furanone modified nanofibres

6.2.3.1 PVA/DMHF

Blends of PVA with 2,5 dimethyl-4-hydroxy-3(2H)-furanone were successfully prepared and electrospun using electrospinning process. The nanofibres obtained had diameters between 150-300 nm and pore sizes of less than 100 nm^2. The introduction of the furanone moiety on the nanofibres was revealed by ATR-FTIR. Thermal degradation and X-ray diffraction studies indicated that there was no significant difference in the degradation patterns of PVA and PVA/DMHF nanofibres.

The furanone compound (2,5 dimethyl-4-hydroxy-3(2H)-furanone) in its free form demonstrated up to 4 log reductions in populations of *S. aureus* Xen 36 cells and about 2 log reductions on cells of *P. aeruginosa* Xen 5, *E. coli* Xen 14, *S. typhimurium* Xen 26, and *K. pneumoniae* Xen 39 after 30 minutes. This furanone also inhibited biofilm formation by up to 5 log over 36 hours of exposure. It also demonstrated good antimicrobial efficiency on mixed-strain cultures of *Pseudomonas aeruginosa* Xen 5, *E. coli* Xen 14, *S. aureus* Xen 36, *S. typhimurium* Xen 26 and *K. pneumoniae* Xen 39. PVA/DMHF nanofibres on the other hand achieved up to 3.5 log reductions in populations of *P. aeruginosa* Xen 5 and *E. coli* Xen 14 cells and about 2.2 log reductions on *S.aureus* Xen 36, cells of *S. typhimurium* Xen 26, and *K. pneumoniae* Xen 39 after 30 minutes. These nanofibres also inhibited biofilm formation of all the strains by up to 2.5 log after 36 hours. PVA/DMHF nanofibres also achieved up to 4 log microbial population reductions on mixed strain cultures over 30 minutes of exposure.

6.2.3.2 SMA-Furanone

Synthesis of 5-(2-(2-aminoethoxy)ethoxy)methyl)-2(5H)furanone and 4-(2-(2-aminoethoxy)-2,5-dimethyl-3(2H)-furanone from 2,5 dimethyl-4-hydroxy-3(2H)-furanone was successful. Their structures and molar masses were confirmed using ^{1}H NMR and ES mass spectroscopy. These furanone compounds were successfully immobilized onto SMA copolymer backbone. The furanone modified SMA was electrospun to obtain nanofibres. SMA copolymers modified with 5-(2-(2-aminoethoxy)ethoxy)methyl)-2(5H)furanone and 4-(2-(2-aminoethoxy)-2,5-dimethyl-3(2H)-furanone

demonstrated a major weight loss in the temperature range between 250-300°C which was not shown by pristine SMA nanofibres. This indicated that the modification of SMA with furanone compounds decreased the thermal stability of SMA nanofibres. Differential scanning calorimetry of SMA copolymers modified with 5-(2-(2-aminoethoxy)ethoxy)methyl)-2(5H)furanone demonstrated structural changes from the zig-zag structure of SMA to a more planar structure. The 4-(2-(2-aminoethoxy)-2,5-dimethyl-3(2H)-furanone modified SMA on the other hand had a higher glass transition temperature of about 170°C compared to the 140°C shown by pristine SMA.

Free 5-(2-(2-aminoethoxy)ethoxy)methyl)-2(5H)furanone achieved up to 2 log reductions in populations of *P. aeruginosa* Xen 5, *E. coli* Xen 14, *S. typhimurium* Xen 26, *S. aureus* Xen 36 and *K. pneumoniae* Xen 39 after 30 minutes of exposure. This furanone compound also inhibited biofilm formation by strains of *P. aeruginosa* Xen 5, *E. coli* Xen 14, *S. typhimurium* Xen 26, *S.aureus* Xen 36 and *K. pneumoniae* Xen 39 by at least 1.5 log after 36 hours. Reduction in viable cell populations of up to 1.5 log was achieved by this furanone in mixed-strain cultures. Nanofibres derived from 5-(2-(2-aminoethoxy)ethoxy)methyl)-2(5H)furanone modified SMA furanone coated filters achieved up to 1.1 log reductions in populations of *P. aeruginosa* Xen 5, *E.coli* Xen 14, *S. typhimurium* Xen 26, *S. aureus* Xen 36 and *K. pneumoniae* Xen 39 after 30 minutes of exposure. These nanofibres also inhibited biofilm formation by strains of *P. aeruginosa* Xen 5, *E. coli* Xen 14, *S. typhimurium* Xen 26, *S. aureus* Xen 36 and *K. pneumoniae* Xen 39 at least 2.5 log after 36 hours and almost the same in mixed-strain cultures (2.4 log inhibition).

Free 4-(2-(2-aminoethoxy)-2,5-dimethyl-3(2H)-furanone recorded reductions of up to 5.5 log in populations of *P. aeruginosa* Xen 5 and *S. typhimurium* Xen 26 after 30 minutes of exposure. Up to 4.5 log reductions were achieved for *Escherichia coli* Xen 14, *S. aureus* Xen 36 and *K.pneumoniae* Xen 39. This furanone also inhibited surface colonization by biofilms of *P. aeruginosa* Xen 5, *E. coli* Xen 14, *S. typhimurium* Xen 26, *S. aureus* Xen 36 and *K. pneumoniae* Xen 39 by almost 3 log after 36 hours. Antibiofouling characterization revealed that the free 4-(2-(2-aminoethoxy)-2,5-dimethyl-3(2H)-furanone showed higher inhibition efficiency (4.2 log) compared to free 2,5-dimethyl-4-hydroxy-(3(2H)-furanone and 5-(2-(2-aminoethoxy)ethoxy)methyl)-2(5H)furanone. Nanofibres made from 4-(2-(2-aminoethoxy)-2,5-dimethyl-3(2H)-furanone modified SMA on the other hand achieved up to 4 log reductions in populations of *P. aeruginosa* Xen 5, followed by *S.typhimurium* Xen 26 which was reduced by up to 3.4 log after 30 minutes of exposure. *Escherichia coli* Xen 14, *S. aureus* Xen 36 and *K. pneumoniae* Xen 39 were all reduced by at least 2.5 log after 30 minutes of exposure. These nanofibres also inhibited biofilm formation by up to 3 log over 36 hours of exposure to the strains. These nanofibres also showed antimicrobial activity of up to 3.75 log after 30 minutes of exposure to the mixed strain culture.

6.3 Concluding remarks

The findings from this study suggest that the main objective of this study which was to fabricate nanofibres with both antibiofouling and antimicrobial properties was met. Further investigations on the mechanical properties of the nanofibres and possible reduction in the amount of leached metal ions would be recommended for future studies especially with the drinking water filtration applications in mind.

Biocide-doped nanofibres reduced bacteria populations of all the tested strains to levels acceptable in drinking water. Copper-doped nanofibres indicated excellent antimicrobial properties when the plate counting technique was employed. Bioluminescence imaging, which quantifies all metabolically active cells (even those which are unculturable), indicated a tendency of the bacteria to enter a stage of dormancy on contact with Cu^{2+} functionalized nanofibres. Biocide-doped and Cu^{2+} containing nanofibres did not show any tendency to inhibit biofilm attachment on surfaces but demonstrated good antimicrobial properties.

Nanofibrous mats emanating from PVA and SMA modified with furanone compounds demonstrated promising results for water treatment applications. These nanofibres demonstrated their potential to not only inactivate (kill) bacteria which come into contact with it, but also repel (inhibit) surface attachment of the strains. Furanone compounds with the core 3(*2H*)-furanone structure demonstrated high activity compared to the 2(5H)-furanone structure.

6.4 Recommendations

Recommendations for further studies include:

- Synthesis of more furanone compounds with the 3(2H) structure.
- Immobilization of the furanone compounds on other polymers like polyacrylonitrile and cellulose acetate which are already used in the water purification industry.
- DNA sequence studies on the specific quorum sensing pathways of the synthesized furanone compounds.
- Post electrospinning functionalization of the nanofibres.
- Improvements on mechanical properties of SMA e.g.co-axial electrospinning with nylon.

Appendix A

Table 1: GC-MS settings

Injector temperature	250 °C
Injection volume	1 ml
Injection mode	Splitless
Purge flow	30 ml/min
Purge time	1 min
Carrier gas	Helium
MS mode	EI+
Scanning mass range	35 to 850 m/z
Scan time	0.15 min
Inter-scan delay	0.05 min

Table 2: Analysis set-up

Pre Injection Time (s)	60
Incubation Temp (ºC)	80
Pre Inc Agitator Speed (rpm)	250
Agitator on time (s)	5
Agitator off Time (s):	2
Extraction Time (s)	600
Desorption Time (s) :	600
GC Runtime (s)	2760